ISSN - 2757-8135

EUROPEAN EYE RESEARCH

The European Eye Research is indexed in OUCI, Scilit, Scope Database, EBSCO and TUBITAK TR Dizin

Owner
Melis Palamar, MD
Ege Universitesi Tip Fakultesi, Goz Hastaliklari AD, Bornova, Izmir, Türkiye
Tel: +90 232 390 37 88
melispalamar@gmail.com

Editor
Filiz Afrashi, MD
Ege Universitesi Tip Fakultesi, Goz Hastaliklari AD, Bornova, Izmir, Türkiye
Tel: +90 232 390 37 88
afrashif@yahoo.com

Contact:
Publisher
KARE
Goztepe Mah. Fahrettin Kerim Gokay Cad. No: 200 D: 2, Goztepe, Kadikoy, Istanbul, Türkiye
Phone: +90-216-550 61 11 Fax: +90-216-550 61 12
e-mail: kare@karepb.com Web: kare@karepb.com

Publications Coordinator: Esra Semerci
Graphic Design: Zeynep Koyun

Owned by on behalf of the Director of European Eye Research, İstanbul: Melis PALAMAR | Executive Editor: Filiz AFRASHI | Publication Type: Periodical

EUROPEAN EYE RESEARCH

NATIONAL ADVISORY BOARD

EUROPEAN
EYE
RESEARCH

CONTENTS

EUROPEAN
EYE
RESEARCH

EDITORIAL

In this issue of our journal, which we are proud to launch as it enters its 6th year, we present 11 original research articles, 2 fascinating case reports, a letter to the editor, and 1 review article.

The first of the original research studies evaluates the effects of two different glaucoma eye drops on posterior segment vascular parameters. The second is another imaging study assessing the effects of energy drinks—which are widely consumed today—on pupil dynamics, as well as retinal and choroidal structures. The third study is an interesting investigation evaluating trends in forensic ophthalmology. The fourth study evaluates the effects of scleral contact lenses applied to keratoconus patients on the anterior segment and tear film. The fifth study is an imaging study on vitreopapillary interface changes in non-ischemic AION, while the subsequent study examines tear film function following eyelid tumor surgery performed using the Laissez-Faire technique. The seventh study evaluated the effects on the cornea in patients who received multiple dexamethasone implants due to macular edema caused by retinal vein occlusion. The eighth study examined the use of large language models in glaucoma education, given the increasing use of artificial intelligence across many fields today. The ninth study investigated the effect of different techniques on corneal strength in deep anterior lamellar keratoplasty. The tenth study evaluated the causes of choroidal neovascularization in the pediatric group. In the eleventh study, a bibliometric analysis of the editorial boards of ophthalmology journals in Turkey was conducted. I believe you will read these highly valuable studies, which cover many areas of ophthalmology, with great interest.

These two fascinating case reports will contribute to our collective education.

In the "Letter to the Editor" section, a commentary has been provided on the article titled "The 100 most-cited articles in Turkish ophthalmology: a bibliometric analysis of research trends and scientific impact," which I believe will be useful.

Finally, the review article will help us recall valuable information regarding ocular histology.

I extend my heartfelt thanks to you, our esteemed researchers, who have walked this path with us in the short time since our journal's inception and have elevated it to significant heights through your valuable contributions; to our referees, who have guided us with their insightful comments; and to our esteemed editorial team.

Sincerely,

Filiz Afrashi, MD

Editor-In-Chief

DOI: 10.14744/eer.2025.63634
Eur Eye Res 2026;6(1):1–10

EUROPEAN EYE RESEARCH

ORIGINAL ARTICLE

Exploring the impact of latanoprostene bunod versus latanoprost on optic disc, macular, and choroidal vasculature: A comparative analysis

Furkan Ozer,[1] Duygu Gulmez Sevim,[2] Metin Unlu,[2] Osman Erdogan,[2] Kuddusi Erkilic[2]

[1]Nevsehir State Hospital, Nevsehir, Turkiye
[2]Department of Ophthalmology, Division of Glaucoma, Erciyes University Medical Faculty, Kayseri, Turkiye

Abstract

Purpose: This study aims to compare the effect of latanoprostene bunod and latanoprost on the vasculature of the posterior segment of the eye.

Methods: The study included 34 eyes of 17 patients diagnosed with primary open-angle glaucoma or ocular hypertension. Of these, 14 eyes of 7 patients were administered latanoprost 0.005% (Latafree, VEM ilaç, Türkiye) once daily (defined as the LAT group), while 20 eyes of 10 patients were administered latanoprostene bunod 0.024% (Vyzulta, Bausch+Lomb, Rochester, NY, USA) once daily (defined as the VYZ group). Intraocular pressure (IOP), macular and optic disc vascular density (VD), as well as submacular and subfoveal choroidal vascular parameters, were assessed for changes within each group over time and compared between groups at all time points (at baseline, month 1, month 3, and month 6).

Result: Latanoprost demonstrated superiority in reducing IOP compared to latanoprostene bunod ($p<0.001$). Nevertheless, a substantial decrease in IOP was observed in both agents by the conclusion of the 6th month, in comparison with the initial baseline level (all $p<0.001$). At the 6th month, peripapillary VD was observed to be higher in the VYZ group ($p=0.001$), whereas the majority of macular VD or choroidal vascular parameters exhibited higher values in the LAT group.

Conclusion: Latanoprostene bunod may protect the optic nerve head from hypoperfusion-related damage by improving peripapillary vascular perfusion. IOP-lowering effect may be more pronounced with latanoprost, but both drugs can effectively lower IOP. In addition, the utilization of latanoprost may increase macular and choroidal vasculature.

Keywords: Choroidal vascularity index; Latanoprost; Latanoprostene bunod; Macular vascular density.

Glaucoma represents a significant global public health concern, with a prevalence that is among the leading causes of blindness worldwide.[1] It is characterized by optic nerve damage and progressive vision loss. The principal objective of glaucoma therapy is to achieve a reduction in intraocular pressure (IOP) in order to mitigate the stress placed on the optic nerve head and thereby safeguard visual function. Among the most frequently prescribed pharmaceutical agents for this indication are prostaglandin analogues, with latanoprost being one of the most commonly utilized agents within this pharmacological class.[2] This therapeutic approach is recommended as the initial treatment for glaucoma by the European Glaucoma Society guidelines.[3]

Cite this article as: Ozer F, Gulmez Sevim D, Unlu M, Erdogan O, Erkilic K. Exploring the impact of latanoprostene bunod versus latanoprost on optic disc, macular, and choroidal vasculature: A comparative analysis. Eur Eye Res 2026;6(1)1–10.

Correspondence: Duygu Gulmez Sevim, M.D. Department of Ophthalmology, Erciyes University Medical Faculty, Kayseri, Turkiye
E-mail: duygugsevim@gmail.com

Submitted Date: 21.05.2025 **Revised Date:** 02.07.2025 **Accepted Date:** 07.08.2025 **Available Online Date:** 29.04.2026

However, more recently, new pharmaceutical agents have been developed for the management of glaucoma. One such agent is latanoprostene bunod, which combines the effects of nitric oxide and prostaglandin analogs.[4] In addition to their effect on IOP, prostaglandin analogs have been demonstrated to exert a modulating influence on the vascular structures of the choroid.[5] It is still of particular interest to examine changes in choroidal and retinal blood flow, as this may elucidate the pathophysiology of optic nerve damage and vision loss in glaucoma patients. Nevertheless, the precise impact of latanoprostene bunod and latanoprost on choroidal and retinal microcirculation remains a subject of ongoing investigation.

The central objective of the study is to undertake a comparative analysis of the choroidal vascular structures as well as the optic disc, macular, and foveal vascular densities (VD), in patients diagnosed with primary open-angle glaucoma or ocular hypertension, utilizing latanoprostene bunod and latanoprost.

Materials and Methods

The study was conducted at the University of XXX, Department of Ophthalmology, Division of Glaucoma. The research was undertaken in accordance with the tenets set forth in the Helsinki Declaration, and this study was approved by the Institutional Review Board of the University (no:2024/251 and date: November 06, 2025). A written informed consent form was signed by all patients following the provision of a comprehensive explanation of the processes involved.

This prospective study included 34 eyes of 17 patients who had not previously received glaucoma treatment. The diagnosis of primary open-angle glaucoma or ocular hypertension was made by D.G.S. Patients who received latanoprost 0.005% (Latafree, VEM ilaç, Türkiye) were assigned to the LAT group (14 eyes of 7 patients), while those who received latanoprostene bunod 0.024% (Vyzulta, Bausch+Lomb, Rochester, NY, USA) were assigned to the VYZ group (20 eyes of the 10 patients). Both latanoprost and latanoprostene bunod were administered once daily (at 10:00 PM) to the respective group of patients.

Patients were excluded if they had any of the following conditions that could affect or disrupt the macula or choroid: diabetic retinopathy, ocular trauma, dense media opacities, age-related macular degeneration, uveitis or scleritis, +3D or more hyperopia, and −6D or more myopia. In addition, the exclusion criteria included any systemic disease, such as hypertension, diabetes mellitus, hyper- or hypothyroidism, and connective tissue disorders.

A comprehensive ophthalmological examination was conducted for all subjects, which included IOP (using a Goldmann applanation tonometer), dilated fundus examination, and slit-lamp biomicroscopic examination. In addition, axial length (Axl) measurements were performed utilising the Nidek AL-Scan device (Nidek Co., Ltd., Gamagori, Japan), while central corneal thickness was determined through the use of the Sirius Scheimpflug tomographer and topographer (CSO, Costruzione Strumenti Oftalmici, Florence, Italy).

ImageJ and Optical Coherence Tomography Angiography (OCTA) Imaging

Macular, foveal, peripapillary, and optic disc VD was obtained by OCTA using the RTVue XR Avanti (Optovue, Inc., Fremont, CA, USA). The device employs a split-spectrum amplitude-decorrelation angiography algorithm, which permits non-invasive imaging of the retinal vasculature. The instrument performs volumetric scans of 304 × 304 A-scans at 70,000 A-scans per second, with an approximate acquisition time of 3.0 s. To assess the superficial capillary plexus and the deep capillary plexus in the macular region, 3 × 3 mm and 6 × 6 mm scan protocols were centered on the fovea. These two layers were accurately distinguished by the automatic segmentation function of the software. The percentage of the total area occupied by blood vessels in the parafoveal and perifoveal zones was calculated as macular vessel density (VD). The peripapillary and optic disc area were analyzed using the 4.5 × 4.5 mm scan protocol, which was centered on the optic nerve head. One horizontal and one vertical scan were performed, with each scan centered on the optic disc.[6] The scans were conducted using 2- and 4-mm diameter rings, with a ring width of 1 mm, centered on the optic disc. Radial peripapillary VD was automatically measured using the device software. The VD within the whole disc, peripapillary area, and inner disc (specifically within the optic disc boundary) was automatically measured by the instrument software, and then calculated as the percentage of area occupied by blood vessels.

Images of macular optical coherence tomography (spectral-domain-OCT, version 1.9.17.0; manufactured by Heidelberg Engineering, Heidelberg, Germany) were captured through horizontal scanning, centered on the central/center foveal region, following pupil dilation. n addition, the enhanced depth imaging (EDI) protocol was employed to ensure accurate visualization of the choroid (Fig. 1). OCT images were used to evaluate choroidal parameters as reported in previous studies.[7-10] The subfoveal choroid

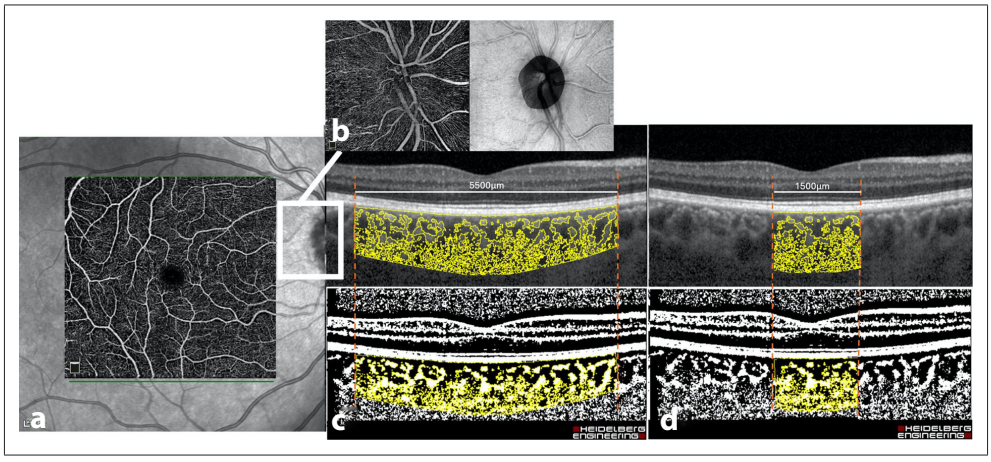

Fig. 1. **(a)** The macular scan image and **(b)** the optic disc scan image obtained by optical coherence tomography (OCT) angiography on the corresponding A-scan OCT image. **(c)** The submacular choroidal area (5500 µm) and the **(d)** subfoveal choroidal area (1500 µm) as presented in the corresponding B-scan OCT image. In the choroidal area, dark areas within the choroid represent the luminal area (vascular spaces), while the remaining lighter regions correspond to stromal tissue.

area (1500 µm width) and the submacular choroid area (5500 µm width) were manually segmented by O.E using the ImageJ software (version 1.54d, National Institutes of Health, Bethesda, MD, USA). The choroidal boundary was delineated from the Bruch's membrane to the choroid-sclera interface. The image was subsequently converted to an 8-bit binary format. The level of brightness was adjusted using the mean value obtained from the lumen of the three principal choroidal vessels within the region of interest (ROI), with the intention of considering the lumen of the choroidal vessels as the actual lumen area. The images were subjected to binarization using Niblack's auto-local thresholding method, to differentiate the luminal area (LA) from the stromal area (SA). The total choroidal area (TCA) was determined by adding together the LA and SA. The choroidal vascular index (CVI) was determined as the ratio of the LA to the TCA.[11,12]

OCTA images with a quality of 6/10 or higher (self-defined by the device) were selected for analysis. All OCT and OCTA imaging was conducted by the same experienced (and blinded) operator at a specific time between 08:30 and 10:30 AM. Furthermore, motion artifacts and segmentation errors were carefully excluded. When calculating the choroidal parameters, manual determination of the choroidal area, including demarcation of the sclerochoroidal border, was performed by one author (xxx) and verified by another author (xxx).

All measurements were collected at the initial visit (defined as the baseline) before the commencement of latanoprost and latanoprostene bunod treatment. Subsequently, measurements were taken at the 1st month, 3rd month, and 6th month visits during the treatment period.

Statistical Analysis

The statistical analyses were conducted using the IBM Statistical Package for the Social Sciences Statistics software, version 22 (IBM, Chicago, USA). Descriptive statistics (frequency, percentage, mean, median, minimum, and maximum values) were used for descriptive parameters. A Levene's test for homogeneity of variance was conducted. In addition, the Pearson Chi-square test was employed to assess nominal-ordinal data, while the Shapiro–Wilk test was utilized to assess the normality of the distribution of continuous variables. The Student's t-test was utilized for the analysis of data that exhibited a normal distribution, whereas data that did not conform to a normal distribution were evaluated using the Mann–Whitney U test and the Wilcoxon test. To perform a comparison of continuous parameters, a linear mixed model was utilized. A $p<0.05$ was deemed to represent a statistically significant result in all analyses.

Results

The study included 34 eyes of 17 patients diagnosed with primary open-angle glaucoma (or ocular hypertension). Table 1 shows the demographic and clinical characteristics of the patients in this study, and there was no significant difference between the groups in these demographic or clinical characteristics (sex: $p=0.43$, age: $p=0.502$, eyes: $p=0.99$, Axl: $p=0.735$, and CCT: $p=0.580$).

No significant change was observed in macular or foveal choroidal vascular parameters, including CVI, LA, TCA, and SA, over time in each group (Table 2). However, at the 6th month, the submacular TCA, LA, and SA, as well as the subfoveal TCA and LA, were observed to be elevated in the

Table 1. Demographic and clinical characteristics

	VYZ	LAT	*P*
Sex (male/female)	4/6	2/5	0.43
Age (years)	56.85±21.0 (median: 65.5 [19–80])	52.86±7.4 (median: 53 [43–63])	0.502
Eyes (right/left)	10/10	7/7	0.99
Axl (mm)	22.80±0.71 (median: 23 [22–24])	22.89±0.82 (median: 23 [22–24])	0.735
Central corneal thickness (µm)	563.60±24.8 (median: 563 [515–607])	568.57±26.4 (median: 562 [544–631])	0.580

Axl: Axial length, VYZ: Vyzulta group, LAT latafree group

LAT group relative to the VYZ group (all each $p<0.001$). In addition, the submacular and subfoveal CVI demonstrated an increase at the 3rd month in the LAT group when compared to the VYZ group (each $p=0.014$).

There was no significant difference over time in macular VD parameters in both groups (Table 3). Conversely, certain macular VD parameters at the 3rd month, including superficial whole area, superficial hemi-superior, superficial hemi-inferior, superficial perifovea, deep whole area, deep hemi-inferior, deep parafovea, deep perifovea, demonstrated higher values in the LAT group in compared to the VYZ group ($p<0.001$, $p<0.001$, $p<0.001$, $p<0.001$, $p=0.003$, $p<0.001$, $p<0.001$ and $p=0.001$, respectively). In addition, all macular VD parameters, except for the deep whole area, were different between the VYZ and LAT groups at month 6 (Table 3). Among these parameters, superficial and deep foveal VD values were higher in the VYZ group, while the other variables were higher in the LAT group (superficial foveal VD [%]: VYZ=21.12±4.9, LAT=15.2±1.5, $p<0.001$; deep foveal VD [%]: VYZ=37.1±4.3, LAT=32±0.5, $p<0.001$) (Table 3).

Inside the optic disc, VD was not different between groups at all time points and did not change over time within each group (all $p>0.05$) (Table 4). In the VYZ group, whole disc VD and peripapillary VD increased at 1 and 6 months, but decreased at 3 months (whole disc VD [%]: baseline=46.7±4, at 1st month=49.9±3, at 3rd month=48.2±2.1 and 6th month=50.4±0.7; peripapillary VD [%]: baseline=51.8±3.2, at 1st month=53.3±3.1, at 3rd month=50.5±2.4 and at 6th month=54.6±1.3). In addition,

Table 2. Comparison of macular and foveal choroidal vascular parameters and IOP

Groups	Sub-macular (5500 µm)				Sub-foveal (1500 µm)			
	mTCA (mm^2)	mLA (mm^2)	mSA (mm^2)	mCVI (%)	fTCA (mm^2)	fLA (mm^2)	fSA (mm^2)	fCVI (%)
VYZ[a] (*n*=20)								
Baseline[x]	1.55±0.8	0.98±0.4	0.55±0.3	65.2±5.3	0.43±0.1	0.27±0.1	0.16±0.08	64±4.3
1st month[y]	1.60±0.8	1.02±0.4	0.58±0.3	65.4±4.9	0.43±0.1	0.27±0.09	0.16±0.07	63.6±4.2
3rd month[z]	1.60±0.9	1.02±0.5	0.57±0.4	65.6±4.5	0.43±0.2	0.27±0.1	0.16±0.08	63.9±3.9
6th month[t]	1.38±0.2	0.87±0.1	0.51±0.04	62.8±1.8	0.40 ±0.04	0.24±0.02	0.16±0.03	61.3±2.3
P[c]	0.264	0.171	0.822	0.06	0.449	0.240	0.321	0,054
LAT[b] (*n*=14)								
Baseline[x]	1.88±0.5	1.15±0.2	0.72 ±0.2	62.0±4.1	0.49±0.1	0.29±0.06	0.19±0.07	61.5±4
1st month[y]	1.78±0.3	1.11±0.2	0.67±0.1	62.5±3.2	0.47± 0.1	0.29±0.05	0.18 ±0.04	61.7±2.2
3rd month[z]	1.88±0.4	1.17±0.2	0.71±0.1	62.3±2	0.51±0.06	0.31±0.03	0.20±0.04	61±1.7
6th month[t]	2.04±0.3	1.28±0.1	0.77±0.1	63.5±2.3	0.53±0.04	0.32±0.02	0.20±0.04	62.2±2.1
P[c]	0.076	0.057	0.451	0.444	0.172	0.077	0.310	0.621
p[ab]								
Baseline	0.183	0.21	0.162	0.074	0.276	0.395	0.184	0.105
1st month	0.428	0.447	0.417	0.071	0.459	0.484	0.442	0.138
3rd month	0.328	0.287	0.18	0.014*	0.128	0.187	0.078	0.014*
6th month	<0.001*	<0.001*	<0.001*	0.319	<0.001*	<0.001*	0.535	0.276

LAT: Latafree group, VYZ: Vyzulta group, CVI: Choroidal vascular index, LA: Luminal area, SA: Stromal area, TCA: Total choroidal area, m: Macular, f: Foveal, P^{ab}: Cross sectional *P*-value; P^{c}: Longitidunal *P*-value; *Statistically significant

Table 3. Comparison of macular and foveal vessel density parameters

Groups	Time	Macular VD (%)					
		Whole area	Hemi superior	Hemi inferior	Fovea	Parafovea	Perifovea
VYZ[a] (*n*=20)	Baseline						
	Superficial	44.9±4.7	44.9±4.7	45.1±4.8	19.02±7.5	47.05±5.4	45.05±4
	Deep	45.6±5.7	45.2±5.4	46±6.2	35±7.9	51.9±4.3	46.5±6.3
	1st month						
	Superficial	46.7±4.3	46.8±4.2	46.6±3.9	19.81±7.6	48.5±4.3	47.4±3.9
	Deep	49.2±6.1	49.2±6.1	48.8±6.6	35.7±8.4	53.8±5.2	50.3±6.7
	3rd month						
	Superficial	44.9±3.5	45±2.9	44.8±2.8	19.84±7.1	47.1±4.3	45.6±3.1
	Deep	44.6±5.7	44.5±5.2	44.2±5.7	35.6±7.1	49.7±4.6	45.4±6
	6th month						
	Superficial	45.5±5.5	45.3±2.6	45.6±3	21.12±4.9	46.7±3.6	46.2±2.8
	Deep	46±.4.2	43.9±4.6	46.1±4.1	37.1±4.3	52.3±3.9	47±4.4
	P[c]						
	Superficial	0.267	0.255	0.314	0.409	0.563	0.119
	Deep	0.059	0.06	0.092	0.554	0.096	0.067
LAT[b] (*n*=14)	Baseline						
	Superficial	47.8±3	47.6±2.4	47.7±3.2	14.3±5.6	47.7±4.1	48.1±4.2
	Deep	46.7±5.8	46.5±6.3	47.4±5.4	30±6.5	54.2±4.6	48.2±6.5
	1st month						
	Superficial	48.4±6.3	46.6±5.8	47.1±5.7	15.2±5.9	49.5±5.3	48±6.6
	Deep	47.5±7.9	47.1±7.8	48.1±8.1	31.8±8.1	56.2±3.8	48.7±9.6
	3rd month						
	Superficial	49.6±2	49.1±2.5	49.9±2.4	21.7±11.9	50.1±3.3	50.8±2
	Deep	50.3±4.2	49.6±5.3	51.1±3.7	36.5±10	56.3±2.2	52.4±4
	6th month						
	Superficial	49±0.8	48.6±0.8	49.5±0.8	15.2±1.5	52.1±1.6	49.7±0.9
	Deep	48±3.3	47.1±3.3	49.2±3.4	32±0.5	54.4±2.2	50.1±3.5
	P[c]						
	Superficial	0.515	0.24	0.158	0.06	0.058	0.113
	Deep	0.247	0.357	0.233	0.103	0.171	0.251
P[Ab]	Baseline						
	Superficial	0.056	0.061	0.082	0.058	0.709	0.057
	Deep	0.587	0.606	0.502	0.061	0.148	0.461
	1st month						
	Superficial	0.345	0.914	0.733	0.07	0.532	0.766
	Deep	0.473	0.396	0.779	0.192	0.153	0.566
	3rd month						
	Superficial	<0.001*	<0.001	<0.001*	0.568	0.037	<0.001*
	Deep	0.003*	0.009	<0.001*	0.777	<0.001*	0.001*
	6th month						
	Superficial	<0.001*	<0.001	<0.001	<0.001	<0.001	<0.001
	Deep	0.158	0.039	0.032	<0.001	0.081	0.041

LAT: Latafree group, VYZ: Vyzulta group, VD: Vessel density, *P*[ab]: Cross sectional *P*-value, *P*[c]: Longitidunal *P*-value, *Statistically significant

Table 4. Comparison of papillary and peripapillary VD parameters

	Time	VYZ[a] (*n*=20)	LAT[b] (*n*=14)	P^{ab}
Whole-Disc VD (%)	Baseline[x]	46.7±4	46.9±5.6	0.894
	1st month[y]	49.9±3	51.1±2.4	0.227
	3rd month[z]	48.2±2.1	47.6±6.6	0.698
	6th month[t]	50.4±0.7	50±0.4	0.107
	P^{c}	0.002*	0.112	-
	p^{xy}	0.058	-	-
	P^{yz}	0.037*	-	-
	P^{zt}	0.005*	-	-
	P^{xt}	0.006*	-	-
Disc-inside VD (%)	Baseline[x]	46.5±6.9	47.1±4.8	0.796
	1st month[y]	48.3±7.6	49.3±7.6	0.69
	3rd month[z]	50.3±8.8	45.6±10	0.159
	6th month[t]	50.1±5.4	48.2±2.3	0.231
	P^{c}	0.190	0.470	-
Disc-peripapillary VD (%)	Baseline[x]	51.8±3.2	53.8±4.1	0.123
	1st month[y]	53.3±3.1	54.2±3.6	0.435
	3rd month[z]	50.5±2.4	53.6±2.5	0.001*
	6th month[t]	54.6±1.3	53±1.1	0.001*
	P^{c}	<0.001*	0.560	-
	P^{xy}	0.108	-	-
	P^{yz}	0.025*	-	-
	P^{zt}	<0.001*	-	-
	P^{xt}	0.032*	-	-

LAT: Latafree group; VYZ: Vyzulta group, VD: Vessel density, P^{ab}: Cross sectional *P*-value, P^{c}: Longitidunal *P*-value. *Statistically significant

when comparing the groups, it was lower in the VYZ group at month 3 and lower in the LAT group at month 6 (at 3rd month: p=0.001 and at 6th month: p=0.001).

Regarding IOP, the baseline, 1st, 3rd, 6th months in the VYZ group were 23.15±2.7 mmHg, 16.25±2.6 mmHg, 16.95±2.1 mmHg, and 15.95±0.3 mmHg (respectively), while in the LAT group were 23.14±2.3 mmHg, 17.35±2.7 mmHg, 16.78±1.9 mmHg, and 14.14±1.0 mmHg (respectively). IOP in the VYZ group was significantly decreased between baseline and 1st month (p<0.001) as well as between baseline and

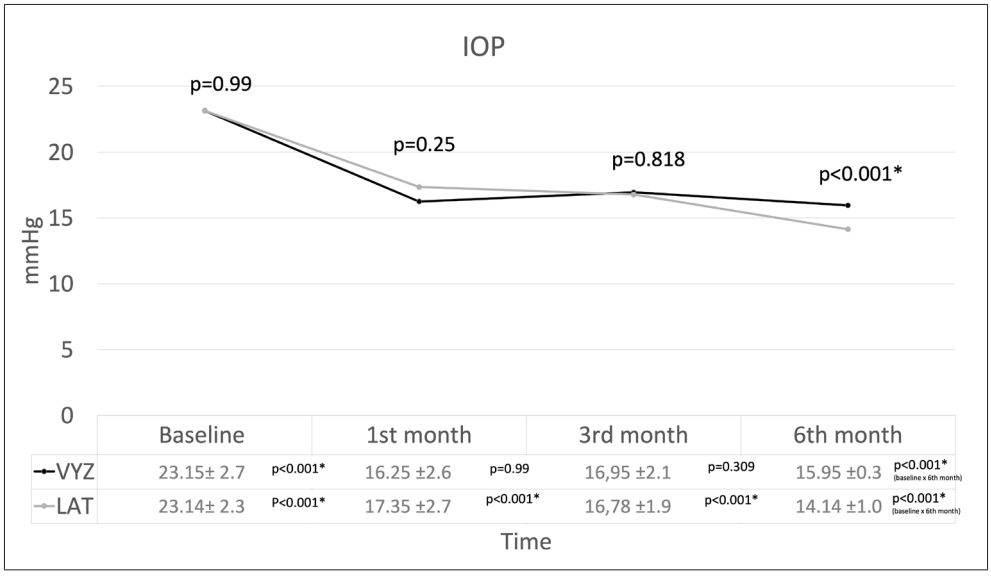

Fig. 2. Changes in intraocular pressure over time in each group and comparison at all time points.

6th month (p<0.001), while it was similar between 1st and 3rd month (p=0.99) as well as 3rd and 6th month (p=0.309). IOP in the LAT group was significantly reduced between baseline and 1st month (p<0.001) as well as between baseline and 6th month (p<0.001). This reduction was also observed between 3rd and 6th months (p<0.001). However, there were comparable IOP values between the 1st and 3rd months in the LAT group. (p=0.99) (Fig. 2). In addition, IOP was lower in the LAT group compared to the VYZ group at month 6 (p<0.001) (Table 4).

The correlation of parameter changes (from baseline to month 6) in each group is shown in Table 5. In the VYZ group, whole disc VD was positively correlated with TCA, LA, and SA (rho=0.596, p=0.006; rho=0.62, p=0.004; and rho=0.556, p=0.011, respectively), while superficial macular VD was negatively correlated with CVI (rho=−0.541 p=0.014). In the LAT group, there was a negative correlation between deep macular VD and CVI (rho=−0.589, p=0.027), while a positive correlation was found between deep macular VD and SA (rho=0.69, p=0.006).

Table 5. Correlations of parameter changes (from baseline to 6-month) in each group.

Parameters	Groups	IOP (mmHg)	w-Superficial macular VD (%)	w-Deep macular VD (%)	w-Optic disc VD (%)
CVI (%)	VYZ				
	Rho	−0.193	−0.541	−0.271	−0.269
	P	0.416	0.014*	0.249	0.251
	LAT				
	Rho	0.001	0.365	−0.589	−0.69
	P	0.997	0.199	0.027*	0.815
TCA (mm^2)	VYZ				
	Rho	0.151	0.127	0.158	0.596
	P	0.526	0.593	0.506	0.006*
	LAT				
	Rho	−0.289	−0.142	0.516	0.413
	P	0.315	0.629	0.059	0.142
LA (mm^2)	VYZ				
	Rho	0.167	0.08	0.124	0.62
	P	0.482	0.737	0.601	0.004*
	LAT				
	Rho	−0.318	−0.018	0.323	0.405
	P	0.268	0.95	0.26	0.151
SA (mm^2)	VYZ				
	Rho	0.135	0.181	0.195	0.556
	P	0.57	0.445	0.409	0.011*
	LAT				
	Rho	−0.221	−0.275	0.69	0.351
	P	0.449	0.341	0.006*	0.218
IOP (mmHg)	VYZ				
	Rho	-	0.238	0.12	0.382
	P	-	0.313	0.613	0.096
	LAT				
	Rho	-	−0.386	−0.233	−0.10
	P	-	0.173	0.423	0.734

CVI: Choroidal vascular index, LA: Luminal area, SA: Stromal area, w: Whole, TCA: Total choroidal area, IOP: Intraocular pressure, LAT: Latafree group, VYZ: Vyzulta group, VD: Vascular density. *Statistically significant

Discussion

Prostaglandin analogs are frequently the preferred choice for the medical management of glaucoma due to their ability to decrease IOP by increasing uveoscleral outflow, a mechanism that has been demonstrated in numerous studies.[13,14] However, certain side effects, including serous retinal detachment and central serous chorioretinopathy, have prompted a noteworthy inquiry into its impact on the choroid and the posterior segment in recent years.[15] Moreover, a new drug, latanoprostene bunod 0.024%, has been shown to reduce IOP by increasing aqueous outflow through both the uveoscleral and trabecular pathways. [16] The effect of latanoprostene bunod on the posterior segment represents an intriguing and attention-grabbing research topic, particularly given that it is a nitric oxide-donating prostaglandin F2α analog.

The present study examined the impact of both latanoprostene bunod and latanoprost on the optic disc vasculature, choroidal vascular structure, and macular vascular area. The findings of the present study indicated that the majority of choroidal vascular parameters exhibited a notable increase in the LAT group compared to the VYZ group at the 6th month. These results suggest that the choroidal vascular effect may be more pronounced in latanoprost than in latanoprostene bunod. Although latanoprostene bunod contains nitric oxide, which has the potential to induce vasodilation, the observed superiority of latanoprost in LA may indicate that nitric oxide does not exert a significant effect on the choroidal area. Furthermore, the results in the area of submacular TCA or SA may indicate that latanoprost has a greater capacity for uveoscleral outflow. This may prove beneficial in reducing IOP, as evidenced by the findings of the current study, which indicated that the LAT group exhibited superior efficacy in lowering IOP compared to the VYZ group. Nevertheless, both medications demonstrated successful IOP reduction by the conclusion of the 6-month trial period.

A number of studies in the literature have indicated that topical prostaglandin analogs can cause a breakdown of the retinal blood-aqueous barrier, resulting in disruption of the posterior lens capsule and subsequent access for inflammatory mediators to reach the macula.[17,18] This, in turn, leads to macular edema due to the breakdown of the blood-retinal barrier caused by the release of the inflammatory mediators.[19] Moreover, some studies have indicated a potential correlation between increased superficial and deep macular VD and macular edema. [20] After 6 months, the higher results on macular VD and submacular choroidal parameters with latanoprost in the current study may be attributed to its vasodilator effect. However, this effect may be deleterious, as it may be a potential trigger for macular edema, serous retinal detachment, or central serous choroidopathy, which may manifest as a side effect of latanoprost. In consideration of the aforementioned side effects, latanoprostene bunod may be regarded as a safer alternative to latanoprost. Nevertheless, as macular or choroidal thickness was not evaluated in the present study, no definitive conclusions can be drawn on this matter.

It is noteworthy that in the VYZ group, despite the absence of a statistically significant change at the various time points, the vast majority of superficial and deep macular VD parameters exhibited an increase at the 1st month, which then underwent a decrease at the 3rd month. Although the nitric oxide present in latanoprostene bunod has a relatively short half-life and a short-term effect on vasodilation, it may nevertheless exert an influence on this change.[21,22] Nevertheless, this effect seems to be transient or perhaps its vasodilatory effect was suppressed by another factor, such as desensitization or rebound. Somehow, it is also possible that vasoconstriction occurred, which could have resulted in a reduction of macular VD. Further investigation is required to gain a deeper understanding of this issue.

It has been demonstrated that the density of microvasculature in the optic disc can be diminished in patients diagnosed with glaucoma.[23,24] Furthermore, these changes can occur at the early stages or periods of glaucoma, which may indicate an early sign of glaucoma. The present study demonstrated that, at the 6th month, the VYZ group exhibited increased whole optic disc and peripapillary VD, which may indicate that the optic disc damage was prevented due to an improvement in optic disc or peripapillary area perfusion. Moreover, at the conclusion of the 6th month, peripapillary VD was observed to be higher in the VYZ group than in the LAT group, which lends support to the superiority of latanoprostene bunod over latanoprost on the peripapillary vasculature. In a comparative study, Liu *et al*.[25] investigated the efficacy of latanoprostene bunod (0.024%) and timolol (0.5%) in reducing IOP and increasing ocular perfusion pressure. Their findings revealed that latanoprostene bunod demonstrated a more pronounced reduction in IOP and an augmented increase in ocular perfusion pressure in comparison to timolol. The increased perfusion observed in their study was found to be associated with a decrease in IOP. However, our peripapillary VD results suggest that a different mechanism may be involved, as latanoprostene bunod demonstrated superior efficacy in increasing peripapillary VD, whereas

latanoprost showed superiority in reducing IOP at the end of the 6-month study period. It is possible that the nitric oxide contained in the latanoprostene bunod can induce selectively vasodilatation within the peripapillary area, thereby increasing perfusion and protecting the optic nerve head from hypoperfusion-related damage. In addition, our correlation results indicate that in patients treated with latanoprostene bunod, alterations in choroidal parameters correlated with changes in peripapillary VD, whereas in those treated with latanoprost, the changes in choroidal parameters correlated with changes in deep macular VD. These correlations may suggest that the efficacy of these drugs differs in the various anatomical structures, such as the choroid, macula, or papillary/peripapillary area. Furthermore, they underscore the importance of considering the relationships between these structures, despite their distinct vascular supply.

The study conducted by Weinreb *et al*.[26] indicated that latanoprostene bunod (0.024%) demonstrated a more pronounced IOP reduction and comparable adverse effects in comparison to latanoprost 0.005%. In addition, some other studies have demonstrated comparable IOP-lowering effects between these two pharmaceutical agents in both animal and human models.[27,28] However, the duration of these studies was limited by their relatively short follow-up periods. The findings of our study indicated that although both eye drops were effective in reducing IOP, the outcomes may vary over a prolonged follow-up period: although the IOP in the 1st month of the present study exhibited a lower value in the VYZ group (though not to a statistically significant), the IOP at the end of 6 months point demonstrated a lower value in the LAT group (which was statistically significant). In addition, the cumulative corneal toxicity caused by benzalkonium chloride (BAK) on the ocular surface may have contributed to this difference in IOP reduction observed at the 6th month between the BAK-containing and preservative-free formulations, possibly by affecting drug bioavailability. Since this study did not directly assess BAK-induced toxicity, further investigations are warranted to explore this potential mechanism.

The present study was subject to certain limitations. Primarily, the patient cohort was small, and the follow-up period was relatively brief. Second, the peripapillary choroidal vasculature was not assessed, which could have provided additional information about choroidal perfusion of the peripapillary area. A third limitation of the study is that the thickness of the choroid was not measured, which would have affected the macular choroidal parameters. Additionally, the lack of assessment of visual acuity prevented the evaluation of the relationship between visual function and vascular changes. The final limitation is the difference in preservative content BAK between the two compared medications; comparing two formulations with similar BAK content would have provided a more balanced evaluation.

In conclusion, although latanoprost 0.005% demonstrated superiority in reducing IOP compared to latanoprostene bunod 0.024%, both agents exhibited a significant reduction in IOP by the end of the 6th month. Moreover, while latanoprost 0.005% may be more efficacious in increasing the vasculature of the submacular or foveal choroidal area and the superficial or deep macular capillary plexus, latanoprostene bunod 0.024% may be more effective in increasing peripapillary VD.

Ethics Committee Approval: This study was approved by The Erciyes University Local Ethics Committee (No:2024/251; date:06/11/2024).

Informed Consent: Written informed consents were obtained from patient and his family.

Peer-review: Externally peer-reviewed.

Authorship Contributions:

Concept: F.O., D.G.S. ; Design: F.O., D.G.S. ; Supervision: M.U., K.E. ; Resource: O.E. ; Materials: M.U., O.E. ; Data Collection and/or Processing: O.E. ; Analysis and/or Interpretation: F.O. ; Literature Search: O.E. ; Writing: F.O. ; Critical Reviews: D.G.S., M.U.

Conflict of Interest: None declared.

Use of AI for Writing Assistance: Not declared.

Financial Disclosure: The authors declared that this study received no financial support.

References

1. Quigley HA, Broman AT. The number of people with glaucoma worldwide in 2010 and 2020. Br J Ophthalmol 2006;90:262–7. [CrossRef]
2. Alm A. Latanoprost in the treatment of glaucoma. Clin Ophthalmol 2014;8:1967-85. [CrossRef]
3. European Glaucoma Society Terminology and Guidelines for Glaucoma, 5th Edition. Br J Ophthalmol 2021;105:1–169. [CrossRef]
4. Lo TC, Chen YY, Hung MC, Chou P. Latanoprostene Bunod 0.024% in the Treatment of Open-Angle Glaucoma and Ocular Hypertension: A Meta-Analysis. J Clin Med 2022;11(15):4325. [CrossRef]
5. El-Nimri NW, Jiang L, Dahanayake D, Sweidan S, Smith BE, Wildsoet CF. Effect of topical latanoprost on choroidal thickness and vessel area in Guinea pigs. Exp Eye Res 2022;225:109286. [CrossRef]

6. Ozer F, Unlu M, Gulmez Sevim D, Sener H, Evereklioglu C. Evaluation of lamina cribrosa and peripapillary vascular density in thyroid orbitopathy and effect of intravenous methylprednisolone therapy. Can J Ophthalmol 2024;59:e489–95. [CrossRef]
7. Unlu M, Ozer F, Sener H, Gulmez Sevim D. Vascular changes of the peripapillary choroidal area in the thyroid orbitopathy. Int Ophthalmol 2024;44:326. [CrossRef]
8. Gahramanov K, Unlu M, Ozer F, Sener H, Erkilic K. Is there a relationship between the keratoconus and the peripapillary choroidal vasculature? Int Ophthalmol 2024;44:404. [CrossRef]
9. Sener H, Ozer F, Unlu M, Gulmez Sevim D. Automated evaluation of parapapillary choroidal microvasculature in thyroid eye disease. Int Ophthalmol 2023;43:4323–31. [CrossRef]
10. Agrawal R, Gupta P, Tan KA, Cheung CM, Wong TY, Cheng CY. Choroidal vascularity index as a measure of vascular status of the choroid: Measurements in healthy eyes from a population-based study. Sci Rep 2016;6:21090. [CrossRef]
11. Sonoda S, Sakamoto T, Yamashita T, et al. Luminal and stromal areas of choroid determined by binarization method of optical coherence tomographic images. Am J Ophthalmol 2015;159:1123–31.e1. [CrossRef]
12. Sonoda S, Sakamoto T, Yamashita T, et al. Choroidal structure in normal eyes and after photodynamic therapy determined by binarization of optical coherence tomographic images. Investig Ophthalmol Vis Sci 2014;55:3893–8. [CrossRef]
13. Matsou A, Anastasopoulos E. Investigational drugs targeting prostaglandin receptors for the treatment of glaucoma. Expert Opin Investig Drugs 2018;27:777–85. [CrossRef]
14. Li T, Lindsley K, Rouse B, et al. Comparative Effectiveness of First-Line Medications for Primary Open-Angle Glaucoma: A Systematic Review and Network Meta-analysis. Ophthalmology 2016;123:129–40. [CrossRef]
15. Cakir I, Pehlivanoglu S, Yalcinkaya G, Altan C. The Effect of Latanoprost on Choroidal Vascularity Index in Glaucoma and Ocular Hypertension. J Glaucoma 2022;31:972–8. [CrossRef]
16. Mehran NA, Sinha S, Razeghinejad R. New glaucoma medications: latanoprostene bunod, netarsudil, and fixed combination netarsudil-latanoprost. Eye (Lond) 2020;34:72–88. [CrossRef]
17. Alm A, Grierson I, Shields MB. Side effects associated with prostaglandin analog therapy. Surv Ophthalmol 2008;53:S93–105. [CrossRef]
18. Ozdemir H, Karacorlu M, Karacorlu SA. Serous detachment of macula in cystoid macular edema associated with latanoprost. Eur J Ophthalmol 2008;18:1014–6. [CrossRef]
19. Holló G, Aung T, Cantor LB, Aihara M. Cystoid macular edema related to cataract surgery and topical prostaglandin analogs: Mechanism, diagnosis, and management. Surv Ophthalmol 2020;65:496–512. [CrossRef]
20. Xu Y, Zhang M, Wang H, Yu S. Associations between the Vessel Density in Deep Vascular Plexus and Macular Edema Recurrences in Patients with Retinal Vein Occlusion. Ophthalmic Res 2024;67:584–93. [CrossRef]
21. Erdinest N, London N, Ovadia H, Levinger N. Nitric Oxide Interaction with the Eye. Vision (Basel) 2021;5:29. [CrossRef]
22. Hardy P, Dumont I, Bhattacharya M, et al. Oxidants, nitric oxide and prostanoids in the developing ocular vasculature: a basis for ischemic retinopathy. Cardiovasc Res 2000;47:489–509. [CrossRef]
23. Yip VCH, Wong HT, Yong VKY, et al. Optical Coherence Tomography Angiography of Optic Disc and Macula Vessel Density in Glaucoma and Healthy Eyes. J Glaucoma 2019;28:80–7. [CrossRef]
24. Akil H, Huang AS, Francis BA, Sadda SR, Chopra V. Retinal vessel density from optical coherence tomography angiography to differentiate early glaucoma, pre-perimetric glaucoma and normal eyes. PLoS One 2017;12:e0170476. [CrossRef]
25. Liu JHK, Slight JR, Vittitow JL, Scassellati Sforzolini B, Weinreb RN. Efficacy of Latanoprostene Bunod 0.024% Compared With Timolol 0.5% in Lowering Intraocular Pressure Over 24 Hours. Am J Ophthalmol 2016;169:249–57. [CrossRef]
26. Weinreb RN, Ong T, Scassellati Sforzolini B, et al. A randomised, controlled comparison of latanoprostene bunod and latanoprost 0.005% in the treatment of ocular hypertension and open angle glaucoma: the VOYAGER study. Br J Ophthalmol 2015;99:738–45. [CrossRef]
27. Zanutigh V, Galetto L, Valvecchia F, Logioco C. Ocular Surface Evaluation after Switch from Latanoprost 0.005% to Latanoprostene Bunod 0.024. J Curr Glaucoma Pract 2023;17:205–9. [CrossRef]
28. Desai SJ, Pumphrey SA, Koethe B. Comparative effects of latanoprost and latanoprostene bunod on intraocular pressure and pupil size in ophthalmologically normal Beagle dogs. Vet Ophthalmol 2022;25:282–90. [CrossRef]

DOI: 10.14744/eer.2025.40469
Eur Eye Res 2026;6(1):11–20

EUROPEAN EYE RESEARCH

ORIGINAL ARTICLE

Effects of energy drink consumption on retinal and choroidal structures and pupil dynamics: A multimodal ocular imaging study

Mustafa Duran,[1] Caner Ozturk,[2] Sabriye Bolat[2]

[1]Department of Ophtalmology, Hitit University Erol Olçok Education and Research Hospital, Corum, Turkiye
[2]Department of Ophtalmology, Hitit University Erol Olçok Education and Research Hospital, Corum, Turkiye

Abstract

Purpose: To evaluate the effects of energy drink (ED) consumption on choroidal thickness (CT), central macular thickness (CMT), choroidal vascularity index (CVI), retinal microvasculature, pupil diameter (PD), intraocular pressure (IOP), central corneal thickness (CCT), and anterior chamber depth (ACD).

Methods: Twenty-seven volunteers with no systemic or ocular diseases were enrolled in this prospective study. CT and CVI by optical coherence tomography (OCT), retinal vessel density (VD) by OCT-angiography, and PD by corneal topography were measured before the ED ingestion. Measurements were performed 1 h and 2 h after ED ingestion again. One week later, the measurements were repeated after the participants consumed 250 mL of water.

Results: There was a significant decrease in temporal CT at 1 h after ED intake compared to baseline (p=0.005). Temporal CT was not significantly different from baseline 2 h after ED intake (p=0.763). There was a significant increase in temporal CT at both 1 and 2 h after water intake (0.039 and 0.022, respectively). Subfoveal CT was significantly lower at 1 h after ED intake compared to baseline (p=0.009), whereas no significant difference in subfoveal CT was found at the end of the 2nd h (p=0.076). Water consumption did not affect subfoveal CT (p=0.473). There was no statistically significant difference in IOP, CCT, ACD, PD, CMT, nasal CT, CVI, and retinal VD measured at 1 and 2 h after both ED and water consumption compared to baseline (p>0.05).

Conclusion: ED consumption resulted in a transient decrease in CT but did not cause significant alterations in other anterior or posterior ocular parameters, including IOP, PD, or retinal microvasculature. These findings suggest that moderate ED intake may induce short-term vascular changes in the choroid without affecting overall retinal or anterior segment structure in healthy individuals.

Keywords: Choroidal thickness; Choroidal vascularity index; Energy drink; Retinal vessel density.

Energy drinks (EDs), widely consumed, especially by students and athletes, are promoted for their effects, such as reducing fatigue, enhancing alertness, and improving performance.[1,2] These beverages typically contain caffeine, taurine, sugars, and various vitamins.[3] Caffeine, a central nervous system stimulant, exerts its effects by antagonising adenosine receptors, while taurine, an amino acid naturally found in the retina, may have vasodilatory properties.[4,5]

Caffeine intake has been associated with systemic effects, such as increased heart rate and blood pressure, as well as

Cite this article as: Duran M, Ozturk C, Bolat S. Effects of energy drink consumption on retinal and choroidal structures and pupil dynamics: A multimodal ocular imaging study. Eur Eye Res 2026;6(1):11–20.

Correspondence: Caner Öztürk, M.D. Department of Ophtalmology, Hitit University Erol Olçok Education and Research Hospital, Corum, Turkiye
E-mail: canerx6@hotmail.com

Submitted Date: 05.05.2025 **Revised Date:** 11.08.2025 **Accepted Date:** 19.08.2025 **Available Online Date:** 29.04.2026

ocular changes, including elevated intraocular pressure (IOP) and reduced macular blood flow.[6] As caffeine and taurine have opposing effects on blood vessels, the combined influence of these two substances on ocular tissues may be complex. The iris, which receives both sympathetic and parasympathetic innervation, may also be affected by ED consumption.[7]

The development of non-invasive, high-resolution imaging modalities, such as optical coherence tomography (OCT) and OCT-angiography (OCT-A) enables detailed evaluation of retinal and choroidal structures. Enhanced depth imaging (EDI) OCT allows for measurement of choroidal thickness (CT) and calculation of the choroidal vascularity index (CVI), while OCT-A provides insights into microvascular changes in the retina.[8,9]

This study aimed to investigate the effects of ED consumption on CT, CVI, retinal microvasculature, and pupil diameter (PD) in healthy individuals using multimodal ocular imaging techniques.

Materials and Methods

This prospective study was approved by the institutional ethics committee and conducted in accordance with the Declaration of Helsinki (approval number: 2024-66). Written informed consent was obtained from all participants. The right eyes of 27 healthy subjects were included.

Participants with ocular pathologies (glaucoma, cataract, uveitis, history of intraocular surgery, retinal and corneal abnormalities, >3D myopia or hyperopia), smoking history, pregnancy, metabolic or systemic disease (including hypertension, diabetes mellitus), present drug or alcohol use were excluded. Participants who had consumed caffeinated beverages or chocolate in the previous 12 h were also excluded, as caffeine is known to remain active in the body for up to 3–6 h.[10]

All participants underwent slit-lamp biomicroscopy, best-corrected visual acuity assessment, and fundus examination. Spherical equivalent (SE) and IOP of the participants were measured with an autorefractometer (Topcon KR-8900; Topcon Corporation, Japan). PD under photopic, mesopic, and scotopic (40 lx illuminance, 4 lx illuminance, 0.4 lx illuminance, respectively) conditions, central corneal thickness (CCT) and anterior chamber depth (ACD) were measured with Sirius topographer (Sirius, Costruzione Strumenti Oftalmici, Italy). Axial length (AL) was obtained with Nidek AL-Scan optic biometry (Nidek Co. Ltd, Japan).

Central macular thickness (CMT), subfoveal CT, and CT at 1000 µm nasal and temporal to the fovea were measured by Heidelberg Spectralis OCT (Heidelberg Engineering GmbH; Germany). An experienced examiner measured CT manually from the retinal pigment epithelium to the sclera using the callipers of the OCT device.

The choroidal structures, including the luminal area (LA) and the total choroidal area (TCA), were calculated using the binarization of EDI-OCT images with the ImageJ software program (version 1.50 a; National Institutes of Health, Bethesda, MD, USA). Stromal area was found from the difference of TCA and LA. The CVI values were calculated using the LA/TCA ratio (Fig. 1).

Retinal vessel density (VD) at the superficial and deep capillary plexuses (SCP, DCP) and choriocapillaris (CC) was assessed using 3 × 3 mm OCT-A scans (Triton OCT, Topcon, Tokyo, Japan) with an early treatment diabetic retinopathy study grid. The central (inner 1 mm) VD and the nasal, inferior, superior, and temporal parafoveal VDs (located between the inner 1 mm and outer 3 mm borders) at the SCP, DCP, and CC levels were evaluated (Fig.2).

Measurements were obtained at baseline, and at 1 and 2 h after ingestion of 250 mL ED (Red Bull®, containing 150 mg/L caffeine, 800 mg/L taurine, small amounts of sugar, and vitamins). One week later, the same protocol was repeated with 250 mL of water. All measurements were performed between 13:30 and 15:30 to minimize diurnal variation.

Statistical Analysis

The Statistical Package for the Social Sciences programme V22 (IBM Corp., Armonk, NY, USA) was used for statistical analysis. Shapiro–Wilk test was used to evaluate the normality of the data. Repeated-measures analysis of variance with Greenhouse-Geisser correction was used for normally distributed variables; the Friedman test was applied for non-normally distributed variables. *Post hoc* Bonferroni correction was applied for multiple comparisons. Paired *t*-tests or Wilcoxon signed-rank tests were used for pairwise analyses. Data are presented as mean±standard deviation. A $p<0.05$ was considered statistically significant.

Results

A total of 27 healthy participants, 14 males and 13 females, were included. No significant gender difference was observed ($p=0.847$). The mean age of the participants was 30.74±5.68 years. Mean systolic and diastolic blood pressures at baseline were 114.62±7.80 and 80.89±5.04 mmHg, respectively. The mean AL was 24.29±0.95 mm.

Table 1 shows CCT, ACD, PD in scotopic, mesopic, and photopic conditions, CT, and CVI values of the participants

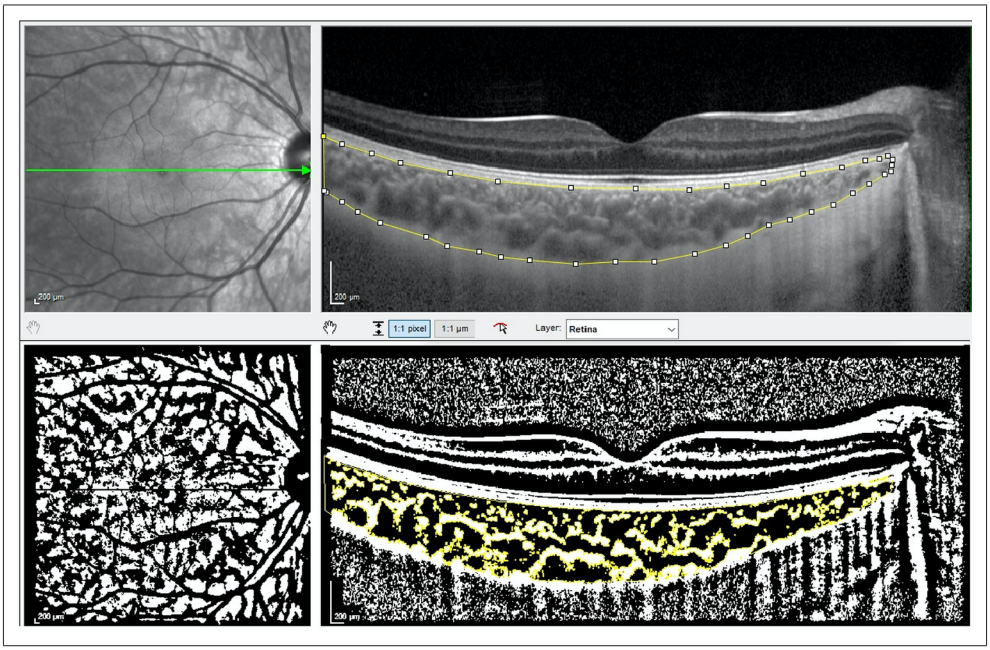

Fig. 1. Marking of the total choroidal area using Image J software. The post-acquisition spectral domain optical coherence tomography image processing demonstrates the binarization of the region of interest utilizing Niblack's auto local threshold technique. Vascular areas appear darker and stromal areas appear lighter.

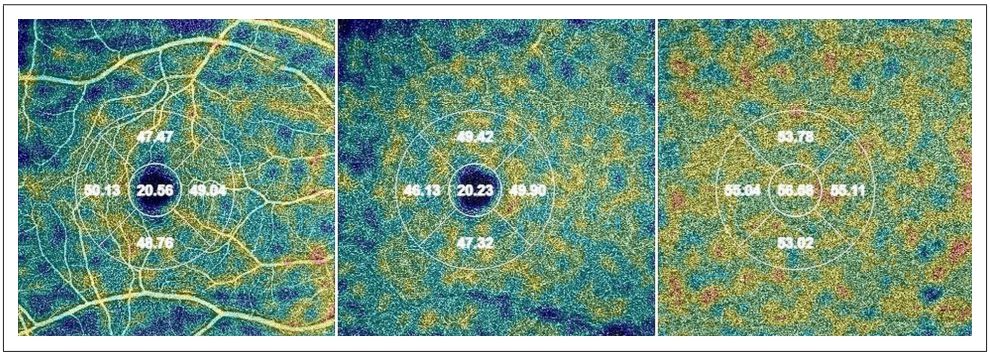

Fig. 2. 1 × 3 mm foveal EDTRS grid showing (a) Superficial vessel density, (b) Deep vessel density, and (c) Coriocapillaris vessel density.

before and after ED and water consumption. Temporal CT decreased significantly 1 h after ED consumption compared to baseline (p=0.005), but returned to baseline levels at 2 h (p=0.763). Temporal CT was significantly increased at both 1 and 2 h after water intake (0.039 and 0.022, respectively). Subfoveal CT was significantly lower at 1 h after ED consumption compared to baseline (p=0.009), whereas no significant difference in subfoveal CT was found at the end of the 2nd h (p=0.076). Water consumption did not significantly change subfoveal CT (p=0.473) (Fig. 3).

No significant difference was found in SE, IOP, CCT, ACD, PD, CMT, nasal CT, and CVI measured at 1 and 2 h after both ED and water consumption compared to baseline (p>0.05).

Table 2 shows the central, superior, inferior, nasal, and temporal parafoveal VDs at the SCP, DCP, and CC levels before and after ED and water consumption. After ED and water consumption, central and parafoveal VD values were not statistically changed (p>0.05).

Direct comparison of ocular parameters between ED and water conditions at baseline, 1 h, and 2 h after intake is shown in Table 3. A significant difference in temporal CT at 1 h was observed between ED and water conditions. ED intake caused a decrease in temporal CT, whereas water intake caused an increase. No other parameters, including subfoveal CT, nasal CT, CVI, PD under various lighting conditions, CMT, or VD at the SCP, DCP, and CC levels, showed significant differences between ED and water conditions at any time point (all p>0.05).

Table 1. Comparison of SE, IOP, CCT, ACD, PD, CMT, CT, and CVI before and after consumption of energy drink and water

Parameter	Baseline (Mean±SD)	After 1 h (Mean±SD)	After 2 h (Mean±SD)	*p*	*p*
SE (Diopters)					
ED	−0.90±0.86	−0.92±0.88	−0.90±0.91	0.952[f]	
Water	−0.90±0.92	−0.92±0.89	−0.93±0.94	0.620[f]	
IOP (mmHg)					
ED	16.70±3.22	16.67±2.80	16.67±2.86	0.994[r]	
Water	17.11±2.33	16.56±2.68	16.70±2.99	0.250[f]	
CCT (µm)					
ED	540.78±41.40	539.44±41.40	539.26±41.86	0.132[r]	
Water	540.93±41.93	540.59±42.01	540.44±41.77	0.104[r]	
ACD (mm)					
ED	3.27±0.22	3.27±0.22	3.27±0.23	0.932[f]	
Water	3.28±0.22	3.28±0.22	3.26±0.22	0.305[r]	
Scotopic PD (mm)					
ED	5.68±0.70	5.80±0.76	5.74±0.70	0.583[r]	
Water	5.78±0.55	5.74±0.69	5.79±0.67	0.890[r]	
Mesopic PD (mm)					
ED	5.43±0.62	5.51±0.82	5.41±0.75	0.570[r]	
Water	5.34±0.67	5.32±0.72	5.37±0.75	0.856[r]	
Photopic PD (mm)					
ED	4.37±0.83	4.26±0.88	4.33±0.89	0.653[r]	
Water	4.11±0.74	4.08±0.85	4.23±0.71	0.474[r]	
CMT (µm)					
ED	261.93±14.40	263.37±15.38	262.48±14.71	0.171[f]	
Water	262.85±14.11	262.70±13.82	261.82±14.95	0.405[f]	
Temporal CT (µm)					
ED	357.85±76.50	347.93±73.73	358.96±80.73	0.003[r]	0–1 0.005[b] 1–2 0.015[b] 0–2 0.763[b]
Water	351.41±82.06	363.48±79.74	364.33±91.24	0.010[r]	0–1 0.039[b] 1–2 0.843[b] 0–2 0.022[b]
Subfoveal CT (µm)					
ED	366.67±85.85	354.56±79.50	361.59±76.95	0.045[r]	0–1 0.009[b] 1–2 0.036[b] 0–2 0.076[b]
Water	363.63±74.13	363.48±90.33	368.96±90.54	0.473[r]	
Nasal CT (µm)					
ED	326.52±81.06	322.44±76.43	327.22±74.67	0.495[r]	
Water	325.41±76.20	330.19±84.54	326.48±81.16	0.648[r]	
CVI (%)					
ED	0.64±0.02	0.65±0.03	0.64±0.02	0.683[r]	
Water	0.65±0.02	0.65±0.02	0.65±0.02	0.736[f]	

[b]: Bonferroni correction. [r]: Repeated measures anova. [f]: Friedman test. SE: Spherical equivalent, IOP: Intraocular pressure, CCT: Central corneal thickness, ACD: Anterior chamber depth, PD: Pupil diameter, CMT: Central macular thickness, CT: Choroidal thickness, CVI: Choroidal vascularity ındex, ED: Energy drink, SD: Standard deviation

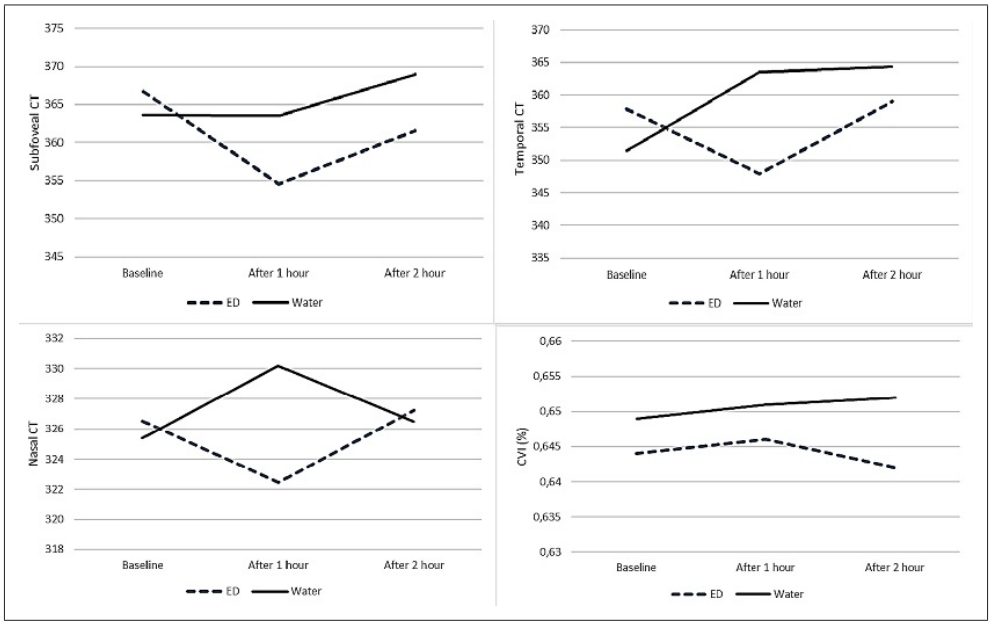

Fig. 3. Time-course changes in choroidal thickness (subfoveal, temporal, nasal) and choroidal vascularity index after energy drink and water intake.

Discussion

EDs have gained popularity across all age groups, particularly among young adults, due to their stimulating effects on the central nervous system. Given the increasing concerns about their cardiovascular and neurological impacts, recent studies have also begun to investigate their potential ocular effects. In this context, our study aimed to assess both anterior and posterior segment responses to ED consumption in healthy individuals using multimodal imaging techniques.

Our findings demonstrated that ED consumption did not significantly affect SE, IOP, CCT, ACD, PD, CMT, nasal CT, CVI, or central and parafoveal VD. However, a transient decrease in temporal and subfoveal CT was observed at 1 h following ED intake, which resolved by the 2nd h.

The effect of caffeinated drinks on PD is currently unclear. Redondo *et al*.[11] found a significant increase in PD 30 min after caffeine intake (4 mg/kg) compared to the placebo drug. A significant increase in PD was also observed by Abokyi *et al*.[12] in those who consumed 250 mg of caffeine-containing beverages. In contrast, the study by Bardak *et al*.[13] showed that there was no change in PD after consumption of coffee containing 57 mg of caffeine. The complex effects of caffeine on both the sympathetic and parasympathetic systems may have resulted in contradictory results.[7] After ED consumption, we found no change in PD under photopic, mesopic, and scotopic light conditions.

The literature on the effect of caffeine on IOP is inconclusive. Jo and Lee[14] reported that IOP increased significantly after drinking caffeinated EDs in healthy participants, whereas there was no significant change in IOP after drinking caffeine-free beverages. In other studies conducted with healthy participants, it was demonstrated that caffeine did not affect IOP.[15,16] In a meta-analysis, Li *et al*.[17] reported that caffeine had no effect on IOP in healthy subjects. However, it increased IOP in patients with open-angle glaucoma and ocular hypertension. In our study, we found no change in IOP after caffeine-containing ED consumption.

It has been shown by color Doppler ultrasound that consumption of caffeine-containing beverages causes narrowing of the arteries supplying the eye, including the ophthalmic artery, central retinal artery, and short posterior nasal ciliary artery.[18] Terai *et al*.[19] showed that retinal vessels narrowed 1 h after consuming 200 mg of caffeine. The choroid, a layer rich in vascular structures, can be strongly affected by this vasoconstrictive effect of caffeine. In our study, we found a significant decrease in subfoveal and temporal CT after ED consumption. In a study comprising 30 healthy male subjects, Toprak *et al*.[20] observed a statistically significant reduction in CT at both 30 min and 1 h following the consumption of caffeine-containing EDs. In contrast, some studies have indicated that ED does not have an impact on CT.[21,22] The discrepancy in results may be attributed to the varying quantities of caffeine present in the EDs utilized in the

Table 2. Comparison of central and parafoveal vessel densities at the superficial capillary plexus, deep capillary plexus, and choriocapillaris before and after consumption of energy drink and water

Parameters	Baseline (Mean±SD)	After 1 h (Mean±SD)	After 2 h (Mean±SD)	*P*-value
SCP (%)				
ED				
Central	20.06±4.50	19.87±3.67	19.79±3.92	0.855[r]
Superior	45.20±3.47	44.89±2.75	45.32±2.91	0.837[f]
Nasal	46.00±2.44	45.41±2.37	45.64±2.15	0.485[r]
Inferior	46.11±2.88	45.42±2.42	46.10±2.87	0.253[f]
Temporal	47.06±2.37	46.14±2.36	46.56±2.57	0.173[r]
Water				
Central	19.82±4.12	19.63±4.27	20.31±4.56	0.204[r]
Superior	45.03±3.14	44.74±2.38	45.07±2.32	0.837[f]
Nasal	44.97±3.10	45.23±2.16	45.91±2.15	0.837[f]
Inferior	44.66±3.36	45.06±2.80	45.59±2.85	0.195[r]
Temporal	45.80±3.22	45.90±2.28	46.45±1.76	0.289[f]
DCP (%)				
ED				
Central	15.95±4.53	15.38±3.87	15.58±4.19	0.638[r]
Superior	46.65±3.45	47.52±2.12	46.82±2.57	0.335[f]
Nasal	47.81±2.40	48.01±2.29	47.82±3.75	0.886[r]
Inferior	47.22±2.61	47.10±1.98	46.77±2.34	0.156[f]
Temporal	44.92±2.23	44.48±2.40	44.75±2.41	0.740[r]
Water				
Central	15.53±4.34	15.17±4.15	16.09±4.32	0.108[r]
Superior	46.39±3.72	46.48±2.31	46.73±2.52	0.335[f]
Nasal	47.42±2.40	47.51±2.40	47.95±1.93	0.484[r]
Inferior	45.87±2.78	46.65±2.25	47.33±2.46	0.972[f]
Temporal	43.91±5.13	43.75±2.74	44.77±2.62	0.071[f]
CC (%)				
ED				
Central	55.19±3.11	54.87±2.43	55.14±2.84	0.818[r]
Superior	52.68±2.31	53.13±1.71	52.78±1.89	0.567[r]
Nasal	52.25±2.29	51.99±2.02	52.70±2.40	0.323[r]
Inferior	52.90±1.69	53.47±1.96	53.65±1.65	0.254[r]
Temporal	53.48±1.78	53.42±1.81	52.96±2.42	0.431[r]
Water				
Central	54.72±2.62	55.14±2.41	55.23±2.72	0.610[r]
Superior	52.30±1.76	52.01±2.13	52.61±2.14	0.748[f]
Nasal	52.30±2.14	52.88±2.11	52.71±2.00	0.437[r]
Inferior	52.97±2.55	53.47±2.03	52.80±2.66	0.964[f]
Temporal	53.39±1.18	53.34±2.09	53.39±1.94	0.772[f]

[r]: Repeated measures anova, [f]: Friedman test. SCP: Superficial capillary plexus, DCP: Deep capillary plexus, CC: Choriocapillaris, ED: Energy drink, SD: Standart deviation

Table 3. Direct comparison of ocular parameters between energy drink and water conditions at baseline, 1 h, and 2 h after intake

Parameter	ED (mean±SD)	Water (mean±SD)	*p*
Scotopic PD (mm)			
Baseline	5.68±0.70	5.78±0.55	0.370[P]
After 1 h	5.80±0.76	5.74±0.69	0.649[P]
After 2 h	5.74±0.70	5.79±0.67	0.499[P]
Mesopic PD (mm)			
Baseline	5.43±0.62	5.34±0.67	0.351[P]
After 1 h	5.51±0.82	5.32±0.72	0.107[P]
After 2 h	5.41±0.75	5.37±0.75	0.685[P]
Photopic PD (mm)			
Baseline	4.37±0.83	4.11±0.74	0.107[P]
After 1 h	4.26±0.88	4.08±0.85	0.188[P]
After 2 h	4.33±0.89	4.23±0.71	0.330[P]
CMT (µm)			
Baseline	261.93±14.40	262.85±14.11	0.056[W]
After 1 h	263.37±15.38	262.70±13.82	0.126[W]
After 2 h	262.48±14.71	261.82±14.95	0.240[W]
Temporal CT (µm)			
Baseline	357.85±76.50	351.41±82.06	0.206[P]
After 1 h	347.93±73.73	363.48±79.74	0.003[P]
After 2 h	358.96±80.73	364.33±91.24	0.267[P]
Subfoveal CT (µm)			
Baseline	366.67±85.85	363.63±74.13	0.086[P]
After 1 h	354.56±79.50	363.48±90.33	0.104[P]
After 2 h	361.59±76.95	368.96±90.54	0.089[P]
Nasal CT (µm)			
Baseline	326.52±81.06	325.41±76.20	0.890[P]
After 1 h	322.44±76.43	330.19±84.54	0.091[P]
After 2 h	327.22±74.67	326.48±81.16	0.887[P]
CVI (%)			
Baseline	0.64±0.02	0.65±0.02	0.294[P]
After 1 h	0.65±0.03	0.65±0.02	0.370[P]
After 2 h	0.64±0.02	0.65±0.02	0.080[P]
SCP central (%)			
Baseline	20.06±4.50	19.82±4.12	0.861[W]
After 1 h	19.87±3.67	19.63±4.27	0.537[P]
After 2 h	19.79±3.92	20.31±4.56	0.247[P]
DCP central (%)			
Baseline	15.95±4.53	15.53±4.34	0.426[P]
After 1 h	15.38±3.87	15.17±4.15	0.630[P]
After 2 h	15.58±4.19	16.09±4.32	0.320[P]
CC central (%)			
Baseline	55.19±3.11	54.72±2.62	0.368[W]
After 1 h	54.87±2.43	55.14±2.41	0.594[P]
After 2 h	55.14±2.84	55.23±2.72	0.891[P]

[P]: Paired *t*-test, [W]: Wilcoxon signed-rank test. PD: Pupil diameter, CMT: Central macular thickness, CT: Choroidal thickness, CVI: Choroidal vascularity ındex, SCP: Superficial capillary plexus, DCP: Deep capillary plexus, CC: Choriocapillaris, ED: Energy drink, SD: Standart deviation

investigation. Another reason why results may vary is that CT can be affected by factors, such as refraction, gender, and age. Our findings are consistent with those reported by Arej *et al*.,[23] who demonstrated a significant decrease in subfoveal CT 1 h after the ingestion of an ED containing caffeine and taurine. At 4 h post-consumption, subfoveal CT returned to baseline. This transient thinning suggests a transient vasoconstrictive effect, likely due to the caffeine content, which may be counteracted by the vasodilatory influence of taurine over time.

Temporal CT showed a modest but statistically significant increase at both 1 and 2 h after water intake. This finding is consistent with previous reports indicating that systemic hydration can temporarily increase CT by improving ocular perfusion and enlarging the vascular compartment.[24,25] This effect is probably caused by an increase in blood volume and reduced blood viscosity, which facilitates choroidal filling. In contrast, ED consumption caused a transient CT reduction, presumably due to caffeine-induced vasoconstriction, which was partially offset by the vasodilatory effect of taurine.

CVI allows assessment of choroidal vascularization with higher reliability and lower variability than CT.[8] Koçak *et al*.[26] showed that subfoveal CVI was significantly decreased in healthy subjects who consumed coffee containing 75 mg caffeine. To our knowledge, this is the first study to evaluate the effect of ED consumption on CVI. Our results demonstrated that there was no statistically significant change in CVI following ED consumption.

There are only a few studies that show the effect of ED on the retinal microvascular blood flow in using OCT-A. Doğan *et al*.[21] reported that VD measurements of the parafoveal and perifoveal deep capillary plexus were significantly higher after ED consumption. Karti *et al*.[27] demonstrated that oral caffeine (200 mg) resulted in a statistically significant decrease in macular flow area (superficial, deep, and CC) and VD. Yilmaz Tugan *et al*.[28] reported a statistically

significant decrease in VD parameters in all segments of the superficial, deep, and peripapillary macular regions after 200 mg orally caffeine intake. In our study, there was no significant change in superficial, deep, and CC VD values. The reason why the VD values were not affected by the consumption of ED can be attributed to the vasodilatory effect of taurine, in contrast to the vasoconstrictive effect of caffeine. The fact that caffeine and taurine may limit each other's effects in ED may explain the conflicting results in the literature. The absence of significant changes in retinal VD following ED intake may be explained by this opposing pharmacological interplay, as well as the relatively low caffeine dose employed in our study. Together, these observations highlight that the ocular response to ED is both component- and dose-dependent and that certain vascular beds, such as the choroid, may be more sensitive to these acute hemodynamic shifts than others. Although most studies, including ours, suggest that moderate ED consumption does not result in major retinal vascular changes, isolated case reports have described severe ocular events following excessive intake. Gupta *et al*.[29] reported a case of acute macular neuroretinopathy in a healthy adult shortly after consuming multiple EDs. Similarly, Pagano *et al*.[30] documented intraretinal hemorrhages and sudden visual loss attributed to high-volume ED ingestion. These cases highlight the need for further investigation into possible individual susceptibility and dose-dependent effects. Importantly, when ED and water conditions were compared directly, only the temporal CT at 1 h differed significantly between the two conditions (p=0.003), confirming that this transient thinning was specific to ED consumption rather than a non-specific, time-dependent change. The absence of significant differences between conditions for other ocular parameters, including subfoveal CT, suggests that the vascular response to ED intake may be more localized to certain choroidal regions. This finding supports the idea that caffeine-induced vasoconstriction, potentially moderated by taurine's vasodilatory properties, has a measurable, yet region-specific, impact on choroidal perfusion.

Our study is valuable because it evaluates how ED consumption affects both anterior segment and posterior segment structures of the eye. In addition, it is the first study to evaluate the effect of ED consumption on CVI. Considering the widespread and increasing use of EDs among young adults, understanding their comprehensive ocular effects is clinically important. Our findings contribute to a growing but still limited body of literature examining the specific impact of EDs on ocular parameters.

Study Limitations

Our study also has some limitations. All participants consumed the same amount of ED, regardless of their body weight. Therefore, the amount of caffeine and taurine per kilogram is different for each participant. The ED consumed by the participants in the study contained 37.5 mg/250 mL of caffeine, which is a relatively low amount when compared to other studies that have examined the effects of ED and caffeine on ocular parameters. The low amount of caffeine may have affected the results. Another limitation of our study is the lack of randomization and masking. While the objective nature of OCT and OCT-A measurements reduces the likelihood of measurement bias, the absence of participant masking could theoretically introduce placebo or expectation effects, particularly with regard to subjective parameters. In addition, the relatively small size of our sample and the inclusion of only young, healthy subjects limit the generalizability of the findings to broader populations, including older individuals or those with ocular or systemic diseases. Studies with larger, more diverse populations and varying caffeine doses may reveal additional effects that were not observed in our cohort.

Conclusion

In this study, we investigated the short-term effects of ED consumption on the anterior and posterior structures of the eye using multimodal imaging techniques. While ED intake did not significantly alter in IOP, CCT, ACD, CVI, foveal, and parafoveal VD, our findings revealed that it induced a transient decrease in temporal and subfoveal CT 1 h after consumption. These results suggest that the components of EDs, particularly caffeine, may cause short-term vascular responses in the choroid through sympathetic stimulation and vasoconstriction, while other ocular structures remain unaffected. The resolution of this effect by the 2nd h may reflect compensatory mechanisms or the opposing action of taurine, a vasodilatory component also present in EDs. This study supports the hypothesis that EDs can temporarily influence ocular perfusion, specifically within the choroid, without causing sustained structural changes in healthy individuals. Further studies with longer follow-up periods and varied caffeine doses are needed to better understand the long-term effects of ED consumption on the eyes.

Ethics Committee Approval: This study was approved by The Ethics committee of Hitit University (2044-66 11/09/2024)

Informed Consent: Written informed consent was obtained from the patient for the preparation of this work.

Peer-review: Externally peer-reviewed.

Authorship Contributions: Concept: M.D., C.O., S.B.; Design: M.D., C.O., S.B.; Supervision: M.D., C.O., S.B.; Resource: M.D., C.O., S.B.; Materials: S.B.; Data Collection and/or Processing: M.D., S.B.; Analysis and/or Interpretation: M.D.; Literature Search: C.O.; Writing: C.O.; Critical Reviews: M.D., C.O.

Conflict of Interest: None declared.

Use of AI for Writing Assistance: Not declared.

Financial Disclosure: The authors declared that this study received no financial support.

References

1. Ulbrich A, Hemberger SH, Loidl A, et al. Effects of alcohol mixed with energy drink and alcohol alone on subjective intoxication. Amino Acids 2013;45:1385–93. [CrossRef]
2. Ishak WW, Ugochukwu C, Bagot K, Khalili D, Zaky C. Energy drinks: psychological effects and impact on well-being and quality of life-a literature review. Innov Clin Neurosci 2012;9:25–34.
3. Bunker ML, McWilliams M. Caffeine content of common beverages. J Am Diet Assoc 1979;74:28–32. [CrossRef]
4. Giles GE, Mahoney CR, Brunyé TT, Gardony AL, Taylor HA, Kanarek RB. Differential cognitive effects of energy drink ingredients: caffeine, taurine, and glucose. Pharmacol Biochem Behav 2012;102:569–77. [CrossRef]
5. Froger N, Moutsimilli L, Cadetti L, et al. Taurine: the comeback of a neutraceutical in the prevention of retinal degenerations. Prog Retin Eye Res 2014;41:44–63. [CrossRef]
6. Yan A, La Rosa A, Chhablani PP, Chhablani J. Caffeine and Vision: Effects on the Eye. Turk J Ophthalmol 2024;54:291–300. [CrossRef]
7. Yoon JJ, Danesh-Meyer HV. Caffeine and the eye. Surv Ophthalmol 2019;64:334–44. [CrossRef]
8. Agrawal R, Gupta P, Tan KA, Cheung CM, Wong TY, Cheng CY. Choroidal vascularity index as a measure of vascular status of the choroid: Measurements in healthy eyes from a population-based study. Sci Rep 2016;6:21090. [CrossRef]
9. WuDunn D, Takusagawa HL, Sit AJ, et al. OCT Angiography for the diagnosis of glaucoma: a report by the American Academy of Ophthalmology. Ophthalmology 2021;128:1222–35. [CrossRef]
10. Nawrot P, Jordan S, Eastwood J, Rotstein J, Hugenholtz A, Feeley M. Effects of caffeine on human health. Food Addit Contam 2003;20:1–30. [CrossRef]
11. Redondo B, Vera J, Carreño-Rodríguez C, Molina-Romero R, Jiménez R. Acute effects of caffeine on dynamic accommodative response and pupil size: a placebo-controlled, double-blind, balanced crossover study. Curr Eye Res. 2020;45:1074–81. [CrossRef]
12. Abokyi S, Owusu-Mensah J, Osei KA. Caffeine intake is associated with pupil dilation and enhanced accommodation. Eye (Lond) 2017;31:615–9. [CrossRef]
13. Bardak H, Gunay M, Mumcu U, Bardak Y. Effect of Single Administration of Coffee on Pupil Size and Ocular Wavefront Aberration Measurements in Healthy Subjects. Biomed Res Int 2016;2016:9578308. [CrossRef]
14. Jo SH, Lee CK. The effect of caffeinated energy drink consumption on intraocular pressure in young adults. Journal of the Korean Ophthalmological Society 2015;56:1096–103. [CrossRef]
15. Adams BA, Brubaker RF. Caffeine has no clinically significant effect on aqueous humor flow in the normal healthy eye. Ophthalmology 1990;97:1030–1. [CrossRef]
16. Kim J, Aschard H, Kang JH, et al. Intraocular pressure, glaucoma, and dietary caffeine consumption: a gene-diet interaction study from the UK Biobank. Ophthalmology 2021;128:866–76. [CrossRef]
17. Li M, Wang M, Guo W, Wang J, Sun X. The effect of caffeine on intraocular pressure: a systematic review and meta-analysis. Graefes Arch Clin Exp Ophthalmol 2011;249:435–42. [CrossRef]
18. Ozkan B, Yüksel N, Anik Y, Altintas O, Demirci A, Çağlar Y. The effect of caffeine on retrobulbar hemodynamics. Curr Eye Res 2008;33:804–9. [CrossRef]
19. Terai N, Spoerl E, Pillunat LE, Stodtmeister R. The effect of caffeine on retinal vessel diameter in young healthy subjects. Acta Ophthalmol 2012;90:e524–8. [CrossRef]
20. Toprak G Sr, Alkan Y. Comparison of the Short-Term Effect of Coffee, Energy Drink, and Water on the Eyes in Young Healthy Subjects. Cureus 2023;15:e48335. [CrossRef]
21. Doğan M, Sabaner MC, Akar AT, et al. Evaluation of the effect of energy drink consumption on retina and choroid: an optical coherence tomography and optical coherence tomography angiography study. Cutan Ocul Toxicol 2020;39:295–7. [CrossRef]
22. Mete A, Kimyon S, Yılmaz A, Er KE, Yılmaz İE, Temizer M. Changes in choroidal thickness following energy drink consumption in healthy subjects. European Journal of Therapeutics 2018;24:210–3. [CrossRef]
23. Arej N, Azar G, Salviat F, et al. Study of choroidal thickness variations after ingestion of a taurine and caffeine-containing energy drink. Clin Nutr ESPEN 2021;43:245–9. [CrossRef]
24. Mansouri K, Medeiros FA, Marchase N, Tatham AJ, Auerbach D, Weinreb RN. Assessment of choroidal thickness and volume during the water drinking test by swept-source optical coherence tomography. Ophthalmology 2013;120:2508–16. [CrossRef]
25. Nagasato D, Mitamura Y, Egawa M, et al. Changes of choroidal structure and circulation after water drinking test in normal eyes. Graefes Arch Clin Exp Ophthalmol 2019;257:2391–9. [CrossRef]
26. Koçak N, Beldağlı C, Yeter V. Acute Effects of Coffee on Peripapillary and Subfoveal Choroidal Parameters in Young Healthy Subjects. Eur J Ophthalmol 2022;32:3584–91. [CrossRef]
27. Karti O, Zengin MO, Kerci SG, Ayhan Z, Kusbeci T. Acute

effect of caffeine on macular microcirculation in healthy subjects: An optical coherence tomography angiography study. Retina 2019;39:964–71. [CrossRef]
28. Yilmaz Tugan B, Subasi S, Pirhan D, Karabas L, Yuksel N, Kucuk KD. Evaluation of macular and peripapillary vascular parameter change in healthy subjects after caffeine intake using optical coherence tomography angiography. Indian J Ophthalmol 2022;70:879–89. [CrossRef]
29. Gupta N, Padidam S, Tewari A. Acute macular neuroretinopathy (AMN) related to energy drink consumption. BMJ Case Rep 2019;12:e232144. [CrossRef]
30. Pagano CW, Wu M, Wu L. Acute visual loss and intraretinal hemorrhages associated to energy drink consumption. Int Ophthalmol 2017;37:1349–51. [CrossRef]

DOI: 10.14744/eer.2025.81904
Eur Eye Res 2026;6(1):21–28

EUROPEAN EYE RESEARCH

ORIGINAL ARTICLE

Trends in forensic ophthalmology consultations

Kader Kasar,[1] Halit Canberk Aydogan,[2] Asena Keles Sahin,[1] Aslıhan Uzun[1]

[1]Department of Ophthalmology, Ordu University, Faculty of Medicine, Ordu, Turkiye
[2]Department of Forensic Medicine, Ordu University Training and Research Hospital, Ordu, Turkiye

Abstract

Purpose: Ocular trauma is a leading cause of monocular blindness worldwide, requiring forensic and medical evaluation. This study retrospectively examines forensic ophthalmology consultations, trauma types, and medicolegal implications.

Methods: A retrospective analysis was conducted on ophthalmology consultation reports from the Forensic Medicine Clinic at Ordu University Training and Research Hospital (2017–2024). All statistical analyses were performed using IBM Statistical Package for the Social Sciences Statistics for Windows, Version 22.0 (IBM Corp., Armonk, NY, USA). The normality of the data was tested using the Shapiro–Wilk test. If the data were normally distributed, descriptive statistics were reported as mean±standard deviation. If the data were not normally distributed, the Mann–Whitney U test was used, and descriptive statistics were presented as Median (Min-Max). Categorical variables were expressed as frequency (n) and percentage (%). For group comparisons of categorical variables, the Fisher-Freeman-Halton exact test, Chi-square test, and Fisher's exact test were used. Statistical significance was set at $\alpha=0.05$. .

Results: A total of 123 eyes from 108 patients were included in the study. Among 108 cases, the mean age was 41.84±17.61 years, and 74.1% were male. Blunt trauma was most common (88.8%), while injuries caused by a sharp object were significantly more frequent in males ($p<0.05$). The mean duration from trauma to forensic evaluation was 3 (0–654) days, with longer delays in trauma from a sharp object cases ($p<0.05$). The presence of an intraocular foreign body was a key finding in a subset of open-globe injuries, which also showed a higher frequency of fundus pathologies ($p<0.05$). Post-traumatic severe visual impairment was recorded in 11.7% of right-eye cases and 4.16% of left-eye cases.

Conclusion: Forensic ocular trauma cases are predominantly associated with blunt injuries, with males being more frequently affected. In forensic medical reporting, assessing functional impairment and the forensic evaluation process with a multidisciplinary approach is of great importance.

Keywords: Blunt trauma; forensic ophthalmology; medicolegal assessment; ocular trauma; trauma with a sharp object; vision loss.

Ocular trauma is one of the leading causes of vision loss worldwide, significantly reducing the quality of life on an individual level while also imposing substantial socioeconomic burdens on society.[1,2] According to the World Health Organization, approximately 55 million people suffer from ocular trauma each year, with nearly 1.6 million cases resulting in permanent blindness.[3,4] In particular, traumatic corneal opacities are among the most common causes of corneal blindness in low- and middle-income countries.[5]

Although the eye constitutes only a small portion of the total body surface area, it is highly exposed to external forces and is particularly vulnerable to physical trauma.

* This paper was presented as an oral presentation at the 5th Turkish Forensic Sciences Congress and the 16th Forensic Medicine Workshop, organized by the TURAZ Science Association between May 16–19, 2024.

Cite this article as: Kasar K, Aydogan HC, Sahin AK, Uzun A. Trends in forensic ophthalmology consultations. Eur Eye Res 2026;6(1):21–28.

Correspondence: Kader Kasar, M.D. Department of Ophthalmology, Ordu University, Faculty of Medicine, Ordu, Turkiye
E-mail: drkaderkasar@hotmail.com
Submitted Date: 03.04.2025 **Revised Date:** 10.07.2025 **Accepted Date:** 28.08.2025 **Available Online Date:** 29.04.2026

[6,7] Consequently, vision impairment due to ocular injuries can lead to significant psychological distress, reduced occupational efficiency, and long-term economic losses.[8]

In the forensic medicine context, ocular trauma is not merely a clinical concern but also serves as a critical forensic indicator, providing key insights into the mechanism, severity, and timing of trauma.[3] Findings such as intraocular hemorrhages, periorbital hematomas, and retinal lesions are of paramount importance in distinguishing cases of physical assault, particularly in child and domestic abuse investigations. Forensically significant ocular injuries necessitate meticulous evaluation not only for criminal legal proceedings but also for medico-legal assessments related to functional impairment and compensation claims.[9] A study conducted by Ligget et al. [10] reported that ocular trauma accounted for 1.3% of emergency department admissions. Similarly, in a study by Üstündağ et al. [11], 180 ocular trauma cases were reported over 20 months in the emergency department of Ordu University Hospital. Doğan et al. [12] identified that 3.1% of trauma cases presenting to forensic medicine units involved ocular trauma. These findings emphasize the necessity of both ophthalmological and forensic evaluations in cases of ocular trauma.

Given that the eye is an anatomically and functionally independent sensory organ, it is crucial to assess each eye separately. Evaluations of visual acuity (VA), visual field integrity, retinal damage, and optic nerve involvement are essential not only for determining the medical impact of trauma but also for forensic classifications of "functional loss" and "permanent visual impairment." Accordingly, forensic ocular consultations should not be limited to diagnostic assessments but must also consider their legal implications.[13]

This study aims to retrospectively analyze forensic ocular consultations requested by the Forensic Medicine Department of Ordu University Training and Research Hospital between 2017 and 2024. The study seeks to examine the distribution of trauma types, their effects on visual function, and the critical multidisciplinary considerations required for forensic reporting. In this regard, the study provides a literature-supported, interdisciplinary perspective on the intersection between ophthalmology and forensic medicine.

Materials and Methods

This study is based on the retrospective evaluation of forensic ophthalmology consultation reports requested by the Forensic Medicine Clinic and prepared by the Ophthalmology Clinic of Ordu University Training and Research Hospital between 2017 and 2024. The research was conducted in accordance with the ethical principles outlined in the 2008 Declaration of Helsinki and was approved by the relevant local ethics committee (Ethics Committee Approval: Decision No. 2025/76 dated July 04, 2025).

All ocular injuries included in this study were classified according to the standardized Birmingham Eye Trauma Terminology (BETT). This system provides an unambiguous, globally accepted framework for defining mechanical eye injuries, categorizing them into closed-globe and open-globe injuries based on the integrity of the corneoscleral wall.[14] To ensure standardized assessment of outcomes, key clinical terms were operationally defined based on VA. "Severe visual impairment" was used to describe cases with a VA of counting fingers, hand motion, or light perception (LP). The term "Complete vision loss" was reserved specifically for cases with no LP, representing a total loss of visual function. Furthermore, the medicolegal terms "functional impairment" and "functional loss" were defined according to the national forensic medicine guideline for the Turkish Penal Code.[15] "Functional impairment" was categorized as a permanent but partial decline in the organ's function (e.g., a measurable decrease in VA that does not render the eye blind). In contrast, "functional loss" was defined as the complete or near-complete cessation of the organ's primary function, rendering it legally non-functional.

All cases included in the study were patients who were referred to the ophthalmology department under official forensic investigation due to suspected ocular trauma. The dataset comprised the following variables: Age, gender, type of trauma (blunt or trauma with a sharp object), affected eye (right, left, or bilateral), the interval between trauma and consultation, type of ocular lesion detected (contusion, laceration, rupture, etc.), level of VA, functional impairment status, and necessity for medical intervention.

All statistical analyses were performed using IBM Statistical Package for the Social Sciences Statistics for Windows, Version 22.0 (IBM Corp., Armonk, NY, USA). Descriptive statistics for continuous variables were presented as mean±standard deviation, minimum, and maximum values. Categorical variables were expressed as frequency (n) and percentage (%).

For group comparisons of categorical variables, the Fisher-Freeman-Halton exact test, Chi-square test, and Fisher's exact test were used. Statistical significance was set at $\alpha = 0.05$.

Results

A total of 108 cases referred to the Ophthalmology Clinic for forensic consultation between 2017 and 2024 were retrospectively analyzed. The age range of the patients varied between 5 and 83 years, with a mean age of 41.84±17.61 years. In terms of gender distribution, 80 (74.1%) of the patients were male, while 28 (25.9%) were female. The time interval between trauma occurrence and forensic medical evaluation exhibited considerable variability. The shortest interval was on the same day, whereas the longest was 654 days. The mean consultation delay was 3 (0–654) days.

Regarding the type of trauma, 96 (88.8%) of cases involved blunt trauma, while 12 (11.2%) involved trauma with a sharp object. Gender-based analysis revealed that trauma with a sharp object injury was significantly more frequent in male patients ($p<0.05$). In addition, when the interval between trauma occurrence and forensic consultation was compared by trauma type, it was observed that trauma with sharp object injuries was associated with a significantly longer delay in presentation ($p<0.05$). Demographic variables stratified by trauma type are detailed in Table 1.

The annual distribution of forensic consultations indicated that the number of cases increased over time, with 7 cases (6.5%) in 2017 and 19 cases (17.6%) in 2024 (Fig. 1).

Regarding seasonal and monthly variations, the highest number of cases occurred in August (*n*=14, 13.0%) and May (*n*=13, 12.0%), while the lowest number of cases was observed in February (*n*=5, 4.6%). Seasonal analysis revealed that trauma cases were most frequent in the summer (*n*=27, 25.0%) and least common in the winter (*n*=21, 19.4%).

Table 1. Sociodemographic characteristics by type of ocular trauma

Age	Type of trauma				*p*
	Blunt trauma		Sharp trauma		
	n=96	%	*n*=12	%	
≤25 years	22	22.9	1	8.3	0.471
26–35 years	16	16.7	3	25	
36–45 years	15	15.6	3	25	
46–55 years	22	22.9	4	33.3	
≥56 years	21	21.9	1	8.3	
Sex					0.034
Female	28	29.2	0	0	
Male	68	70.8	12	100	
Time to ophthalmic evaluation (days)	Blunt trauma (*n*=94)		Sharp trauma (*n*=14)		0.225
	3 (0–654)		5 (1–180)		

Among the 123 eyes analyzed, 109 cases (88.6%) were classified as closed-globe injuries, whereas 14 cases (11.3%) involved open-globe injuries. Laterality assessment revealed that the left eye was affected in 57 cases (52.8%), the right eye in 36 cases (33.3%), and bilateral involvement was present in 15 cases (13.9%).

In terms of specific lesions, contusion was the most common finding, primarily seen in closed-globe injuries and observed in 104 eyes (84.5%). The 14 open-globe injuries consisted of 12 full-thickness lacerations from sharp trauma (9.7%) and 2 ruptures from blunt trauma (1.6%). An intraocular foreign body (IOFB) was detected in 8 eyes (6.5%), all of which were, by definition, classified as open-globe injuries.

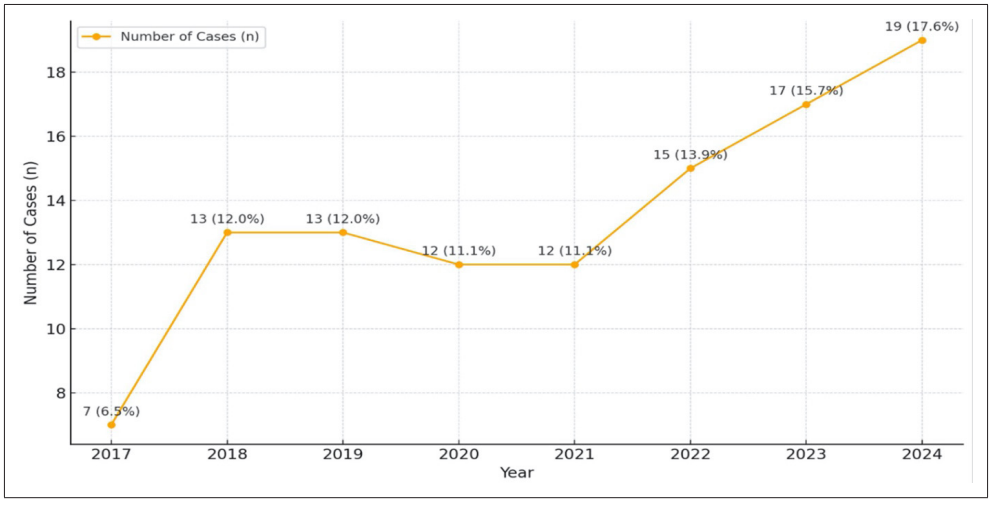

Fig. 1. Annual distribution of cases between 2017 and 2024.

Similarly, corneal, anterior segment, and fundus findings were significantly more frequent in open-globe injuries compared to closed-globe injuries ($p<0.05$). In addition, 70.6% of closed-globe injuries were classified as treatable with basic medical intervention, whereas all open-globe injuries required advanced medical or surgical interventions (Table 2).

Table 2. Distribution of ocular findings and injury characteristics by trauma type

Structural ınjury	**Consultation evaluation parameter**				***p***
	Closed globe injury		**Open globe injury**		
	***n*=109**	**%**	***n*=14**	**%**	
Contusion	104	95.4	0	0	<0.001
Lamellar laceration	5	4.6	0	0	
Laceration	0	0	12	85.7	
Rupture	0	0	2	14.3	
Affected eye	*n*=94	%	*n*=14	%	0.295
Right eye	30	31.9	6	42.9	
Left eye	49	52.1	8	57.1	
Bilateral	15	16	0	0	
Presence of intraocular foreign body	*n*=109	%	*n*=14	**%**	<0.001
Present	0	0	8	57.1	
Absent	109	100	6	42.9	
Periorbital finding	*n*=109	%	*n*=14	%	
Present	84	77.1	9	64.3	0.326
Absent	25	22.9	5	35.7	
Conjunctival finding	*n*=109	%	*n*=14	%	
Present	61	56	10	71.4	0.270
Absent	48	44	4	28.6	
Corneal finding	*n*=109	%	*n*=14	%	
Present	7	6.4	8	57.1	<0.001
Absent	102	93.6	6	42.9	
Fundus finding	*n*=109	%	*n*=14	%	
Present	12	11	6	42.9	0.006
Absent	97	89	8	57.1	
Anterior segment finding	*n*=109	%	*n*=14	%	
Present	9	8.3	7	50	<0.001
Absent	100	91.7	7	50	
Orbital bone fracture	*n*=109	%	*n*=14	%	
Present	16	14.7	2	14.3	1.000
Absent	93	85.3	12	85.7	
Accompanying systemic trauma find	*n*=94	%	*n*=14	%	0.882
Present	49	52.1	7	50	
Absent	45	47.9	7	50	
Basic medical ınterventıon status	*n*=109	%	*n*=14	%	<0.001
Treatable with basic medical intervention	77	70.6	0	0	
Not treatable with basic medical intervention	32	29.4	14	100	

Based on the results of the visual function assessment, no visual loss was observed in 37 of the 51 right eyes (72.5%) with closed-globe injuries, while 8 eyes (15.7%) exhibited functional impairment. In contrast, among the right eyes with open-globe injuries, functional loss was recorded in 6 eyes (11.8%). Regarding the left eye, 58 of the 72 eyes (80.6%) with closed-globe injuries maintained normal visual function, and functional impairment was identified in 6 eyes (8.3%). Among the left eyes affected by open-globe injuries, functional impairment was observed in 5 eyes (6.9%), and functional loss was present in 3 eyes (4.2%). These findings underscore the fact that open-globe injuries are more frequently associated with functional loss compared to closed-globe injuries and tend to result in a poorer visual prognosis (Table 3).

Based on the clinical findings and visual functional assessments, a classification scheme was developed to assist forensic evaluation. This classification integrates visual outcomes with treatment needs and is intended to guide standardized medico-legal reporting. The details of this framework are presented in Table 4.

Discussion

The classification of ocular trauma in this study was based on the BETT, which categorizes injuries into two primary types: open-globe and closed-globe.[14] This distinction is critical, as open-globe injuries, defined by a full-thickness defect of the corneoscleral wall, carry a significantly different prognostic and therapeutic profile compared to closed-globe injuries, where the globe remains intact.

Table 3. Functional status of the right and left eye following trauma

Right eye, (*n*=51)	**Ocular function-consultation evaluation result**				***p***
	Closed globe injury		**Open globe injury**		
	***n*=45**	**%**	***n*=6**	**%**	
No visual loss	37	82.2	0	0	<0.001
Functional ımpairment	8	17.8	0	0	
Functional loss	0	0	6	100	
Left eye, (*n*=72)	*n*=64	%	*n*=8	%	<0.001
No visual loss	58	90.6	0	0	
Functional ımpairment	6	9.4	5	62.5	
Functional loss	0	0	3	37.5	

In our study, this classification was used alongside a multidisciplinary approach, considering the forensic medical assessment criteria outlined in the "Evaluation of Injury Offenses in Forensic Medicine under the Turkish Penal Code (2019)" guideline (Table 4).[15]

In our study, 88.6% of eyes involved closed-globe injuries, whereas 11.4% presented with open-globe injuries. Hösükler et al. [16] reported a 94.6% prevalence of closed-globe injuries and a 5.4% prevalence of open-globe injuries in their study. The literature consistently highlights that closed-globe injuries are more common, often resulting from blunt trauma mechanisms.[17,18] While both injury types carry the risk of permanent ocular sequelae, open-globe injuries pose a significantly higher risk for severe complications, primarily due to disruptions in corneal and scleral integrity.[19] In our cohort, blunt trauma was the predominant mechanism, a finding consistent with existing literature. These injuries most commonly manifested as closed-globe injuries, with clinical findings such as contusion, subconjunctival hemorrhage, and periorbital ecchymosis being frequently observed, which underscores the typical presentation of this trauma type.

Among the key prognostic factors in open-globe injuries, the presence of an IOFB is of particular concern, as it can significantly impact visual outcomes. Studies indicate that IOFBs may induce retinal toxicity over time and increase the risk of proliferative vitreoretinopathy, leading to further complications in long-term visual prognosis.[17-20] Consistent with these findings, our study also found that the presence of foreign bodies, as well as corneal and fundus abnormalities, was significantly higher in open-globe injuries ($p<0.05$).

In our study, 41.5% of cases involved right-eye trauma, while 12.2% exhibited bilateral ocular involvement. Üstündağ et al. [11] reported that both eyes were affected at an equal rate in their study. However, literature findings regarding laterality in ocular trauma remain controversial. Some studies suggest that right-eye injuries are more prevalent, which has been hypothesized to be associated with the dominance of right-hand usage in the majority of individuals, leading to asymmetrical reflex movements and exposure patterns.[21] Nonetheless, this remains a topic of ongoing debate, as some researchers report a higher prevalence of left-eye injuries, whereas others support the predominance of right-eye involvement.[22,23]

Traumatic ocular injuries are more frequently observed in males, a finding well-established in epidemiological studies.[3,6] In our study, 74.1% of cases were male, while

Table 4. Forensic medicine criteria to be considered during ophthalmology consultation report preparation

Pathology	Forensic assessment
Ecchymosis/hematoma or superficial lacerations on eyelids/periorbital area	Treatable with basic medical ıntervention
Subconjunctival hemorrhage without visual impairment or cosmetic-functional defect	Treatable with basic medical ıntervention
Corneal abrasion or contusion without perforation	Treatable with basic medical ıntervention
Iris, uvea, vitreous injuries (e.g., intraocular hemorrhage)	Not treatable with basic medical ıntervention
Traumatic lens lesions (subluxation, luxation, cataract, hyphema)	Not treatable with basic medical ıntervention
Enucleation or evisceration	Not treatable with basic medical ıntervention
Lacrimal canal injuries	Not treatable with basic medical ıntervention
Choroidal rupture	Not treatable with basic medical ıntervention
Retinal trauma (edema, laceration, detachment, hemorrhage)	Not treatable with basic medical ıntervention
Scleral and/or conjunctival perforation	Not treatable with basic medical ıntervention
Globe perforation	Not treatable with basic medical ıntervention
Persistent traumatic epiphora	Not treatable with basic medical ıntervention
Traumatic ptosis	Not treatable with basic medical ıntervention
Trichiasis, entropion, ectropion (post-traumatic)	Not treatable with basic medical ıntervention
Traumatic strabismus (non-intracranial origin)	Not treatable with basic medical ıntervention
Optic nerve injury (non-intracranial origin)	Not treatable with basic medical ıntervention
Fracture of a single orbital bone	2 points
Fracture of multiple orbital bones or open/comminuted fracture	3 points
Light perception only, hand motion, finger counting, visual acuity 1/10–3/10	Loss of function
Visual acuity 4/10–7/10	Permanent functional ımpairment
Traumatic strabismus	Permanent functional ımpairment
Hemianopia	Permanent functional ımpairment
Persistent traumatic epiphora	Permanent functional ımpairment
Total traumatic ptosis	Permanent functional ımpairment
Diplopia	Permanent functional ımpairment

25.9% were female, further reinforcing this trend. This male predominance has been linked to greater engagement in outdoor activities, physical labor, and high-risk occupations, which contribute to a higher susceptibility to ocular trauma.[24]

In Turkey, studies conducted in emergency departments have reported mean ages for ocular trauma cases ranging between 18.6 and 27.8 years.[11,22,25] However, international studies indicate that this average extends up to 30 years.[26] In forensic medicine studies, the mean age has been reported as 35 years.[12,16] Consistent with these findings, the mean age in our study was 41.84±17.61 years, aligning more closely with forensic medicine reports.

This age discrepancy may be attributable to the broader age distribution typically observed in forensic cases. In addition, older individuals may undergo more frequent forensic evaluations due to an increased risk of post-traumatic complications. Another contributing factor to the higher mean age in our study may be the higher life expectancy in the region where the research was conducted.[27]

The Forensic Medicine Clinic at our hospital was established in 2017, and as the clinic developed and the number of personnel increased, a progressive rise in ophthalmology consultation requests was observed in our study. Analyzing the seasonal distribution of traumatic ocular injuries, we identified that the highest number of cases occurred in August and May. The existing literature supports this trend, suggesting that ocular trauma is more frequent during the summer months, largely due to increased participation in outdoor activities, recreational sports, and a rise in occupational accidents.[16,28,29] The findings of our study are consistent with these reports.

Our study also revealed that a significant proportion of open-globe injuries required advanced medical intervention, as

they were not manageable with basic medical treatment ($p<0.01$). In a study by Üstündağ et al.[11], only four cases of open-globe injuries resulted in total blindness. Similarly, Doğan et al.[12] reported that 7.6% of cases exhibited permanent functional impairment. However, in our study, this proportion was found to be 8.3%, suggesting a higher incidence of severe ocular sequelae compared to previous reports.

A thorough and timely ophthalmological evaluation is of paramount importance in the forensic assessment of patients presenting with ocular trauma. This is particularly critical in forensic reporting, where the collaboration between ophthalmologists and forensic medicine specialists is essential. In forensic ophthalmology consultations, repeated assessments may be required due to changes in clinical findings or the need for additional examinations. Our study demonstrated that the time interval between trauma and consultation was significantly longer for trauma with a sharp object injury, suggesting that these cases undergo extended follow-up evaluations, potentially due to the need for a more detailed assessment of functional loss or the prolonged recovery period following trauma with a sharp object.

Study Limitations

As a retrospective study, our research has inherent limitations. The study only included data from forensic ophthalmology consultation reports, which means that sociodemographic characteristics and other medico-legal factors, such as the assessment of permanent facial scars in cases involving ptosis, could not be extensively analyzed. Furthermore, considerations related to compensation law were not addressed in detail, as they fall outside the scope of this study.

Ethics Committee Approval: This study was approved by The Ethics Committee of Ordu university

(Decision No. 2025/76 dated July 04, 2025).

Informed Consent: Written informed consents were obtained from patient and his family.

Peer-review: Externally peer-reviewed.

Authorship Contributions: Concept: K.K., H.C.A., A.K.S., A.U.; Design: K.K., H.C.A., A.K.S., A.U.; Supervision: K.K., A.K.S., A.U.; Resource: K.K., H.C.A.; Materials: K.K., H.C.A.; Data Collection and/or Processing: K.K., H.C.A.; Analysis and/or Interpretation: K.K., H.C.A.; Literature Search: K.K., H.C.A.; Writing: K.K., H.C.A.; Critical Reviews: K.K., A.K.S., A.U.

Conflict of Interest: None declared.

Use of AI for Writing Assistance: Not declared.

Financial Disclosure: The authors declared that this study received no financial support.

References

1. Thylefors B. Epidemiological patterns of ocular trauma. Aust N Z J Ophthalmol 1992;20:95–8. [Crossref]
2. Whitcher JP, Srinivasan M, Upadhyay MP. Corneal blindness: a global perspective. Bull World Health Organ 2001;79:214–21.
3. Omolase CO, Omolade EO, Ogunleye OT, Omolase BO, Ihemedu CO, Adeosun OA. Pattern of ocular injuries in owo, Nigeria. J Ophthalmic Vis Res 2011;6:114–8. [Crossref]
4. Bashir MT, Bouamra O, Kirwan JF, Lecky FE, Bourne RRA. Ocular injuries among patients with major trauma in England and Wales from 2004 to 2021. Eye (Lond) 2024;38:2761–7. [Crossref]
5. Kate A, Basu S. Corneal blindness in the developing world: The role of prevention strategies. F1000Res 2024;12:1309. [Crossref]
6. Négrel AD, Thylefors B. The global impact of eye injuries. Ophthalmic Epidemiol 1998;5:143–69. [Crossref]
7. Türkiye Özürlüler Araştırması, Devlet İstatistik Enstitüsü Başkanlığı. 2002 Yayın no: 2913. Available at: https://cdn.tbmm.gov.tr/KKBSPublicFile/D24/Y3/T10/WebOnergeMetni/c411849e-1874-4add-98b9-c49012b0aca4.pdf Accessed on 10 Apr, 2026. [Article in Turkish]
8. Pham AT, Whitescarver TD, Beatson B, Purt B, Yonekawa Y, Shah AS, et al. Ophthalmic trauma: the top 100 cited articles in Ophthalmology journals. Eye 2022;36:2328–33. [Crossref]
9. Pérez-Sales P, López Martin S, Parras Cordovés M. Assessment and litigation of ocular injuries by less-lethal weapons. Torture 2024;34:4–21. [Crossref]
10. Liggett PE, Pince KJ, Barlow W, Ragen M, Ryan SJ. Ocular trauma in an urban population. Review of 1132 cases. Ophthalmology 1990;97:581–4. [Crossref]
11. Üstündağ M, Orak M, Gülooğlu C, Sayhan MB, Özhasenekler A. Retrospective evaluation of eye injury victims presented to emergency department. Turk J Emerg Med 2007;7:64–7
12. Doğan B, Kılıboz T, Garbioğlu A, Karbeyaz K, Gürsoy HH. Evaluation of ocular trauma in Forensic Medicine. Osmangazi J Med 2021;43:234–8. [Article in Turkish]
13. Çelik C, Ata U. Concepts of Persistent Weakening or Loss of Function of One of The Senses or Organs in the Turkish Penal Code: Systematic Review. Adli Tıp Bülteni 2022;27:279–87. [Article in Turkish] [Crossref]
14. Kuhn F, Pieramici DJ. Classification of mechanical eye injuries. In: Ocular Traumatology. Berlin, Heidelberg: Springer Berlin Heidelberg; 2008. p. 13–16.
15. Balcı Y, Çolak B, Gürpınar K, Anolay NN. Türk Ceza Kanunu'nda tanımlanan yaralama suçlarının adli tıp açısından değerlendirilmesi rehberi. Available at: https://www.atk.gov.tr/tckyaralama24-06-19.pdf. [Article in Turkish]
16. Hösükler E, Erkol ZZ, Yazgı BK. Göz travması olgularının Adli Tıp Yönünden analizi. Fırat Med J 2022;27:186–90. [Article in Turkish]

17. Kızıloğlu M, Kızıloğlu TG, Akkaya ZY. Prognostic Factors in Blunt Eye Trauma. TJO 2013;43:33–8.
18. Cillino S, Casuccio A, Di Pace F, Pillitteri F, Cillino G. A five-year retrospective study of the epidemiological characteristics and visual outcomes of patients hospitalized for ocular trauma in a Mediterranean area. BMC Ophthalmology 2008;8:1–9. [Crossref]
19. Alem KD, Arega DD, Weldegiorgis ST, Agaje BG, Tigneh EG. Profile of ocular trauma in patients presenting to the department of ophthalmology at Hawassa University: Retrospective study. PLoS One 2019;14:e0213893. [Crossref]
20. Tsujinaka M, Akaza K, Nagai A, Nakamura I, Bunai Y. Usefulness of post-mortem ophthalmological endoscopy during forensic autopsy:a case report. Med Sci Law 2005;45:85–8. [Crossref]
21. Rahman, S, Hossain A, Alam S, Rahman A. Mechanical eye trauma epidemiology, prognostic factors, and management controversies-An update. Ophthalmol 2021;11:305–18. [Crossref]
22. Ferráez, JLP, Martínez, RP. Epidemiological characteristics of ocular trauma, classified according to the ocular trauma score. Rev Med Univ Auton Sinaloa 2022;29:1–10. [Article in Spanish]
23. Özdemir M, Yaşlar T, Şimşek Ş, Durmuş A. Göz travması olgularımızn epidemiyolojik değerlendirmesi. Van Tıp Dergisi 2002;9:6-11 [Article in Turkish]
24. Joseph E, Zak R, Smith S, Best WR, Gamelli RL, Dries DJ. Predictors of blinding or serious eye injury in blunt trauma. J Trauma 1992;33:19–24. [Crossref]
25. Alpay A, Özcan Ö, Uğurbaş SC, Uğurbaş SH. Batı Eye injuries at a tertiary health center in the west Black Sea region, Turkey. Turk J Trauma Emerg Surg. 2012;18:118–24. [Crossref]
26. Çakırer D, Güzey M, Dikici K, Tolun H. Göz travması olgularımızın epidemiyolojik incelemesi. T Klin Oftalmoloji 1995;4:13–6. [Article in Turkish]
27. Schein OD, Hibberd PL, Shingleton BJ, Kunzweiler T, Frambach DA, Seddon JM, et al. The spectrum and burden of ocular injury. Ophthalmology 1988;95:300–5. [Crossref]
28. TUİK coğrafi veriler. Available at: https://cip.tuik.gov.tr/ Accessed on: 19 Feb, 2025
29. Maurya RP, Srivastav T, Singh VP, Mishra CP, Al-Mujaini A. The epidemiology of ocular trauma in Northern India: A teaching hospital study. Oman J Ophthalmol 2019;12:78–83. [Crossref]

DOI: 10.14744/eer.2025.97659
Eur Eye Res 2026;6(1):29–35

EUROPEAN EYE RESEARCH

ORIGINAL ARTICLE

Analysis of tear meniscus and anterior segment alterations in keratoconus patients after scleral contact lens

Cisil Erkan Pota, Yusuf Samet Atlıhan

Department of Ophthalmology, Akdeniz University Medical Faculty, Antalya, Turkiye

Abstract

Purpose: The objective of the study is to evaluate the effects of scleral contact lenses (ScL) wear on tear meniscus parameters and anterior segment changes in patients with keratoconus (KC).

Methods: This prospective study included 37 eyes of 23 KC patients fitted with ScLs (ICD FlexFit scleral lens, ABB Optical Group, USA). Best-corrected visual acuity (BCVA) and lens fitting parameters were assessed. Tear meniscus depth (TMD), tear meniscus area (TMA) and tear meniscus height (TMH) were evaluated using anterior segment optical coherence tomography (AS-OCT) along with anterior chamber depth (ACD), anterior chamber angle (ACA), anterior chamber volume (ACV), pupil diameter, and central corneal thickness (CCT) were measured before lens application and after 4 h of wear using corneal topography.

Results: According to the ABCD classification, 25 eyes were Stage 1, 9 eyes were Stage 2, and 3 eyes were Stage 3. The fitted ScLs had an average vault of 4369±453 µm, an average diameter of 16.1±0.37 mm, and a mean base curve of 7.64±0.71 mm. BCVA improved significantly after ScL from 0.25±0.11 to 0.018±0.05 logMAR. The mean tear reservoir thickness was 315±50 µm. Although no statistically significant changes were observed in parameters such as ACA, ACD, ACV, and CCT, a significant reduction in TMH, TMD, and TMA values was observed after lens wear ($p<0.001$).

Conclusion: ScLs are an effective treatment option to improve visual quality in patients with KC. Although scleral lenses have no direct contact with the cornea, TMH decreased within hours of wear. Changes in anterior segment parameters, as well as lens fitting, can be evaluated using AS-OCT and corneal topography.

Keywords: Anterior segment parameters; meniscus height; scleral contact lenses; tear fluid reservoir; tear meniscus depth; tear tear meniscus area

Rigid, gas-permeable lenses that are supported by the conjunctival tissue covering the scleral surface and that vault over the limbus and cornea have been defined as scleral contact lenses (ScLs). While ScLs are in direct contact with the conjunctiva, there is a tear reservoir between the limbus and the cornea. A lens that is completely on the sclera is considered a ScL, regardless of its size.[1]

ScL lenses are used to correct corneal irregularities, to treat ocular surface diseases, and for cosmetic purposes. Even after successful corneal surgery, ScL lenses are an effective treatment option to restore vision in most patients due to residual corneal irregularities and astigmatism (AST). They provide a method that improves vision and creates a smooth optical surface by correcting the visual distortions caused by an irregular cornea.[2]

In addition, the tear reservoir between the cornea and the lens ensures continuous hydration of the cornea, protection, and moisture, which is beneficial in the

Cite this article as: Erkan Pota Ç, Atlıhan YS. Analysis of tear meniscus and anterior segment alterations in keratoconus patients after scleral contact lens. Eur Eye Res 2026;6(1):29–35.

Correspondence: Cisil Erkan Pota, M.D. Department of Ophthalmology, Akdeniz University Medical Faculty, Antalya, Turkiye
E-mail: cisilerkann@gmail.com
Submitted Date: 13.06.2025 **Revised Date:** 09.08.2025 **Accepted Date:** 04.09.2025 **Available Online Date:** 29.04.2026

treatment of ocular surface diseases. This is particularly effective in cases of severe dry eye disease, neurotrophic keratopathy and graft-versus-host disease. In addition, it provides mechanical protection in cases such as entropion, trichiasis, and chemical injury and supports the healing of persistent epithelial defects.[1,3]

Another important feature of ScL lenses is their ability to reduce the need for keratoplasty in patients with severe corneal disease.[4] The scope of their clinical applications is constantly expanding. Their role in the tear film and the health of the ocular surface has also attracted considerable interest. Changes in the tear film when wearing contact lenses can directly affect the quality of vision. As the front surface of contact lenses is the most important refractive surface, it is important that the optical surface is always clean and sufficiently hydrated. Disturbing the stability of the tear film can increase light scattering and lead to optical aberrations. However, innovative lens materials and designs, such as those used in ScL, aim to minimize these effects by optimizing the protection of the ocular surface.

Changes in tear film stability during contact lens wear have been associated with factors such as thinning of the lipid component, acceleration of the tear film thinning process, and an increase in evaporation rate.[5] A better understanding of how these changes affect the tear reservoir is critical to discovering the therapeutic potential of ScL. Current studies aim to gain more insight into the clinical efficacy of these lenses, particularly by assessing the height of the tear meniscus and other tear film parameters.[5]

Approximately half of the contact lens wearers report symptoms such as dryness, stinging, and discomfort. ScLs tend to be more demanding in terms of wearing comfort and the fitting process, especially compared to soft contact lenses.[6] In this context, a stable tear film and ocular surface play a crucial role in the successful use of ScLs and in facilitating patient adaptation.[7]

In recent years, the therapeutic potential of ScLs has attracted considerable attention due to their effects on the health of the ocular surface and tear film. Examination of the tear meniscus in ScL wearers using anterior segment optical coherence tomography (AS-OCT) may not only improve the understanding of the clinical efficacy of these lenses, but also provide new perspectives for therapeutic approaches.

Our aim in this study is to investigate the short-term effects of scleral lenses in individuals with keratoconus (KC), to evaluate changes in tear film parameters and anterior segment parameters, and to perform an analysis of clinical findings related to the lens fitting process.

Materials and Methods

This study was conducted at the Akdeniz University Hospital, Department of Ophthalmology. The project was approved by This study was approved by the Akdeniz University Medical Faculty Institutional Ethics Committee (Date: 24.04.2025, Decision no: 378). Informed consent was obtained from all participants after explaining the study requirements. The clinical study adhered to the principles of the Declaration of Helsinki.

Inclusion Criteria

1. Age between 16 and 55 years
2. No contraindications to contact lens use
3. Diagnosis of KC.

Exclusion Criteria

1. Pre-existing systemic or ocular diseases affecting contact lens use
2. History of eye trauma or corneal surgery
3. Previous ScLs use
4. Presence of any anterior segment pathology, corneal abnormalities other than KC, chronic dry eye, Sjögren's syndrome, Meibomian gland dysfunction, ocular cicatricial pemphigoid, or any other disease that may cause dry eye.

Application of the Scleral Lens

The ScLs were manufactured from a cross-linked copolymer (ICD FlexFit Scleral Lens, ABB Optical Group, USA) with diameters ranging from 14.50 to 17.00 mm, a central thickness between 0.10 and 2.00 mm, a refractive index of 1.432 and an oxygen permeability (Dk/t) of 130×10^{-11} (cm^2/s) [(mL O_2/mL × mmHg)].

The ABCD grading system was used to classify KC.[8] Measurements were taken before and 4 h after lens application. Each participant underwent an ophthalmological examination, including visual acuity, refraction measurement, slit lamp biomicroscopy, and corneal topography with the Pentacam (Oculus Optikgeräte GmbH, Wetzlar, Germany). The tear meniscus was assessed using optical coherence tomography (OCT) (Triton, Topcon, Tokyo, Japan).

The subjects were fitted with scleral lenses of different diameters (ICD FlexFit Scleral Lens, ABB Optical Group, Atlanta, USA). All ScLs used in this study were selected from a diagnostic fitting set and fitted according to the instructions. Lens fitting was performed according to the fitting instructions provided by the manufacturer.

An attempt was made to keep the thickness of the fluid reservoir (FR) close to the recommended values for the lens.[9] After insertion of the lens, the initial fitting was assessed with a slit-lamp examination. During this evaluation, the position of the lens, the fluorescein distribution, the presence of air bubbles, the pressure of the lens periphery on the conjunctiva, and conjunctival blanching were assessed to determine the suitability of the lens.

Patients had no previous history of contact lens wear (scleral lenses, rigid gas permeable contact lenses, hybrid lenses, or soft contact lenses). The patients who underwent corneal cross-linking had a postoperative period of more than 1 year. In all participants, the ScL was filled with preservative-free artificial tears before insertion. The thickness of the FR between the cornea and the posterior lens surface was checked using AS-OCT, and the most suitable lenses were fitted for each patient. After fitting, the final overrefraction was performed. All lenses used in this study were spherical; astigmatic lenses were not fitted during the study. The lens fitting was considered acceptable for all subjects involved in the study.

At baseline (without ScL) and 4 h after the application of ScL, tear meniscus depth (TMD), tear meniscus height (TMH), and tear meniscus area (TMA) were analyzed with AS-OCT (Triton, Topcon, Tokyo, Japan) (Fig. 1).

AS-OCT was performed in combination with a slit-lamp to examine the parameters of the tear meniscus of the lower eyelid, with the image taken at the 6 o'clock position just below the center of the pupil. The TMA was calculated based on previous studies as the triangular area bounded by the anterior margin of the lower eyelid, the anterior corneal margin, and the anterior border of the tear meniscus. ImageJ software (version 1.53t; National Institutes of Health, Bethesda, MD, USA) was used for image analysis (http://imagej.nih.gov/ij/).[10] During the measurements, the measurement tool integrated in the OCT software was used to mark the height and depth of the tear meniscus to obtain linear measurements in micrometers (μm).[11] The same anatomical points were then identified in the ImageJ software, and the measurements obtained from the OCT device were entered as a reference scale (Fig. 2). These linear measurements were used to calculate the area of the tear meniscus using ImageJ software. The corresponding region was manually delineated in ImageJ based on the same anatomical landmarks, and the reference length obtained from the OCT device was applied. The software then automatically calculated the enclosed area and reported the result in square micrometers (μm^2) (Fig. 3). To avoid the effects of delayed blinking, OCT measurements were performed immediately after blinking. Measurements were taken between 1 and 2 p.m. to avoid the effects of diurnal variations (ambient lighting was 10 lux).

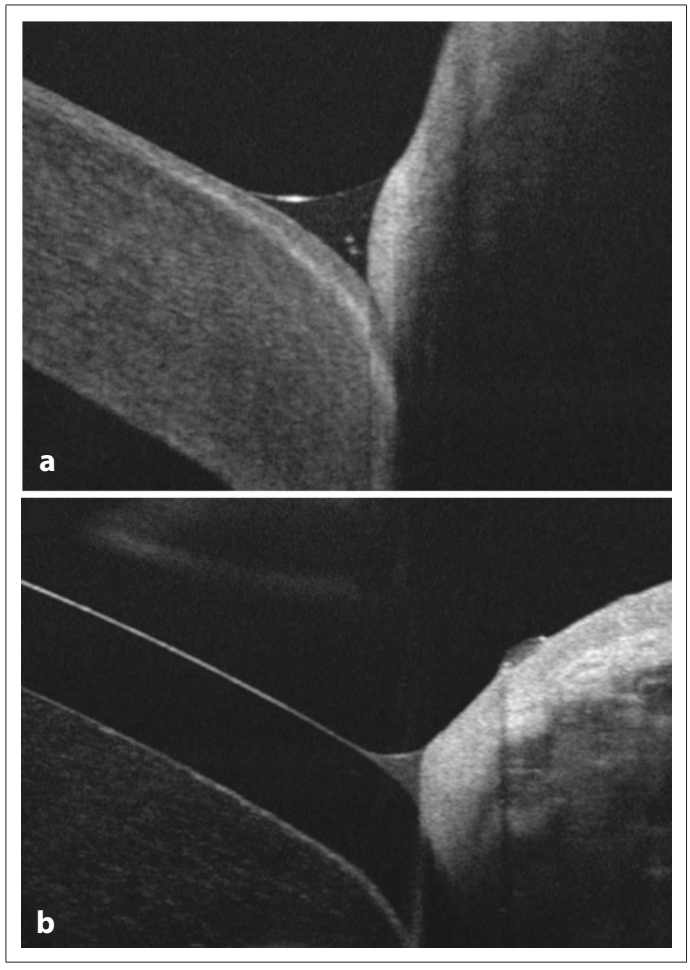

Fig. 1. Visualization of tear meniscus with anterior segment optical coherence tomography; **(a)** Image of tear meniscus before scleral lens. **(b)** Image of a tear meniscus after a scleral lens.

The thickness of the tear reservoir was measured with OCT of the anterior segment by measuring the distance between the corneal apex and the inner surface of the lens (Fig. 4).[12]

Before wearing the ScL, patients' corneal topography was measured, including Kmax (steep keratometric value), Kmean (mean of Kflat and Ksteep), thinnest corneal thickness (TCT), central corneal thickness, and AST.

In addition, anterior chamber parameters such as anterior chamber angle (ACA), anterior chamber volume (ACV), anterior chamber depth (ACD), and pupil diameter were measured and compared using corneal topography both before wearing the ScL and 4 h after fitting the lenses.

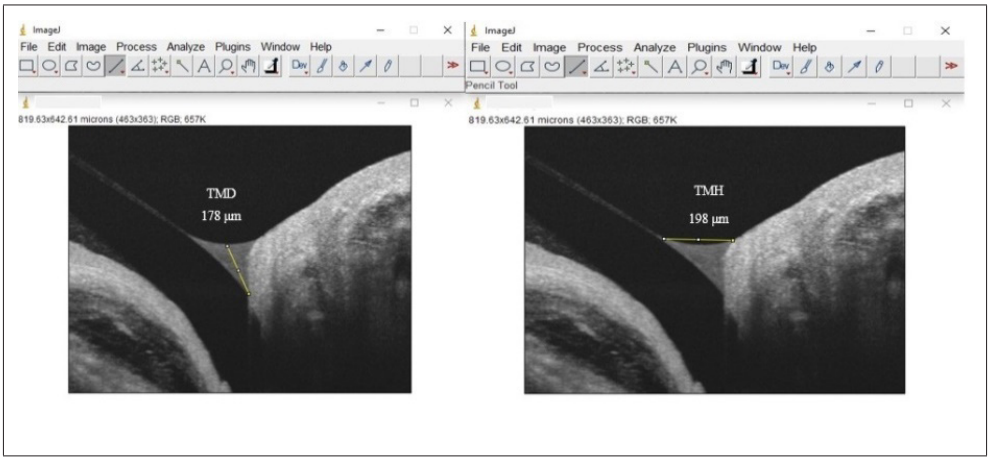

Fig. 2. Measurement of tear meniscus depth and tear meniscus height using ImageJ software.

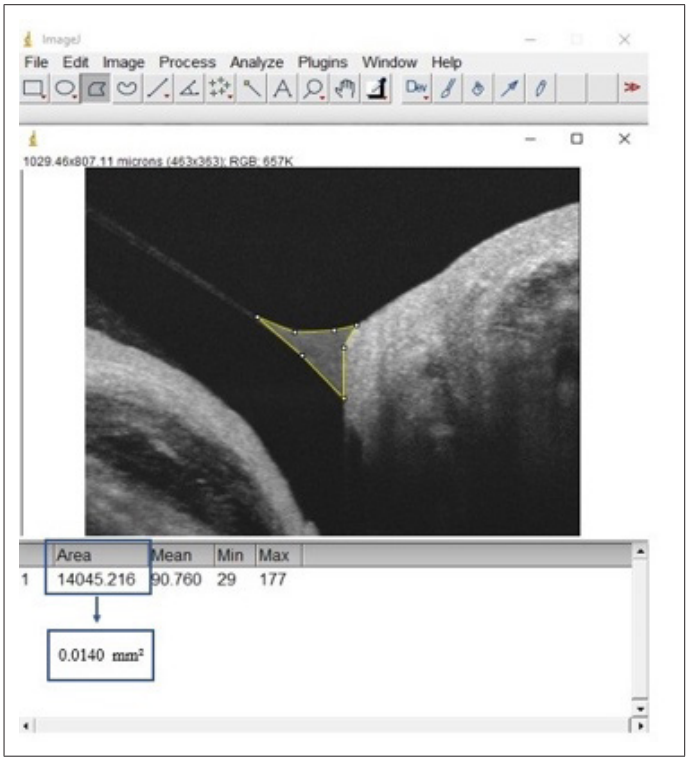

Fig. 3. Measurement of tear meniscus area using ImageJ software, blue box indicating.

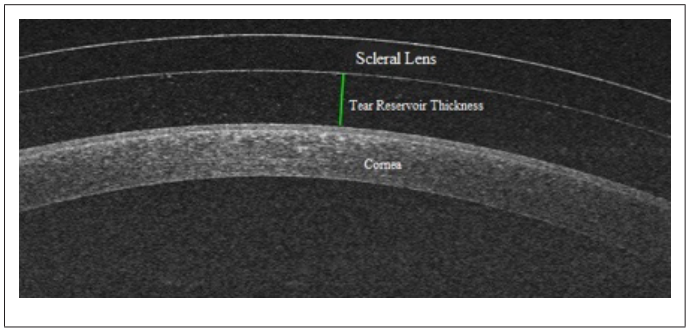

Fig. 4. Evaluation of tear reservoir thickness with anterior segment optical coherence tomography.

Statistical Analysis

The IBM Statistical Package for Social Sciences (SPSS) software (version 26.0; SPSS Inc., Chicago, IL, USA) was used for the statistical analyses. In the power analysis conducted with the GPower 3.1 programme, the effect size was set at 0.90 power (1-beta), 0.05 margin of error (alpha), and the minimum sample size to be included in the study was n=21.[13] The normality of the sample distribution was tested using the Kolmogorov–Smirnov test. For descriptive statistics, non-normally distributed variables were expressed as median (minimum–maximum) and normally distributed variables as mean±standard deviation. For the comparison of continuous variables, the Wilcoxon signed-rank test was used for data that did not follow a normal distribution, and the paired-samples t-test was used for normally distributed data.

Results

The study included 37 eyes of 23 patients diagnosed with KC who showed improved visual acuity after ScL fitting. Of the patients, 12 (52.17%) were male, and 11 (47.83%) were female. Sixteen right eyes (43.25%) and 21 (56.75%) left eyes were included. The mean age of the patients was 33±11.5 years (range: 16–51). According to the ABCD classification, 25 eyes were in Stage 1, 9 eyes in Stage 2, and 3 eyes in Stage 3. Had undergone corneal cross-linking treatment. In total, 12 eyes of 7 patients underwent corneal crosslinking treatment.

Before lens application, the best-corrected visual acuity (BCVA) was 0.25±0.11 logMAR, while after lens application, the BCVA improved to 0.018±0.05 logMAR. In all cases, OCT of the AS-OCT showed an adequate tear reservoir, no significant compression of the midperipheral conjunctiva,

Table 1. Data are expressed as mean±standard deviation (minimum–maximum)

	Mean±standard deviation (minimum–maximum)
Age (years)	33±11.5 (16–51)
Kmax (D)	52.6±4.11 (48–61)
Kmean (D)	46.5±2.3 (44–50)
Astigmatism (D)	4.6±1.9 (2.9–8.6)
TCT (µm)	475±38 (431–555)
Tear reservoir thickness (µm)	315±50 (180–425)
ScL vault (µm)	4369±453 (3800–5200)
ScL diameter (mm)	16.1±0.37 (15.5–16.3)
ScL base curve (mm)	7.64±0.71 (6.25–8.85)

Kmean: Arithmetic mean of the steepest curve (Kmax) and the flattest curve; TCT: Thinnest corneal thickness; ScL: Scleral lens; D: Diopters; µm: Micrometer; mm: Millimeter.

and optimal edge alignment was observed on both slit-lamp biomicroscopy and AS-OCT evaluation.

The mean TCT was 475±38 µm, Kmax was 52.6±4.11 D, Kmean was 46.5±2.3 D and AST was 4.6±1.9 D. The lens-related parameters are summarized in Table 1. The mean thickness of the tear reservoir was 315±50 µm. The fitted ScLs had a mean curvature of 4369±453 µm, a mean diameter of 16.1±0.37 mm, and a mean base curve of 7.64±0.71 mm.

Visual acuity improved significantly after lens wear (from 0.25±0.11 logMAR to 0.018±0.05 logMAR). No statistically significant difference in pupil diameter, TCT, ACA, ACV, or ACD was observed after wearing the ScL. However, a statistically significant decrease in TMH, TMD, and TMA values was observed (p<0.001) (Table 2).

Table 2. Evaluation of visual acuity, tear meniscus values, and anterior segment parameters of the patients before and after scleral lens fitting

	Before scleral lens	After scleral lens	*p*
Visual acuity (Snellen)	0.57±0.13 (0.40–0.70)	0.96±0.1 (0.70–1)	<0.001
Visual acuity (logMAR)	0.25±0.11 (0.15–0.40)	0.018±0.05 (0–0.15)	<0.001
TMH (mm)	0.293±0.085 (0.115–0.378)	0.199±0.051 (0.110–0.331)	<0.001
TMD (mm)	0.216±0.059 (0.100–0.270)	0.154±0.042 (0.105–0.218)	<0.001
TMA (mm^2)	0.0268±0.0102 (0.006–0.039)	0.0155±0.0071 (0.0044–0.025)	<0.001
Pupil Diameter (mm)	3.7±1 (2.21–5.66)	3.94±0.98 (2.89–5.35)	0.480
CCT (µm)	485±50.2 (457–556)	486±50.5 (430–550)	0.728
ACD (mm)	3.79±0.4 (3–4.15)	3.71±0.91 (1.44–4.33)	0.543
ACA (°)	35.8±9.1 (21.5–43.8)	34.6±8.4 (23–38)	0.516
ACV (mm^3)	186.2±32.8 (103–251)	183.7±43.1 (105–250)	0.226

SD: Standard deviation; logMAR: Logarithm of the minimum angle of resolution; mm: Millimeter; µm: Micrometer; TMA: Tear meniscus area, TMD: Tear meniscus depth; TMH: Tear meniscus height; CCT: Central corneal thickness; ACV: Anterior chamber volume; ACD: Anterior chamber depth; ACA: Anterior chamber angle are expressed as mean±SD.

Discussion

In this study, the use of ScL improved visual acuity in all patients. We found that OCT imaging of the anterior segment is a useful method to evaluate the thickness of the tear reservoir during ScL fitting. A reduction in tear meniscus parameters was noted 4 h after wearing ScL.

KC leads to irregular AST and distortion of the corneal shape, resulting in visual disturbances.[14] In the early stages of KC, vision can often be corrected with spectacles; however, as the disease progresses, the use of ScL becomes a critical treatment option.[15] Previous studies have investigated lens fitting and tear reservoir using AS-OCT. In one study, the average thickness of the tear reservoir after 5 h of ScL wear was reported to be 294.3±137.5 µm, which is comparable to the results of our study. The study showed that removing and reapplying a scleral lens with fresh saline can increase the thickness of the FR. However, this change in the thickness of the FR had no significant effect on visual acuity, the extent of light disturbance, or the quality of vision.[16]

ScLs have no direct contact with the cornea, which means that the lens is subject to less mechanical stress and is less uncomfortable. Studies have shown that ScLs are more favorable for KC patients in terms of comfort and visual acuity than other lens types.[17] Although the FR between the lens and the ocular surface provides additional comfort by relieving dry eye discomfort, some patients wearing these lenses may experience blurred vision throughout the day.[15,18,19] Although the FR formed between the lens and the cornea generally maintains the moisture balance of the tear film and alleviates dry eye symptoms, some patients wearing ScL may experience blurred vision, foreign-body sensation, and temporary visual disturbances after removing the lens. For this reason, regular follow-up care is important for ScL wearers.

An important cause of blurred vision in ScL wearers is midday fogging (MDF). Previous studies have investigated the effects of these values on MDF. In one study, white blood cells, primarily neutrophils, were found in the tear film under ScLs, and individuals with higher corneal clearance from their ScLs are more likely to suffer from MDF.[18] In another study, an increased concentration of MMP-9 and MMP-10 was found in the FR after wearing ScLs for several hours.[21] It is assumed that changes in the FR during the course of the day can cause this situation. Further studies are needed to investigate the change in fluid in the FR throughout the day and its effects on MDF.

In a study examining anterior chamber changes after ScL application in healthy individuals, a decrease in ACD and ACA values was noted, but the difference was not statistically significant.[9] The aforementioned study found that the clinical significance of anterior chamber and trabecular iris angle changes was limited in healthy individuals with open angles.[9] In our study, there was a similar decrease in ACA, ACV, and ACD values, but the difference was not statistically significant.

In our study, a significant decrease in TMD, TMH, and TMA values was observed after ScL was used. Previous studies have found that the use of soft contact lenses leads to lower TMA values and makes the tear meniscus more unstable and susceptible to evaporation.[22] According to the data obtained in our study, a 42.1% decrease in TMA was observed during the day when wearing ScL.

During the use of ScL, the thickness of the lens and the presence of FR can lead to symptoms of corneal hypoxia. The oxygen permeability values and thin design of modern ScL have led to the notion that this hypoxic effect can be eliminated, but definitive evidence on this topic is not yet available.[15] The thickness of the FR between the lens and the cornea may reduce oxygen delivery.[20] Previous studies have found that the target thickness of the reservoir varies between 200 and 600 µm.[23,24] Taking into account factors such as ScL thickness, oxygen permeability, and tear exchange, the thickness of the FR has been associated with the development of corneal edema. Previous studies have shown that individuals with healthy corneas can generally tolerate ScLs with FR of 700–800 µm during short-term wear (≥100 min), provided the lens material has a high oxygen permeability.[12] It has been reported that central corneal edema in ScL increases with FR thickness, but reaches a plateau at around 600 µm.[12] In our study, the mean thickness of the FR was calculated to be 315±50 µm, similar to the values of 250–400 µm previously reported by manufacturers for lens fitting.[9]

There are some limitations to our study. The first is the small number of patients and the short duration of lens use. The data of the patients after a long-term follow-up are not available. Larger studies are needed to assess long-term outcomes. Another limitation of our study is that there is no subjective or biochemical data on MDF. A final limitation is that no subgroup analysis could be performed because the number of subgroups was unequal, and the number of eyes in some groups was small. The strength of our study is that this is the first study in the literature to prospectively compare TMD, TMA, and TMH values and evaluate them with anterior segment parameters after wearing ScL.

Conclusion

ScL offers significant improvement in vision for people with KL. Although these lenses avoid direct contact with the cornea, a significant reduction in tear meniscus measurements was observed after only a few hours of wear. This emphasizes the need to regularly check the tear film and FR dynamics in patients wearing ScL.

Ethics Committee Approval: This study was approved by the Akdeniz University Medical Faculty Institutional Ethics Committee (Date: 24.04.2025, Decision no: 378).

Informed Consent: Written informed consent was obtained.

Conflict of Interest: None declared.

Financial Disclosure: The author declared that this study has received no financial support.

Use of AI for Writing Assistance: None declared.

Authorship Contributions: Concept: Ç.E.P., Y.S.A.; Design: Ç.E.P., Y.S.A.; Supervision: Ç.E.P.; Resource: Ç.E.P., Y.S.A.; Materials: Ç.E.P., Y.S.A.; Data collection and/or processing: Ç.E.P., Y.S.A.; Analysis and/or interpretation: Ç.E.P., Y.S.A.; Literature review: Ç.E.P., Y.S.A.; Writing: Ç.E.P., Y.S.A.; Critical review: Y.S.A.

Peer-review: Externally peer-reviewed.

References

1. Schornack MM. Scleral lenses: a literature review. Eye Contact Lens 2015;41:3–11. [CrossRef]
2. Pullum KW, Whiting MA, Buckley RJ. Scleral contact lenses: the expanding role. Cornea. 2005;24:269–77. [CrossRef]
3. Bavinger JC, DeLoss K, Mian SI. Scleral lens use in dry eye syndrome. Curr Opin Ophthalmol 2015;26:319–24. [CrossRef]
4. Koppen C, Kreps EO, Anthonissen L, Van Hoey M, Dhubhghaill SN, Vermeulen L. Scleral lenses reduce the need for corneal transplants in severe keratoconus. Am J Ophthalmol 2018;185:43–7. [CrossRef]

5. Montani G, Martino M. Tear film characteristics during wear of daily disposable contact lenses. Clin Ophthalmol 2020 4;14:1521–31. [CrossRef]
6. Guillon M, Maissa C. Dry eye symptomatology of soft contact lens wearers and nonwearers. Optom Vis Sci 2005;82:829–34. [CrossRef]
7. Downie LE, Craig JP. Tear film evaluation and management in soft contact lens wear: a systematic approach. Clin Exp Optom 2017;100(5):438–58. [CrossRef]
8. Belin MW, Duncan JK. Keratoconus: The ABCD grading dystem. Klin Monbl Augenheilkd 2016;233:701–7. [CrossRef]
9. Queiruga-Piñeiro J, Barros A, Lozano-Sanroma J, Fernández-Vega Cueto A, Rodríguez-Uña I, Merayo-LLoves J. Assessment by optical coherence tomography of short-term changes in iop-related structures caused by wearing scleral lenses. J Clin Med. 2023;12:4792. [CrossRef]
10. Czajkowski G, Kaluzny BJ, Laudencka A, Malukiewicz G, Kaluzny JJ. Tear meniscus measurement by spectral optical coherence tomography. Optom Vis Sci 2012;89:336–42. [CrossRef]
11. Karadeniz Ugurlu S, Altın Ekin M, Aytogan H. Assessment of tear meniscus by optical coherence tomography in patients with canalicular laceration repair. Int Ophthalmol 2020;40:13–8. [CrossRef]
12. Fisher D, Collins MJ, Vincent SJ. Fluid Reservoir Thickness and Corneal Edema during Open-eye Scleral Lens Wear. Optom Vis Sci 2020;97:683–9. [CrossRef]
13. Faul F, Erdfelder E, Lang AG, Buchner A. G*Power 3: a flexible statistical power analysis program for the social, behavioral, and biomedical sciences. Behav Res Methods 2007;39:175–91. [CrossRef]
14. Ciftci MD, Degirmenci C, Palamar M. Evaluation of scleral thickness in patients with keratoconus. Eye Contact Lens 2025;51:214–9. [CrossRef]
15. Şengör T, Aydın Kurna S. Update on contact lens treatment of keratoconus. Turk J Ophthalmol 2020;50:234–44. [CrossRef]
16. Seco R, Macedo-de-Araújo RJ, González-Méijome JM. Influence of scleral lens removal and reapplication on fluid reservoir thickness and visual quality after 5 h of lens wear. Cont Lens Anterior Eye 2025;48:102392. [CrossRef]
17. Levit A, Benwell M, Evans BJW. Randomised controlled trial of corneal vs. scleral rigid gas permeable contact lenses for keratoconus and other ectatic corneal disorders. Cont Lens Anterior Eye 2020;430:543–52. [CrossRef]
18. Postnikoff CK, Pucker AD, Laurent J, Huisingh C, McGwin G, Nichols JJ. Identification of leukocytes associated with midday fogging in the post-lens tear film of scleral contact lens wearers. Invest Ophthalmol Vis Sci 2019;60:226–33. [CrossRef]
19. Alipour F, Kheirkhah A, Jabarvand Behrouz M. Use of mini scleral contact lenses in moderate to severe dry eye. Cont Lens Anterior Eye 2012;35:272–6. [CrossRef]
20. Bergmanson JP, Walker MK, Johnson LA. Assessing scleral contact lens satisfaction in a keratoconus population. Optom Vis Sci 2016;93:855–60. [CrossRef]
21. Walker MK, Lema C, Redfern R. Scleral lens wear: Measuring inflammation in the fluid reservoir. Cont Lens Anterior Eye 2020;43:577–84. [CrossRef]
22. Guillon M, Maissa C. Contact lens wear affects tear film evaporation. Eye Contact Lens 2008;34:326–30. [CrossRef]
23. Arlt C. Clinical effect of tear layer thickness on corneal edema during scleral lens wear. Aalen University; 2015. [Article in Master's Thesis].
24. Tan B, Zhou Y, Yuen TL, Lin K, Michaud L, Lin MC. Effects of scleral-lens tear clearance on corneal edema and post-lens tear dynamics: A pilot study. Optom Vis Sci 2018;95:481–90. [CrossRef]

DOI: 10.14744/eer.2025.04834
Eur Eye Res 2026;6(1):36–43

EUROPEAN EYE RESEARCH

ORIGINAL ARTICLE

Vitreopapillary interface features in patients with non-arteritic anterior ischemic optic neuropathy

Selda Celik Dulger,[1] Seyfullah Ikbal Aksu,[1] Bayazıt Ilhan[2]

[1]Department of Ophthalmology, Ankara Etlik City Hospital, Ankara, Turkiye
[2]Department of Ophthalmology, Health Sciences University, Ulucanlar Eye Education and Research Hospital, Ankara, Turkiye

Abstract

Purpose: The objective of this study was to evaluate the vitreopapillary interface features in patients with acute and non-acute non-arteritic anterior ischemic optic neuropathy (NAION) compared with healthy controls.

Methods: This is a retrospective cohort study and included 30 affected eyes (group 1) and 30 unaffected fellow eyes (group 2) from 30 NAION patients and 30 eyes from 30 age- and sex-matched healthy controls (group 3). Posterior vitreous detachment (PVD), peripapillary wrinkles (PPWs), and peripapillary superficial vessel protrusion (PSVP) at the vitreous-peripapillary interface were assessed from optical coherence tomography slices.

Results: The average age of the patients was 60.7±10.7 years, and the average age of the controls was 57.4±9.5 years (p=0.213). The prevalence of complete PVD at the time of acute presentation was 23.3% in group 1, 0.0% in group 2, and 16.7% in group 3 (p=0.004). At the 3rd month, the prevalence of complete PVD increased to 30% in group 1 and remained unchanged in group 2. The number of PPWs was 5.33±2.96, 3.57±1.43, and 1.37±0.76 in groups 1, 2, and 3, respectively (p<0.001) at baseline. At the 3rd month, the PPW in group 1 was significantly greater than that in group 2 (p=0.011). The number of PSVPs was 8.4±3.47 in group 1, 10.7±1.82 in group 2, and 7.43±1.28 in group 3 at baseline (p<0.001). There was no significant difference in the number of PSVPs among the groups at the end of 3-month follow-up (p=0.96).

Conclusion: PVD was present in almost one-third of eyes that had suffered NAION, and the affected eyes had PVD significantly more frequently than the unaffected eyes. The increased PPW in the affected eyes of NAION patients may be related to optic nerve head edema. NAION patients had more superficial vessel protrusion in the subacute period regardless of ischemic episode.

Keywords: Non-arteritic anterior ischemic optic neuropathy; Papillary vitreous detachment; Peripapillary superficial vessel protrusion; Peripapillary wrinkles; Vitreopapillary traction.

Non-arteritic anterior ischemic optic neuropathy (NAION) is the most common acute optic neuropathy, presenting as painless, unilateral loss of vision in the elderly population.[1,2] Presumed pathophysiology of NAION was acute hypoperfusion or circulatory insufficiency of the short posterior ciliary arteries, which is the most accepted, but no single mechanism has been fully proven.[3]

There are numerous examples of retinal damage and hemorrhages occurring during spontaneous or surgical separation of the vitreous or internal limiting membrane. Disc and peripapillary tissue also are known to be susceptible to vitreous separation.[4] Parsa and Hoyt[4] ignored the microvascular ischemic theory as a primary pathogenic mechanism. Rather, they proposed a purely

Cite this article as: Celik Dulger S, Aksu SI, Ilhan B. Vitreopapillary interface features in patients with non-arteritic anterior ischemic optic neuropathy. Eur Eye Res 2026;6(1):36–43.

Correspondence: Selda Celik Dulger, M.D. Ankara Etlik City Hospital, Department of Ophthalmology, Ankara, Turkiye
E-mail: drsldclk@gmail.com

Submitted Date: 07.05.2025 **Revised Date:** 12.09.2025 **Accepted Date:** 16.09.2025 **Available Online Date:** 29.04.2026

tractional etiology causing optic neuropathy resulting from shearing forces on the optic nerve head (ONH) and peripapillary tissue during the progression of posterior vitreous detachment (PVD). In support of this theory, Modarres *et al*.[5] performed pars plana vitrectomy to release vitreopapillary attachments from the swollen ONH in eyes with NAION and reported favorable outcomes. Visual field improvement has been reported after spontaneous PVD in a patient diagnosed with NAION.[6]

One possible mechanism is that optic disc edema in NAION may be initiated by PVD, causing alterations in the vitreopapillary interface.[7] It is postulated that edema may lead to transient hypoperfusion, which further exacerbates optic disc edema. Thus, a potentially self- perpetuating cycle is initiated. Peripapillary capillary compression during PVD, further ischemia, venous stasis, and ultimately axonal damage, may be initiated by this cascade. Understanding the characteristics of patients with NAION who also develop PVD is crucial to elucidate this potential association.[8,9] Despite the proposed clinical relationship of both conditions, detailed investigations of the possible role of PVD in the context of NAION remain limited.

On the basis of the vitreous traction hypothesis proposed in the pathogenesis of NAION, this study aimed to evaluate PVD and vitreopapillary interface characteristics in acute and non-acute NAION patients compared with normal subjects using optical coherence tomography (OCT).

Materials and Methods

This was a retrospective cohort study and included data of patients with NAION who were admitted to the neuro-ophthalmology unit of a tertiary hospital in Ankara between January and September 2023. The study was approved by the local ethics commission (ethics number: AEŞH-BADEK-2024-932) and was conducted in accordance with the Declaration of Helsinki.

The diagnosis of NAION was based on the presence of several key clinical features, including sudden visual loss, color vision impairment, a relative afferent pupillary defect, a characteristic visual field defect, and associated optic disc edema. Eyes were excluded if they presented more than 3 weeks after the onset of symptoms. All potential causes of optic neuropathy, including inflammatory, hereditary, traumatic, toxic, and other factors, were excluded. The exclusion criteria for both the NAION and control groups were as follows: Retinal pathology, high myopia, glaucoma, significant media opacity affecting image quality on OCT, history of previous ocular trauma or surgery, and axial length (AL) exceeding 25.5 mm. Information was also collected regarding the subjects' medical history and smoking status.

The healthy control subjects were recruited from patients who presented to the outpatient clinic for refractive problems. The inclusion criteria were best corrected visual acuity (BCVA) ≥20/20; normal slit-lamp biomicroscopy and fundus examination; a normal visual field; a normal-appearing ONH; and no history of ocular, neurologic, or systemic disease.

All subjects (both at baseline and at 3 months for NAION patients) underwent a comprehensive ophthalmological examination. This included BCVA, intraocular pressure (IOP) measurement, and slit-lamp biomicroscopy. A dilated fundus examination was conducted with a +90 diopter lens, and color vision was assessed using the Ishihara color blindness test plates. In addition, AL and anterior chamber depth were evaluated through the Lenstar LS900 (Haag-Streit AG, Switzerland) and spherical equivalent with the Visuref 150 (Carl Zeiss Meditec AG, Jena, Germany). Visual field examinations were conducted on all NAION patients through the Humphrey Field Analyzer 3 (Carl Zeiss Meditec, Inc., USA). Incomplete and complete PVD, vitreous attachments to the ONH, peripapillary wrinkle (PPW), and peripapillary superficial vessel protrusion (PSVP) were evaluated from circular and macular OCT slices.

Optic disc and macular OCT images were obtained through the Heidelberg Engineering spectral domain OCT (SD-OCT) system (Heidelberg Engineering, Heidelberg, Germany). All OCT images were acquired by a single experienced technician. Circular peripapillary and macular OCT slices were employed to assess the presence of papillary vitreous detachment, PPW, and superficial vessel protrusion at the vitreous-peripapillary interface. The definition of PVD in this study was a complete stage 4 PVD without any presence of the premacular bursa or posterior vitreous cortex on any scans of the OCT.[10] Partial PVD was defined as a sharp and discrete hyperreflective linear image with focal attachments to the ONH, reproducible on at least one other scan. PSVP is defined as the protrusion of peripapillary superficial retinal vessels from the surface of the nerve fiber layer, as observed in circular peripapillary OCT images. It is hypothesized to be the result of vitreous traction.[11] PPWs are situated in the retinal nerve fiber layer in proximity to the disc surface or at a distance of half a disc diameter from the disc edge, manifesting as closely spaced circumferential corrugations.[12] Two blinded specialists conducted independent evaluations and recorded the OCT

parameters. A different specialist conducted a separate evaluation of the data.

Statistical Analysis

The data were analyzed using IBM Statistical Package for the Social Sciences (SPSS) (International Business Machines, SPSS) Statistics 23 (SPSS Inc., Chicago, IL, USA). The data were examined for compliance with a normal distribution through the Shapiro–Wilk and Kolmogorov–Smirnov tests. For the analysis of independent variables, the independent samples *t*-test was used to determine if the independent variables fit a normal distribution, and the Mann–Whitney *U*-test was used to determine if they did not fit a normal distribution. A Chi-square test was used for the categorical variables. For the analysis of dependent variables, the dependent samples *t*-test was used to determine if the dependent variables fit the normal distribution, and the Wilcoxon signed-rank test was used to determine if they did not fit a normal distribution. The Kruskal–Wallis test was used to compare non-normally distributed data for groups of three or more. Dunn's test was used for multiple comparisons. One-way ANOVA was employed to compare normally distributed data. Bonferroni and Duncan tests were used for multiple comparisons for groups of three or more. The findings were presented as the mean±standard deviation and median (min-max) for quantitative data and as the frequency for categorical data. Statistical significance was defined at $P<0.050$.

Results

This study examined 30 affected eyes (group 1) and 30 unaffected fellow eyes (group 2) from 30 NAION patients and 30 eyes from 30 age- and sex-matched healthy control patients (group 3). Overall, 18 female and 12 male patients with a mean age of 60.7±10.7 years and 19 female and 11 male healthy controls with a mean age of 57.4±9.5 years were studied ($p=0.213$). In the NAION group, 50% of the patients had diabetes mellitus, and 56.7% had essential hypertension. NAION was detected in the right eye in 56.7% of the patients and the left eye in 43.3% of the patients. The mean BCVA in group 1 was 1.13±0.88 (LogMAR), that in group 2 was 0.34±0.38 (LogMAR), and that in group 3 was 0.27±0.27 (LogMAR). The color vision was 3.2±4.8 in group 1, 11.33±2.26 in group 2, and 12.00±0.00 in group 3. Significant difference was found between group 1 and group 2 in terms of BCVA and color vision ($p<0.001$). The spherical equivalent was 0.26±1.62 diopters (D), 0.31±1.66 D, and 0.20±1.37 D in groups 1, 2, and 3, respectively ($p=0.964$). At the first presentation, the mean disc areas of group 2 were 1.81±0.26 mm^2. The demographic and other clinical characteristics of the groups are presented in Table 1.

Complete PVD was observed in 23.3% (7/30) of the group 1 on SD-OCT at baseline. No complete PVD was observed in group 2, and 5 of 30 eyes (16.7%) presented complete PVD in group 3. Group 1 and group 2 differed significantly in terms of complete PVD ($P=0.004$). There was no significant difference in complete PVD between group 1 and group 3, and between group 2 and group 3 ($p>0.05$). There was no significant difference in terms of partial PVD among the three groups at the time of presentation ($p>0.05$) (Fig. 1 and Table 2). At the baseline, the three groups differed significantly in terms of PPW ($p<0.001$). The mean value of PPW was 5.33±2.96 in group 1, 3.57±1.43 in group 2, and 1.37±0.76 in group 3. Superficial vessel protrusion did not differ between groups 1 and 3 ($p>0.05$). Group 2 had significantly greater PSVP than did group 1 and group 3 ($p<0.001$) (Table 3).

While the complete PVD was 23.3% of group 1 at the time of presentation, it increased to 30% at the 3rd month ($p<0.001$). The prevalence of partial PVD of group 2 did not differ significantly at the end of the 3-month follow-up. At the

Table 1. Demographic characteristics of NAION patients and controls

n (%) for categorical variables	Control (*n*=30)		NAION (*n*=30)		*p*
	n	%	*n*	%	
Sex					
Male	11	36.7	12	40.0	1.000
Female	19	63.3	18	60.0	
Systemic disease (DM)					
Yes	8	26.7	15	50.0	0.111
No	22	73.3	15	50.0	
Systemic disease (HT)					
Yes	10	33.3	17	56.7	0.119
No	20	66.7	13	43.3	
Cigarette use					
Yes	12	40.0	12	40.0	1.000
No	18	60.0	18	60.0	
Continuous variables	**Mean±S.D**		**Mean±S.D**		***p***
Age[t]	57.47±9.57 58.5 (40–71)		60.77±10.71 62 (35–79)		0.213

*$p<0.05$; *t*: Independent Sample *t*-test, categorical parameters; Chi-square test. NAION: Non-arteritic anterior ischemic optic neuropathy, SD: Standard deviation

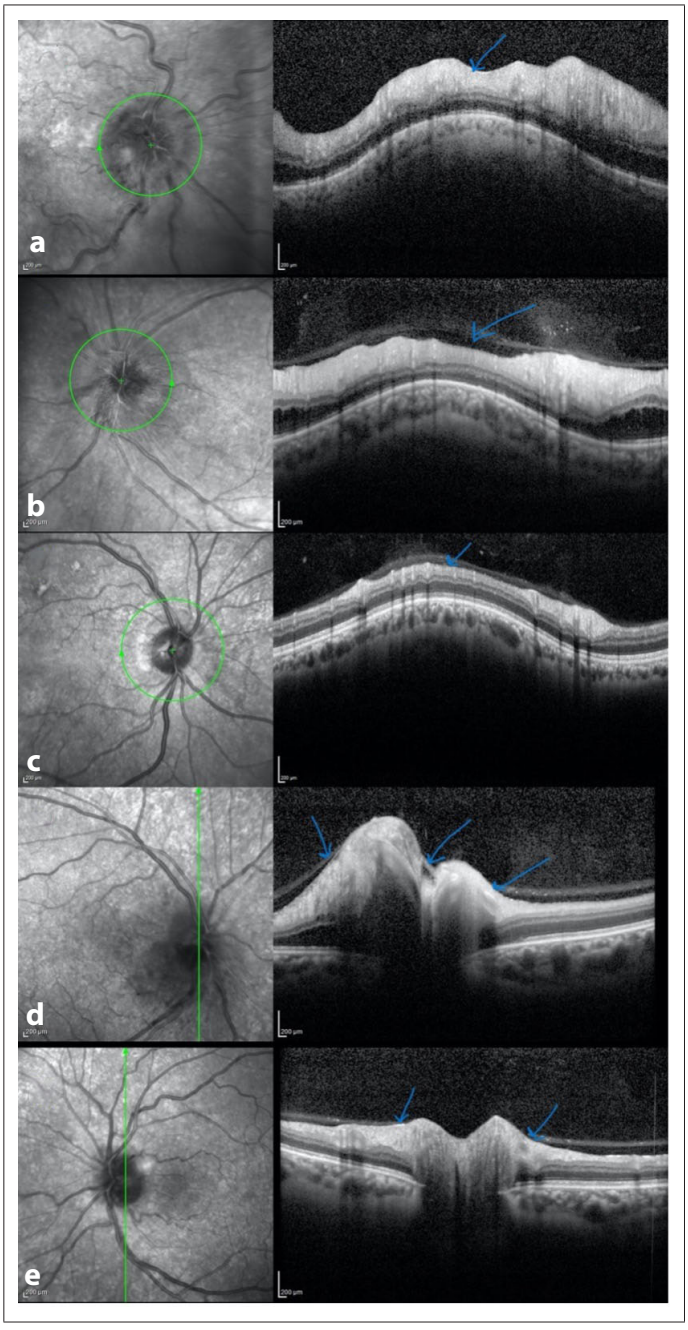

Fig. 1. Spectral domain optical coherence tomography (OCT) scan showing complete posterior vitreous detachment in a patient with acute non-arteritic anterior ischemic optic neuropathy (NAION) **(a)**, incomplete posterior vitreous detachment in a patient with acute NAION **(b)**, and no posterior vitreous detachment in a patient with acute NAION at circular **(c)**, horizontal **(d)**, vertical **(e)**, OCT slices (blue arrow).

3rd month, no significant change in the PPW was observed in group 1, whereas a significant increase in the PSVP was observed (p=0.353, p<0.001, respectively) (Fig. 2). In group 2, no significant change was observed in the complete or partial PVD at the end of the 3-month follow-up (p>0.05).

Table 2. Comparison of PVD status of affected and unaffected eyes in NAION patients at baseline and 3rd month

n (%) for categorical variables	Unaffected eye (n=30)		Affected eye (n=30)		p
	Number	%	Number	%	
PVD 0. month					
No	17a	56.7	5b	16.7	0.000**
Incomplete	13a	43.3	18a	60.0	
Complete	0a	0.0	7b	23.3	
PVD 3. month					
No	17a	56.7	4b	13.3	0.000**
Incomplete	13a	43.3	17a	56.7	
Complete	0a	0.0	9b	30.0	

*p<0.05; **p<0.01, Categorical variable: Chi-square test, a,b: There is no significant difference between groups having the same letter. NAION: Non-arteritic anterior ischemic optic neuropathy, PVD: Posterior vitreous detachment

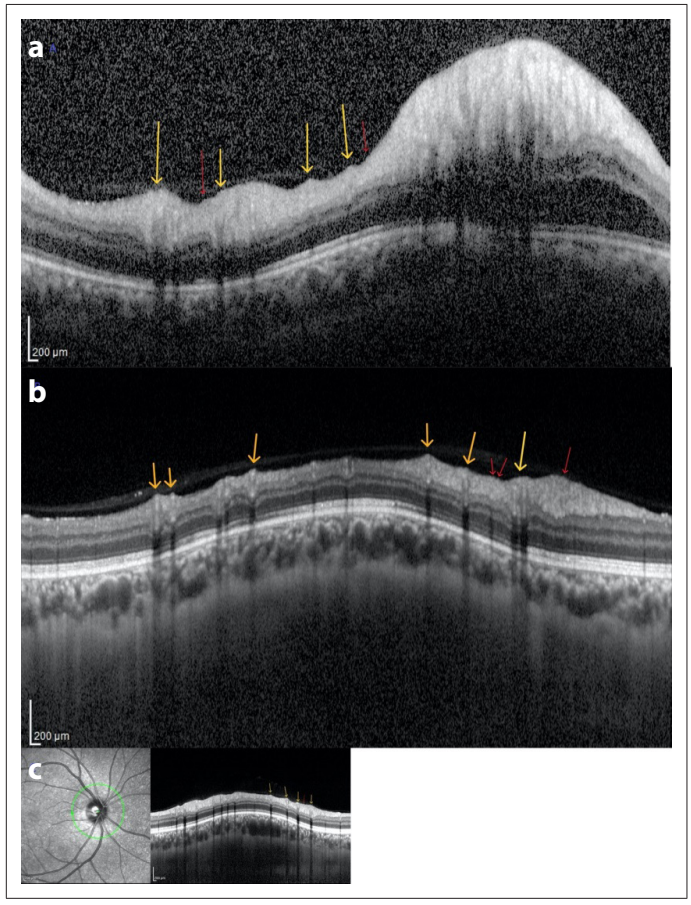

Fig. 2. Spectral domain optical coherence tomography scan showing peripapillary wrinkles (red arrow) and peripapillary superficial vessel protrusion (yellow arrow) in a patient with acute non-arteritic anterior ischemic optic neuropathy **(a)** and in the same patient at the 3rd month **(b)**, in the healthy control group **(c)**.

Table 3. Comparison of baseline ocular characteristics of the affected and unaffected eyes in the NAION group and healthy eyes

n (%) for categorical variables	Healthy eye (*n*=30)		Unaffected eye (*n*=30)		Affected eye (*n*=30)		*p*
	n	%	*n*	%	*n*	%	
Eye							
Right	30	100.0	13	43.3	17	56.7	0.000**
Left	0	0.0	17	56.7	13	43.3	
PVD							
No	8[ab]	26.7	17[b]	56.7	5[a]	16.7	0.004**
Incomplete	17[a]	56.7	13[a]	43.3	18[a]	60.0	
Complete	5[ab]	16.7	0[b]	0.0	7[a]	23.3	
Visual field							
Generalized		0	0		12		
Inferior altitudinal		0	0		11		
Superior altitudinal		0	0		4		
Quadranopic		0	0			3	
Continuous variables	**Mean±SD Med. (Min.-Max.)**		**Mean±SD Med. (Min.-Max.)**		**Mean±SD Med. (Min.-Max.)**		
Spherical equivalent[F]	0.20±1.37 −0.12 (−2–3.5)		0.31±1.66 0 (−4.25–4.5)		0.26±1.62 0 (−2.5–5)		0.964
ACD [F]	3.4±0.273.4 (3.02–4.09)		3.35±0.53 3.25 (2.5–4.6)		3.34±0.57 3.3 (2.36–4.68)		0.880
AL[F]	24.03±1.04 24.03 (22.23–26.95)[a]		23.00±0.90 22.97 (21.36–26.06)b		22.97±0.91 22.97 (21.29–26.04)b		0.000**
BCVA[H] (LogMAR)	0.27±0.27 0.2 (0–1)[a]		0.34±0.38 0.19 (0–1.4)[a]		1.13±0.88 1 (0–2.7)[b]		0.000**
Color vision[F]	12.00±0.00 12 (12–12)[a]		11.33±2.26 12 (0–12)[a]		3.2±4.8 0 (0–12)[b]		0.000**
IOP[F]	13.6±2.16 14 (10–18)		13.4±3.15 12 (9–20)		13.7±3.72 12.5 (8–21)		0.929
PPW[F]	1.37±0.76 1 (0–3)[a]		3.57±1.43 3 (2–9)[b]		5.33±2.96 5 (1–11)[c]		0.000**
PSVP[F]	7.43±1.28 8 (5–10)[a]		10.7±1.82 11 (6–15)[b]		8.4±3.47 9 (3–17)[a]		0.000**

*p<0.05; **p<0.01. Categorical variable: Chi-square test, F: One-way ANOVA test, H: Kruskal–Wallis H Test. a,b,c: There is no significant difference between groups having the same letter. SD: Standard deviation, NAION: Non-arteritic anterior ischemic optic neuropathy, PVD: Papillary vitreous detachment, ACD: Anterior chamber depth, AL: Axial length, BCVA: Best corrected visual acuity, IOP: Intraocular pressure, PPW: Peripapillary wrinkle, PSVP: Peripapillary superficial vessel protrusion, LogMAR: Logarithm of the minimum angle of resolution

Similarly, PPWs or PSVP in group 2 did not differ from the first presentation to the 3rd month (p=0.354, 0.174, respectively). At the 3rd month, a significant difference in the complete PVD persisted between group 1 and group 2 (p<0.001). The percentage of vitreous attachment to the ONH was 13.3% in group 1 and 56.7% in group 2 (p<0.001) (Table 2). The PPW in group 1 was significantly greater than that in group 2 (p=0.011). PSVP reveals no change in group 2 at the end of 3-month follow-up (p=0.96). The differences in BCVA and color vision were statistically significant in group 1 and group 2 at the 3rd month, which was similar to the findings at baseline (p=0.001) (Table 4). IOP did not differ at baseline or at 3rd month among the three groups (p>0.05).

Discussion

Our study investigated vitreopapillary interface characteristics such as PVD, PPW, and PSVP in patients

Table 4. Comparison of ocular characteristics of the affected and unaffected eyes in NAION group at baseline and 3rd month

	Month	Unaffected eye (n=30)	Affected eye (n=30)	p[1]
		Mean.±S.D	Mean.±S.D	
VA	Month 0	0,34±0,38	1,13±0,88	**0,000****
	Month 3	0,33±0,39	0,92±0,86	**0,001****
	p[2]	0,945	0,108	
Color vision	Month 0	11,33±2,26	3,20±4,80	**0,000****
	Month 3	10,67±3,28	4,03±5,16	**0,000****
	p[2]	0,324	0,205	
IOP	Month 0	13,40±3,15	13,70±3,72	0,737
	Month 3	13,87±2,96	14,00±3,35	0,871
	p[2]	0,313	0,545	
PPW	Month 0	3,57±1,43	5,33±2,96	**0,005****
	Month 3[a]	3,43±1,25	4,80±2,99	**0,011***
	p[2]	0,354	0,353	
PSVP	Month 0	10,70±1,82	8,40±3,47	**0,002****
	Month 3	10,97±1,50	10,93±3,26	0,960
	p[2]	0,174	**0,001****	

p<0,05, **p<0,01. p1: comparison of baseline and 3rd month measurements of two groups. (Independent Sample T Test, [a] Mann–Whitney U test), *p2: Comparison of baseline and 3rd month measurements in each group. (Paired Sample T Test, [a] Wilcoxon Test)), NAION: non-arteritic anterior ischemic optic neuropathy, VA: visual acuity, IOP: intraocular pressure, PPW: peripapillary wrinkle, PSVP: peripapillary superficial vessel protrusion.

with NAION. In this study, eyes with NAION had partial or complete PVD which is more common than the prevalence of PVD in the unaffected eyes. The prevalence of complete PVD increased to 30% in the affected eyes at the 3rd month visit, and remained unchanged in the fellow eyes. The prevalence of vitreous attachment was significantly greater in the unaffected fellow eyes than in the affected eyes both at baseline and 3rd month. Complete PVD showed no difference between the affected eyes and the healthy eyes.

Previous studies have suggested an association between PVD and the development of NAION.[4,13] Rabbani *et al*.[14] reported a PVD prevalence of 18.9% in patients with NAION and a significant association between PVD prevalence and advancing age. They suggested that there might not be a direct causal link between PVD and optic nerve ischemic neuropathy but rather a shared risk factor of advancing age. Others reported 30% and 25.3% of vitreous detachment in patients with NAION and a similar prevalence in the fellow eyes.[9,13] Thompson *et al*.[9] reported that complete PVD was identified in OCT sections before NAION onset in eight patients with NAION, which negates the possibility that tractional vitreous forces are involved in the pathogenesis of NAION. They proposed that if the pathogenesis of NAION was primarily mechanical, PVD should be actively developing at the time of the acute NAION. In our study, because the rates of complete PVD in the affected eyes were significantly greater than in the fellow eyes, the traction forces exerted by PVD may have facilitated the development of NAION, at least in some of the cases with small discs. Another likely speculation is that ONH edema may alter the vitreopapillary interface and trigger PVD formation. In addition, while the prevalence of complete PVD increased in the affected eyes at the end of 3 months, there was no change in the fellow eye, supporting the possibility that an acute NAION episode may contribute to the development of PVD. Shen and MacIntosh[6] reported a case developing PVD so shortly after an acute NAION episode, and her visual field worsened at the time of PVD, but improved spontaneously in a month afterward. They speculated that there is an association between two entities and suggested that vitreous traction on the ONH causes structural alterations to the axons. Over time, the release of traction on the nerve may permit restoration of normal axonal architecture and even visual recovery. If this speculation is true, triggering PVD by ONH edema secondary to acute NAION may contribute positively to visual outcomes but needs further investigation.

Previous studies have reported that vitreopapillary traction may play a role in the pathogenesis of a number of conditions such as optic nerve edema, NAION, and intra- and peripapillary hemorrhages.[4,15,16] It is a well-known condition that small and cupless discs, called disc-at-risk discs, are important in the pathogenesis of NAION. It has been shown that vitreopapillary attachments are stronger on cupless discs.[4] A recent study revealed a higher rate of focal vitreopapillary and vitreovascular attachments on crowded discs than on non-crowded discs. They suggested that crowded discs may have stronger vitreopapillary attachments, producing stronger traction forces on the vessel wall, resulting in the disruption of blood flow in NAION.[17] Similarly, Kahraman *et al*.[18] reported a strong association between vitreopapillary adhesion and crowded discs, and ONH perfusion decreased in the adhesion group. The vitreopapillary traction hypothesis proposes that traction on the ONH may cause an elongation of the nerve fibers and damage its nourishing blood vessels, resulting in disc edema due to axonal cytoskeletal damage and impaired blood flow. According to this hypothesis, ischemia still plays

an important role in the pathogenesis of NAION, but is not the primary cause of NAION.[19] Vasculopathic risk factors and characteristic sudden vision loss in NAION are indicators of ischemia. The "disc at risk" not only creates a compartment syndrome but may also contribute to strong vitreal attachments revealed in recent studies. The tractional hypothesis may be acting through the crowded disc.

A recent study suggested PPWs and PSVP as potential indicators of traction caused by papillary vitreous detachment in NAION. Kupersmith *et al*.[12] detected PPW on OCT slices in eyes with NAION and proposed that they are a common response to stress and strain resulting from swelling of the ONH and edema extending to the peripapillary retina. In our series, the PPW in the affected eyes was significantly greater than that in the fellow eyes and healthy eyes. From baseline to the 3rd month, the change in the PPW was not significant in the affected eyes or in the fellow eyes. We proposed that the increased PPW in the affected eyes of NAION patients may be related to ONH edema rather than traction due to PVD.

Li *et al*.[11] reported that 44% of eyes with acute NAION and 90% of eyes with non-acute NAION presented with PSVP. They detected a higher number of vitreous-pulled superficial vessels in the superior quadrant, consistent with more damaged visual field defects in a patient with NAION. In our study, significantly higher PSVP was observed in the unaffected fellow eyes compared to the affected and healthy eyes at the time of presentation. Three months later, PSVP in the affected eyes was similar to that in the unaffected eyes. The increased prevalence of vessel protrusion in non-acute NAION eyes observed in both our study and that of Li *et al*.[11] has been interpreted as suggestive of ONH edema in the acute period, which may potentially serve as a complicating factor in the detection of PSVP. Higher rates of PSVP in the NAION cohort compared to the healthy eyes suggest that stronger vitreopapillary adhesion in crowded discs may cause greater vitreous pulled-vessels in eyes of patients with NAION. Future studies are needed to determine whether PSVP and PPW play a role in the presumed tractional theory of NAION.

Some limitations of our study are the relatively small sample size and cross-sectional design. Another is the lack of OCT slices from patients presenting with pre-NAION status and comparison with the post-NAION appearance to interpret whether a causal relationship exists. Prospective studies with larger sample sizes and well-documented vitreopapillary interface features during acute NAION could be useful in elucidating this issue.

Conclusion

PVD was present almost one-third of eyes with NAION, and the affected eyes had PVD significantly more frequently than the unaffected eyes. The increased PPW in the affected eyes of NAION patients may be related to ONH edema rather than traction due to PVD. The presumed strong vitreopapillary attachments in crowded discs may cause greater vitreous pulled-vessels in the eyes of patients with NAION. A better understanding of the vitreopapillary status of such patients may lead to improved therapeutic and diagnostic interventions that will result in more favorable visual outcomes in this vulnerable population.

Ethics approval and consent to participate: This study was approved by the Ethical Committee of Ankara Etlik City Hospital (AEŞH-BADEK-2024-932 30/10/2024).

Peer-review: Externally peer-reviewed.

Authorship Contributions: Concept: S.C.D., S.I.A., B.I.; Design: S.C.D., S.I.A., B.I.; Supervision: S.C.D., S.I.A., B.I.; Resource: S.C.D., B.I.; Materials: S.I.A.; Data Collection and/or Processing: S.C.D., S.I.A.; Analysis and/or Interpretation: S.C.D.; Literature Search: S.C.D.; Writing: S.C.D.; Critical Reviews: S.C.D., B.I.

Conflict of Interest: None declared.

Use of AI for Writing Assistance: Not declared.

Financial Disclosure: The authors declared that this study received no financial support.

References

1. Francois J, Verriest G, Neetens A, de Rouck, Hanssens M. Pseudo-papillites vasculaires. Ann Ocul (Paris) 1962;195:830-885.
2. Miller GR, Smith JL. Ischemic optic neuropathy. Am J Ophthalmol 1966;62:103–15. [CrossRef]
3. Hayreh SS. Anterior ischaemic optic neuropathy. III. Treatment, prophylaxis, and differential diagnosis. Br J Ophthalmol 1974;58:981–9. [CrossRef]
4. Parsa CF, Hoyt WF. Nonarteritic anterior ischemic optic neuropathy (NAION): A misnomer. Rearranging pieces of a puzzle to reveal a nonischemic papillopathy caused by vitreous separation. Ophthalmology 2015;122(3):439–42. [CrossRef]
5. Modarres M, Sanjari MS, Falavarjani KG. Vitrectomy and release of presumed epipapillary vitreous traction for treatment of nonarteritic anterior ischemic optic neuropathy associated with partial posterior vitreous detachment. Ophthalmology 2007;114(2):340–4. [CrossRef]
6. Shen B, MacIntosh PW. Posterior vitreous detachment associated with non-arteritic ischaemic optic neuropathy. Neuroophthalmology 2016;40(5):234–6. [CrossRef]

7. Arnold AC, Hepler RS. Fluorescein angiography in acute nonarteritic anterior ischemic optic neuropathy. Am J Ophthalmol 1994;117(2):222–30. [CrossRef]
8. Chen CS, Johnson MA, Flower RA, et al. A primate model of nonarteritic anterior ischemic optic neuropathy. Invest Ophthalmol Vis Sci 2008;49(7):2985–92. [CrossRef]
9. Thompson AC, Bhatti MT, Gospe SM. Spectral-Domain Optical Coherence Tomography of the Vitreopapillary Interface in Acute Nonarteritic Anterior Ischemic Optic Neuropathy. Am J Ophthalmol 2018;195:199–208. [CrossRef]
10. Uchino E, Uemura A, Ohba N. Initial stages of posterior vitreous detachment in healthy eyes of older persons evaluated by optical coherence tomography. Arch Ophthalmol 2001;119:1475–9. [CrossRef]
11. Li D, Sun S, Liang J, et al. Papillary vitreous detachment as a possible accomplice in non-arteritic anterior ischaemic optic neuropathy. Br J Ophthalmol 2023;108(4):607–12. [CrossRef]
12. Kupersmith MJ, Sibony PA, Dave S. Nonarteritic anterior ischemic optic neuropathy induced retinal folds and deformations. Investig Ophthalmol Vis Sci 2017;58(10):4286–91. [CrossRef]
13. Hayreh SS, Jonas JB. Posterior vitreous detachment: Clinical correlations. Ophthalmologica 2004;218(5):333–43. [CrossRef]
14. Rabbani M, Sanjari MS, Sadeghi A, Neshaste-Saz H, Rabbani Z, Khiabani S. A retrospective study of posterior vitreous detachment in patients with non-arteritic anterior ischemic optic neuropathy referred to Rasoul Akram hospital in 2022-2023. BMC Ophthalmol 2025;25(1). [CrossRef]
15. Katz B, Hoyt WF. Intrapapillary and peripapillary hemorrhage in young patients with incomplete posterior vitreous detachment. Signs of vitreopapillary traction. Ophthalmology 1995;102:349–54. [CrossRef]
16. Cibis GW, Watzke RC, Chua J. Retinal haemorrhages in posterior vitreous detachment. Am J Ophthalmol 1975;80:1043–6. [CrossRef]
17. Hondur AM, Moazami G, Hondur G, Tezel TH. Vitreopapillary Findings in Nonarteritic Ischemic Optic Neuropathy versus Healthy Eyes: A Clinical and OCT Comparison. Ophthalmology 2025;132(3):327–34. [CrossRef]
18. Kahraman HG, Guven YZ, Koc F. Effect of vitreopapillary interface adhesions on optic disc: an OCTA study. Int Ophthalmol 2025;45(1):249. [CrossRef]
19. Martin-Gutierrez MP, Petzold A, Saihan Z. NAION or not NAION? A literature review of pathogenesis and differential diagnosis of anterior ischaemic optic neuropathies. Eye 2024;38(3):418–25. [CrossRef]

DOI: 10.14744/eer.2025.07769
Eur Eye Res 2026;6(1):44–49

EUROPEAN EYE RESEARCH

ORIGINAL ARTICLE

Evaluation of tear function after spontaneous granulation healing (laissez–faire technique) in eyelid tumor surgery

Burak Ulas, Altan Atakan Ozcan, Nilufer Topaktas

Department of Ophthalmology, Cukurova University Faculty of Medicine, Adana, Türkiye

Abstract

Purpose: The purpose of this study was to evaluate the tear dynamics and ophthalmological findings in patients who underwent spontaneous granulation healing after eyelid tumor excision.

Methods: Ten eyes of 10 patients with complaints of eyelid tumors were included in the study. Demographic information of the patients, presence of systemic diseases, pathological diagnosis, size of the lesion, size of the excised area, tear dynamics (Schirmer-I test, tear break-up time), and ocular findings of the lid left for secondary healing after excision were evaluated retrospectively.

Results: Ten patients (five females and five males) with a mean age of 68±14.4 years were followed up with spontaneous granulation healing after eyelid excision. The healing time of the eyelids was 21.5±4.9 days. The mean value of the Schirmer-I test was 11.7±1.25 mm before the operation, and the mean Schirmer-I test was 7.42±2.14 mm at the 1st month after the operation ($p<0.001$). Tear break-up time was found to be 12.8±2.36 s preoperatively and 8 ± 2.51 s at the 1st month postoperatively ($p=0.003$). A positive correlation was found between age and the length of the eyelid healing time ($r=0.685$, $p=0.045$).

Conclusion: Spontaneous granulation healing after eyelid tumor excision may lead to a significant reduction in tear stability. Despite these changes in tear dynamics, the technique appears to be a feasible option for eyelid reconstruction, offering satisfactory healing without major complications.

Keywords: Eyelid tumor; Laissez-Faire technique; spontaneous granulation healing; tear dynamics.

Approximately 5–10% of cutaneous malignancies manifest in the periocular region, necessitating careful clinical management due to the functional and cosmetic significance of the area. Excision of these lesions from the area is used quite frequently in the diagnosis and treatment of the disease.[1-3] The main function of the eyelids is to protect the conjunctiva and cornea by providing tear dynamics on the ocular surface.[4,5] Due to previous eyelid surgeries, deterioration in tear dynamics and cosmetic malformations may occur. It is a well-established fact that eyelid tumor surgery can mechanically alter the corneoscleral and conjunctival interface sufficiently to worsen or aggravate dry eye symptoms.[4,5] Ocular surface problems may be seen in patients secondary to the deterioration of eyelid function, and ocular complaints such as burning and stinging, foreign body sensation, and blurred vision may occur.[4-7] To prevent such complications, surgical reconstruction of the eyelid defect following tumor excision has long been the standard and preferred approach.[7,8] As an alternative to this point of view, it was first described by Brown and Fryer in 1957 that the eyelid defect created to reduce the surgical burden

Cite this article as: Ulas B, Ozcan AA, Topaktas N. Evaluation of tear function after spontaneous granulation healing (Laissez–Faire technique) in eyelid tumor surgery. Eur Eye Res 2026;6(1):44–49.

Correspondence: Burak Ulas, M.D. Department of Ophthalmology, Cukurova University Faculty of Medicine, Adana, Türkiye
E-mail: drburakulas@gmail.com

Submitted Date: 24.06.2025 **Revised Date:** 21.08.2025 **Accepted Date:** 22.09.2025 **Available Online Date:** 29.04.2026

could be left to secondary healing.[9-12] These investigators were the first to consider secondary healing after eyelid lesion excision as an alternative to surgical repair.[11-14] Concerns about this technique included disruption of tear dynamics and the development of dry eye syndrome, unpredictability, and long surgical recovery time, as well as poor cosmetic and functional outcomes associated with bleeding and infection.[12-14] Laissez–Faire technique has some surgical advantages: First, secondary intention healing provides a simple, cost-effective, and time-efficient reconstructive option, eliminating the need for complex flap or graft procedures; second, this technique also allows close post-operative monitoring of the surgical field, which is particularly advantageous in tumors with a high risk of recurrence.

The increase in interest in techniques that reduce the duration of surgery time during the pandemic has led to an increase in studies on this subject. The purpose of the present study is to evaluate the tear dynamics and ophthalmological findings of patients who were left to secondary healing after eyelid tumor excision.

Materials and Methods

Ten eyes of 10 patients who applied to Cukurova University Faculty of Medicine, Department of Ophthalmology, Oculoplasty Unit, with the complaint of eyelid mass in 2021–2024 were included in the study. This study was approved by the Cukurova University Faculty of Medicine Institutional Human Subjects Ethical Committee (Approval number: September 01, 2023-136-25). The present study was conducted in accordance with the principles of the Declaration of Helsinki. All patients' written informed consent was provided for participation in the study. All patients underwent extensive ophthalmological examinations before surgery. All patients were operated on with a wide excision technique under local anesthesia.

The margin of excision was marked with a surgical pencil as 4 mm from the border of the visible mass. The mass was excised by making a pentagonal cut. If necessary, cauterization was performed before the end of the surgery to control bleeding. After removal of the mass, the defect was followed up for secondary healing. It was recommended to use topical tobramycin ointment 3 times a day for proper wound care, and to use artificial tears (polyvinyl alcohol 1.4%; povidone 0.6%) 5 times a day to prevent ocular surface damage. Control examinations of the patients were performed on the 1st day, 1st week, and 1st, 3rd, and 6th months postoperatively.

The pathological diagnoses of the patients, the size of the lesion, the size of the excised area, and the ocular findings of the valve left for secondary healing were evaluated. Healing time, follow-up time, visual acuity, Schirmer-I test, fluorescein tear break-up time, dye area status, presence of complications, surgical margins, and the need for additional surgery were evaluated and recorded. Schirmer-I test was performed without anesthesia using special filter paper strips. The Schirmer test strip was placed beneath the temporal lid margin between the palpebral conjunctiva of the lower eyelid and the bulbar conjunctiva of the eye. The eyes were closed for 5 min, and the wet portion of the Schirmer test strip was measured in millimeters. The measurement of fluorescein tear break-up time was performed after 2% sodium fluorescein solution was instilled onto the inferior conjunctival fornix. After that, the tear film was assessed with a cobalt blue filter of a slit lamp to show the first precorneal hypofluorescent spot. The time to interruption of the normal homogeneous fluorescence pattern was recorded in seconds to define the tear break-up time.

Statistical Analysis

For comparison of two related (paired) continuous variables, the paired samples t-test or the Wilcoxon Signed Rank test was used, depending on whether the statistical hypotheses were fulfilled or not. To evaluate the correlations between measurements, the Pearson Correlation Coefficient or Spearman Rank Correlation Coefficient was used, depending on whether the statistical hypotheses were fulfilled or not. Categorical variables were expressed as numbers and percentages, whereas continuous variables were summarized as mean and standard deviation, and as median and minimum-maximum, where appropriate. All analyses were performed using IBM Statistical Package for the Social Sciences Statistics Version 20.0 statistical software package. The statistical level of significance for all tests was considered to be 0.05.

Results

The secondary healing of 10 patients (five females and five males) with a mean age of 68±14.4 years after eyelid tumor excision was followed. Systemic disease was present in 4 (57.1%) of these patients (benign prostatic hypertrophy, hypertension, and thyroid disease). The anterior segment and fundus were normal on slit-lamp examination. Six (60%) of the masses were in the left eye. All of the masses were in the lower eyelid. Six of them were located on the lateral eyelid. The mean area excised in the operation was 0.35 cm^2, and the mean lesion size in the excised area was 0.24 cm^2.

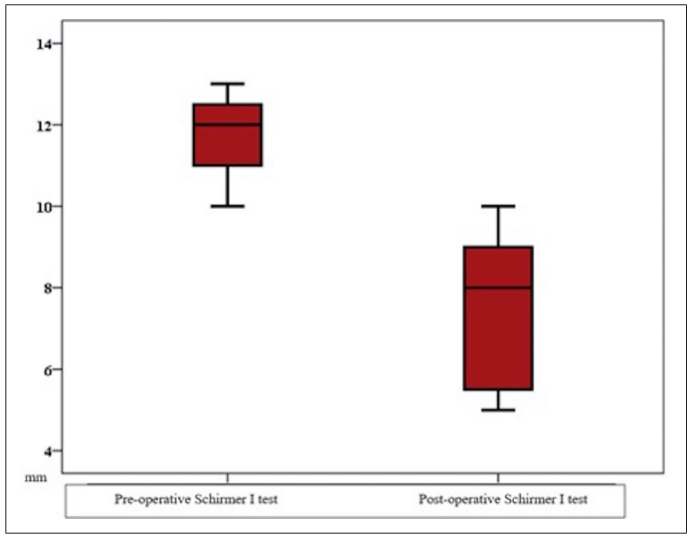

Fig. 1. Pre-operative and post-operative 1st month Schirmer-I test graph of patients operated for eyelid tumor.

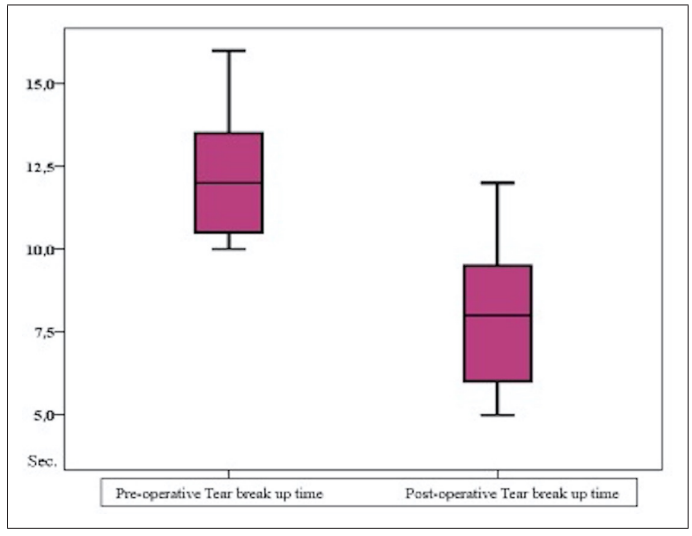

Fig. 2. Pre-operative and post-operative 1st month tear break-up time graph of patients operated for eyelid tumor.

After eyelid tumor excision, 7 (70%) patients were diagnosed with basal cell carcinoma nodular type, 1 patient (10%) with squamous cell carcinoma *in situ*, and 2 (20%) with intradermal nevus. The secondary healing time of the eyelids was 21.5±4.9 days. An average follow-up period of 3.1 months was recorded after the surgical procedure.

In the 1st week after the operation, 4 (40%) patients had a corneal dye area, and 2 (20%) had a conjunctival dye area. There was no dye area in 4 patients (40%). There was no difference between best-corrected visual acuity before and after the operation (average LogMAR 0.7). The mean Schirmer-I test was 11.7±1.25 mm before the operation, and 7.42±2.14 mm at the 1st month postoperatively, and it was found to decrease significantly (p<0.001) (Table 1 and Fig. 1).

Tear break-up time was found to be 12.8±2.36 s preoperatively and 8±2.51 s in the 1st month after the operation, and it decreased significantly (p=0.003) (Fig. 2). At the end of the 3rd month, it was observed that all the eyelids reached their natural contour (Figs. 3-5). A significant correlation was found between age and eyelid healing time (correlation coefficient 0.685, p=0.045). It was determined that gender, lesion size, excision size, and eyelid location (lateral/medial) had no effect on eyelid healing time (p>0.05). None of the patients developed complications during or after the operation, and did not need a secondary operation. Surgical margins were intact in all patients.

Discussion

A variety of techniques have been developed for the reconstruction of eyelid defects following tumor excision. Moesen and Paridaens[15] and Ding *et al*.[16] both reported successful outcomes using local tissue flaps and free grafts, respectively, for lower eyelid reconstruction. Bengoa-González *et al*.[17] described a modified Cutler–Beard technique for upper eyelid reconstruction, which also yielded positive results. These studies collectively suggest that a range of techniques can be effective for eyelid tumor reconstruction, with the choice depending on the specific case and the expertise of the surgeon.[15-17] Allowing the defect in the tissue to heal without additional procedures after surgical intervention is called secondary granulation healing (Laissez–Faire technique).[9,12] Secondary intention healing, a method of allowing wounds to heal on their own

Table 1. Preoperative and postoperative first month Schirmer-I test and tear break-up time results of patients operated for eyelid tumor

	Pre-operative Schirmer-I (mm)	Post-operative Schirmer-I (mm) (1st month)		Pre-operative tear breakup time (sec)	Post-operative tear break-up time (1st month) (sec)	
Mean	11.71	7.42	p<0.001	12.28	8	p=0.003
±Standart deviation	1.25	2.14		2.36	2.5	
Min-Max	10-13	5-10		10-16	5-12	

Fig. 3. Our patient followed up with an eyelid tumor (intradermal nevus); in the pre-operative **(a)**, post-operative 1st day **(b)**, post-operative 7th day (c), post-operative 1st month **(d)**, post-operative 3rd month **(e)** clinical appearance, the improvement pattern, and eyelid contours improved.

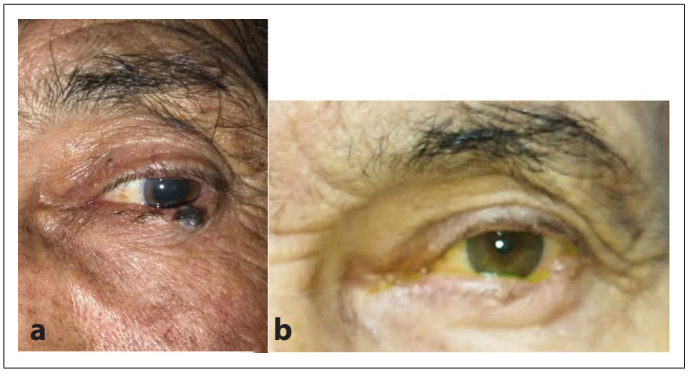

Fig. 4. **(a)** A 76-year-old male patient complaining of a mass in the lower eyelid, whose biopsy result showed nodular basal cell carcinoma. **(b)** At the 1st post-operative control, it was observed that the eyelid had healed and had a natural contour.

without surgical reconstruction, has been found to be a safe and effective option for managing defects following the excision of benign lid margin tumors.[10-14] This technique has also been successfully used in periocular reconstruction, with satisfactory functional and cosmetic results in the majority of cases.[9-12] In some situations, modifications to the reconstruction technique, such as basal and lateral block resection, may be necessary to ensure complete removal of residual tumor tissue.[18]

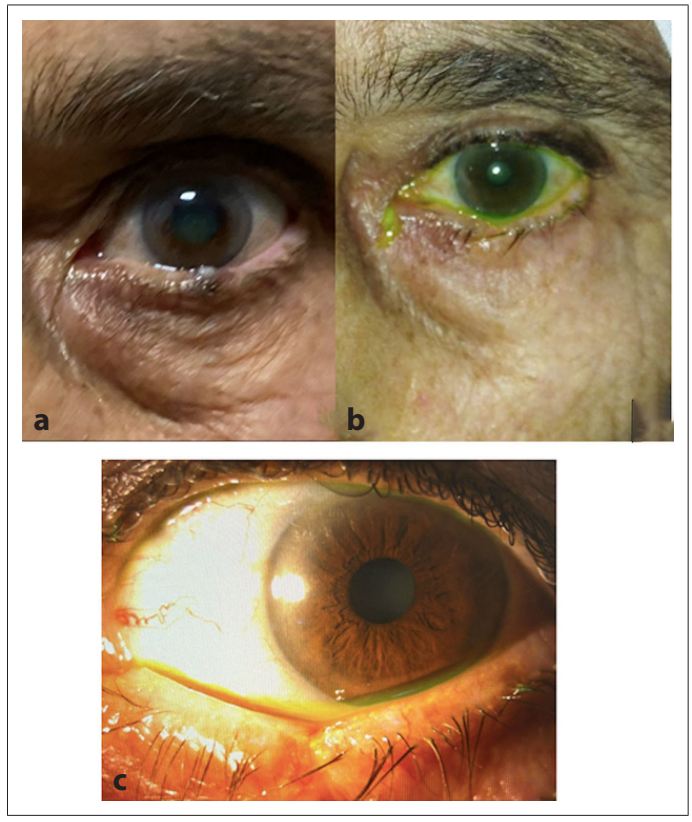

Fig. 5. **(a)** A 77-year-old female patient had a lesion on her left lower eyelid that has been developing for 3 months (pre-operative). Post-operative recovery is observed at the 2nd week **(b)** and 1st month **(c)**.

Spontaneous wound healing after excision of lid tumors has also been shown to lead to satisfactory cosmetic and functional outcomes, with no need for secondary surgery in some cases.[19]

Secondary healing has not been favored as a primary treatment modality, as long recovery times of several weeks are associated with disadvantages such as unpredictable cosmetic results, tissue deterioration, and risk of wound infection.[9-11] However, with the pandemic period, the approach to patients in need of surgery with short operation time and technique, with easy-to-apply techniques, has gained importance. This idea has also increased the interest in secondary healing practices and results. The advantages of this technique are that it is cost-effective, provides a short surgical time, is comfortable for the patient and the surgeon, allows the follow-up of tumors with a high risk of recurrence, and provides a suitable basis for secondary surgery.

According to Lowry *et al.*,[11] 83% of patients (49 out of 59) with periocular skin defects achieved satisfactory functional and cosmetic results. They stated that they observed ectropion, trichiasis, and hypertrophic scar as complications in 10 patients.[11] In their study, Shankar *et al.*[12] achieved

satisfactory functional and esthetic results in 23 of 25 patients (92%). They stated that there is a need for secondary intervention in a patient with viable granulation tissue. Previous studies have demonstrated that variables including defect location, skin pigmentation, wound dimensions, and depth are valuable in forecasting the success of secondary intention healing.[10-14] In addition, Lowry *et al*.[11] described that many of the complications associated with periocular secondary healing were similar and comparable to those reported for primary reconstruction.

In the present study, all 10 patients had good functional and cosmetic results, the surgical margins were intact, and none of them required secondary surgery. In a case series by Mehta,[13] post-operative ectropion necessitated secondary repair in only one of 11 patients who had undergone excision of lesions at the eyelid margin. All cases demonstrated complete wound healing within 6 weeks, with progressive cosmetic enhancement observed over the following 6–8 weeks. The average recovery period in the present study was 4 weeks, whereas esthetic outcomes continued to improve during the following 6–8 weeks.

Kibbi *et al*.,[14] in a series of 39 patients, observed that age had no effect on recovery; it was stated that this result could be due to the fact that only three of the patients were 85 years old and over. However, in the present study, it was determined that age may have an effect on the recovery period, and this result was thought to be due to the more balanced age distribution of our cases. Although there was a positive correlation between age and recovery time in our study, the power analyses were around 60% because the sample size was small, which is below the ideal desired power rate. In the study conducted by Kibbi *et al*.,[14] it was determined that a defect located in the region medial to the healing may cause worse results, and this situation was thought to be due to the wider lesions in that region. Kibbi *et al*.[14] found that the size of the defect had an effect on healing. However, in the present study, the effect of defect location and defect size on healing was not significant. It was thought that the limited number of our sample may have contributed to this result.

Eyelid surgeries can compromise ocular surface homeostasis by altering key anatomical and functional structures such as the lacrimal gland, meibomian glands, and orbicularis oculi muscle, potentially leading to tear film instability and dry eye symptoms.[4,5,20] Disruption of the eyelid margin and periocular tissues during tumor excision may negatively affect tear production and distribution, even in the absence of direct trauma to the lacrimal apparatus. In the present study, tear function was evaluated using the Schirmer-I test and fluorescein tear break-up time, supported by slit-lamp examination of the ocular surface. Both parameters showed a statistically significant decline 1 month postoperatively, indicating an early post-operative deterioration in tear dynamics following secondary healing. Specifically, the Schirmer-I values decreased from a pre-operative mean of 11.7±1.25 mm to 7.42±2.14 mm (P<0.001), whereas tear break-up time dropped from 12.8±2.36 s to 8.0±2.51 s (p=0.003). These findings align with previous reports suggesting that even minimally invasive eyelid procedures may contribute to post-operative dry eye by destabilizing the tear film.[4,5] While none of the patients in this series developed chronic ocular surface complications, the significant short-term reduction in tear metrics highlights the importance of careful post-operative monitoring and supportive treatment, especially during the early healing phase. Further research is warranted to determine whether these changes persist beyond the early post-operative period and to identify potential protective strategies in eyelid tumor surgeries managed with the Laissez–Faire technique.

The pandemic period has led to an increased need for more comfortable and faster techniques for patients and oculoplasty surgeons. The interest in this technique has increased because it provides a short time in surgery, allows tissue follow-up of the excised area for possible recurrences, and tissue care can be made more simply than large reconstruction techniques such as flaps and grafts.

This study has several limitations that should be acknowledged. First, the retrospective design inherently introduces potential selection and information biases, which may affect the generalizability of the findings. Second, the relatively small sample size limits the statistical power of the analyses, particularly in assessing subgroup effects such as lesion location, lesion size, and systemic comorbidities. Another important limitation of the present study is the relatively short follow-up period (mean: 3.1 months), which does not allow for the assessment of late complications or the persistence of tear dysfunction beyond the early post-operative phase. Finally, the absence of a control group undergoing primary reconstruction prevents direct comparison between Laissez-Faire and other reconstructive approaches. In addition, although no patient required secondary surgery in our series, this finding should be interpreted with caution, as the limited number of cases prevents broader generalization of this result. Moreover, the absence of a control group (e.g., patients undergoing primary reconstruction) restricts the ability to compare the Laissez–Faire technique directly with

standard reconstructive approaches, which would have significantly strengthened the conclusions. Despite these limitations, this study contributes valuable preliminary data on the functional implications of spontaneous granulation healing after eyelid tumor excision and highlights the need for prospective, controlled studies with larger cohorts.

Conclusion

While the Laissez-Faire technique may represent a feasible and well-tolerated alternative for eyelid reconstruction following tumor excision, our findings demonstrate a significant short-term decline in tear function parameters. This highlights the importance of careful patient selection and close post-operative monitoring. Given the small sample size and limited follow-up, further prospective studies with larger cohorts and control groups are needed to clarify the long-term safety, efficacy, and functional outcomes of this approach.

Ethics Committee Approval: This study was approved by Cukurova University Faculty of Medicine Non-Interventional Clincal Trials Ethics Committee (01.09.2023 date; number 136).

Informed Consent: Written informed consent was obtained from the patients.

Peer-review: Externally peer-reviewed.

Authorship Contributions: Concept: A.A.O., B.U. NT; Design: A.A.O., B.U.; Supervision: A.A.O.; Resource: B.U., N.T.; Materials: A.A.O., B.U., NT.; Data Collection and/or Processing: A.A.O., B.U., N.T.; Analysis and/or Interpretation: A.A.O., B.U.; Literature Search: A.A.O., B.U., NT; Writing: A.A.O., B.U., N.T.; Critical Reviews: A.A.O, B.U.

Conflict of Interest: The authors declared that they have no conflict of interest.

Use of AI for Writing Assistance: Not declared.

Financial Disclosure: The authors declared that this study received no financial support.

REFERENCES

1. Ulas B, Ozcan A, Sulanc B, Acikalin A. Evaluation of histopathology results in eyelid tumors: 20-year experience at a Turkish tertiary referral center. J Fr Ophthalmol 2025;48:104543. [Crossref]
2. Echchaoui A, Benyachou M, Houssa A, et al. Management of eyelid carcinomas: retrospective bicentric study of 64 cases and review of the literature. J Fr Ophthalmol 2016;39:187–94. [Crossref]
3. Lasudry J. Management of eyelid tumors: general considerations. J Fr Ophtalmol 2011;34:741–54. [Crossref]
4. Gonnermann J, Klein JP, Klamann MKJ, et al. Dry eye symptoms in patients after eyelid reconstruction with full-thickness eyelid defects: using Tomey TG-1000 thermographer. Ophthalmic Research 2012;48:192–8. [Crossref]
5. Aksu Ceylan N, Yeniad B. Effects of Upper Eyelid Surgery on the Ocular Surface and Corneal Topography. Turk J Ophthalmol 2022;52:50–6. [Crossref]
6. Sendul SY, Akpolat C, Yılmaz Z, Eryilmaz OT, Guven D, Kabukcuoglu F. Clinical and pathological diagnosis and comparison of benign and malignant eyelid tumors. J Fr Ophtalmol 2021;44:537–43. [Crossref]
7. Poignet B, Gardrat S, Dendale R, et al. Basal cell carcinomas of the eyelid: results of initial surgical management. J Fr Ophtalmol 2019;42:1094–9. [Crossref]
8. Brown JB, Fryer MP. Carcinoma of eyelids and canthal region. Geriatrics 1957;12:181–4.
9. DaCosta J, Oworu O, Jones CA. Laissez-faire: how far can you go? Orbit 2009;28:12–15. [Crossref]
10. Zitelli JA. Secondary intention healing: an alternative to surgical repair. Clin Dermatol 1984;2:92–106. [Crossref]
11. Lowry JC, Bartley GB, Garrity JA. The role of secondintention healing in periocular reconstruction. Ophthal Plast Reconstr Surg 1997;13:174–88. [Crossref]
12. Shankar J, Nair RG, Sullivan SC. Management of peri-ocular skin tumours by laissez-faire technique: analysis of functional and cosmetic results. Eye (Lond) 2002;16:50–53. [Crossref]
13. Mehta HK. Spontaneous reformation of lower eyelid. Br J Ophthalmol 1981;65:202–8. [Crossref]
14. Kibbi N, Khan Y, Leffel DJ, Christensen SR, Suozzi KC. Predicting outcomes following second intent healing of periocular surgical defects, Arch Dermatol Res. 2021;313:483–9. [Crossref]
15. Moesen I, Paridaens D. A technique for the reconstruction of lower eyelid. Br J Ophthalmol 2007;91:1695–7. [Crossref]
16. Ding JP, Chen B, Yao J. Lateral orbital propeller flap technique for reconstruction of the lower eyelid defect. Ann R Coll Surg Engl 2018;100:e103–5. [Crossref]
17. Bengoa-González A, Laslau BM, Martin-Clavijo A, Mencia-Gutierrez E, Lago-Llinas MD. Reconstruction of upper eyelid defects secondary to malignant tumors with a newly modified Cuttler-Beard technique with tarsoconjunctival flap. J Ophthalmol 2019;6838415. [Crossref]
18. Sharma RL, Sharma ML, Mahajan D. Basal and lateral block resection for residual eyelid tumor during second stage reconstruction at 3 weeks. Archives of International Surgery 2015;5:177.
19. Lee JM, Lee H, Lee TE, Park M, Baek S. Second intention healing after shave excision of benign tumors on the lid margin. Ann Dermatol 2011;23:463–7. [Crossref]
20. Ulas B, Ozcan A, Yar K, Kaya I, Binokay H. Evaluation of visual field and ocular surface parameters by clinical comparison after blepharoplasty for dermatochalasis. J Fr Ophthalmol 2024;47:104135. [Crossref]

DOI: 10.14744/eer.2025.09821
Eur Eye Res 2026;6(1):50–59

EUROPEAN EYE RESEARCH

ORIGINAL ARTICLE

The impact of repeated intravitreal dexamethasone implants on the cornea in patients with macular edema due to retinal vein occlusion

Ulviye Kivrak,[1,2] Nesrin Tutas Gunaydin,[3] Selin Ciftci,[1] Erdi Karadag,[1] Fatma Isil Sozen Delil,[1] Guzide Akcay[1]

[1]Department of Ophthalmology, University of Health Sciences, Kartal Dr. Lütfi Kırdar City Hospital, Istanbul, Turkiye
[2]Department of Advanced Neurologıcal Sciences, Istanbul University Institute of Graduate Studies in Health Sciences, Istanbul, Turkiye
[3]Department of Ophthalmology, Istanbul Arel University, Istanbul, Turkiye

Abstract

Purpose: This study aimed to assess the impact of repeated 700 µg intravitreal dexamethasone implant (IDI) applications on corneal parameters in patients with macular edema (ME) secondary to retinal vein occlusion (RVO).

Methods: This retrospective pilot study included 62 patients with RVO and 63 control subjects. RVO patients received two or more IDI treatments. Detailed eye examinations, including posterior segment evaluations, corneal topography, and endothelial parameters, were retrieved from the patients' medical records.

Results: The study involved 23 patients with central RVO (CRVO) and 39 with branch RVO (BRVO). Ischemic RVO was present in 52.2% of CRVO and 48.7% of BRVO patients. The mean age of RVO patients was 64.79±10.00 years; for the control group, it was 65.03±9.02 years (p=0.068). Patients received an average of 6.58±3.38 IDI injections. Eyes treated with IDI showed significantly worse best-corrected visual acuity and increased central macular thickness compared to fellow eyes and controls (p<0.001 and p=0.031, respectively). Central corneal thickness was significantly thinner in eyes that received IDI, and anterior corneal depth, anterior and posterior corneal curvature, total high-order corneal aberrations, trefoil, and spherical values were significantly higher (p<0.05). In addition, endothelial cell density was significantly lower, and the mean cell area, minimum cell area, and maximum cell area were higher in the eyes that received IDI (p<0.05).

Conclusion: Repeated IDI injections adversely affect corneal topographic and endothelial parameters in RVO-related ME. These changes were associated with the type and localization of RVO, ischemic status, number of IDI administrations, and lens status.

Keywords: Corneal endothelium; corneal topography; intravitreal dexamethasone implant; retinal vein occlusion; specular microscopy.

* This manuscript has been oraly represented at 47th National Spring Symposium of the Turkish Ophthalmological Association (TOD).

Cite this article as: Kivrak U, Tutas Gunaydin N, Ciftci S, Karadag E, Sozen Delil FI, Akcay G. The impact of repeated intravitreal dexamethasone implants on the cornea in patients with macular edema due to retinal vein occlusion. Eur Eye Res 2026;6(1):50–59.

Correspondence: Ulviye Kivrak, M.D. Department of Ophthalmology, University of Health Sciences, Kartal Dr. Lütfi Kırdar City Hospital; Department of Advanced Neurologıcal Sciences, Istanbul University Institute of Graduate Studies in Health Sciences, Istanbul, Turkiye
E-mail: dr.ulviyekivrak@hotmail.com
Submitted Date: 18.06.2025 **Revised Date:** 11.09.2025 **Accepted Date:** 23.09.2025 **Available Online Date:** 29.04.2026

Retinal vein occlusion (RVO) is the second most common retinal vascular disease, presenting as central RVO (CRVO), hemi-central, or branch RVO (BRVO).[1,2] In RVO, increased pressure in the capillary plexus and reduced blood flow lead to ischemia. Secondary to ischemia, vascular endothelial growth factor (VEGF) and pro-inflammatory cytokines increase, causing damage to the blood-retinal barrier and increased vascular permeability. Consequently, macular edema (ME), ischemia, and complications arising from retinal neovascularization develop.[3] In RVO, ME is the most frequent cause of vision loss and is treated with intravitreal corticosteroids and anti-VEGF agents in CRVO and BRVO. Laser therapy may also be used for patients with BRVO.[1]

The intravitreal dexamethasone implant (IDI) (Ozurdex, Allergan Inc., Irvine, California, USA) is a biodegradable, slow-release implant containing 700 µg of preservative-free dexamethasone (DEX). IDI exhibits anti-inflammatory properties and reduces VEGF release.[4,5] Unlike most anti-VEGF treatments, it has a longer duration of effect, lasting 4–6 months, thereby improving patient adherence to treatment.[6]

The SHASTA study demonstrated that IDI is effective and safe in improving visual acuity and central macular thickness (CMT) in patients with RVO receiving multiple IDI treatments for ME. This study reported no adverse effects other than cataract progression and ocular hypertension, which have been observed in other studies.[7] Kwak *et al*.[8] showed that 400 µg IDI had no toxic effects in rabbit corneal, lens, and retinal models. In addition, several studies have investigated the impact of a single application of IDI on the corneal endothelium in patients with RVO.[9,10] Only one study reported no changes in corneal endothelial parameters after an average of 1.5±0.8 (range, 1–3) IDI injections in 12 patients with RVO for ME.[9] However, no study has shown the effect of repeated IDI implant application in ME due to RVO on both corneal topographic and specular microscopic parameters in cases that require much more frequent procedures.

This study aimed to evaluate changes in corneal topographic and endothelial parameters, as measured by specular microscopy, in patients with ME due to RVO who underwent multiple IDI treatments.

Materials and Methods

This retrospective study was conducted between January 2019 and November 2023 at the Department of Ophthalmology of Kartal Dr. Lütfi Kırdar City Hospital. Ethical approval was obtained from the hospital's ethics committee, and the study was conducted in accordance with the principles of the Declaration of Helsinki (Protocol No: 2023/514/250/12). The study included 62 patients aged >18 years who required two or more injections due to ME secondary to RVO and 63 age- and sex-matched healthy controls with minor symptoms such as refractive errors. Exclusion criteria were the presence of any of the following: coexisting neurologic or metabolic disease, corneal disease, infection, endothelial cell count (ECN) <1000/mm^2, retinal disease other than RVO, uveitis, optic nerve disease, contact lens use, previous ocular trauma or surgery except for cataract surgery (patients with a history of complicated cataract surgery or those whose interval between the initial IDI injection and cataract surgery was <6 months were excluded from the study), and intraocular pressure (IOP) that could not be controlled with antiglaucoma treatment.

Patient data were retrieved from the medical records, including sex, laterality, best-corrected visual acuity (BCVA) using Snellen charts, IOP using a Goldmann applanation tonometer, pachymetry, findings of biomicroscopic examination of the anterior and posterior segments, fundus fluorescein angiography (FFA) images, optical coherence tomography (OCT) measurements, corneal topographic and specular microscopic parameters, number of IDI administered, lens status, and any comorbidities.

Measurements of both eyes of patients with RVO, and only one eye of healthy controls, were randomly selected. The retinal nerve fiber layer (RNFL) and CMT were measured using a spectral-domain OCT (Topcon, Japan) device. Before IDI treatment, all patients with RVO underwent evaluation with FFA (Canon CF-1® system, Japan). Patients were classified into two groups: CRVO and BRVO, based on the location of RVO, and further categorized as ischemic or non-ischemic according to the extent of ischemia.

IDI was performed by an experienced ophthalmologist. Following the application of proparacaine hydrochloride (Alcaine 0.5%, Alcon Pharmaceuticals, Couver, Belgium) and disinfection of the eyelid and ocular surface with 5% povidone-iodine, the IDI was injected into the vitreous cavity through the pars plana using a 22-gauge (G) needle with a preloaded implant applicator, positioned 3.5 and 4 mm behind the limbus for phakic and pseudophakic eyes, respectively. After the IDI injection, IOP was measured for each patient, and retinal artery perfusion was evaluated. To prevent infection, all patients were prescribed tobramycin 0.3% (Tobradex, Alcon, UK) 4 times daily for 1 week following IDI. During the follow-up visits, the number of

IDI injections administered due to ME development was recorded for each patient. Detailed information regarding the procedure was provided to all patients before IDI treatment, and written consent was obtained from each participant before treatment.

The corneal topographic parameters of all participants were evaluated by the same experienced technician using the Scheimpflug imaging system (Sirius Topography, CSO, Florence, Italy). To optimize corneal imaging, the participants were instructed to refrain from blinking immediately before each measurement to eliminate ocular surface dryness. Anterior segment parameters, including central corneal thickness (CCT), anterior chamber depth (ACD), corneal volume (CV), anterior and posterior corneal curvature (ACC, PCC, respectively), and the root mean square values of total high-order corneal aberrations (HOAs) within the central 6 mm of the cornea were recorded.

In addition, corneal endothelial cell parameters of all participants were evaluated using the central analysis method by the same experienced technician using non-contact specular microscopy (Tomey EM-4000; Tomey Corporation). This method determined results using the ImageNet software program after manually marking at least 110 neighboring cells. The ECN, endothelial cell density (ECD), mean cell area (MCA), minimum cell area (CAmin), maximum cell area (CAmax), coefficient of variation in cell area (CV%), and hexagonal cell ratio (HEX) were recorded for all participants.

Statistical Analysis

Statistical analyses were performed using R version 2.15.3 (R Core Team, Vienna, Austria, 2013). Data reporting included mean, standard deviation, frequency, and percentage. The normality of the quantitative data was assessed using the Shapiro–Wilk test and graphical examinations. An independent samples *t*-test was used for pairwise comparisons of quantitative variables, showing a normal distribution between the two groups. A one-way analysis of variance was used for comparisons involving more than two groups, and a paired samples *t*-test was used for comparisons within groups. Pearson's Chi-squared test was used to compare categorical data. Pearson's correlation analysis was used to determine the level of relationship between quantitative variables. Fisher's z-transformation was used to compare correlation coefficients. Statistical significance was set at $P<0.05$. An a priori power analysis was conducted using G*Power 3.1 to determine the minimum required sample size. Assuming a medium effect size (Cohen's d=0.5), a significance level of 0.05, and a statistical power of 0.80, the required total sample size was calculated as 102 participants (51 per group).

Results

This study included the eyes of 23 patients with CRVO and 39 patients with BRVO (38.5% inferior BRVO and 61.5% superior BRVO), and randomly selected only one eye of 63 eyes from control patients. According to the FFA results, 52.2% (n=12) of patients with CRVO and 48.7% (n=19; 14 superior, five inferior) of patients with BRVO were diagnosed with ischemic RVO. The mean age of RVO patients was 64.79±10.00 years, compared to 65.03±9.02 years in the control group (P=0.068). Among patients, the mean number of IDI administrations was 6.58±3.38 (2-14). Laser treatment for ischemia was added to the treatment of the 26 patients with RVO. Thirty-eight patients had a history of uncomplicated cataract surgery, 24 patients were phakic, and all control group patients were phakic. Patients whose IOP remained 21 mmHg or higher, despite medical treatment, were excluded from the study. There were no statistically significant differences in age or sex between the patient and control groups. The demographic and clinical characteristics of the study participants are presented in Table 1.

Significant differences in BCVA and CMT were observed upon analysis of the eyes in the IDI group, the fellow eyes, and the control group. BCVA was significantly lower in eyes that received IDI than in fellow eyes and the control group ($P<0.001$, for all comparisons), whereas CMT was significantly higher (P=0.031 and P=0.001, respectively). There were no significant differences between the groups regarding IOP and mean RNFL thickness.

In terms of corneal topographic parameters, CCT was significantly thinner in eyes that received IDI than in fellow eyes and the control group ($P<0.001$). ACD was statistically deeper in eyes that received IDI than in fellow eyes and the control group ($P<0.001$ for all comparisons). ACC and PCC were significantly higher in eyes receiving IDI than in the control group ($P<0.001$ for all). Total HOAs, including trefoil and spherical aberrations, were also significantly higher in eyes that received IDI than in fellow eyes and the control group ($P<0.05$) (Table 2).

In the endothelial parameters, ECN and ECD were significantly lower in eyes that received IDI compared to fellow eyes and the control group ($P<0.001$ for all comparisons). The MCA, CAmin, and CAmax were significantly higher in eyes that received IDI than in fellow eyes and the control group ($P<0.005$, for all comparisons) (Table 2).

Table 1. Demographic and clinic features of all study participants

Parameters	RVO patients (%)	Control group (%)	All participant (%)	*P*
Age (mean±SD)	64.79±10.00	65.03±9.02	64.87±10.67	[a]0.068
Gender				
Female/male, *n* (%)	31 (50)/31(50)	42 (66.7%)/21 (33.3)		[b]0.059
Parameters	**BRVO patients**	**CRVO patients**	**RVO patients**	***P***
IDI number (mean±SD)	5.26±3.19	7.13±3.68	6.58±3.38	[a]0.329
Ischemic status				
Ischemic RVO	19 (48.7)	12 (52.2)	31 (50)	[b]0.793
Non-ischemic RVO	20 (51.3)	11 (47.8)	31 (50)	
Treatment				
IDI	22 (56.4)	14 (60.9)	36 (58.1)	[b]0.731
IDI+LASER	17 (43.6)	9 (39.1)	26 (41.9)	
Laterality of eye				
Right	20 (51.3)	13 (56.5)	33 (53.2)	[b]0.690
Left	19 (48.7)	10 (43.5)	29 (46.8)	

RVO: Retinal vein occlusion, BRVO: Branch retinal vein occlusion, CRVO: Central retinal vein occlusion, IDI: Intravitreal dexamethasone implant, [a]Independent *t*-test, [b]Pearson Chi-square test

Table 2. Comparison of corneal topographic and specular microscopy parameters of participants

Parameters	The eye of RVO[1]	The fellow eye[2]	Control eye[3]	[a]p (1 and 2)	[a]p (1 and 3)	[b]p (2 and 3)
BCVA (logMAR)	0.72±0.45	0.10±0.14	0±0	**<0.001***	**<0.001***	0.285
IOP (mm Hg)	15.48±3.62	14.92±3.08	15.37±3.04	0.173	0.143	0.139
Average RNFL (µm)	100.94±22.71	104.13±12.52	105.92±11.48	0.164	0.126	0.406
CMT (µm)	280.03±68.56	257.80±36.53	247.94±24.41	**0.031***	**0.001***	0.054
CCT (µm)	520.24±37.53	536.13±33.17	542.75±29.47	0.057	**<0.001***	0.054
CV, mm^3	55.69±5.38	57.23±11.64	56.36±2.77	0.302	0.384	0.566
ACD, mm	3.71±0.61	3.42±0.54	3.32±0.42	**<0.001***	**<0.001***	0.224
ACC, D	9.54±7.67	6.23±5.72	4.95±2.04	0.131	**<0.001***	0.235
PCC, D	18.95±13.73	15.90±10.50	11.40±4.98	0.610	**<0.001***	0.545
Total HOAs	0.84±0.61	0.63±0.46	0.58±0.27	**0.034***	**0.003***	0.111
COMA	0.43±0.40	0.40±0.30	0.36±0.18	0.554	0.178	0.307
Trefoil	0.47±0.53	0.30±0.32	0.25±0.17	**0.017***	**0.002***	0.056
Spheric	0.32±0.25	0.25±0.18	0.24±0.10	**0.036***	**0.026***	0.798
ECD (cells/mm^2)	2149.55±463.87	2462.35±342.72	2554.94±277.19	**<0.001***	**<0.001***	0.099
CV (%)	39.90±7.31	38.94±6.61	38.40±4.99	0.384	0.180	0.608
HEX (%)	43.53±6.76	45.58±6.76	45.79±7.65	0.065	0.083	0.869
Mean cell area	490.03±127.17	416.71±89.25	395.84±42.87	**<0.001***	**<0.001***	0.097
Min cell area	116.60±37.75	100.11±27.09	98.90±20.46	**0.008***	**0.002***	0.779
Max cell area	1227.06±459.56	993.71±377.60	929.44±218.55	**0.001***	**<0.001***	0.248
ECN	191.55±57.63	226.53±42.90	230.97±38.60	**<0.001***	**<0.001***	0.544

BCVA: Best-corrected visual acuity, RNFL: Retinal nerve fiber layer, CMT: Central macular thickness, IOP: Intraocular pressure, CCT: Central corneal thickness, CV: Corneal volume, ACD: Anterior chamber depth, ACC: Anterior corneal curvature, PCC: Posterior corneal curvature, HOA: High order aberration, ECD: Endothelial cell density, CV (%): Coefficient of variation of cell size, HEX: Percentage of hexagonality, D: Diopters, AL: Axial length, ECN: Endothelial number. [a]Independent groups *t*-test, [b]Dependent groups *t*-test, * $P<0.05$

Regarding the differences between eyes that received IDI and fellow eyes in RVO patients, positive correlations were found between the number of IDI injections and BCVA (logMAR) (r=0.278, P=0.029) as well as CV% (r=0.287, P=0.024). Negative correlations were observed between the number of IDI injections and both CCT (r=–0.259, P=0.042) and HEX (r=–0.354, P=0.005). No statistically significant relationships were found between the number of IDI injections and the other corneal topographic and endothelial parameters (Table 3). According to the relationship between the number of IDI injections and both corneal topographic and endothelial parameters based on lens status, no significant correlations were observed in phakic eyes receiving IDI injections (P>0.05). In pseudophakic eyes that received IDI, a positive correlation was found between the number of IDI injections and the CV% (r=0.330, P=0.043). Negative correlations were found between the number of IDI injections and CCT (r=–0.334, P=0.040) and HEX (r=–0.349, P=0.012). There were no statistically significant differences in the correlation levels between the number of IDI injections and other parameters based on lens status (P>0.05) (Table 4).

Table 3. Comparison of the differences between the eye with RVO and the fellow eye by the number of IDI

The difference between the RVO eye and the fellow eye	IDI number	
	r	*P*
BCVA (logMAR)	0.278	**0.029***
IOP (mm Hg)	0.157	0.222
Average RNFL (μm)	0.191	0.137
CMT (μm)	0.047	0.717
CCT (μm)	–0.259	**0.042***
CV, mm^3	–0.032	0.807
ACD, mm	0.158	0.220
ACC, D	–0.132	0.310
PCC, D	–0.184	0.151
Total HOAs	0.165	0.200
COMA	0.008	0.950
Trefoil	–0.172	0.180
Spheric	–0.070	0.589
ECD (cells/mm^2)	–0.146	0.258
CV (%)	0.287	**0.024***
HEX (%)	–0.354	**0.005***
Mean cell area	0.103	0.426
Min cell area	0.082	0.524
Max cell area	0.088	0.495
ECN	–0.190	0.139

IDI: Intravitreal dexamethasone implant, BCVA: Best-corrected visual acuity, RNFL: Retinal nerve fiber layer, CMT: Central macular thickness, IOP: Intraocular pressure, CCT: Central corneal thickness, CV: Corneal volume, ACD: Anterior chamber depth, ACC: Anterior corneal curvature, PCC: Posterior corneal curvature, HOA: High order aberration, ECD: Endothelial cell density, CV (%): Coefficient of variation of cell size, HEX: Percentage of hexagonality, D: Diopters, AL: Axial length, ECN: Endothelial number. r=Pearson correlation coefficient, *P<0.05.

Significant differences were found based on the classification of RVO into BRVO (superior and inferior BRVO) and CRVO groups, as well as for BCVA and spherical HOA values, according to the differences between the eyes receiving IDI and the fellow eyes in patients with RVO. The BCVA was significantly lower in the CRVO group than in the BRVO group (P=0.012). *Post hoc* evaluations using the Bonferroni test indicated that this difference was significant between the inferior BRVO and CRVO groups (P=0.009), whereas no differences were observed among the other groups (P>0.05). A statistically significant difference was found for spherical values when compared based on RVO localization (P=0.033). *Post hoc* evaluations using the Bonferroni test revealed a significant difference between the superior BRVO and CRVO groups (P=0.043), with no differences observed among the other groups (P>0.05) (Table 5). Regarding ischemic condition, the ischemic group exhibited significantly lower BCVA and CMT values and higher HOA and COMA values than the non-ischemic group (P=0.025, P=0.017, P=0.043, P=0.002, respectively) (Table 6).

Discussion

IDI, the first approved medical treatment for ME secondary to RVO, has shown significant improvement in BCVA and CMT after a single IDI treatment.[11] Studies have demonstrated a similar efficacy and safety profile to that of the initial treatment when IDI is repeated after 6 months, although an increase in cataract cases has been reported.[12] The most common adverse effects observed after IDI include cataracts and increased IOP.[12-14] In this study, we evaluated patients who received multiple IDI treatments for RVO-related ME and observed changes in corneal topographic and specular microscopic parameters associated with the type and localization of RVO, ischemic status, number of IDI treatments, and lens status.

Some studies have investigated corneal topographic changes in eyes that underwent IDI application.[10,15] Güler

Table 4. Comparison of differences between the eye with RVO and the fellow eye according to IDI number and lens status

The difference between the RVO eye and the fellow eye	Phacic		Pseudophacic		Comparing correlation levels	
	IDI number		IDI number			
	r	p	r	*P*	z	*P*
CCT (μm)	−0.040	0.852	−0.334	**0.040***	1.113	>0.05
CV, mm^3	−0.053	0.806	−0.017	0.919	0.131	>0.05
ACD, mm	0.161	0.451	0.053	0.751	0.396	>0.05
ACC, D	0.054	0.805	−0.236	0.155	0.676	>0.05
PCC, D	−0.240	0.259	−0.195	0.240	0.171	>0.05
Total HOAs	0.209	0.326	0.071	0.670	0.511	>0.05
COMA	0.194	0.363	−0.056	0.737	0.915	>0.05
Trefoil	0.022	0.917	−0.225	0.173	0.909	>0.05
Spheric	0.049	0.819	−0.117	0.484	0.603	>0.05
ECD (cells/mm^2)	−0.053	0.805	−0.039	0.816	0.051	>0.05
CV (%)	0.030	0.888	0.330	**0.043***	1.133	>0.05
HEX (%)	−0.183	0.393	−0.349	**0.032***	0.649	>0.05
Mean cell area	0.007	0.972	0.006	0.971	0.004	>0.05
Min cell area	0.266	0.210	−0.033	0.846	1.107	>0.05
Max cell area	−0.096	0.656	0.049	0.769	0.527	>0.05

CCT: Central corneal thickness, CV: Corneal volume, ACD: Anterior chamber depth, ACC: Anterior corneal curvature, PCC: Posterior corneal curvature, HOA: High order aberration, ECD: Endothelial cell density, CV (%): Coefficient of variation of cell size, HEX: Percentage of hexagonality, D: Diopters, AL: Axial length, ECN: Endothelial number. r=Pearson correlation coefficient *P<0.05

et al. [10] found no significant change in CCT after a single-dose IDI treatment in patients with RVO. In their study, they attributed this to the fact that the IOP increase that may occur due to the DEX implant does not increase enough to disrupt the endothelial pump function or directly change the mechanical properties of the cornea, which has non-linear viscoelastic tissue properties.[10,16] Bayat *et al*. [15] reported a statistically significant decrease in CCT in the 1st month after single-dose IDI application due to diabetes mellitus (DM)-related ME, linking this change to apoptosis in the corneal endothelium induced by steroids. Nevertheless, other corneal parameters did not show significant changes in these studies.[10,15] In our study, a statistically significant reduction in CCT was observed in eyes that received multiple IDI treatments compared to both fellow eyes and the control group. In addition, significant increases were noted in other corneal topographic parameters, including ACD, ACC, PCC, total HOAs, and spherical and trefoil aberrations. We hypothesized that the thinning observed in CCT and changes in corneal curvature could be attributed to increased corneal DEX concentration due to repeated IDI applications and the pharmacokinetic properties of DEX in the eye. Naageshwaran's study on rabbits' eyes showed that the highest concentration after intracameral DEX injection was in the cornea, followed by the iris-ciliary body and aqueous humor, respectively.[17] This was attributed to the diffusion of lipophilic DEX from the corneal endothelium to the stroma and epithelium. The avascular cornea serves as a reservoir for DEX due to its lack of rapid elimination. Previous studies have also shown that glucocorticoid receptors are present in epithelial, keratocyte, and endothelial cells of the cornea, with low concentrations promoting cell proliferation. In contrast, high doses may induce apoptosis and necrosis in epithelial and endothelial cells.[18] Therefore, the increased DEX concentration may induce apoptosis in corneal cells, which could be the underlying cause of the observed changes in the cornea; however, no histopathological or biochemical verification has been conducted to support this view. Some studies have investigated topographic changes in the cornea after 20-23-25-27G vitrectomy,[19-21] and it was also considered that wound healing and contraction in repeated sclerotomies performed during IDI application may contribute to some changes in corneal curvature. However, no study has yet investigated the simultaneous changes in relation to parameters such as the application

Table 5. Comparison of the difference between the eye with RVO and the fellow eye according to the location of retinal vein occlusion

The difference between the RVO eye and the fellow eye	CRVO (*n*=23)	BRVO (*n*=39)		*P*
		Inferior (*n*=15)	Superior (*n*=24)	
BCVA (logMAR)	0.79±0.46	0.34±0.41	0.64±0.49	**0.012***
IOP (mm Hg)	0.83±3.17	1.19±3.08	0.08±3.48	0.573
Average RNFL (μm)	2.3±24.14	−1.5±9.37	−9.63±12.45	0.059
CMT (μm)	21.04±81.41	−2.75±39.39	19.43±68.11	0.316
CCT (μm)	−1.95±23.4	−8.06±22.67	2.67±22.63	0.216
CV, mm^3	0.96±3.42	−1.5±7.67	−3.78±17.27	0.405
ACD, mm	0.32±0.51	0.37±0.75	0.19±0.45	0.529
ACC, D	2.41±6.27	−0.31±8.17	0.83±6.8	0.281
PCC, D	−0.7±22.34	−2.44±11.07	−0.83±11.51	0.919
Total HOAs	0.2±0.52	0.16±0.75	0±0.49	0.345
COMA	0.03±0.29	0.01±0.48	0.06±0.41	0.917
Trefoil	0.24±0.48	0.18±0.52	0.01±0.29	0.197
Spheric	0.16±0.26	0.12±0.24	0.04±0.25	**0.033***
ECD (cells/mm^2)	338.85±519.99	403.63±701.07	379.25±355.39	0.695
CV (%)	−0.87±10.94	2.88±8.05	1.17±6.32	0.472
HEX (%)	−0.43±6.79	−3.38±11.42	−2.46±8.03	0.606
Mean cell area	82.44±149.83	84.38±211.66	64.04±86.84	0.583
Min cell area	22.64±40.34	19.56±47.56	17.5±34.06	0.320
Max cell area	248.69±433.31	242.38±501.6	149.63±363.52	0.446
ECN	−43.88±96.13	−37.79±71.44	−29.96±51.71	0.806

BRVO: Branch retinal vein occlusion, CRVO: Central retinal vein occlusion, BCVA: Best-corrected visual acuity, RNFL: Retinal nerve fiber layer, CMT: Central macular thickness, IOP: Intraocular pressure, CCT: Central corneal thickness, CV: Corneal volume, ACD: Anterior chamber depth, ACC: Anterior corneal curvature, PCC: Posterior corneal curvature, HOA: High order aberration, ECD: Endothelial cell density, CV (%): Coefficient of variation of cell size, HEX: Percentage of hexagonality, D: Diopters, AL: Axial length, ECN: Endothelial number. One-way analysis of variance, *P<0.05.

site and injection frequency. Grandinetti *et al*. [19] observed no changes in corneal parameters following 23G and 25G vitrectomy. In contrast, changes in corneal curvature were noted in the 1st month post-20G vitrectomy, returning to pre-operative levels by the 3rd month. Slusher *et al*. [20] specifically noted an increased incidence of astigmatism following repeated pars plana vitrectomy through the same sclerotomy sites.

Studies evaluating its impact on human corneal endothelial cells have also been conducted.[22,23] Jamil *et al*. [22] used specular microscopy to demonstrate that the use of 0.4 mg intracameral DEX did not have a toxic effect on the corneal endothelium. Ilhan *et al*. [9] found no changes in the corneal endothelium of patients with RVO 6 months after IDI treatment for ME. In this study, 19 patients with ME due to RVO received a single-dose IDI application, and 12 patients had an average of 1.5±0.8[1-3] IDI injections. Güler *et al*. [10] found no significant change in corneal endothelial parameters in the 1st month after single-dose IDI in patients with RVO, but observed a significant decrease in ECD in the 3rd month. Bayat *et al*.[15] reported a reduction in ECD in the 1st month after single-dose IDI application in

Table 6. Comparison of the differences between the eye with RVO and the fellow eye according to ischemic status

The difference between the RVO eye and the fellow eye	Ischemic (*n*=31)	Non-ischemic (*n*=31)	*P*
BCVA (logMAR)	0.76±0.47	0.49±0.48	**0.025***
IOP (mm Hg)	0.39±3.32	0.74±3.17	0.669
Average RNFL (µm)	0.16±18.57	−0.55±15.62	0.548
CMT (µm)	4.63±82.62	14±50.33	**0.017***
CCT (µm)	−4.9±16.32	1.32±24.25	0.240
CV, mm^3	−3.29±16.3	0.21±1.68	0.244
ACD, mm	0.32±0.64	0.26±0.47	0.677
ACC, D	2.77±6.99	−0.17±6.33	0.091
PCC, D	−2.74±19.68	0.65±11.57	0.412
Total HOAs	0.03±0.38	−0.26±0.66	**0.043***
COMA	0.18±0.37	0.12±0.34	**0.002***
Trefoil	0.13±0.4	0.1±0.48	0.833
Spheric	0.08±0.24	0.06±0.28	0.773
ECD (cells/mm^2)	−324.26±563.04	−301.35±407.79	0.855
CV (%)	0.39±9.75	1.55±7.62	0.603
HEX (%)	−1.97±10.05	−2.13±7.02	0.942
Mean cell area	73.87±157.94	72.77±116.29	0.975
Min cell area	14.9±46.18	18.06±49.8	0.796
Max cell area	294.68±573.29	172.03±505.08	0.375
ECN	−35.81±59.05	−34.16±71.8	0.922

BCVA: Best-corrected visual acuity, RNFL: Retinal nerve fiber layer, CMT: Central macular thickness, IOP: Intraocular pressure, CCT: Central corneal thickness, CV: Corneal volume, ACD: Anterior chamber depth, ACC: Anterior corneal curvature, PCC: Posterior corneal curvature, HOA: High order aberration, ECD: Endothelial cell density, CV (%): Coefficient of variation of cell size, HEX: Percentage of hexagonality, D: Diopters, AL: Axial length, ECN: Endothelial number. Independent groups *t*-test, *$P<0.05$

patients with DM, attributing this to the combined effect of DM and IDI. In our study, patients underwent at least two IDI applications; the average number of IDI treatments was 6.58±3.38 (range, 2–14). In cases of ME due to RVO, there was a decrease in ECD and an increase in ACA, CAmin, and CAmax after multiple IDI treatments. We also found a positive correlation between IDI count and CV (%) and a negative correlation between CCT and HEX. These endothelial changes might reflect a response secondary to steroid-induced apoptosis and the toxic effects, or stress associated with repeated IDI applications.

Salvi *et al*. [24] demonstrated that CCT increased by approximately 13.81% in the immediate post-operative period (1 h) following cataract surgery, remained elevated by 6.44% on the first post-operative day compared to pre-operative values, and gradually returned to near-baseline levels by the end of the first post-operative week (0.57% difference). Similarly, Ventura *et al*. [25] reported that CCT returned to pre-operative levels within 3–12 months post-surgery. Following cataract surgery, surgical trauma may lead to increased irregularity in the size, hexagonality, and shape of endothelial cells. However, these changes have been shown in various studies to stabilize over time.[26,27] In our study, all patients had undergone cataract surgery at least 6 months before the first IDI. The observed negative correlations between the number of IDI injections and both CCT and HEX, along with the positive correlation with CV depending on lens status, may be attributed to the facilitated anterior segment penetration of DEX in pseudophakic eyes following repeated IDI administration.

Vural *et al*. [28] reported that CCT was thinner in CRVO patients than in BRVO patients. They associated this with the difference in pathophysiology between CRVO and BRVO. In the subgroups of this study, the spherical aberration value was significantly higher in patients with CRVO compared to those with BRVO. In addition, total HOAs and COMA values were significantly higher, and CMT values were lower in the ischemic group than in the non-ischemic group. We attributed these findings to the increased need for repeated IDI treatments in these patient groups.

This study has certain limitations. First, this was a pilot study conducted with a small sample size due to the limited number of patients available for subgroup analyses. The study was cross-sectional; changes in corneal topographic and endothelial parameters before and after IDI application were not evaluated comparatively, constituting another study limitation. In this context, the changes that may develop secondary to RVO could not be fully distinguished from those potentially induced by IDI.

Studies have demonstrated that repeated IDI application for RVO-related ME improves visual acuity and reduces ME. However, no study has evaluated the effect of repeated IDI application on corneal topographic parameters and endothelial measurements evaluated using specular microscopy. In this study, it was found that multiple IDI applications performed for ME due to RVO may lead to statistically significant changes in corneal parameters. New studies evaluating pre- and post-IDI parameters in a larger patient population will help assess corneal changes that may develop due to repeated IDI application.

Ethics Committee Approval: This study was approved by The

Informed Consent: Written informed consent was obtained from the patient for the preparation of this work.

Peer-review: Externally peer-reviewed.

Authorship Contributions:

Concept: U.K., S.C., E.K., G.A.; Design: U.K., N.T.G., E.K., G.A.; Supervision: U.K., N.T.G.; Materials: U.K., S.C., E.K., F.I.D.S.; Data Collection and/or Processing: U.K., S.C., E.K., F.I.D.S.; Analysis and/or Interpretation: U.K., N.T.G., S.C., E.K., F.I.D.S., G.A.; Literature Search: U.K., N.T.G., G.A.; Writing: U.K.; Critical Reviews: U.K., N.T.G., G.A.

Conflict of Interest: None declared.

Use of AI for Writing Assistance: Not declared.

Financial Disclosure: The authors declared that this study received no financial support.

References

1. Nicholson L, Talks SJ, Amoaku W, Talks K, Sivaprasad S. Retinal vein occlusion (RVO) guideline: executive summary. Eye (Lond) 2022;36:909–12. [CrossRef]
2. Lendzioszek M, Bryl A, Poppe E, Zorena K, Mrugacz M. Retinal Vein Occlusion-Background Knowledge and Foreground Knowledge Prospects-A Review J Clin Med 2024;13:3950. [CrossRef]
3. Tang Y, Cheng Y, Wang S, Wang Y, Liu P, Wu H. Review: The Development of Risk Factors and Cytokines in Retinal Vein Occlusion. Front Med (Lausanne) 2022;9:910600. [CrossRef]
4. Barnes PJ. Corticosteroid effects on cell signalling. Eur Respir J 2006;27:413–26. [CrossRef]
5. Alkholief M, Kalam MA, Raish M, et al. Topical sustained-release dexamethasone-loaded chitosan nanoparticles: assessment of drug delivery efficiency in a rabbit model of endotoxin-induced uveitis. Pharmaceutics 2023 3;15:2273. [CrossRef]
6. Moisseiev E, Goldstein M, Waisbourd M, Barak A, Loewenstein A. Long-term evaluation of patients treated with dexamethasone intravitreal implant for macular edema due to retinal vein occlusion. Eye (Lond) 2013;27:65–71. [CrossRef]
7. Capone A Jr, Singer MA, Dodwell DG, et al. Efficacy and safety of two or more dexamethasone intravitreal implant injections for treatment of macular edema related to retinal vein occlusion (Shasta study). Retina 2014;34:342–51. [CrossRef]
8. Kwak HW, D'Amico DJ. Evaluation of the retinal toxicity and pharmacokinetics of dexamethasone after intravitreal injection. Arch Ophthalmol 1992;110:259–66. [CrossRef]
9. Ilhan N, Coskun M, Ilhan O, et al. Effect of intravitreal injection of dexamethasone implant on corneal endothelium in macular edema due to retinal vein occlusion. Cutan Ocul Toxicol 2015;34:294–7. [CrossRef]
10. Güler HA, Örnek N, Örnek K, et al. Effect of dexamethasone intravitreal implant (Ozurdex®) on corneal endothelium in retinal vein occlusion patients : Corneal endothelium after dexamethasone implant injection. BMC Ophthalmol 2018;18:235. [CrossRef]
11. Haller JA, Bandello F, Belfort R Jr, et al. Randomized, sham-controlled trial of dexamethasone intravitreal implant in patients with macular edema due to retinal vein occlusion. Ophthalmology 2010;117:1134–46.e3. [CrossRef]
12. Haller JA, Bandello F, Belfort R Jr, et al. Dexamethasone intravitreal implant in patients with macular edema related to branch or central retinal vein occlusion twelve-month study results. Ophthalmology 2011;118:2453–60. [CrossRef]
13. Boyer DS, Yoon YH, Belfort R Jr, et al. Three-year, randomized, sham-controlled trial of dexamethasone intravitreal implant in patients with diabetic macular edema. Ophthalmology 2014;121:1904–14. [CrossRef]
14. Chiquet C, Dupuy C, Bron AM, et al. Intravitreal dexamethasone implant versus anti-VEGF injection for treatment-naïve patients with retinal vein occlusion and macular edema: a 12-month follow-up study. Graefes Arch Clin Exp Ophthalmol 2015;253:2095–102. [CrossRef]
15. Bayat AH, Karataş G, Kurt MM, Elçioğlu MN. The corneal effects of intravitreal dexamethasone implantation. Ther Adv Ophthalmol 2020;12:2515841420947544. [CrossRef]
16. Franco S, Lira M. Biomechanical properties of the cornea measured by the Ocular Response Analyzer and their association with intraocular pressure and the central corneal curvature. Clin Exp Optom 2009;92:469–75. [CrossRef]
17. Naageshwaran V, Ranta VP, Toropainen E, et al. Topical pharmacokinetics of dexamethasone suspensions in the rabbit eye: Bioavailability comparison. Int J Pharm 2022;615:121515. [CrossRef]
18. Bourcier T, Forgez P, Borderie V, Scheer S, Rostène W, Laroche L. Regulation of human corneal epithelial cell proliferation and apoptosis by dexamethasone. Invest Ophthalmol Vis Sci 2000;41:4133–41.
19. Grandinetti AA, Kniggendorf V, Moreira LB, Moreira Junior CA, Moreira AT. A comparison study of corneal topographic changes following 20-, 23-, and 25-G pars plana vitrectomy. Arq Bras Oftalmol 2015;78:283–5. [CrossRef]
20. Slusher MM, Ford JG, Busbee B. Clinically significant corneal astigmatism and pars plana vitrectomy. Ophthalmic Surg Lasers 2002;33:5–8. [CrossRef]
21. Avitabile T, Castiglione F, Bonfiglio V, Castiglione F. Transconjunctival sutureless 25-gauge versus 20-gauge standard vitrectomy: correlation between corneal topography and ultrasound biomicroscopy measurements of sclerotomy sites. Cornea 2010;29:19–25. [CrossRef]
22. Jamil AZ, Ahmed A, Mirza KA. Effect of intracameral use of dexamethasone on corneal endothelial cells. J Coll Physicians Surg Pak 2014;24:245–8.
23. Vinciguerra P, Albé E, Vinciguerra R, et al. Long-term resolution of immunological graft rejection after a dexamethasone intravitreal implant. Cornea 2015;34:471–4. [CrossRef]

24. Salvi SM, Soong TK, Kumar BV, Hawksworth NR. Central corneal thickness changes after phacoemulsification cataract surgery. J Cataract Refract Surg 2007;33:1426–8. [CrossRef]
25. Ventura AC, Wälti R, Böhnke M. Corneal thickness and endothelial density before and after cataract surgery. Br J Ophthalmol 2001;85:18–20. [CrossRef]
26. Bourne RR, Minassian DC, Dart JK, Rosen P, Kaushal S, Wingate N. Effect of cataract surgery on the corneal endothelium: modern phacoemulsification compared with extracapsular cataract surgery. Ophthalmology 2004;111:679–85. [CrossRef]
27. Lundberg B. Corneal endothelial changes seven years after phacoemulsification cataract surgery. Int Ophthalmol 2024;44:169. [CrossRef]
28. Vural GS, Karahan E. Central corneal thickness, axial length, anterior chamber and optic disc structure in patients with central and branch retinal vein occlusion. Eur J Ophthalmol 2022:1120672122131705. [CrossRef]

DOI: 10.14744/eer.2025.93723
Eur Eye Res 2026;6(1):60–69

EUROPEAN EYE RESEARCH

ORIGINAL ARTICLE

Use of large language models in turkish information materials for glaucoma patient education: evaluation of readability, accuracy and comprehensiveness

Ali Dal,[1] Murat Erdag,[2] Betul Dikme,[1] Bunyamin Kutluksaman[1]

[1]Department of Ophthalmology, Tayfur Ata Sokmen Faculty of Medicine, Mustafa Kemal University, Hatay, Turkiye
[2]Department of Ophthalmology, Fırat Faculty of Medicine, Fırat University, Elazığ, Turkiye

Abstract

Purpose: This study aims to evaluate the readability of the Turkish Ophthalmology Association's (TOA) glaucoma patient education brochure and to assess the capabilities of GPT-4.0, Gemini, and DeepSeek in generating Turkish patient education materials with respect to readability, accuracy, and comprehensiveness.

Methods: The TOA's patient education brochure on glaucoma was evaluated for readability using the Ateşman and Bezirci-Yilmaz formulae. The questions from the TOA booklets were presented independently to the GPT-4.0, Gemini, and DeepSeek models. The replies generated by these models were readability tested using the same formulas. In addition, qualified ophthalmologists evaluated the accuracy and comprehensiveness of the artificial intelligence (AI)-generated responses. AI-generated responses were converted to Q1 and Q2 formats to test text simplification. These versions were reevaluated for readability, accuracy, and comprehensiveness to see if simplification increased intelligibility without affecting medical accuracy.

Results: The TOA brochure had a higher readability level than the recommended patient education standard. Bezirci-Yilmaz scores showed that Gemini and DeepSeek had significantly lower readability than the TOA brochure (p=0.007 and p=0.033, respectively), whereas GPT-4.0 showed no significant difference (p=0.077). Ateşman scores indicated no significant difference between TOA and AI-generated texts. Gemini showed significantly higher comprehensiveness than GPT-4.0 (p=0.042), whereas accuracy scores did not differ significantly among the models. Readability improved for Gemini following simplification (p=0.013 and p=0.005, respectively), whereas GPT 4.0 and DeepSeek remained unchanged. After simplification, the comprehensiveness score decreased for Gemini, whereas GPT-4.0 and DeepSeek maintained their comprehensiveness.

Conclusion: While large language models hold promise for use as glaucoma patient information materials, it is essential to rigorously evaluate the accuracy and comprehensiveness of the content they produce.

Keywords: Glaucoma; large language models; readability.

Cite this article as: Dal A, Erdağ M, Dikme B, Kutluksaman B. Use of large language models in Turkish information materials for glaucoma patient education: Evaluation of readability, accuracy, and comprehensiveness. Eur Eye Res 2026;6(1):60–69.

Correspondence: Ali Dal, M.D. Department of Ophthalmology, Mustafa Kemal University, Hatay, Turkiye
E-mail: alidal19@hotmail.com

Submitted Date: 24.07.2025 **Revised Date:** 28.09.2025 **Accepted Date:** 09.10.2025 **Available Online Date:** 29.04.2026

Glaucoma represents a leading cause of irreversible blindness on a global scale. Current estimates indicate that approximately 3.6 million cases of blindness among individuals aged 50 and older can be attributed to glaucoma. Projections suggest that by the year 2040, this condition is anticipated to impact over 110 million individuals worldwide.[1,2] Due to the asymptomatic onset and gradual progression of the disease, diagnosing and treating glaucoma present significant challenges, even in developed countries with established screening programs.[3]

In managing glaucoma, effectively controlling intraocular pressure through the appropriate use of medications can significantly reduce the risk of vision loss for most patients.[4] Non-adherence to treatment is a critical factor that significantly impacts the long-term visual prognosis of patients.[5] Research indicates that adherence to glaucoma treatment is notably low, particularly within the initial 6 months. During this timeframe, there was a significant decline in the number of patients who continued their treatment.[6] Reasons for non-adherence to treatment include patients' insufficient understanding of glaucoma, apprehensions regarding treatment, potential side effects of medications, and the belief that the medications may not be effective. Research indicates that these issues can be addressed through enhanced patient education and the implementation of effective communication strategies.[7,8]

To ensure patient compliance with treatment, it is essential that they receive accurate and comprehensive information about the treatment process. At the outset of treatment, key aspects such as medication dosages, administration timing, intervals between medications, and the technique for instilling drops should be thoroughly explained. Written informational materials provided to patients serve as valuable resources to facilitate the correct implementation of the treatment.[9] International guidelines suggest that patient education materials should be written at a readability level of at least sixth grade to ensure they are easily understood by patients and their families.[10] In addition to the educational brochures offered to patients, there is a growing trend of individuals seeking health information through digital platforms, including the internet, social media, and artificial intelligence (AI)-driven chatbots.[11] Research indicates that patients who seek information from sources such as the internet tend to exhibit greater adherence to their treatment plans.[12]

Large language models (LLMs) are advanced AI systems that have been trained on extensive datasets, enabling them to generate coherent and contextually relevant natural language text.[13] These systems possess the capability to generate medical information and educate patients by analyzing content sourced from the Internet. Models such as ChatGPT from OpenAI, Gemini from Google, and DeepSeek from DeepSeek AI are being increasingly utilized in the medical sector for patient education and the creation of informational content.[8,14] There are concerns about the accuracy, comprehensiveness, and readability of the content generated by LLMs.[15] In addition, Bard and Bing, which are also widely used AI tools in the healthcare field, are developed by Google and Microsoft, respectively.

In Turkey, the Turkish Ophthalmology Association (TOA) provides educational resources for patients regarding glaucoma and various other eye conditions on its official website (https://oftalmoloji.org.tr). In the context of chronic diseases such as glaucoma, it is essential that the information provided is clear, precise, and thorough, enabling patients to make well-informed decisions.[16] This study evaluated glaucoma patient information brochures created by TOA, focusing on their readability through the Ateşman and Bezirci-Yilmaz formulas. Questions presented in a question-answer format were posed to language models, and the responses generated by GPT-4.0, Gemini, and DeepSeek were analyzed for accuracy, comprehensiveness, and readability. In addition, the study assessed whether simplifying the AI-generated responses could enhance readability.

The primary objective of this study is to assess the readability level of TOA patient information brochures and to evaluate the effectiveness, readability, accuracy, and comprehensiveness of LLMs in generating Turkish patient education materials specifically for glaucoma patients.

Materials and Methods

In our research, we utilized the information provided on the glaucoma unit's webpage of the TOA website, which serves public informational purposes, as our primary data source. This guide is structured around common questions related to glaucoma, such as "What is glaucoma?" and "What causes glaucoma?" Each response in the guide was assessed individually using the Ateşman and Bezirci-Yilmaz readability formulas. Our study exclusively relied on publicly accessible data and literature. Given that no animal or human subjects were involved, approval from an ethics committee and patient consent were not necessary.

Use of Language Models

The questions from the glaucoma unit's public web page were submitted, without alteration, to ChatGPT-4.0, DeepSeek,

and Gemini, which are the most widely utilized LLMs.[17] Each question was posed on a separate chat page, and the responses were documented to develop new patient education brochures. We evaluated three LLMs: ChatGPT-4 (OpenAI, April 2025 version), Gemini Advanced 1.5 (Google, 2025 version), and DeepSeek-Chat (2025 version). All responses were generated between May 10 and 20, 2025, to ensure consistency. Standardized prompts were used for all models (see Supplementary File 1 for the complete prompt texts). Each model was run with default parameters (temperature= 0.7, maximum token limit =1024, randomness/seed = default).

Furthermore, these responses were requested to be reorganized into "Question 1" and "Question 2" formats to evaluate the capability of LLMs to adapt the texts for lower education levels.

- **Question 1: "***Can you rearrange the text I shared below so that a 6*th *grader can understand it?***"**
- **Question 2: "***Can you edit the text I shared below to make it simpler to understand?***"**

A total of 72 patient-style questions were extracted from the official TOA glaucoma brochure and used as the study dataset. For each question, responses were generated from three LLMs in three different formats: Initial response (IR), Question 1 format (Q1), and Question 2 format (Q2). This process yielded a total of 648 individual responses ($72 \times 3 \times 3$). Each response was analyzed separately using both the Ateşman and Bezirci-Yilmaz readability indices, and was independently evaluated for accuracy and comprehensiveness by two glaucoma specialists. Inter-rater agreement between the two glaucoma specialists was assessed using intraclass correlation coefficients (ICC, two-way random effects model, and absolute agreement).

Readability Criteria

Ateşman readability criterion

The Ateşman readability measure assigns a score ranging from 0 to 100 based on the average length of sentences and words. In this system, scores of 90–100 are deemed suitable for individuals at the 4th-grade level and below. Scores between 80 and 89 correspond to the 5th or 6th grade, whereas scores of 70–79 are appropriate for the 7th or 8th grade. Scores ranging from 60 to 69 indicate a 9th or 10th grade level of education, and scores of 50–59 are suitable for the 11th or 12th grade. Scores between 40 and 49 reflect an education level equivalent to an associate degree (13–15th grade), whereas scores of 30–39 are indicative of undergraduate graduation. Finally, scores of 29 and below are associated with graduate-level education.[17]

Bezirci-Yilmaz readability criterion

The Bezirci-Yilmaz readability criterion assesses text complexity by calculating a score based on the average sentence length and the number of syllables in the words used. Scores ranging from 1 to 8 are deemed suitable for primary education, whereas scores between 9 and 12 are appropriate for high school. For undergraduate education, scores from 12 to 16 are recommended, and scores exceeding 16 are considered suitable for academic levels.[18]

Comprehensiveness and accuracy of LLMs' production of patient-targeted information.

Responses from language models were assessed for both accuracy and comprehensiveness by referencing the information available on the public website of the glaucoma unit. The evaluation of the accuracy and breadth of the materials was conducted by specialist physicians A.D. and B.K., who possess extensive knowledge of glaucoma and actively manage glaucoma patients in their clinical practice. The evaluations were conducted independently by both reviewers and then discussed together to reach a consensus on each response.

For comprehensiveness, responses were rated as "not comprehensive" (1 point) for responses lacking important detail, "somewhat comprehensive" (2 points) for responses that included minimal but essential information, "moderately comprehensive" (3 points) for responses that provided a reasonable level of detail, "comprehensive" (4 points) for responses that addressed the most critical issues, and "very comprehensive" (5 points) for responses that provided comprehensive and detailed information.

Accuracy was scored as "poor" (1 point) for responses that contained significant inaccuracies that could mislead patients and potentially cause harm, "fair" (2 points) for responses that may contain factual errors but are unlikely to mislead or harm patients, and "good" (3 points) for responses that were free of errors.[20]

Statistical Analysis

In the analysis of the data, a one-way analysis of variance (ANOVA) was used to determine whether there were statistically significant differences between the groups. The normality of the data distribution was assessed using the Shapiro–Wilk test, and the homogeneity of variances was evaluated using Levene's test. When the ANOVA test indicated significant differences between group means, the Tukey honestly significant difference (HSD) *post hoc* test was applied to identify which specific groups differed. Effect sizes (η^2 for ANOVA and Cohen's d for

pairwise comparisons) and 95% confidence intervals (CIs) were reported alongside *P*-values to ensure transparent interpretation of the results. Statistical analyses were conducted using IBM Statistical Package for the Social Sciences Statistics for Windows, Version 26.0 (IBM Corp., Armonk, NY, USA). $p<0.05$ was considered statistically significant.

Results

Ateşman Readability Scores

In the analyses of the Ateşman readability score (as the Ateşman readability score increases, the level of education required to understand the text decreases), it was observed that the first answers produced by GPT-4.0, Gemini, and DeepSeek models had higher readability scores compared to the TOA brochure, but these differences were not found to be statistically significant (TOA and GPT-4.0: p=0.758, TOA and Gemini: p=0.101, TOA and DeepSeek: p=0.082). In addition, no statistically significant difference was found in the pairwise comparisons between GPT-4.0, Gemini, and DeepSeek models ($p>0.05$) (Table 1).

The evaluation of readability scores for Ateşman revealed that the IRs generated by GPT-4.0 and Gemini were assessed at a 9–10th grade level, whereas the responses from the DeepSeek model were rated at a 7–8th grade level. In the GPT-4.0 model, the simplification process (Q1 and Q2) did not produce a significant change in readability. On the other hand, a significant increase in readability scores was detected in Q1 and Q2 formats in Gemini and DeepSeek models. In the Gemini model, the readability score of the IRs was notably lower than that of the simplified formats (Q1 and Q2). Likewise, in the DeepSeek model, the readability scores following the simplification process demonstrated a significant improvement compared to the original responses (Table 2).

Bezirci-Yilmaz Readability Scores

The one-way ANOVA revealed a statistically significant difference in Bezirci-Yilmaz readability scores among the

Table 1. Ateşman and Bezirci-Yilmaz readability scores of the initial responses from TOA, GPT-4.0, Gemini, and DeepSeek models

Outcome	TOA (Mean±SD)	GPT-4.0 (Mean±SD)	Gemini (Mean±SD)	DeepSeek (Mean±SD)	Comparison	Mean difference	95% CI (Lower–upper)	*p*	Effect size (Cohen's d)
Ateşman readability score	58.61±12.41	62.85±8.84	68.91±5.78	72.11±3.38	TOA versus GPT-4.0	4.24	−3.2–11.6	0.758	0.18
					TOA versus Gemini	10.30	2.1–18.5	0.101	0.45
					TOA versus DeepSeek	13.50	4.3–21.7	0.082	0.51
					GPT-4.0 versus Gemini	6.06	−1.2–13.8	0.503	0.30
					GPT-4.0 versus DeepSeek	9.26	1.0–17.5	0.106	0.39
					Gemini versus DeepSeek	3.20	−2.6–9.0	0.711	0.15
Bezirci-Yilmaz Score	13.02±3.27	8.64±4.10	6.83±0.87	6.92±1.24	TOA versus GPT-4.0	−4.38	−9.1–0.3	0.077	0.42
					TOA versus Gemini	−6.19	−10.2–−2.1	**0.007**	0.71
					TOA versus DeepSeek	−6.10	−10.0–−2.2	**0.033**	0.68
					GPT-4.0 versus Gemini	−1.81	−4.3–0.7	0.724	0.15
					GPT-4.0 versus DeepSeek	−1.72	−4.5–0.9	0.098	0.14
					Gemini versus DeepSeek	0.09	−1.0–1.2	0.911	0.02

Statistically significant results ($p<0.05$) are indicated in bold. TOA: Turkish Ophthalmology Association's, CI: Confidence interval, SD: Standard deviation. Effect sizes are reported as Cohen's d. *Post hoc* comparisons adjusted with Bonferroni correction

Table 2. Comparison of Ateşman readability scores and education levels among the IR, Q1, and Q2 formats of GPT-4.0, Gemini, and DeepSeek

Model	Format	Ateşman score (Mean±SD)	Education level	Comparison	Mean difference	95% CI (Lower–upper)	*p*	Effect size (Cohen's d)
GPT-4.0	IR	62.85±8.83	9–10th Grade	IR versus Q1	0.53	−1.2–2.3	0.365	0.07
	Q1	63.38±7.90	9–10th Grade	IR versus Q2	0.32	−1.5–2.1	0.866	0.04
	Q2	63.18±8.84	9–10th Grade	Q1 versus Q2	−0.21	−2.1–1.7	0.912	0.02
Gemini	IR	68.91±5.78	9–10th Grade	IR versus Q1	4.19	1.1–7.2	**0.035**	0.61
	Q1	73.10±3.22	7–8th Grade	IR versus Q2	8.12	3.9–12.3	**0.004**	0.95
	Q2	77.03±2.73	7–8th Grade	Q1 versus Q2	3.93	1.8–6.0	**0.007**	0.72
DeepSeek	IR	72.11±3.38	7–8th Grade	IR versus Q1	3.53	0.9–6.2	**0.014**	0.58
	Q1	75.64±3.56	7–8th Grade	IR versus Q2	5.54	2.1–8.9	**0.004**	0.82
	Q2	77.65±6.23	7–8th Grade	Q1 versus Q2	2.01	0.5–3.7	**0.020**	0.44

Statistically significant results ($p<0.05$) are indicated in bold. IR: Initial response; CI: Confidence interval; SD: Standard deviation. Effect sizes are reported as Cohen's d. *Post hoc* comparisons adjusted with the Tukey honestly significant difference test

groups (p=0.007). Tukey HSD *post hoc* analysis showed that the IRs generated by Gemini and DeepSeek had significantly lower readability scores compared to the TOA brochure (p=0.007 and p=0.033, respectively). In contrast, the difference between GPT-4.0 and the TOA brochure was not statistically significant (p=0.077). Furthermore, no significant differences were found among the LLMs themselves, including GPT-4.0 versus Gemini (p=0.724), GPT-4.0 versus DeepSeek (P=0.098), and Gemini versus DeepSeek (p=0.911) (Table 1).

When comparing the IRs of the LLMs (GPT-4.0, Gemini, and DeepSeek) with the answers formatted in Q1 and Q2, a statistically significant enhancement in readability was observed exclusively for the Gemini model (IR and Q1: p=0.013, IR and Q2: p=0.005). In contrast, the GPT-4.0 and DeepSeek models did not exhibit a significant difference in readability scores following the simplification process (p>0.05). Furthermore, no significant differences were identified between the responses in Q1 and Q2 formats across any of the models (p>0.05) (Table 3).

Comprehensiveness and Accuracy Results

The evaluation of the accuracy and comprehensiveness scores of the responses generated by the LLMs revealed variability among the models, particularly in comprehensiveness. Specifically, when assessing accuracy, no statistically significant differences were identified between the GPT-4.0, Gemini, and DeepSeek models across all three formats (Table 4). Each question was posed on a separate chat page. Inter-rater reliability analysis demonstrated excellent agreement for accuracy ratings (ICC = 0.84, 95% CI: 0.79–0.88) and good agreement for comprehensiveness ratings (ICC=0.76, 95% CI: 0.69–0.82), confirming consistency between evaluators.

The analysis of comprehensiveness scores revealed that the Gemini model achieved the highest score in its IRs, demonstrating a statistically significant difference when compared to GPT-4.0 (p=0.042). However, no significant difference was found between the Gemini and DeepSeek models (p=0.103). In addition, the comparison between GPT-4.0 and DeepSeek models showed no significant difference in comprehensiveness (p=0.077).

Upon evaluating the Q1 and Q2 formats after simplification, the comprehensiveness scores for GPT-4.0 and DeepSeek remained largely unchanged. In contrast, a decline in the comprehensiveness score of the Gemini model was noted. A comparison of the responses from the LLM models in the Q1 format revealed a statistically significant difference between Gemini and both GPT-4.0 and DeepSeek, with P=0.025 for each comparison. However, no statistically significant difference was observed in the responses within the Q2 format (Tables 4 and 5).

In our study, we compared the responses of the Gemini, DeepSeek, and GPT-4.0 models across different formats (IR, Q1, and Q2) to assess their comprehensiveness and identify any statistically significant differences (Fig.1). The analysis of the Gemini model revealed a significant difference in comprehensiveness between the first response and the simplified Q1 format (p=0.011). However, no significant difference was observed between the Q1 and Q2 formats (p=0.465). For the DeepSeek model, the

Table 3. Comparison of Bezirci-Yilmaz readability scores and education levels among the IR, Q1, and Q2 formats of GPT-4.0, Gemini, and DeepSeek

Model	Format	Bezirci-Yilmaz Score (Mean±SD)	Education level	Comparison	Mean difference	95% CI (Lower–upper)	*p*	Effect size (Cohen's d)
GPT-4.0	IR	8.64±4.10	Primary school	IR versus Q1	0.14	−1.0–1.3	0.848	0.03
	Q1	8.78±3.27	Primary school	IR versus Q2	0.10	−0.9–1.2	0.888	0.02
	Q2	8.74±3.28	Primary school	Q1 versus Q2	−0.04	−1.0–0.9	0.825	0.01
Gemini	IR	6.83±0.87	Primary school	IR versus Q1	−1.01	−1.8–−0.3	**0.013**	0.78
	Q1	5.82±0.49	Primary school	IR versus Q2	−1.18	−2.0–−0.4	**0.005**	0.81
	Q2	5.65±0.58	Primary school	Q1 versus Q2	−0.17	−0.7–0.3	0.252	0.25
DeepSeek	IR	6.92±1.24	Primary school	IR versus Q1	−0.61	−1.6–0.4	0.222	0.28
	Q1	6.31±1.71	Primary school	IR versus Q2	−0.01	−1.2–1.1	0.261	0.02
	Q2	6.91±1.92	Primary school	Q1 versus Q2	0.60	−0.7–1.9	0.779	0.19

Statistically significant results ($P<0.05$) are indicated in bold. IR: Initial response; CI: Confidence interval; SD: Standard deviation. Effect sizes are reported as Cohen's d. *Post hoc* comparisons adjusted with the Tukey honestly significant difference test

Table 4. Accuracy scores of GPT-4.0, Gemini, and DeepSeek across IR, Q1, and Q2 formats

Format	GPT-4.0 (Mean±SD)	Gemini (Mean±SD)	DeepSeek (Mean±SD)	Comparison	Mean difference	95% CI (Lower–upper)	*p*	Effect size (Cohen's d)
IR	2.88±0.35	3.00±0.25	2.75±0.34	GPT-4.0 versus Gemini	−0.12	−0.4–0.1	0.317	0.35
				GPT-4.0 versus DeepSeek	0.13	−0.2–0.4	1.000	0.20
				Gemini versus DeepSeek	0.25	−0.1–0.6	0.317	0.38
Q1	2.51±0.23	2.63±0.34	2.61±0.40	GPT-4.0 versus Gemini	−0.12	−0.3–0.1	0.317	0.36
				GPT-4.0 versus DeepSeek	−0.10	−0.3–0.2	1.000	0.28
				Gemini versus DeepSeek	0.02	−0.3–0.3	0.317	0.04
Q2	2.39±0.37	2.72±0.40	2.42±0.36	GPT-4.0 versus Gemini	−0.33	−0.6–−0.1	0.317	0.55
				GPT-4.0 versus DeepSeek	−0.03	−0.3–0.2	1.000	0.08
				Gemini versus DeepSeek	0.30	0.0–0.6	0.317	0.50

Statistically significant results ($p<0.05$) are indicated in bold. IR: Initial response; CI: Confidence interval; SD: Standard deviation. Effect sizes are reported as Cohen's d. *Post hoc* comparisons adjusted with the Tukey honestly significant difference test

Table 5. Comprehensiveness scores of GPT-4.0, Gemini, and DeepSeek across IR, Q1, and Q2 formats

Format	GPT-4.0 (Mean±SD)	Gemini (Mean±SD)	DeepSeek (Mean±SD)	Comparison	Mean difference	95% CI (Lower–upper)	*p*	Effect size (Cohen's d)
IR	3.25±0.71	3.88±0.35	3.50±0.84	GPT-4.0 versus Gemini	−0.63	−1.2–0.1	**0.042**	0.72
				GPT-4.0 versus DeepSeek	−0.25	−0.8–0.3	0.077	0.30
				Gemini versus DeepSeek	0.38	−0.1–0.9	0.103	0.46
Q1	2.00±0.51	2.50±0.53	2.00±0.42	GPT-4.0 versus Gemini	−0.50	−0.9–0.1	**0.025**	0.82
				GPT-4.0 versus DeepSeek	0.00	−0.4–0.4	1.000	0.00
				Gemini versus DeepSeek	0.50	0.1–0.9	0.025	0.81
Q2	2.00±0.48	2.13±0.64	2.00±0.56	GPT-4.0 versus Gemini	−0.13	−0.5–0.3	0.537	0.22
				GPT-4.0 versus DeepSeek	0.00	−0.4–0.4	1.000	0.01
				Gemini versus DeepSeek	0.13	−0.3–0.6	0.537	0.20

Statistically significant results ($p<0.05$) are indicated in bold. IR: Initial response; CI: Confidence interval; SD: Standard deviation. Effect sizes are reported as Cohen's d. *Post hoc* comparisons adjusted with the Tukey honestly significant difference test

comparisons indicated no statistically significant difference in comprehensiveness between the IR and the Q1 format (p=0.076). Similarly, the analysis of the GPT-4 model showed no significant difference between the IR and the Q1 format (p=0.092). Furthermore, when examining accuracy rates, no significant differences were found between the IR and Q1

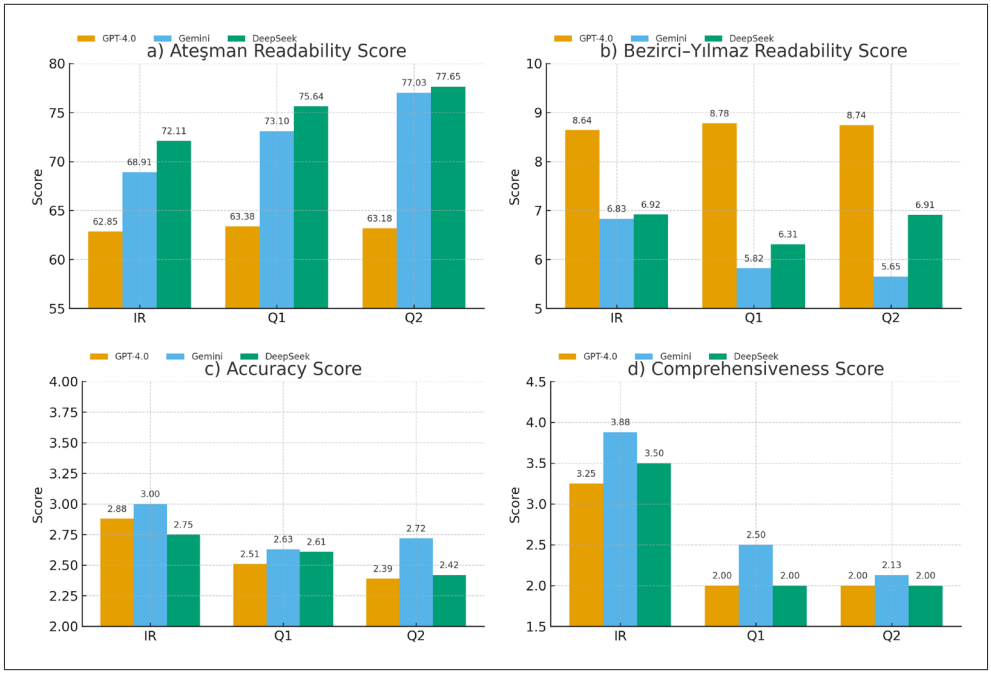

Fig. 1. Summary of main outcomes across GPT-4.0, Gemini, and DeepSeek in three response formats (IR, Q1, and Q2). **(a)** Ateşman readability scores, **(b)** Bezirci-Yilmaz readability scores, **(c)** Accuracy scores, and **(d)** Comprehensiveness scores. IR: Initial response; Q1: First simplified version, Q2: Second simplified version.

formats across all three LLM models (GPT-4.0, Gemini, and DeepSeek) (with p=0.141, 0.097, and 0.102, respectively).

Discussion

This study evaluated the readability of the glaucoma patient information brochure created by TOA, as well as the effectiveness and reliability of LLMs in delivering Turkish information to glaucoma patients. The findings allow for a direct comparison between traditional brochures prepared for Turkish-speaking patients and the content generated by LLMs. The results suggest that AI-based models have the potential to produce more accessible materials that may enhance patient understanding and adherence.

Effective patient information brochures should be easily understood by individuals with a low level of education while providing comprehensive and accurate information.[21] The American Medical Association advises that patient education materials should be written at a readability level of 6th grade or lower.[8] A recent study indicated that the patient information materials from the American Academy of Ophthalmology were developed at an 8th-grade reading level, which exceeds the recommended patient education level of 6th grade.[16] In our study, we found that the readability level of the brochures prepared by TOA was assessed to be at the 11–12th grade according to the Ateşman formula and at the undergraduate level according to the Bezirci-Yilmaz formula, both exceeding the recommended level. These results suggest that a higher level of education is necessary for a better understanding of patient information materials in ophthalmology. This situation should be considered to enhance clarity in patient education. However, when readability is increased, there is a risk of reduced comprehensiveness. In our study, readability was primarily enhanced by reducing sentence length and simplifying word choices, which allowed the content to become more accessible without altering its scope. Nevertheless, to ensure that simplified brochures maintain their comprehensiveness, additional strategies such as supplementary information layers and visual aids may be incorporated to preserve the depth and accuracy of patient education materials.

While AI-based language models can enhance patient education by increasing knowledge, it is essential to thoroughly assess the accuracy, comprehensiveness, and readability of the content they generate.[14] The results of our study showed that the responses produced by GPT-4.0 had a similar level of readability as the TOA brochure, but the responses produced by Gemini and DeepSeek required a lower level of training to be meaningfully understood compared to the Bezirci-Yilmaz formula. This finding shows that some LLMs can produce more understandable Turkish content. Previous studies have suggested that AI-supported approaches to reduce the level of education required to understand patient information materials may be beneficial for patient education.[20] Our research substantiates this perspective.

In the research conducted by Yalla *et al*.,[16] it was noted that ChatGPT-4.0 demonstrated a higher accuracy level compared to other AI models such as Bing and Bard. However, our study revealed no significant differences in accuracy among the ChatGPT-4.0, Gemini, and DeepSeek models. Regarding comprehensiveness, while the previous study[22] indicated that ChatGPT provided the most thorough answers, our findings showed that the Gemini model achieved the highest comprehensiveness score, with GPT-4.0 and DeepSeek offering lower levels of comprehensiveness. Although the accuracy scores were similar among the models, differences in understandability and comprehensiveness may reflect variations in training datasets, linguistic adaptation, and the ability of each model to process Turkish-specific language structures. This discrepancy highlights the challenge of objectively comparing models and underscores the need for standardized benchmarks and larger expert panels in future studies to ensure consistent and unbiased evaluation across multiple dimensions. Prior research has explored the capacity of LLMs to customize patient education materials to align with health literacy, thereby enhancing the accessibility of health information. These studies have demonstrated that LLMs can effectively adjust content to accommodate lower reading levels.[23] Our research aligns with these findings, demonstrating that structuring patient education materials based on individual health literacy levels can enhance the understanding of the disease and promote informed health decisions.[22,24]

The utilization of AI -driven models for patient information materials presents certain risks. While the content generated by these models appears realistic and fluent, it relies solely on statistical word associations and lacks a genuine reasoning process.[25] The reliability and contextual coherence of the information generated by LLMs can be called into question. It is important to note that the evaluations in this study were performed in May 2025. Given the rapid evolution of AI models, future updates may alter the performance and content generation capabilities of these systems. Models such as ChatGPT from OpenAI are notable for their propensity to generate false or fabricated content, often referred to as "hallucinations" or "confabulations," which significantly restricts their applicability in patient education.[26] In our

study, no hallucinations or major factual inaccuracies were observed in the responses generated by the LLMs. Patients are progressively utilizing the internet and AI-driven models to obtain health-related information.[27] Research indicates that the accuracy of information retrieved from Google searches related to glaucoma is notably low, with considerable discrepancies in the reliability of such information. In this context, the utilization of LLMs as patient information resources may offer a distinct advantage compared to conventional online information sources; however, it is imperative that they are meticulously assessed for accuracy and reliability. Our research indicates that LLMs deliver precise and comprehensive information for educating glaucoma patients in Turkish.

When interpreting the results of our study, it is essential to acknowledge several limitations. First, the questions assessed were derived from glaucoma patient information brochures created by TOA, which may not fully encompass the inquiries or needs most frequently expressed by patients. Nonetheless, the thoroughness of LLMs' responses was evaluated against the TOA brochures, based on the assumption that these materials offer the most accurate and comprehensive information available. The study was conducted exclusively in Turkish, which may limit its applicability to other languages and cultural contexts. In addition, reliance on TOA materials alone may not capture the full spectrum of ophthalmology patient resources, and the generalizability of findings across different populations and healthcare settings remains limited. Furthermore, assessments of accuracy and comprehensiveness were conducted utilizing subjective rating scales. Nevertheless, this limitation is mitigated as comprehensiveness is directly evaluated against TOA brochures, whereas accuracy scores are derived from numerical values rather than a binary "true or false" system. Major language models undergo continuous updates, with new information being integrated periodically. The responses generated by the LLMs in our study were derived from a specific timeframe, indicating that the results may evolve over time. Therefore, longitudinal analyses and repeated evaluations are necessary to ensure consistency of model performance over time. In addition, the readability formulas used in this study (Bezirci-Yilmaz and Ateşman) only measure sentence and word complexity and do not assess the factual accuracy of the content. The good-to-excellent inter-rater agreement supports the robustness of our evaluation process, although future studies with larger expert panels could provide further validation. Furthermore, the default configurations of the language models were employed; variations in prompts or customized settings could potentially alter the outcomes. Future research should consider conducting longitudinal analyses to assess the consistency of these models over time and to evaluate how their accuracy and comprehensiveness are affected by information updates.

Conclusion

In summary, this study demonstrates that LLMs may serve as valuable tools in patient information processes. The comparison between the TOA brochure and the content generated by the LLMs in terms of readability, accuracy, and comprehensiveness provides preliminary insights into the possible usability of AI-based systems as patient education materials, while highlighting the need for further validation in broader contexts. The advancement of AI-supported patient education models holds the potential to transform patient education and information processes. Using AI-generated materials without expert oversight carries risks, including potential hallucinations, incomplete explanations, or oversimplification of complex medical information. Therefore, LLMs should be regarded as supportive tools rather than standalone resources, and all outputs must be reviewed and validated by specialists before being shared with patients. However, further comprehensive studies are necessary to ensure accuracy, reliability, and patient safety before these models can be effectively integrated into clinical practice.

Ethics Committee Approval: Ethics committee approval was not required.

Informed Consent: Written informed consent was obtained.

Conflict of Interest: None declared.

Financial Disclosure: The author declared that this study has received no financial support.

Use of AI for Writing Assistance: None declared.

Authorship Contributions: Concept: A.D.; Design: A.D.; Supervision: A.D., B.K.; Resource: A.D., B.D.; Data collection and/or processing: A.D., B.D.; Analysis and/or interpretation: A.D., B.K.; Writing: A.D., B.D.; Critical review: M.E., B.K.

Peer-review: Externally peer-reviewed.

References

1. Bourne RRA, Steinmetz JD, Saylan M. Causes of blindness and vision impairment in 2020 and trends over 30 years, and prevalence of avoidable blindness in relation to VISION 2020: the Right to Sight. An analysis for the Global Burden of Disease Study. Lancet Glob Health 2021;9:e144–60.
2. Barkana Y, Dorairaj S. Re: Tham: Global prevalence of glaucoma and projections of glaucoma burden through 2040: a systemat-

ic review and meta-analysis. Ophthalmology 2015;122:e40–1. [CrossRef]
3. Mitchell P, Smith W, Attebo K, Healey PR. Prevalence of open-angle glaucoma in Australia. The Blue Mountains Eye Study. Ophthalmology 1996;103:1661-9. [CrossRef]
4. Sleath B, Blalock S, Covert D, Stone JL, Skinner AC, Muir K, et al. The relationship between glaucoma medication adherence, eye drop technique, and visual field defect severity. Ophthalmology 2011;118:2398-402. [CrossRef]
5. Fu DJ, Ademisoye E, Shih V, McNaught AI, Khawaja A. Survival of medical treatment success in primary open-angle glaucoma and ocular hypertension. Br J Ophthalmol 2024;108:1701-7. [CrossRef]
6. Tapply I, Broadway DC. Improving adherence to topical medication in patients with glaucoma. Patient Prefer Adherence 2021;15:1477–89. [CrossRef]
7. McDonald S, Ferguson E, Hagger MS, Foss AJE, King AJ. A theory-driven qualitative study exploring issues relating to adherence to topical glaucoma medications. Patient Prefer Adherence 2019;13:819-28. [CrossRef]
8. Lee GG, Goodman D, Chang TCP. Impact of demographic modifiers on readability of myopia education materials generated by large language models. Clin Ophthalmol 2024;18:3591-604. [CrossRef]
9. Kharod BV, Johnson PB, Nesti HA, Rhee DJ. Effect of written instructions on accuracy of self-reporting medication regimen in glaucoma patients. J Glaucoma 2006;15:244-7. [CrossRef]
10. Weiss BD. Help patients understand: manual for clinicians. 2nd ed. Chicago: American Medical Association; 2007.
11. Yang Z, Wang D, Zhou F, Song D, Zhang Y, Jiang J, et al. Understanding natural language: Potential application of large language models to ophthalmology. Asia Pac J Ophthalmol (Phila) 2024;13:100085. [CrossRef]
12. Haynes RB, McDonald HP, Garg AX. Helping patients follow prescribed treatment: clinical applications. JAMA 2002;288:2880-3. [CrossRef]
13. Cohen SA, Brant A, Fisher AC, Pershing S, Do D, Pan C. Dr. Google vs. Dr. ChatGPT: exploring the use of artificial intelligence in ophthalmology by comparing the accuracy, safety, and readability of responses to frequently asked patient questions regarding cataracts and cataract surgery. Semin Ophthalmol 2024;39:472-9. [CrossRef]
14. Srinivasan N, Samaan JS, Rajeev ND, Kanu M U, Yeo YH, et al. Large language models and bariatric surgery patient education: a comparative readability analysis of GPT-3.5, GPT-4, Bard, and online institutional resources. Surg Endosc 2024;38:2522-32. [CrossRef]
15. Goodman RS, Patrinely JR, Stone CA, Zimmerman E, Donald RR, Sam S, et al. Accuracy and reliability of chatbot responses to physician questions. JAMA Netw Open 2023;6:e2336483. [CrossRef]
16. Yalla GR, Hyman N, Hock LE, Zhang Q, Shukla AG, Kolomeyer NN. Performance of artificial intelligence chatbots on glaucoma questions adapted from patient Brochures. Cureus 2024;16:e56766. [CrossRef]
17. Ateşman E. Türkçede okunabilirliğin ölçülmesi. Dil Dergisi 1997;58:71-4. [Article in Turkish]
18. Bezirci B, Yılmaz AE. A software library for measurement of readability of texts and a new readability metric for Turkish. Dokuz Eylül Üniversitesi Mühendislik Fakültesi Fen ve Mühendislik Dergisi 2010;12:17-25.
19. Kianian R, Sun D, Crowell EL, Tsui E. The use of large language models to generate education materials about uveitis. Ophthalmol Retina 2024;8:195-201. [CrossRef]
20. Postacı SA, Dal A. The ability of large language models to generate patient information materials for retinopathy of prematurity: evaluation of readability, accuracy, and comprehensiveness. Turk J Ophthalmol. 2024;54:330-6. [CrossRef]
21. Cohen SA, Fisher AC, Xu BY, Song BJ. Comparing the accuracy and readability of glaucoma-related question responses and educational materials by Google and ChatGPT. J Curr Glaucoma Pract 2024;18:110-6. [CrossRef]
22. Killeen OJ, Niziol LM, Cho J, Heisler M, Resnicow K, Darnley-Fisch D, et al. Glaucoma medication adherence 1 year after the support, educate, empower personalized glaucoma coaching program. Ophthalmol Glaucoma 2023;6:23-8. [CrossRef]
23. Newman-Casey PA, Niziol LM, Lee PP, Musch DC, Resnicow K, Heisler M. The impact of the Support, Educate, Empower personalized glaucoma coaching pilot study on glaucoma medication adherence. Ophthalmol Glaucoma 2020;3:228–37. [CrossRef]
24. Vaishya R, Misra A, Vaish A. ChatGPT: Is this version good for healthcare and research? Diabetes Metab Syndr 2023;17:102744. [CrossRef]
25. Bernstein IA, Zhang YV, Govil D, Majid I, Chang RT, Sun Y, Shue A, Chou JC, et al. Comparison of ophthalmologist and large language model chatbot responses to online patient eye care questions. JAMA Netw Open 2023;6:e2330320. [CrossRef]
26. Quaranta L, Novella A, Tettamanti M, Pasina L, Weinreb RN, Nobili A. Adherence and persistence to medical therapy in glaucoma: an overview. Ophthalmol Ther 2023;12:2227–40. [CrossRef]
27. Wang J, Shi R, Le Q, Shan K, Chen Z, Zhou X, et al. Evaluating the effectiveness of large language models in patient education for conjunctivitis. Br J Ophthalmol 2025;109:185–91. [CrossRef]

DOI: 10.14744/eer.2025.82621
Eur Eye Res 2026;6(1):70–77

EUROPEAN EYE RESEARCH

ORIGINAL ARTICLE

Exploring corneal strength: Comparative analysis of big bubble and manual lamellar dissection in deep anterior lamellar keratoplasty

Emine Esra Karaca,[1] Yonca Asfuroglu,[2] Gokhan Celik,[1,3] Asim Burak Gunduz,[1] Ozlem Evren Kemer[1]

[1]Department of Ophthalmology, University of Health Sciences, Ankara Bilkent City Hospital, Ankara, Turkiye
[2]Department of Ophthalmology, Ankara Bilkent City Hospital, Ankara, Turkiye
[3]Department of Ophthalmology, Mersin University Faculty of Medicine, Mersin, Turkiye

Abstract

Purpose: To compare the long-term visual outcomes and corneal biomechanical properties following deep anterior lamellar keratoplasty (DALK) using either the big bubble (BB) technique or manual lamellar dissection (MLD) in patients with advanced keratoconus. In addition to evaluate the relationship between residual stromal bed (RSB) thickness and post-operative visual and biomechanical parameters in MLD-DALK eyes, and to assess the reliability of intraocular pressure (IOP) measurements.

Methods: A total of 78 eyes from patients with keratoconus who underwent DALK (43 BB-DALK, 35 MLD-DALK) and completed 18 months of post-operative follow-up were retrospectively analyzed. Corneal hysteresis (CH), corneal resistance factor (CRF), cornea-compensated IOP (IOPcc), Goldmann correlated IOP (IOPg), and best-corrected visual acuity (BCVA) were assessed. In the MLD group, RSB thickness was measured using anterior segment OCT. Biomechanical assessments were performed using the Ocular Response Analyzer.

Results: At 18 months, CH and CRF were comparable between groups ($p>0.05$), as were BCVA and other topographic parameters. The mean RSB thickness in the MLD group was 75.8±27.7 µm, with no significant correlation between RSB and visual or biomechanical metrics. In both groups, IOPcc was significantly higher than IOPg ($p<0.01$), though IOP readings were not correlated with RSB thickness.

Conclusion: MLD-DALK offers similar visual acuity and biomechanical outcomes to BB-DALK and is a viable alternative when BB formation fails. Clinicians should consider using measurements IOPcc for accurate post-operative monitoring, as traditional methods may underestimate true IOP in DALK patients.

Keywords: Big bubble; corneal hysteresis; deep anterior lamellar keratoplasty; manual lamellar dissection.

Cite this article as: Karaca EE, Asfuroglu Y, Celik G, Gunduz AB, Evren Kemer O. Exploring corneal strength: Comparative analysis of big bubble and manual lamellar dissection in deep anterior lamellar keratoplasty. Eur Eye Res 2026;6(1):70–77.

Correspondence: Emine Esra Karaca, M.D. Department of Ophthalmology, University of Health Sciences, Ankara Bilkent City Hospital, Ankara, Turkiye
E-mail: dremineesra@gmail.com

Submitted Date: 08.08.2025 **Revised Date:** 05.10.2025 **Accepted Date:** 03.11.2025 **Available Online Date:** 29.04.2026

Deep anterior lamellar keratoplasty (DALK) is a surgical technique frequently employed to treat keratoconus, a progressive disorder where the cornea thins and protrudes outward. This method selectively replaces the damaged anterior corneal layers while keeping the healthy endothelial structure intact, offering a less invasive option. DALK is ideal for keratoconus as it removes abnormal corneal tissue and substitutes it with a donor cornea, correcting the irregular corneal shape and enhancing vision.[1-3]

The conventional surgical technique used in DALK for keratoconus involves creating a "big bubble" (BB) within the corneal stroma, typically using the Anwar BB technique.[4] This gas-filled cavity facilitates separation of the anterior from the posterior corneal layers, allowing precise removal of diseased tissue while preserving the endothelium. When BB (type 1 bubble) formation is unsuccessful, alternative techniques, such as manual lamellar dissection (MLD), can be employed, providing a viable option for successful transplantation while preserving posterior stromal integrity, although this approach often results in variable residual stromal bed (RSB) thickness. Depending on the type of bubble achieved, the graft may be positioned either directly on Descemet's membrane (type 2 bubble) or on the pre-Descemet/Dua's layer (type 1 bubble), and then sutured in place.[5]

An ocular response analyzer (ORA) is a diagnostic tool used to assess the biomechanical properties of the cornea.[6] It measures corneal hysteresis (CH) and corneal resistance factor (CRF), which represents the ability of the cornea to absorb and dissipate energy during the application and removal of force.[7] In keratoconus, the cornea typically exhibits reduced CH due to its weakened structure. By measuring the CH and other parameters, the ORA provides valuable information for diagnosing and monitoring keratoconus.[8,9] After DALK, the biomechanical properties of the cornea may be altered by surgical intervention and healing.

Only a few reports have investigated differences between BB and MLD techniques in DALK. Akdemir *et al*.[10] compared CH and CRF values in BB-DALK and MLD-DALK and found no significant differences. However, their study did not include a quantitative assessment of RSB thickness, which may influence post-operative biomechanics. Other studies also lacked a detailed analysis of the relationship between RSB and corneal biomechanics.

Therefore, in this study, we aimed to compare long-term visual and biomechanical outcomes between BB-DALK and MLD-DALK, while additionally incorporating anterior segment OCT–based RSB thickness measurements in MLD cases. To our knowledge, this is the milestone study to investigate whether residual stromal thickness correlates with visual function, CH, and intraocular pressure (IOP) parameters, thereby addressing an important gap in the present literature.

The aim of this study was to evaluate whether RSB, measured by anterior segment optical coherence tomography (AS-OCT), influences post-operative visual acuity, corneal biomechanics, and IOP, and to determine whether MLD-DALK provides comparable outcomes to BB-DALK in advanced keratoconus.

Materials and Methods

This retrospective, non-randomized, comparative study included 78 eyes diagnosed with keratoconus eligible for corneal transplantation. This study was conducted in accordance with the Declaration of Helsinki and approved by the Ankara Bilkent City Hospital Ethics Committee (approval number: E-22-3135). Informed consent forms were obtained from all participants in the study. The selection of participants was based on the records of patients from Ankara Bilkent City Hospital- Corneal and External Diseases Services. To determine the appropriate sample size for this retrospective comparative study, a priori power analysis was conducted using G*Power 3.1.9.7 software. A medium effect size (Cohen's d=0.5) was predicted based on prior research that assessed corneal biomechanics following DALK procedures. The required sample size was determined to be 64 participants in total, with 32 participants in each group, with an alpha error probability of 0.05 and a desired statistical power of 0.80 for a two-tailed Mann–Whitney U test. Considering potential data exclusions and missing values, the study included 78 eyes (43 BB-DALK, 35 MLD-DALK), which exceeded the minimum sample size requirement and thereby ensured sufficient power to detect significant intergroup differences in CH and other biomechanical parameters. Participants included in both groups had severe keratoconus according to the Amsler-Krumeich classification. The groups were comparable in terms of pre-operative severity. Only patients aged >18 years who underwent a comprehensive eye examination and at least 18 months of post-operative follow-up were included. Exclusion criteria comprised Individuals with systemic illnesses or eye conditions other than keratoconus, such as cataracts, uveitis, glaucoma, trauma, vitreoretinal issues, dry eyes, or corneal infections. Patients who experienced graft rejection or Descemet's membrane perforation during

DALK were also excluded. All patients underwent thorough ocular examinations, including best-corrected visual acuity (BCVA), slit lamp examination, endothelial cell density with a specular microscope, and Pentacam topography (Oculus, Wetzlar, Germany), both before surgery and at specified post-operative intervals (1 week, 1 month, 3 months, 6 months, 12 months, and 18 months post-operatively). ORA (Reichert, Inc., Depew, NY, USA) was used to assess the corneal biomechanics 18 months post-operatively. The ORA provides two pressure-derived parameters, CH and CRF. Anterior segment photographs were recorded at all follow-up appointments. AS-OCT (Swept Source-OCT, Triton, Topcon, Japan) was utilized to measure the RSB thickness post-operatively (Fig. 1) in patients who underwent MLD-DALK. The measurements were performed in the central zone. Three consecutive measurements were performed, and the average value was computed to ensure accuracy. Furthermore, Figure 2 shows an OCT image of the BB-DALK surgery after 18 months without any RSB.

All surgeries were performed by one of the two experienced corneal surgeons (OEK and EEK). Under general anesthesia, partial-thickness trephination of the recipient cornea was performed, ensuring that it did not perforate the Descemet's membrane. Anwar's BB (Type 1 bubble) or MLD techniques were used to achieve a complete separation of the stroma from Descemet's membrane. For the BB group, conventional 8 mm diameter trephination was performed to a stromal depth between 60% and 80% using a suction trephine. Air was introduced using a 30-gauge needle angled at 45° with its bevel oriented downward. Following the formation of a large bubble, peripheral paracentesis was performed to reduce IOP. After the initial incision, a viscoelastic substance was introduced between the stroma and the layer preceding Descemet's membrane. The stroma was then segmented into four sections and delicately detached from the pre-Descemet's layer. If the BB formation failed despite two or three attempts, manual dissection of the stroma with blunt-tipped fine scissors and a blunt spatula was performed. At the end of both surgeries, an 8.5 mm donor cornea, excluding Descemet's membrane, was sutured in the recipient bed using 16 interrupted 10-0 nylon sutures. Moxifloxacin ophthalmic drops (Vigamox 0.5%; Alcon Laboratories Inc., Fort Worth, TX, USA) and dexamethasone ophthalmic drops (Maxidex 0.1%; Alcon Laboratories Inc.) were administered 6 times a day for 2 weeks post-operatively. After 2 weeks, the drops were adjusted according to the graft status at post-operative visits. All patients stopped receiving dexamethasone ophthalmic drops at the end of 1 year. The patients were assessed every week in the 1st month and every month in the 1st year. Ruptured and loose sutures were removed during routine examinations. At 12 months, all sutures were removed.

Data were analyzed using the Statistical Package for the Social Sciences software (version 25.0; IBM Corp, Armonk, NY, USA). Descriptive statistics were computed for all variables. For the analysis of continuous data, mean±standard deviation was used, while categorical variables were evaluated as the number of cases and percentages (%). The Mann–Whitney U test was employed to evaluate the significance of the difference between the mean values of the two groups. Statistical significance was set at $p<0.05$.

Results

Forty-three eyes with BB-DALK and 35 with MLD-DALK were included in this study. The demographic and topographic data of the patients are shown in Table 1 in terms of the pre-operative and post-operative 18-month periods.

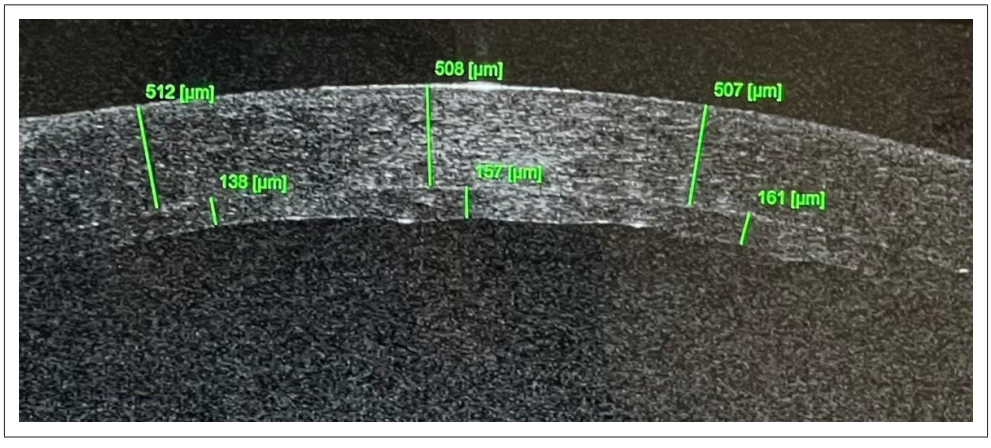

Fig. 1. Anterior segment optic coherence tomography image of a deep anterior lamellar keratoplasty with manual lamellar dissection technique patient, residual stromal bed thickness, and calculation method.

Table 1. Demographic data and comparison of pre-operative and post-operative 18th-month refractive and topographic outcomes between groups

Parameters	BB-DALK	MLD-DALK	*p*
Age (years)	38.58±16.11	44.08±18.42	0.219
Gender (F/M)	23/20	22/13	0.132
Pre-op manifest refraction (SE)	-7.71±3.81	-8.01±4.11	0.088
Pre-op Kmax (D)	68.80±8.12	66.71±7.25	0.486
Pre-op topographic astigmatism	6.21±2.88	5.59±3.01	0.221
Pre-op Central corneal thickness (µm)	418±41.12	403.12±38.33	0.337
Pre-op BCVA (logMAR)	0.96±0.83	1.02±1.02	0.552
Pre-op ECD (cell/mm^2)	2902±403.42	2874±48.12	0.712
Post-op manifest refraction (SE)	-0.23±4.17	-0.43±4.87	0.606
Post-op Kmax (D)	46.01±4.12	45.98±4.54	0.918
Post-op topographic astigmatism	3.87±3.45	3.32±3.76	0.590
Post-op Central corneal thickness (µm)	547.86±59.90	588.75±72.62	**0.019***
Post-op BCVA (logMAR)	0.56±0.37	0.67±0.34	0.096
Post-op ECD (cell/mm^2)	2171.79±605.84	2291.65±660.61	0.396

BB-DALK: Deep anterior lamellar keratoplasty with big bubble technique, MLD-DALK: Deep anterior lamellar keratoplasty with manual lamellar dissection technique, SE: Spherical equivalent, K: Keratometry, D: Diopters, BCVA: Best corrected visual acuity, ECD: Endothelial cell density. *Level of statistical significance $P<0.05$

Table 2. Corneal biomechanics values at post-operative 18th month

Parameters	BB-DALK	MLD-DALK	*p**
CH (mmHg)	8.01±1.90	8.68±1.94	0.123
CRF (mmHg)	9.03±2.24	9.66±2.19	0.173
IOPcc (mmHg)	20.50±6.47	19.93±4.29	0.833
IOPg (mmHg)	17.74±6.59	17.9±4.5	0.520

BB-DALK: Deep anterior lamellar keratoplasty with big bubble technique, MLD-DALK: Deep anterior lamellar keratoplasty with manual lamellar dissection technique, CH: Corneal hysteresis, CRF: Corneal resistance factor, IOPcc: Cornea-compensated factor, IOPg: Goldmann-correlated intraocular pressure

Graft survival rates were 100% in the BB-DALK and MLD-DALK groups at 18 months. Post-operative complications occurred in 5 eyes (6.9%) in the BB-DALK group (1 suture abscesses, 2 loose sutures) and 4 eyes (11.4%) in the MLD-DALK group (2 suture abscesses, 2 loose sutures) (p=0.97) during the follow-up period, patients presenting with loose sutures underwent suture removal and subsequent re-suturing. In cases where a suture abscess developed, the affected suture was removed, and following a 2-week course of topical moxifloxacin drops (Vigamox 0.5%; Alcon Laboratories Inc., Fort Worth, TX, USA) therapy leading to resolution of the abscess, re-suturing was performed.

Patients in both groups were pre-operatively classified as having severe keratoconus according to the Amsler-Krumeich criteria. Pre-operative severity was comparable between groups in terms of spherical equivalent (SE), BCVA, maximum keratometry (Kmax), central corneal thickness (CCT), and endothelial cell count. Post-operative SE, BCVA, Kmax, CCT, and endothelial cell count values were similar between the groups. In the MLD-DALK group, the average RSB was 75.85±27.70 µm. The mean CH, CRF, cornea-compensated IOP (IOPcc), and Goldmann-correlated IOP (IOPg) values of the BB-DALK and MLD-DALK eyes are shown in Table 2. The patients showed CH of 8.01±1.90 and 8.68±1.94 mmHg, CRF of 9.03±2.24 and 9.66±2.19 mmHg,

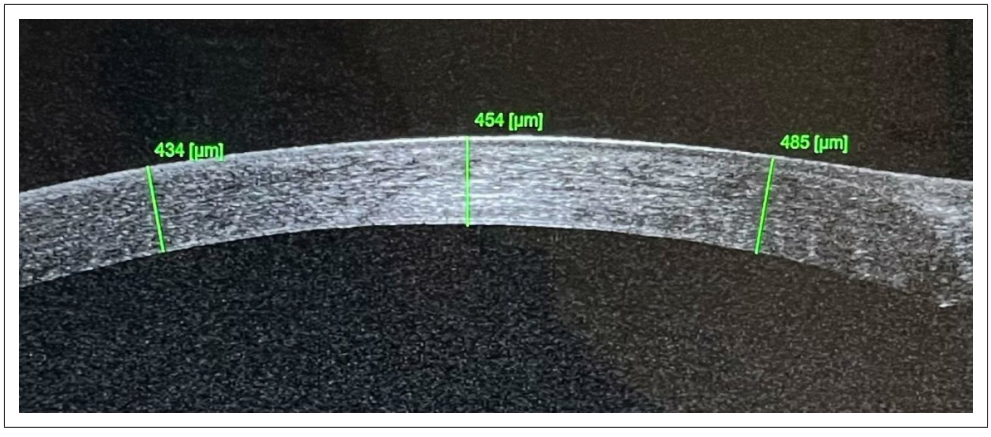

Fig. 2. Anterior segment optic coherence tomography image of a deep anterior lamellar keratoplasty with big bubble technique patient.

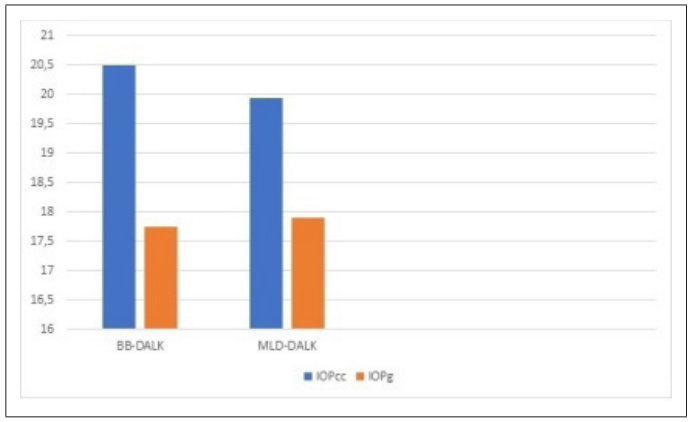

Fig. 3. Comparison of cornea-compensated intraocular pressure (IOP) and Goldmann-correlated IOP within the groups.

IOPcc of 20.50±6.47 and 19.93±4.29 mmHg, and IOPg of 17.74±6.59 and 17.9±4.5 mmHg in the BB-DALK and MLD-DALK eyes, respectively (p>0.05). The IOPcc values were higher than the IOPg values in both the BB-DALK and MLD-DALK groups (p<0.01) (Fig. 3). IOPcc, IOPg, CH, and CRF did not correlate with RSB in the MLD-DALK group (Fig. 4a-d). No significant correlations were observed between CCT and CH, CRF, IOPg, or IOPcc in eyes with BB-DALK and MLD-DALK.

Discussion

In recent years, DALK has become a suitable surgical method for treating keratoconus, where the endothelium and Descemet's membrane are intact.[11-15] The term of graft survival, complication rates, patient-reported outcomes, and corneal stability in this study provides a broader perspective on the efficacy of BB-DALK and MLD-DALK. The high graft survival rates in both groups align with previous reports of DALK's favorable long-term outcomes compared to penetrating keratoplasty, likely due to preserved endothelial integrity. Complication rates were low and similar between groups, suggesting that MLD-DALK remains a safe alternative when BB formation fails, despite its technically demanding nature. The stability of K max and CCT over time reinforces the biomechanical equivalence observed in CH and CRF measurements, suggesting that neither technique compromises long-term corneal integrity. These findings highlight the versatility of DALK and support its use in keratoconus management, particularly in cases where BB-DALK is not feasible.

The ORA can measure two pressure-derived parameters: CH and CRF. While CH represents viscoelastic characteristics, CRF measures the total resistance of the cornea.[16,17] In

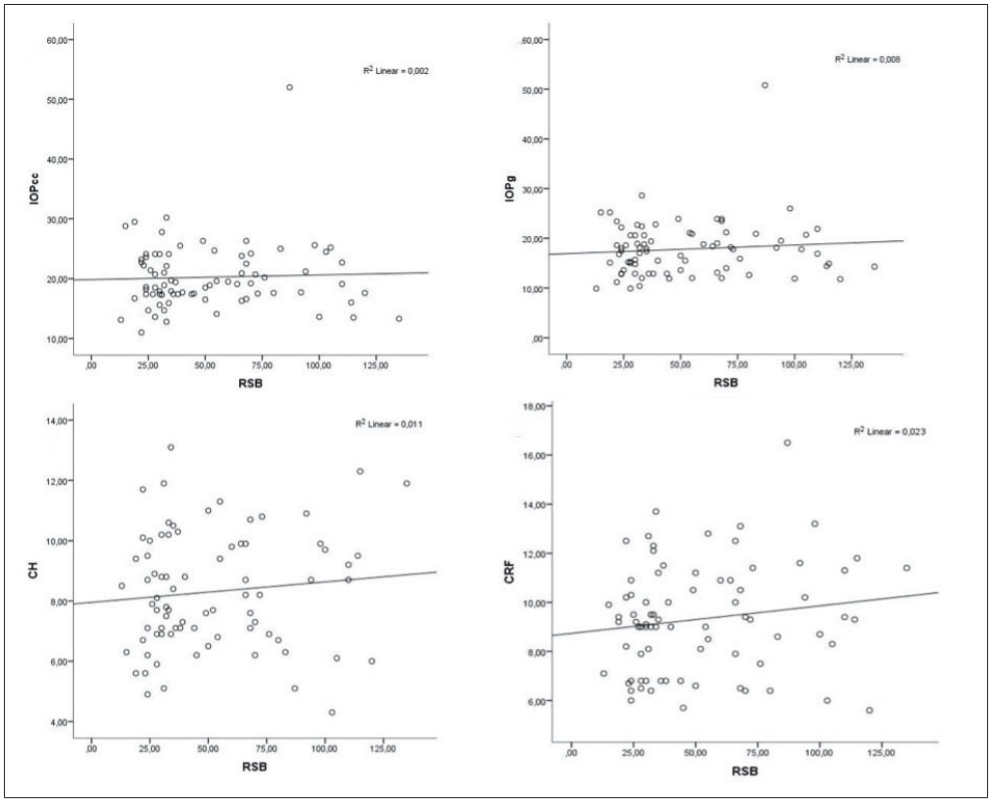

Fig. 4. Correlation between (a) residual stromal bed and cornea-compensated intraocular pressure (IOP), (b) Goldmann-correlated IOP, (c) corneal resistance factor, and (d) corneal hysteresis in the deep anterior lamellar keratoplasty with manual lamellar dissection technique group.

many studies conducted on keratoconic eyes, CH and CRF were found to be lower than those in normal eyes.[18,19] Hosny *et al.* [9] compared the biomechanical features of the cornea in eyes with previous PK and DALK using the ORA. They found that keratoconic eyes that underwent PK had significantly lower CH and CRF values than those that had undergone previous DALK. They also reported that post-DALK keratoconic eyes were similar to normal corneas in terms of corneal biomechanics. They concluded that an intact host Descemet's membrane acts as a strong barrier and maintains corneal rigidity.[9] In another study, Abdelkader found that corneal biomechanics were better in post-DALK eyes than in post-PK eyes at 3 months. However, these results have been reported to be comparable at 1 year.[20] In the BB-DALK technique, the thickness of the RSB cannot be quantified, which is indicative of the complete exposure of Descemet's membrane, as intended by the Anwar technique. In the present study, qualitative assessments using AS-OCT alongside intraoperative surgical records in patients who underwent BB-DALK confirmed the absence of residual stromal tissue, thereby validating the effective execution of the technique. These findings suggest that BB-DALK achieves a more uniform stromal clearance compared to MLD-DALK. Furthermore, the lack of correlation between the mean RSB thickness (75.8 µm) observed in MLD-DALK and post-operative biomechanical parameters CH, CRF, as well as BCVA, indicates that the absence of RSB in BB-DALK has minimal impact on these outcomes. This supports the notion that both techniques yield comparable results in terms of corneal biomechanics. Although we reported the mean RSB thickness, we did not perform subgroup analyses stratifying eyes into thinner versus thicker RSB categories. Similarly, correlation analyses exploring whether RSB thickness might subtly influence biomechanical behavior beyond the mean values were limited. Future studies with larger cohorts are warranted to better elucidate these potential associations.

In addition to CH and CRF measurements, ORA provides more accurate IOP results, as it is not significantly affected by CCT, corneal curvature, or axial length.[21] Feizi *et al.* [22] showed that after DALK, IOP values measured using ORA were significantly higher than those measured using Goldmann applanation tonometry (GAT). This study also observed that IOP_{CC}, which is less influenced by corneal properties than GAT, yielded the highest results.[22] Similar to Feizi's study, we found that IOPcc values were significantly higher than IOPg values in both the BB-DALK and MLD-DALK groups. In our study, IOPcc values were found to be significantly higher than IOPg values in both the BB-DALK and MLD-DALK groups ($p<0.01$). This observation aligns with previous findings by Feizi *et al*. [22] and suggests that changes in corneal properties following DALK may influence IOP measurements. Given that IOPcc, as measured by ORA, is less affected by parameters, such as CCT, corneal curvature, or axial length, this discrepancy likely reflects alterations in corneal biomechanics post-surgery. Specifically, the removal of diseased stroma and integration of donor tissue during DALK may modify the cornea's elastic properties and resistance, resulting in higher IOPcc readings compared to IOPg values obtained through GAT. This difference carries significant clinical implications. First, prolonged use of topical steroids, common in DALK patients, raises the risk of steroid-induced ocular hypertension or glaucoma. The finding that IOPcc exceeds IOPg suggests that traditional GAT measurements may underestimate true IOP in these patients, potentially leading to missed diagnoses of elevated IOP. Consequently, employing methods, such as ORA, which are less influenced by corneal biomechanics, could provide a more accurate assessment of IOP in the post-operative period. Second, the disparity between IOPcc and IOPg underscores the need for further investigation into how surgical modifications and healing processes affect corneal biomechanical parameters. Factors, such as donor stromal thickness, recipient bed characteristics, or suturing techniques may contribute to this difference and warrant exploration. Briefly, the elevated IOPcc relative to IOPg highlights the importance of a cautious approach to IOP monitoring in both BB and MLD DALK patients. Clinicians should consider incorporating ORA-derived IOPcc values into their diagnostic and management strategies, particularly for glaucoma screening or steroid therapy monitoring, to ensure more reliable outcomes. These findings emphasize the need for standardized IOP measurement protocols in the long-term follow-up of DALK patients and encourage future studies to further elucidate this phenomenon. Although Anwar's BB technique is considered to be the most successful approach for DALK, MLD is another viable option that could eliminate the need for PK.[4,23] In this study, we aimed to investigate and compare the effects of these two techniques on corneal biomechanics. We found that CH and CRF were similar between the MLD-DALK and BB-DALK techniques. This also suggests that the similarity of CF and CRF in the BB DALK and MLD DALK groups indicates that MLD DALK can be safely continued in patients where BB DALK cannot be performed. We emphasize that in the future, surgical procedures can be comfortably continued

with MLD DALK without encountering the complications associated with PKP due to similar CF and CRF values among subtypes of DALK surgery.

Akdemir *et al*.[10] studied the biomechanics of corneas that underwent DALK using the BB or MLD technique for keratoconus. Similar to our study, they concluded that the two methods used to perform successful DALK were not superior in terms of corneal biomechanical properties. In addition to their study, we evaluated the possible correlation between the RSB thickness and ORA findings in the MLD-DALK group. We concluded that an average of 75.8 µm RSB thickness did not affect the visual acuity or the effect of the RSB on corneal biomechanics.

In our study, the MLD-DALK technique was employed in cases where the BB-DALK technique failed to achieve a successful BB, such as due to difficulties in separating the stroma from Descemet's membrane. This approach may introduce a selection bias, as patients in the MLD-DALK group could represent more challenging cases with potentially thinner peripheral corneas or greater disease severity. To address this potential bias and enhance the reliability of our findings, we compared DALK types. Although the MLD DALK group appeared to have a thinner mean corneal thickness, higher mean K values, and higher mean disease stage, no statistically significant difference was found between the two groups. This finding suggests that the impact of selection bias may be reduced, rendering CH comparable between the groups.

The first limitation of our study is the exclusion of patients who underwent PKP. The primary reason for this is our longstanding shift away from performing PKP, particularly in patients with keratoconus. The second limitation of our study is the relatively small sample size, retrospective and non-randomized nature. Although the necessary numbers were obtained in the G power analysis, studies with larger samples would yield better results. Another important limitation is that the biomechanical evaluation was based solely on ORA. Although ORA provides clinically useful data, its relatively low repeatability and interobserver variability must be acknowledged. Moreover, more advanced devices, such as the Corvis ST could have provided dynamic and more reproducible biomechanical parameters. The lack of such complementary tools limits the comprehensiveness of our biomechanical assessment. The inclusion of such a device could offer a more comprehensive biomechanical profile of the cornea following BB-DALK and MLD-DALK, potentially revealing subtle differences not captured by the ORA. Future studies are encouraged to incorporate the Corvis ST or similar technologies to validate and expand upon our findings, particularly in assessing the long-term impact of RSB thickness and surgical technique on corneal stability and rigidity. On the other hand, since MLD was specifically performed in cases where BB formation failed, the retrospective and non-randomized nature of the study inevitably introduces a selection bias. These patients may inherently represent more complex keratoconus cases, and this factor should be considered when interpreting our findings.

This study compared the effects of BB and MLD techniques in DALK on corneal biomechanics and visual outcomes in patients with keratoconus. At 18 months post-operatively, CH and CRF values were similar between the BB-DALK and MLD-DALK groups ($p>0.05$). Similarly, no significant difference was observed in BCVA between the two techniques ($p>0.05$). In the MLD-DALK group, the mean RSB thickness was measured as 75.8±27.7 µm, yet no significant correlation was found between RSB thickness and BCVA, CH, CRF, or IOP parameters. Notably, IOPcc values were significantly higher than IOPg values in both groups ($p<0.01$), underscoring the importance of using IOP measurement methods less influenced by corneal biomechanics (e.g., ORA-derived IOPcc) following DALK. In conclusion, the MLD-DALK technique yields comparable outcomes to BB-DALK in terms of visual acuity and corneal biomechanics. In cases where the BB technique is not feasible, MLD-DALK serves as a safe and effective alternative, potentially eliminating the need for penetrating keratoplasty. Ophthalmologists should keep in mind that a cautious approach to IOPcc monitoring is essential, as IOPcc is higher than IOPg in both subtypes of the DALK surgical technique. Larger-scale studies are needed to evaluate the long-term outcomes.

Conclusion

The MLD-DALK technique yields comparable outcomes to BB-DALK in terms of visual acuity and corneal biomechanics. In cases where the BB technique is not feasible, MLDDALK serves as a safe and effective alternative, potentially eliminating the need for penetrating keratoplasty. Ophthalmologists should keep in mind that a cautious approach to IOPcc monitoring is essential, as IOPcc is higher than IOPg in both subtypes of the DALK surgical technique.

Acknowledgment: We would like to express our sincere gratitude to all the staff members of the Cornea Department for their invaluable support and dedication throughout this study. Their expertise, assistance, and commitment to patient care greatly contributed to the successful completion of this research.

Ethics Committee Approval: This study was approved by The Ankara Bilkent City Hospital Ethic Committee (approval number: E-22-3135).

Informed Consent: Written informed consents were obtained from patient and his family.

Peer-review: Externally peer-reviewed.

Authorship Contributions: Concept: E.E.K., Y.A., O.E.K.; Design: E.E.K., O.E.K.; Supervision: O.E.K.; Resource: E.E.K.; Materials: Y.A., G.C., A.B.G.; Data Collection and/or Processing: Y.A., G.Ç., A.B.G.; Analysis and/or Interpretation: E.E.K., Y.A., G.C., A.B.G., O.E.K.; Literature Search: E.E.K., Y.A., G.C.; Writing: E.E.K., G.Ç.; Critical Reviews: E.E.K., O.E.K.

Conflict of Interest: None declared.

Use of AI for Writing Assistance: Not declared.

Financial Disclosure: The authors declared that this study received no financial support.

References

1. Pellegrini M, Yu AC, Busin M. Deep anterior lamellar keratoplasty for keratoconus: Elements for success. Saudi J Ophthalmol 2022;36:36–41. [CrossRef]
2. Parker JS, van Dijk K, Melles GR. Treatment options for advanced keratoconus: A review. Surv Ophthalmol 2015;60:459–80. [CrossRef]
3. Shimazaki J, Shimmura S, Ishioka M, Tsubota K. Randomized clinical trial of deep lamellar keratoplasty vs penetrating keratoplasty. Am J Ophthalmol 2002;134:159–65. [CrossRef]
4. Anwar M, Teichmann KD. Big-bubble technique to bare Descemet's membrane in anterior lamellar keratoplasty. J Cataract Refract Surg 2002;28:398–403. [CrossRef]
5. Bhatt UK, Fares U, Rahman I, Said DG, Maharajan SV, Dua HS. Outcomes of deep anterior lamellar keratoplasty following successful and failed "big bubble". Br. J. Ophthalmol 2012;96:564–9. [CrossRef]
6. Kaushik S, Pandav SS. Ocular Response Analyzer. J Curr Glaucoma Pract 2012;6:17–9. [CrossRef]
7. Murphy ML, Pokrovskaya O, Galligan M, O'Brien C. Corneal hysteresis in patients with glaucoma-like optic discs, ocular hypertension and glaucoma. BMC Ophthalmol 2017;17:1. [CrossRef]
8. Schweitzer C, Roberts CJ, Mahmoud AM, Colin J, Maurice-Tison S, Kerautret J. Screening of forme fruste keratoconus with the ocular response analyzer. Invest Ophthalmol Vis Sci 2010;51:2403–10. [CrossRef]
9. Hosny M, Hassaballa MA, Shalaby A. Changes in corneal biomechanics following different keratoplasty techniques. Clin Ophthalmol 2011;5:767–70. [CrossRef]
10. Akdemir MO, Acar BT, Acar S. Biomechanics in DALK: Big bubble vs manual lamellar dissection. Arq Bras Oftalmol 2020;83:87–91. [CrossRef]
11. Lim L, Pesudovs K, Coster DJ. Penetrating keratoplasty for keratoconus: visual outcome and success. Ophthalmology 2000;107:1125–31. [CrossRef]
12. Feizi S, Javadi MA, Jamali H, Mirbabaee F. Deep anterior lamellar keratoplasty in patients with keratoconus: big-bubble technique. Cornea 2010;29:177–82. [CrossRef]
13. Espandar L, Carlson AN. Lamellar keratoplasty: a literature review. J Ophthalmol 2013;2013:894319. [CrossRef]
14. Reinhart WJ, Musch DC, Jacobs DS, Lee WB, Kaufman SC, Shtein RM. Deep anterior lamellar keratoplasty as an alternative to penetrating keratoplasty a report by the american academy of ophthalmology. Ophthalmology 2011;118:209–18. [CrossRef]
15. Al-Torbak AA, Al-Motowa S, Al-Assiri A, et al. Deep anterior lamellar keratoplasty for keratoconus. Cornea 2006;25:408-12.
16. Luce DA. Determining in vivo biomechanical properties of the cornea with an ocular response analyzer. J Cataract Refract Surg. 2005;31:156–62. [CrossRef]
17. Sullivan-Mee M, Billingsley SC, Patel AD, Halverson KD, Alldredge BR, Qualls C. Ocular Response Analyzer in subjects with and without glaucoma. Optom Vis Sci 2008;85:463–70. [CrossRef]
18. Kirwan C, O'Malley D, O'Keefe M. Corneal hysteresis and corneal resistance factor in keratoectasia: findings using the Reichert ocular response analyzer. Ophthalmologica 2008;222:334–7. [CrossRef]
19. Shah S, Laiquzzaman M, Bhojwani R, Mantry S, Cunliffe I. Assessment of the biomechanical properties of the cornea with the ocular response analyzer in normal and keratoconic eyes. Invest Ophthalmol Vis Sci 2007;48:3026–31. [CrossRef]
20. Abdelkader A. Influence of different keratoplasty techniques on the biomechanical properties of the cornea. Acta Ophthalmol 2013;91:e567–72. [CrossRef]
21. Medeiros FA, Weinreb RN. Evaluation of the influence of corneal biomechanical properties on intraocular pressure measurements using the ocular response analyzer. J Glaucoma 2006;15:364–70. [CrossRef]
22. Feizi S, Hashemloo A, Rastegarpour A. Comparison of the ocular response analyzer and the Goldmann applanation tonometer for measuring intraocular pressure after deep anterior lamellar keratoplasty. Invest Ophthalmol Vis Sci 2011;52:5887–91. [CrossRef]
23. Javadi MA, Mohammad-Rabei H, Feizi S, Daryabari SH. Visual Outcomes of Successful versus Failed Big-Bubble Deep Anterior Lamellar Keratoplasty for Keratoconus. J Ophthalmic Vis Res 2016;11:32–6. [CrossRef]

DOI: 10.14744/eer.2025.82787
Eur Eye Res 2026;6(1):78–85

EUROPEAN EYE RESEARCH

ORIGINAL ARTICLE

Choroidal neovascularization in the pediatric age group

Isil Kefeli,[1] Taylan Ozturk,[2] Ziya Ayhan,[1] Mahmut Kaya,[3] Ali Osman Saatci[1]

[1]Department of Ophthalmology, Dokuz Eylül University Faculty of Medicine, Izmir, Turkiye
[2]Department of Ophthalmology, Izmir Tinaztepe University, Izmir, Turkiye
[3]Private Practice, Izmir, Turkiye

Abstract

Purpose: The purpose of the study is to evaluate the clinical features, underlying etiology, and clinical outcomes of choroidal neovascularization (CNV) in the pediatric population.

Methods: This is a retrospective, single-center, interventional case series. A total of 12 eyes of 12 consecutive pediatric patients with CNV with various etiologies were analyzed. The main clinical parameters included the underlying causes, best-corrected visual acuity before and after the treatment, characteristics of the CNV, and the treatment strategies.

Results: There were four girls and eight boys with a median age of 12.3± 3 years (range: 7–17 years). Eight of 12 patients have completed the 6-month follow-up. The mean follow-up period was 32.8± 41 months (range: 6–132 months) in those 8 patients. Overall, five of them were treated. Four patients were treated with intravitreal anti-vascular endothelial growth factor (anti-VEGF) administration and the remaining patient with photodynamic therapy. Visual acuity improved from logMAR 0.54±0.2 (range: logMAR 0.8–0.2) to logMAR 0.26±0.18 (range: logMAR 0.5–0.1) at the last visit in the treated eyes. All anti-VEGF-treated patients required only a single injection.

Conclusion: CNV, a sight-threatening disease, is rarely seen in the pediatric age group. Families could be hesitant about the intravitreal treatment, but anti-VEGF injections seemed very helpful in our group of treated patients.

Keywords: Aflibercept; anti-vascular endothelial growth factor; choroidal neovascularization; optical coherence tomography angiography; photodynamic therapy; ranibizumab.

Choroidal neovascularization (CNV) is a rare macular disorder that can lead to serious visual impairment in pediatric patients.[1-4] Although CNV is less common in pediatric patients compared to the adult population, it has more devastating consequences, given that a legally blind child faces significant challenges in education and social development.[1,5] Pediatric CNVs can be idiopathic, but several underlying disorders, including inflammatory/infectious diseases, degenerative diseases, traumatic events, neoplastic diseases, and hereditary retinal dystrophies, can be present.[3-5]

The morphological characteristics of pediatric CNV differ from those of adult CNV. While thickening and calcification of Bruch's membrane and diffuse disruption of the retinal pigment epithelium (RPE) are frequently seen in older patients with age-related macular degeneration (AMD), these findings are not commonly seen in children.[6] Besides, most cases of CNV in older patients with AMD have multiple in-growth sites, whereas CNV in children is more likely to have a solitary in-growth site.[7,8] It is believed that these morphological features can be the explanation for the possible spontaneous CNV regression in children.[8]

Cite this article as: Kefeli I, Ozturk T, Ayhan Z, Kaya M, Saatci AO. Choroidal neovascularization in the pediatric age group. Eur Eye Res 2026;6(1):78–85.

Correspondence: Isil Kefeli, M.D. Department of Ophthalmology, Dokuz Eylul University Faculty of Medicine, Izmir, Turkiye
E-mail: isilkefeli@gmail.com
Submitted Date: 11.03.2025 **Revised Date:** 27.10.2025 **Accepted Date:** 14.11.2025 **Available Online Date:** 29.04.2026

The management strategy can be somewhat different than that of adult patients with CNV. Treatment options for pediatric CNV depend on the etiology and include photodynamic therapy (PDT), thermal laser photocoagulation, surgical removal of the membrane, and/or intravitreal anti-vascular endothelial growth factor (anti-VEGF) agents.[8-10]

Herein, we report a case series of 12 eyes of 12 patients under 18 years of age presenting with CNV and share our experience.

Materials and Methods

Medical records of all patients under 18 years old who presented with CNV to our clinic between 2007 and 2023 were retrospectively analyzed. All of the patients were examined by one of us (AOS). The study was conducted by the ethical standards of the Declaration of Helsinki. Approval was obtained from the Local Ethics Committee (registration code: 8618-GOA, September 09, 2024). Patient demographics, fundus characteristics, treatment approach, and outcomes were examined. Multimodal imaging methods, such as optical coherence tomography angiography (OCTA), fluorescein angiography (FA), and optical coherence tomography (OCT), were used to diagnose CNV.

CNV lesions were classified as follows: Type 1 (a neovascular complex between the Bruch's membrane and RPE, originating from the choroid), type 2 (located above the RPE), and type 3 (intraretinal, retinal angiomatous proliferation).[3,11-14]

According to the macular photocoagulation study (MPS) protocol, CNV lesions were classified as classic (early lacy hyperfluorescence), occult (late leakage or leakage from an indistinct focus), or minimally classic depending on the pattern of fluorescein findings.[15]

Active CNV was defined as the presence of subretinal or intraretinal fluid, new or persistent leakage on FA, and/or flow signal corresponding to the CNV complex on OCTA. Regression was defined as the resolution of subretinal/intraretinal fluid and absence of leakage or flow signal on multimodal imaging.

CNV location was defined according to criteria established by the MPS and classified as subfoveal (for lesions within the foveal avascular zone [FAZ]), juxtafoveal (for lesions <200 µm from the FAZ), or extrafoveal (for lesions >200 µm from the FAZ) locations. Lesions located adjacent to the disc or within one disc diameter from the optic disc border were considered peripapillary CNVs.

The treatment decision was made on an individual basis, considering the etiology and ocular conditions.

All intravitreal injections were performed under general anesthesia using standard aseptic technique. Retreatment was considered in cases of persistent or recurrent activity on OCT after 4–6 weeks. Patients were monitored every 4 to 6 weeks as possible till the foveal stabilization was obtained, then followed with extended intervals.

Statistical Analysis

IBM Statistical Package for the Social Sciences Statistics Standard Concurrent User, version 26 (IBM Corp., Armonk, New York, USA) was used for analyzing data and worked at a 95% confidence level. Descriptive statistics were presented as the number of units, percentage, mean± standard deviation, minimum, and maximum values. Due to the small sample size and the paired nature of the data, changes in best-corrected visual acuity (BCVA) were analyzed using the Wilcoxon signed-rank test. Visual acuities were converted to logMAR equivalents and processed.

Results

Overall, 12 eyes of 12 pediatric patients with CNV were scrutinized. The mean age was 12.3±3 (range: 7–17 years). There were eight (67%) boys and four (33%) girls. All patients had unilateral CNV.

Patient's characteristics have been shown in Table 1. The follow-up period in 4 patients was <6 months, as they were lost to follow-up after the initial visit. Thus, eight patients could be followed for 6 months or more. In those, the average follow-up was 32.8±41 months (range: 6–132 months). None of the patients had any concomitant systemic disease.

CNV was associated with several eye diseases: Optic disc drusen in three eyes (25%), laser pointer injury in two eyes (17%), uveitis in two eyes (17%), Bietti crystalline dystrophy in one eye (8%), and best disease in one eye (8%). One of our patients developed CNV after laser injury at the workplace (8%). Idiopathic CNV was diagnosed in two eyes (17%) without any underlying ocular disease (Table 1).

While CNV location was subfoveal in 8 eyes (67%), it was peripapillary in three eyes (25%). In one eye, the CNV lesion was located extrafoveally (8%) (Fig. 1 and 2). Lesion type was Type 2 in eight eyes (67%) and Type 1 in four (33%) eyes.

The mean BCVA at the first visit, in all eyes, was logMAR 0.54± 0.32 (range: logMAR 0–1). The mean BCVA in peripapillary located eyes was logMAR 0.13± 0.1(range: logMAR 0–0.2) and was found to be better than in subfoveal located eyes. The mean BCVA in eyes with subfoveal CNV was logMAR 0.7±0.2 (range: logMAR 1–0.5) at initial visit.

Table 1. Demographic and clinical data of 12 children with CNV

Eye no.	Patient age (years)/sex	Etiology	Location	CNV type	CNV status at presentation	BCVA at presentation	Treatment received	Interval between presentation and last visit	CNV status during last visit	BCVA at last visit
1	7/F	Best's disease	Subfoveal	Type 1	Active	20/125	None	10 months	Active	20/125
2	14/M	Bietti crystalline dystrophy	Subfoveal	Type 2	Active	20/100	Ranibizumab ×1	24 months	Quiescent	20/25
3	14/F	Uveitis	Subfoveal	Type 1	Inactive	20/63	Aflibercept ×1	24 months	Quiescent	20/32
4	9/M	Laser pointer injury	Subfoveal	Type 2	Active	Unavailable	None	None	Active	None
5	13/M	Optic disc drusen	Peripapillary	Type 2	Active	20/32	PDT ×1	132 months	Quiescent	20/25
6	14/M	Optic disc drusen	Peripapillary	Type 2	Active	20/32	None	None	Active	None
7	17/F	Uveitis	Subfoveal	Type 1	Active	20/125	Ranibizumab ×1	24 months	Quiescent	20/63
8	11/M	Idiopathic	Subfoveal	Type 2	Active	20/63	Aflibercept ×1	6 months	Quiescent	20/50
9	9/M	Laser pointer injury	Subfoveal	Type 2	Active	20/200	None	6 months	Active	20/200
10	11/F	Optic disc drusen	Peripapillary	Type 1	Active	20/20	Observation	36 months	Quiescent	20/20
11	15/M	Laser injury at workplace	Subfoveal	Type 2	Active	20/100	None	None	Active	None
12	14/M	Idiopathic	Extrafoveal	Type 2	Active	Unavailable	None	None	Active	None

CNV was considered active in 11 of 12 eyes. Among those with active CNV, 5 eyes underwent treatment. Four eyes of four patients could not receive treatment because they were lost to follow-up, considering the presence of active CNV at the first visit. Parents of 3 patients denied any injection treatment after hearing the possible treatment complications in detail. In one of our uveitic patients, the CNV lesion was inactive at the initial visit, so she was observed. CNV in all eyes remained regressed with a mean BCVA of logMAR 0.38± 0.36 (range: logMAR 0–1) at the last visit.

In our clinic, intravitreal anti-VEGF agents were the first treatment of choice for CNV in pediatric patients, and all injections were performed under general anesthesia. An equal number of patients were treated with ranibizumab (Lucentis®; Novartis, Basel, Switzerland; 0.5 mg in 0.05 mL) (*n*=2) and aflibercept (Eylea®; Bayer, Leverkusen, Germany; 2 mg in 0,05 mL) (*n*=2). All of them remained stable with a single injection only, and no recurrences were observed during the follow-ups. One eye was treated successfully with PDT, diagnosed before the anti-VEGF era.

Five eyes had responded well to treatment (4 eyes underwent anti-VEGF injections and 1 eye underwent PDT), showing increased visual acuity from logMAR 0.54±0.2 (range: logMAR 0.8–0.2) to logMAR 0.26± 0.18 (range: logMAR 0.5–0.1) at the last visit. Although the Wilcoxon signed-rank test did not reach conventional statistical significance (p=0.063), the effect size was large, indicating a clinically meaningful improvement in BCVA despite the small sample size. BCVA remained stable in three eyes of three patients, whose parents did not consent to intravitreal anti-VEGF therapy and remained untreated.

Figure 3 shows the OCT and fundus images of an 11-year-old boy with idiopathic CNV before intravitreal anti-VEGF treatment. After a single dose of intravitreal anti-VEGF treatment, his fundus and OCT findings remained regressed (Fig. 4).

Discussion

In the current study, we evaluated the clinical features of 12 eyes of 12 pediatric patients with CNV. In our case series, the most common

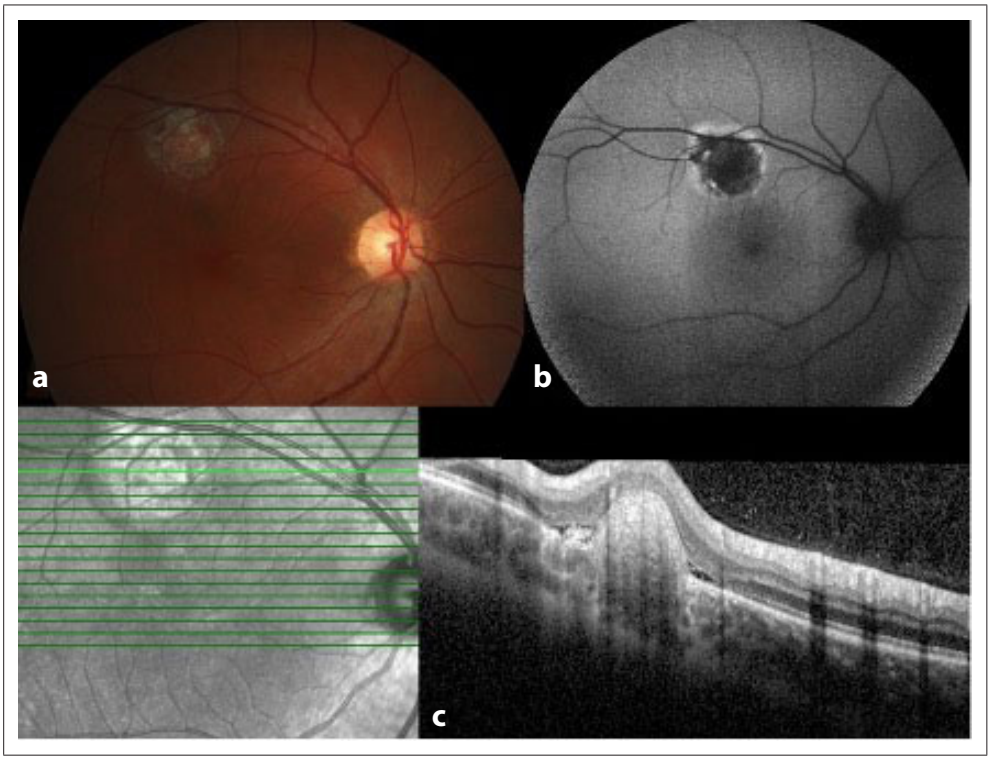

Fig. 1. Right eye, patient 12, at the presentation. **(a)** Color fundus picture revealing an extrafoveal yellowish lesion, together with a tiny intraretinal hemorrhage. **(b)** Fundus autofluorescence imaging showing a hypoautofluorescent lesion surrounded by a hyperautofluorescent rim superior to the fovea. **(c)** Optical coherence tomography exhibiting a minute subretinal fluid with subretinal hyperreflectance.

etiologies were optic disc drusen (25%). Previous large series on pediatric CNV were summarized in Table 2.

In the Intelligent Research in Sight (IRIS) registry, Finn *et al.*[16] reported the features of 2353 eyes with pediatric CNV. In their study, the most common etiology was posterior uveitis/inflammatory chorioretinal disease in 19.4% of patients. Other common etiologies were myopia (18.4%) and hereditary dystrophy (5.4%). In 38.2% of eyes, CNV was claimed as idiopathic.

In parallel to the previous studies, CNV was located subfoveally (67%) in most eyes in our group. However, in

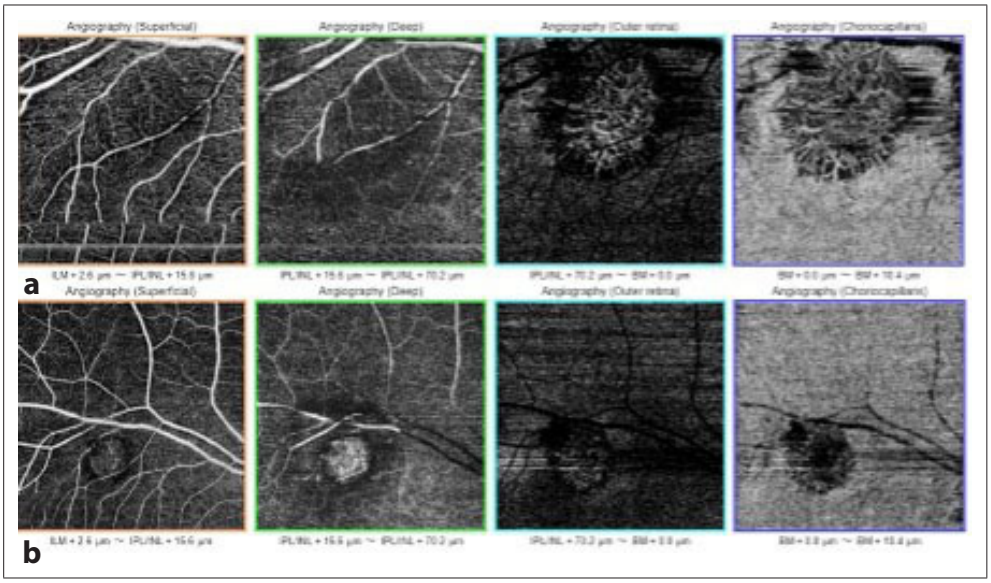

Fig. 2. Right eye, Patient 12, at the presentation. 3 × 3 mm **(a)** and 6 × 6 mm **(b)** Optical coherence tomography angiography slabs demonstrating the neovascular complex exquisitely.

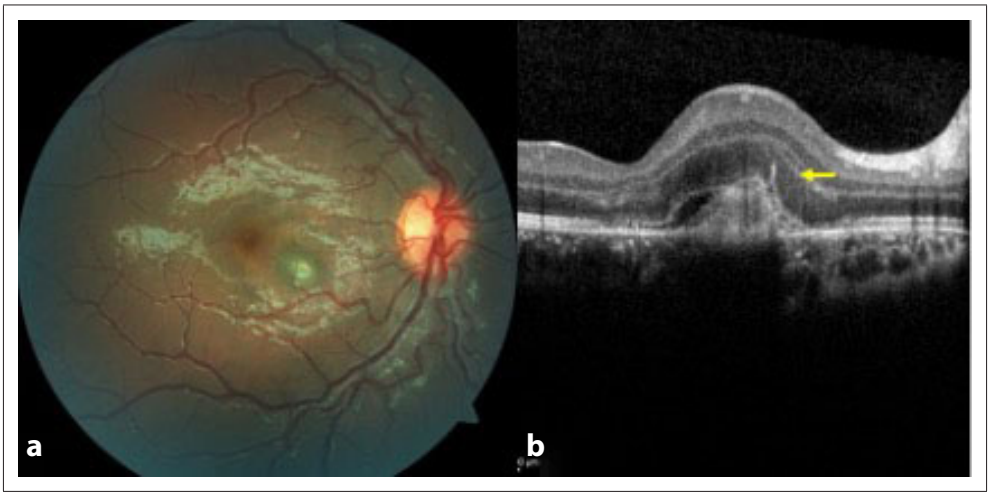

Fig. 3. Right eye, Patient 8. At the presentation, **(a)** Color fundus picture depicting the extrafoveal. Yellowish lesion, optical coherence tomography section **(b)** depicting the subretinal hyperreflective area with some subretinal fluid and hyperreflective finger-like projections (pitchfork sign) (yellow arrow).

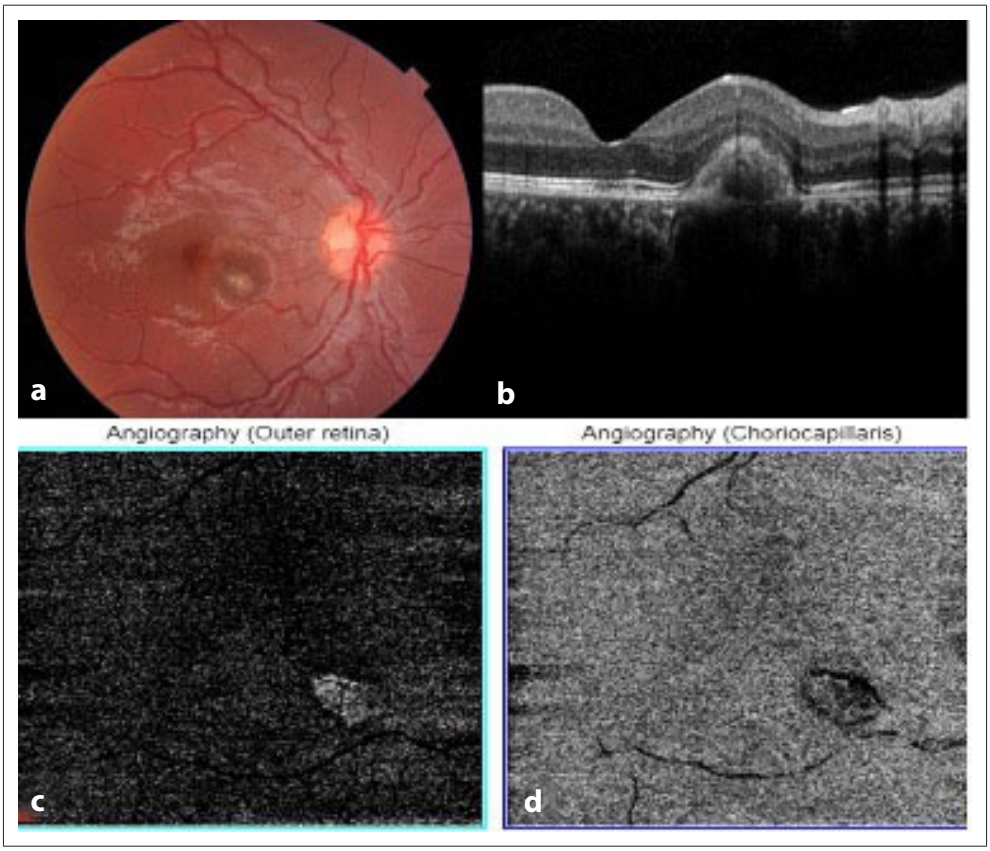

Fig. 4. Right eye, Patient 8, after the anti-vascular endothelial growth factor (anti-VEGF) treatment. **(a and b)** Optical coherence tomography section and the color fundus. Picture demonstrating the regressed lesion without any subretinal fluid following a single dose of intravitreal anti-VEGF (aflibercept 2 mg) treatment. **(c and d)** Outer retina and choriocapillaris slabs revealing the neovascular tuft on optical coherence tomography angiography.

three eyes with optic disc drusen, the CNV location was peripapillary. Peripapillary CNV has been reported to be associated with preexisting ocular pathology rather than being idiopathic, like the subfoveal CNVs.[7,17] Peripapillary CNV may occur as a consequence of various optic nerve diseases such as idiopathic intracranial hypertension, chronic papilledema, pseudopapilledema, optic disc drusen, malignant hypertension, and optic nerve head

Table 2. Previous large series in the literature on pediatric CNV

Study (year)	Number of eyes (patients)	Nature of study	Average follow-up (months)	Most common etiology (%)	Treatment / no. of eyes	Average injections per eye	BCVA at presentation	BCVA at final visit
Rishi et al. (2013)	36 (27)	Single-centre, retrospective	26 (range: 0.07-111.8)	Inflammatory (41.7)	Anti-VEGF/2 (bevacizumab 1.25 mg) PDT/5 TTT/6 Laser/1	4	20/600	20/400
Kozak et al. (2014)	45 (39)	Multi-centre, retrospective	12.8 (range: 3-60)	Inflammatory (38.4)	Anti-VEGF/45 (ranibizumab 0.5 mg and bevacizumab 1.25 mg)	2.79 (1-13)	20/150	20/100
Barth et al. (2016)	10 (8)	Single-centre, retrospective	35 (range: 6-120)	Choroidal osteoma (30)	Anti-VEGF/7 (aflibercept 2 mg, ranibizumab 0.5 mg and bevacizumab 1.25 mg) PDT/3	5.4 (2-10)	logMAR 0.48	logMAR 0.46
Padhi et al. (2017)	43 (35)	Multi-centre, retrospective	Range: 6-84	Retinal dystrophy (39.5)	Anti-VEGF/27 (ranibizumab, bevacizumab and pegaptanib) PDT/1 Laser/1	2.1	Overall visual gain	logMAR 0.43
Ranjan et al. (2021)	26 (23)	Single-centre, retrospective	28.1 (range: 8-72)	Inflammatory (61.5)	Anti-VEGF/19 (ramibizumab 0.5 mg and bevacizumab 1.25 mg)	2	20/125	20/50
Zhang et al. (2021)	33 (30)	Single-centre, prospective	29 (range: 6-60)	Congenital abnormalities (30) Inflammatory (30)	Anti-VEGF/25 (aflibercept 2 mg and ranibizumab 0.5 mg) Surgery/1	1.4	logMAR 0.96	logMAR 0.85
Current study	12 (12)	Single-centre, retrospective	32.8 (range: 6-132)	Optic disc drusen (25) Laser point injury (17) Uveitis (17)	Anti-VEGF/4 (aflibercept 2 mg and ranibizumab 0.5 mg) PDT/1	1	logMAR 0.54	logMAR 0.38

PDT: Photodynamic therapy; TTT: Transpupillary thermotherapy

anomalies.[18] Notably, Rishi *et al*.[7] reported that in their case series, all patients with peripapillary CNV had optic disc drusen.

In our study, a total of 5 eyes underwent treatment. Treatment modalities were tailored individually for each patient. Underlying ocular diseases, CNV location, activation, and systemic conditions were the determining factors.

The initial treatment strategy for pediatric CNV in our clinic was intravitreal anti-VEGF agents. The increasing use of intravitreal anti-VEGF agents has been a major advancement in the management of vitreoretinal diseases in pediatric patients, including CNV. However, it is not currently known whether the short-term suppression of systemic VEGF results in long-term neurodevelopmental outcomes, especially in younger children.[2,19-23]

Previous reports showed that pediatric CNVs had fewer recurrences and required fewer injections in contrast to CNVs that occurred in adults. Finn *et al*.[16] mentioned in their IRIS study that CNV was most likely to be managed with anti-VEGF agents in pediatric patients. In their study, 68.4% of eyes treated with anti-VEGF agents required 3 or fewer injections.[16]

In a subgroup analysis of the MINERVA study – in the open-label, non-randomized study arm – Hykin *et al*.[24] showed that ranibizumab 0.5 mg treatment for 12 months was beneficial for improving BCVA in adolescent patients with CNV with a relatively small number of injections. Their results were consistent with previously published literature in the young population, as we mentioned before. Table 2 summarizes previous large series in the literature on pediatric CNV treated with anti-VEGF.[1-4,7,25]

In all patients, injections were performed under general anesthesia. None of them required more than 1 anti-VEGF injection. Among 4 eyes with subfoveal CNV, the mean BCVA for eyes that underwent treatment was logMAR 0.62±0.15 (range: 0.8–0.5) at presentation which improved to mean logMAR 0.3±0.2 (range: 0.5–0.1) on regression, suggesting the favorable impact of intravitreal anti-VEGF treatment for active disease. Therefore, according to the efficacy and favorable prognosis of limited anti-VEGF therapy, it is recommended that timely treatment for CNV should be considered in the pediatric population.[3,7,25]

One of our patients with peripapillary CNV due to optic disc drusen underwent PDT in 2007. The use of PDT in pediatric CNV has been reported in some case series and reports before. The results of these studies have demonstrated the safety and efficacy of PDT in pediatric CNV.[26-29] In addition, sometimes unfavorability to PDT may be observed, and intravitreal anti-VEGF injections may be necessary in cases of resistance to PDT.[30] In our patient, BCVA increased after he underwent PDT, and intravitreal anti-VEGF treatment was not required afterwards.

In uveitic cases with CNV, if the disease is also active, systemic treatment for the uveitis control is mandatory.[23] In our patient with intermediate uveitis, oral azathioprine (1.5 mg/kg/day) was administered in association with the intravitreal anti-VEGF treatment. Uveitis activity was monitored by careful clinical examination and FA when deemed necessary. No serious side effects were observed in any patient during the follow-up period.

The limitations of our study are its retrospective design, small number of cases, and the lack of a standard protocol. The small sample size and incomplete follow-up of some patients limit the generalizability of our findings. The loss to follow-up in one-third of cases might have created a selection bias. The study period (2007–2023) spans major advances in imaging modalities and treatment protocols, from the pre-anti-VEGF era to the utilization of OCTA and newer intravitreal agents. This heterogeneity may have affected the diagnostic sensitivity, treatment selection, and thereby the clinical outcome.

Conclusion

CNV in the pediatric population is a serious condition with severe visual consequences. In our series, intravitreal anti-VEGF treatment was an effective, safe option with no serious side effects even with a small number of injections. Since there is no standardized treatment protocol for pediatric patients, every patient should be thoroughly evaluated individually, and appropriate treatment should be selected.

Ethics Committee Approval: This study was approved by The Ethics Committee of Dokuz Eylul University (registration code: 8618-GOA, September 09, 2024).

Informed Consent: Written informed consents were obtained from patient and his family.

Peer-review: Externally peer-reviewed.

Authorship Contributions: Design: T.O., A.O.; Supervision: A.O.S.; Resource: ; Materials: I.K., Z.A., M.K.; Data Collection and/or Processing: I.K., T.O.; Analysis and/or Interpretation: I.K., T.O.; Literature Search: I.K.; Writing: I.K., A.O.S.; Critical Reviews: A.O.S.

Conflict of Interest: None declared.

Use of AI for Writing Assistance: Not declared.

Financial Disclosure: The authors declared that this study received no financial support.

References

1. Padhi TR, Anderson BJ, Abbey AM, et al. Choroidal neovascular membrane in paediatric patients: clinical characteristics and outcomes. Br J Ophthalmol 2018;102:1232–7. [CrossRef]

2. Kozak I, Mansour A, Diaz RI, et al. Outcomes of treatment of pediatric choroidal neovascularization with intravitreal antiangiogenic agents: the results of the KKESH International Collaborative Retina Study Group. Retina 2014;34:2044–52. [CrossRef]
3. Zhang T, Wang Y, Yan W, et al. Choroidal Neovascularization in Pediatric Patients: Analysis of Etiologic Factors, Clinical Characteristics and Treatment Outcomes. Front Med (Lausanne) 2021;8:735805. [CrossRef]
4. Barth T, Zeman F, Helbig H, Oberacher-Velten I. Etiology and treatment of choroidal neovascularization in pediatric patients. Eur J Ophthalmol 2016;26:388–93. [CrossRef]
5. Gilbert C, Foster A, Négrel AD, Thylefors B. Childhood blindness: a new form for recording causes of visual loss in children. Bull World Health Organ 1993;71:485-9.
6. Spraul CW, Grossniklaus HE. Characteristics of Drusen and Bruch's membrane in postmortem eyes with age-related macular degeneration. Arch Ophthalmol 1997;115:267–73. [CrossRef]
7. Rishi P, Gupta A, Rishi E, Shah BJ. Choroidal neovascularization in 36 eyes of children and adolescents. Eye (Lond) 2013;27:1158–68. [CrossRef]
8. Melberg NS, Thomas MA, Burgess DB. The surgical removal of subfoveal choroidal neovascularization. Ingrowth site as a predictor of visual outcome. Retina 1996;16:190–5. [CrossRef]
9. Uemura A, Thomas MA. Visual outcome after surgical removal of choroidal neovascularization in pediatric patients. Arch Ophthalmol 2000;118:1373–8. [CrossRef]
10. Goshorn EB, Hoover DL, Eller AW, Friberg TR, Jarrett WH 2nd, Sorr EM. Subretinal neovascularization in children and adolescents. J Pediatr Ophthalmol Strabismus 1995;32:178–82. [CrossRef]
11. Kuehlewein L, Bansal M, Lenis TL, et al. Optical Coherence Tomography Angiography of Type 1 Neovascularization in Age-Related Macular Degeneration. Am J Ophthalmol 2015;160:739–48.e2. [CrossRef]
12. Lumbroso B, Rispoli M, Savastano MC. Longitudinal optical coherence tomography-angiography study of type 2 naive choroidal neovascularization early response after treatment. Retina 2015;35:2242–51. [CrossRef]
13. Ong SS, Hsu ST, Grewal D, et al. Appearance of pediatric choroidal neovascular membranes on optical coherence tomography angiography. Graefes Arch Clin Exp Ophthalmol 2020;258:89–98. [CrossRef]
14. Veronese C, Maiolo C, Huang D, et al. Optical coherence tomography angiography in pediatric choroidal neovascularization. Am J Ophthalmol Case Rep 2016;2:37–40. [CrossRef]
15. Macular Photocoagulation Study Group. Subfoveal neovascular lesions in age-related macular degeneration. Guidelines for evaluation and treatment in the macular photocoagulation study. Arch Ophthalmol 1991;109:1242–57. [CrossRef]
16. Finn AP, Fujino D, Lum F, Rao P. Etiology, Treatment Patterns, and Outcomes for Choroidal Neovascularization in the Pediatric Population: An Intelligent Research in Sight (IRIS®) Registry Study. Ophthalmol Retina 2022;6:130–8. [CrossRef]
17. Keles A, Karaman SK. Intravitreal aflibercept treatment for choroidal neovascularization secondary to laser pointer. Oman J Ophthalmol 2020;13:146–8. [CrossRef]
18. Rishi P, Bharat RPK, Rishi E, et al. Choroidal neovascularization in 111 eyes of children and adolescents. Int Ophthalmol 2022;42:157–66. [CrossRef]
19. Chen Y, Cunningham A, Kotagiri A. The danger of laser pointer-induced retinal damage in children: a large United Kingdom case series and survey of public awareness. J Pediatr Ophthalmol Strabismus 2023;60:52–9. [CrossRef]
20. Kaya M, Yagci BA. Bilateral macular injury following red laser pointer exposure: A case report. Eur Eye Res 2021;1:170-3. [CrossRef]
21. Wu AL, Wu WC. Anti-VEGF for ROP and Pediatric Retinal Diseases. Asia Pac J Ophthalmol (Phila) 2018;7:145–51.
22. Ruparelia S, Sundaram A, Dahrab M, Symonds C, Cruess A. Response of Pediatric Choroidal Neovascularization to Anti-Vascular Endothelial Growth Factor. Cureus 2021;13:e20195. [CrossRef]
23. Kayabaşı M, Ataş F, Saatci AO. Unilateral macular neovascularization formation during the follow-up of a 15-year-old boy with Bietti crystalline dystrophy and the successful treatment outcome with a single intravitreal ranibizumab injection. GMS Ophthalmol Cases 2023;13:Doc06.
24. Hykin PG, Staurenghi G, Wiedemann P, et al. Ranibizumab 0.5 mg treatment in adolescents with choroidal neovascularization: subgroup analysis data from the minerva study. Retin Cases Brief Rep 2021;15:348–55. [CrossRef]
25. Ranjan R, Salian R, Verghese S, et al. Pediatric choroidal neovascularization: Etiology and treatment outcomes with anti-vascular endothelial growth factors. Eur J Ophthalmol 2022;32:235567. [CrossRef]
26. Yıldırım C, Çetin EN, Yayla K, Avunduk AM, Yaylalı V. Photodynamic therapy for unilateral idiopathic peripapillary choroidal neovascularization in a child. Int Ophthalmol 2011;31:333–5. [CrossRef]
27. Mimouni KF, Bressler SB, Bressler NM. Photodynamic therapy with verteporfin for subfoveal choroidal neovascularization in children. Am J Ophthalmol 2003;135:900–2. [CrossRef]
28. Lipski A, Bornfeld N, Jurklies B. Photodynamic therapy with verteporfin in paediatric and young adult patients: long-term treatment results of choroidal neovascularisations. Br J Ophthalmol 2008;92:655–60. [CrossRef]
29. Rego-Lorca D, Catalá-Mora J, López-de-Eguileta A, Díaz-Cascajosa J. Choroidal neovascularization in children: etiology, clinical characteristics and treatment outcomes. Arch Soc Esp Oftalmol (Engl Ed) 2024;99:534-9. [CrossRef]
30. Schadlu R, Blinder KJ, Shah GK, et al. Intravitreal bevacizumab for choroidal neovascularization in ocular histoplasmosis. Am J Ophthalmol 2008;145:875–8. [CrossRef]

DOI: 10.14744/eer.2025.30092
Eur Eye Res 2026;6(1):86–96

EUROPEAN EYE RESEARCH

ORIGINAL ARTICLE

A bibliometric analysis of the editorial boards of ophthalmology journals in Türkiye: Academic productivity, institutional affiliations, gender distributions, subspecialties, and geographical distributions

Mubeccel Bulut,[1] Ali Hakim Reyhan,[2] Cagri Mutaf[2]

[1]Department of Ophthalmology, Necip Fazil City Hospital, Kahramanmaras, Turkiye
[2]Department of Ophthalmology, Harran University, Sanliurfa, Turkiye

Abstract

Purpose: This research examines the current status of nine ophthalmology journals in Türkiye by analyzing their editorial and advisory boards in terms of gender representation, geographical distributions, academic seniority, and subspecialty areas.

Methods: This study examined the editorial and advisory boards of nine Turkish ophthalmology journals by analyzing demographic profiles and publication records obtained from institutional websites and bibliometric databases, National Institutes of Health iCite, and Dimensions.ai. Information regarding the subspecialties of Turkish academics was sourced from the Turkish Ophthalmological Association website. The iCite data provided metrics such as total publications, publications per year, total citations, citations per year, and relative citation ratio (RCR), while the dimensions database yielded complementary metrics, including total publications, total citations, mean citations per publication, field citation ratio, RCR, and percentage of cited publications.

Results: Professors constituted the majority (75.66%) of the 393 editors and advisory board members, and 37.25% were women. Geographically, 87.25% of editors were based in Türkiye, with major concentrations in Ankara (31.61%), Istanbul (21.47%), and Izmir (13.12%). Institutional analysis demonstrated diverse affiliations, with independent and private practice physicians constituting 8.10% (n=40) of the members, followed by physicians affiliated with private hospitals at 6.48% (n=32). Performance metrics from the iCite and dimensions databases identified the Turkish Journal of Ophthalmology as the leading body, with 88.71±84.5 publications, 2108.92±3046.14 citations, and an RCR of 1.24±0.86.

Conclusion: Enhancing the global impact of Turkish ophthalmology journals involves increasing transparency in editorial selection, promoting gender-balanced representation, fostering international collaboration, and addressing regional disparities through strategic diversity initiatives.

Keywords: Academic titles; bibliometric analysis; citation metrics; editorial boards; gender distribution; geographical distribution; ophthalmology journals.

Cite this article as: Bulut M, Reyhan AH, Mutaf C. A bibliometric analysis of the editorial boards of ophthalmology journals in Türkiye: academic productivity, institutional affiliations, gender distributions, subspecialties, and geographical distributions. Eur Eye Res 2026;6(1):86–96.

Correspondence: Mubeccel Bulut, M.D. Department of Ophthalmology, Necip Fazil City Hospital, Kahramanmaras, Turkiye
E-mail: mubeccelbagdas@gmail.com

Submitted Date: 04.11.2025 **Revised Date:** 08.01.2026 **Accepted Date:** 26.01.2026 **Available Online Date:** 29.04.2026

The editorial boards of scientific journals are highly important bodies that ensure quality control in academic publishing and determine publication policies. The composition of editorial boards directly affects journals' scientific quality and impact.[1] The academic profiles, institutional affiliations, and demographic characteristics of editorial board members thus represent important indicators for understanding the ecosystem of scientific publishing.

Journals in the field of general clinical ophthalmology serve as vital platforms for disseminating advances in the diagnosis, management, and treatment of eye diseases. These peer-reviewed publications not only provide a repository of cutting-edge research but also play an important role in shaping ophthalmologists' academic and professional trajectories.[2,3] These journals also contribute to the improvement of clinical standards and the overall progression of ophthalmology as a discipline by promoting evidence-based practice and a culture of continuous learning.

Ophthalmology journals in Türkiye play a crucial role in publishing and disseminating scientific studies in the field of eye diseases. They facilitate the sharing of academic knowledge in ophthalmology and also contribute to raising scientific standards. Editorial boards determine the publication quality of these journals and the scientific management of the processes involved. The demographic structure of these boards is of great importance to understanding journals' scientific impact and publication policies.[4]

The question of gender distributions in editorial boards has become an important research topic in academic publishing. Global analysis has shown that women are under-represented on the editorial boards of ophthalmology journals.[5] The under-representation of women in these influential positions not only reflects broader societal inequalities but also perpetuates systemic biases within the academic ecosystem. Gender inequalities in editorial boards can affect the diversity of perspectives in decision-making processes and potentially influence the selection of research topics, peer review practices, and publication outcomes.

Institutional affiliations and geographical distributions play an important role in shaping the academic ecosystem. Geographical proximity enhances the intensity and frequency of scientific collaboration, thereby strengthening the impact of research outputs.[6] Institutional prestige increases the likelihood of being published in high-impact journals.[7] These factors directly affect academic productivity and scientific communication, playing a critical role in determining research quality and visibility. International collaboration and institutional connections are of considerable strategic importance to enhancing scientific productivity and integration into global academic networks for researchers in developing countries.

Bibliometric analysis tools play a crucial role in evaluating scientific impact and monitoring academic communications. The dimension database provides researchers with comprehensive data analysis capabilities by integrating a wide range of academic resources, including publications, grants, patents, clinical trials, and policy documents.[7] Its advanced search features and user-friendly interface mean that researchers can easily examine complex datasets and identify emerging trends and key contributors. Similarly, the iCite platform facilitates a more accurate assessment of scientific impact by providing comprehensive citation metrics and impact indicators for biomedical publications.[8] Innovative features such as the relative citation ratio (RCR), which normalizes citation rates for a specific field and time period, facilitate the comparison of scientific impacts across different research domains.

Focusing solely on quantitative criteria (such as publication and citation counts) is not by itself sufficient for the evaluation of scientific research. A comprehensive assessment requires consideration of various qualitative factors, including academic title, institutional affiliation, geographical location, academic background, and subspecialty areas. The Leiden Manifesto serves as an important guide in this regard, recommending that qualitative indicators should also be taken into account in research evaluation.[9] Accordingly, the combined use of quantitative and qualitative indicators in scientific assessments enables a more comprehensive and equitable evaluation of the scientific contributions of researchers and institutions.

This study examined the current academic ecosystem of Turkish ophthalmology publishing via a multidimensional analysis of the editorial boards of relevant journals published in Türkiye. Indicators of academic productivity, institutional affiliations, geographical distributions, academic titles, and the gender distributions of editors and advisors were examined. The findings obtained will contribute to the development of strategies aimed at enhancing academic productivity, promoting diversity, and strengthening institutional collaboration.

Materials and Methods

This study analyzed the editorial compositions and academic contributions of nine ophthalmology journals published in

Türkiye; Archieves of Ophthalmological Research, Beyoğlu Eye Journal, Current Retina Journal, Journal of Glaucoma and Cataract, European Eye Research, MN Ophthalmology, Retina-vitreus, Turkish Journal of Ophthalmology, Türkiye Klinikleri Journal of Ophhthalmology. The selection criteria for these journals were as follows: All active ophthalmology journals published in Türkiye and indexed in Web of Science (WOS), Scopus, total return index, and other national and international indexes were included in the study. The journals included in the study were selected from among those that were actively publishing, with publicly available editorial and/or advisory board information, and that had been regularly publishing articles for at least 1 year. Data were collected from December 1 to 31, 2024

The first step involved identifying these journals' editorial teams. Information regarding the chief editors, editors, assistant editors, and members of the scientific advisory boards were systematically collected from each journal's official website. Several demographic parameters were analyzed for each identified academic, including titles (professor, associate professor, assistant professor, or specialist physician), gender distribution, geographical location (city of practice), and institutional affiliations (universities, private clinics, public hospitals, or international institutions). Information regarding the subspecialties of Turkish academics was obtained from the Turkish Ophthalmological Association website.

Based on this comprehensive data collection, this study employed a hierarchical approach to analyze the editorial structures of the journals, systematically categorizing leadership roles into three principal groups: (1) Editor-in-Chief/Co-Editor, (2) Associate Editor, and (3) Editorial or Advisory Board members. This classification was necessitated by the observed variation in editorial organization across journals. While some journals appoint an editor-in-chief, others designate co-editors; similarly, certain journals maintain an editorial board, whereas others have an advisory board. By consolidating these roles into three overarching categories, the study ensured a consistent and comprehensive evaluation of editorial governance, accommodating the structural differences present among the journals.

The identified individuals' academic publication records were next analyzed to evaluate their scholarly contributions and impact. Two widely recognized online databases were employed for this comprehensive bibliometric analysis, the National Institutes of Health iCite[10] and Dimensions.ai.[11] Five key bibliometric parameters were examined using iCite, total publications, publications per year, total citations, citations per year, and RCR. The Dimensions database provided complementary metrics, including total publications, total citations, mean citations per publication, field citation ratio (FCR), RCR, and percentage of cited publications.

Since the data used in the study were obtained from publicly available sources, ethical approval was not required. The study adhered to the principles outlined in the Declaration of Helsinki, ensuring that all data collection and analysis processes were conducted ethically and with respect for the rights and privacy of the individuals involved. The data collection and analysis were conducted systematically and independently verified by two researchers in order to ensure the inter-rater reliability and accuracy of the findings.

The analysis employed descriptive statistics, percentage distributions, and bibliometric indicators to characterize both the demographic composition and academic impact profiles of editorial board members.

Results

All journals are indexed in Tübitak/Ulakbim except for Archives of ophthalmological research. The Turkish Journal of Ophthalmology is the only one of these journals indexed in WOS. In addition, the Turkish Journal of Ophthalmology Journal of Retina-vitreus Beyoğlu Eye Journal are indexed in Scopus, while PubMed/MEDLINE indexes both the Turkish journal of ophthalmology and Beyoglu eye journal.

The editorial structures of the nine ophthalmology journals revealed a total of 502 editorial board positions, which were held by 434 ophthalmologists. Closer examination showed that 378 ophthalmologists served on the editorial board of only one journal, while 43 individuals held positions on the editorial boards of two different journals. In addition, 10 ophthalmologists were members of three different editorial boards, and three academics served simultaneously on the editorial boards of four distınct journals. Ophthalmologists whose credentials could not be reliably verified were excluded from the study.

The composition and distribution of editorial positions revealed distinct patterns across different hierarchical levels. Among editor-in-chief and co-editor positions, all members (100%) held full professorial titles, with a gender distribution of 25% female and 75% male representatives. For associate editor positions, the academic ranking revealed a predominance of full professors (82.76%), followed by associate professors (17.24%), with no assistant professors represented. The gender

distribution among associate editors exhibited 41.38% female and 58.62% male representation. In terms of the editorial/advisory board category, the distribution revealed 74.19% full professors, 19.52% associate professors, and 6.29% assistant professors, with an overall gender composition of 42.08% women and 57.92% men (Fig. 1).

In the gender distribution of editors, only MN Ophthalmology was leading in terms of female representation. Regarding academic ranks, the majority of editorial positions were held by full professors, with Türkiye Klinikleri Ophthalmology journal exhibiting the highest concentration of senior academics (Fig. 2). The academic positions, gender demographics, and editorial structures of the nine Turkish ophthalmology journals are summarized in Table 1.

The geographical distribution of editorial and advisory board members demonstrated clear national trends. The vast majority of editors were based in Türkiye, with only a small proportion representing other countries. While a few journals maintained exclusively domestic editorial boards, others included a more diverse international presence. Notably, participation from countries outside Türkiye remained limited overall (Table 2). Three major metropolitan areas – Ankara, Istanbul, and Izmir – emerged as the primary centers of editorial leadership, reflecting the established academic infrastructure in these cities.

The bibliometric analysis of Turkish ophthalmology journals, utilizing both the iCite and dimensions databases, revealed a clear stratification in academic performance and influence across the field. According to iCite data,

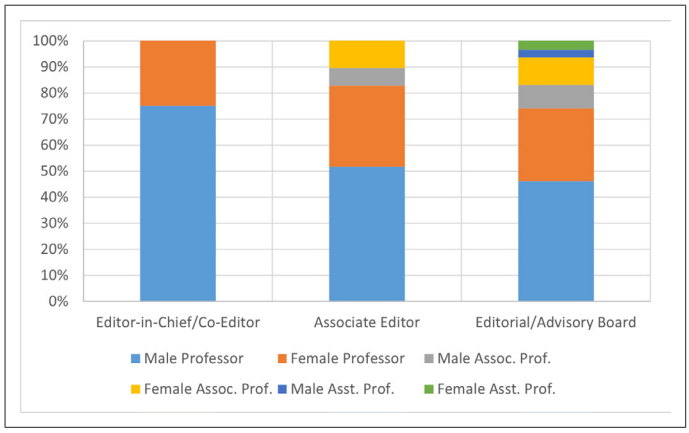

Fig. 1. The distribution of academic ranks and gender across editorial positions (Editor-in-chief/co-editor. associate editor. and editorial/advisory board) in Turkish ophthalmological journals. Each bar represents the proportion of male and female members within each academic rank for the specified editorial role. The slash (/) in position titles indicates alternative naming conventions used by different journals. Percentages are calculated within each editorial position.

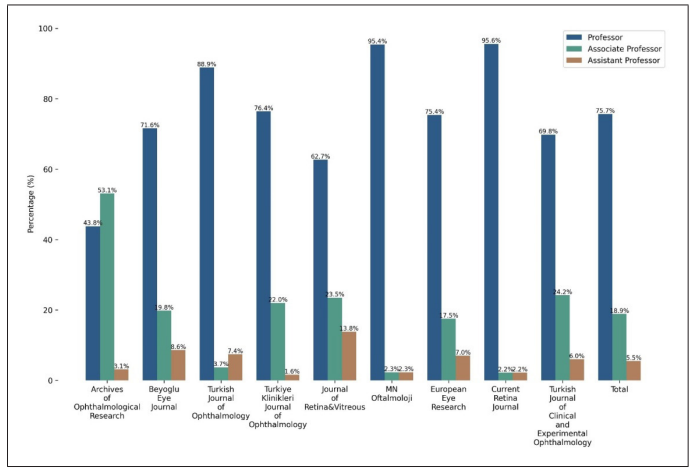

Fig. 2. Distributions of academic titles across ophthalmology journals. The bar chart illustrates the percentage distribution of professors, associate professors, and assistant professors/specialist physicians across nine ophthalmology journals and the overall total.

the Turkish journal of ophthalmology consistently demonstrated the highest level of academic impact (88.71 ± 84.5 publications, 2108.92 ± 3046.14 citations, RCR: 1.24 ± 0.86) among all nine journals analyzed. This journal led in key metrics such as publication output and citation rates, establishing itself as the most influential publication in the field. The journal of Retina and Vitreous also performed strongly, closely following the leader in most performance indicators. Other journals, including the Beyoğlu eye journal and European eye research, exhibited more moderate levels of impact, while MN Ophthalmology and Türkiye Klinikleri Journal of Ophthalmology exhibited developing performance patterns, characteristic of newer or more specialized publications. Editorial/Advisory Board members had noticeably higher publication and citation counts compared to other editorial positions. However, the high standard deviations observed in this group (±1125.24 for publications and ±16505.03 for citations) indicate considerable variability among members. When comparing associate editors with editor-in-chief/co-editors, associate editors exhibited slightly higher metrics, with more publications (63.48 ± 46.23 vs. 54.42 ± 46.25) and higher numbers of publications per year (3.35 ± 1.98 vs. 2.74 ± 1.76). Editor-in-chief/co-editors exhibited higher total citations (904.58 ± 1555.69 vs. 712.62 ± 608.19) (Table 3).

The dimensions database further supported these findings, highlighting considerable variation in bibliometric performance among the journals. The Turkish Journal of Ophthalmology again stood out with the highest mean numbers of publications and citations, as well as the strongest

Table 1. Academic position, gender demographics, and editorial structure of Turkish ophthalmology journals' editorial board members

Turkish ophthalmologic academic journals	Professor	Associate professor	Assistant professor/ specialist	Female	Male
	n (%)	*n* (%)	*n* (%)	*n* (%)	*n* (%)
Archives of ophthalmological research	13 (41.94)	17 (54.84)	1 (3.23)	11 (35.48)	20 (64.52)
Beyoğlu eye journal	58 (69.88)	16 (19.28)	9 (10.84)	40 (48.19)	43 (51.81)
Turkish journal of ophthalmology	25 (89.29)	1 (3.57)	2 (7.14)	13 (46.43	15 (53.57)
Türkiye Klinikleri journal of ophthalmology	94 (76.42)	27 (21.95)	2 (1.63)	55 (44.72)	68 (55.28)
Journal of Retina and Vitreous	34 (62.96)	13 (24.07)	7 (12.96)	12 (22.22)	42 (77.78)
MN ophthalmology	43 (95.56)	1 (2.22)	1 (2.22)	24 (53.33)	21 (46.67)
European eye research	43 (75.44)	10 (17.54)	4 (7.02)	25 (43.86)	32 (56.14)
Current retina journal	43 (95.56)	1 (2.22)	1 (2.22)	11 (24.44)	34 (75.56
Turkish journal of clinical and experimental ophthalmology	25 (69.44)	9 (25)	2 (5.56)	18 (50)	18 (50)
Editorial structure					
Editor-in-chief/co-editor	12 (100)	0 (0)	0 (0)	3 (25)	9 (75)
Associate editor	24 (82.76)	5 (17.24)	0 (0)	12 (41.38)	17 (58.62)
Editorial/advisory board	342 (74.19)	90 (19.52)	29 (6.29)	194 (42.08)	267 (57.92)
Total	378 (75.3)	95 (18.92)	29 (5.78)	209 (41.63)	293 (58.37)

n: Number, %: Distribution percentage. Data were collected from official journal websites between December 1 and 31, 2024. Percentages are calculated within each journal or editorial structure category. "Assistant Professor/Specialist" includes both assistant professors and specialist physicians without academic titles. Gender distribution is based on publicly available information; in cases of ambiguity. Data were cross-checked with institutional profiles. Descriptive statistics were calculated for all metrics (mean±standard deviation)

RC). Second-tier journals, such as the Journal of Retina and Vitreous and European eye research, maintained moderate citation impacts and publication counts. The remaining journals exhibited comparable but lower RCR values, reflecting their emerging status within the academic community. In addition, editors-in-chief and co-editors exhibited strong academic profiles, with an average of 92 publications and 1,391 citations. Similarly, associate editors demonstrated consistent academic performance, with approximately 82 publications and 1,052 citations. In line with the data from the iCite database, Editorial/Advisory Board members displayed greater academic diversity; this group includes both researchers with very high numbers of publications and citations, as well as those with more modest academic outputs (Table 4).

The analysis of ophthalmology subspecialties revealed clear differences in both representation and academic influence. Medical Retina emerged as the most prominent subspecialty among editorial board members, followed by Vitreoretinal surgery and cornea and ocular surface. In contrast, fields such as contact lens and electrodiagnostic were represented by a smaller proportion of members (Fig. 3).

Despite its limited representation, the contact lens subspecialty was noteworthy for its remarkable academic impact. This field demonstrated the highest levels of publication productivity and citation influence, outperforming other subspecialties in both RCR and FCR. Conversely, areas such as electrodiagnostic and neuro-ophthalmology, while clinically significant, exhibited lower citation metrics, indicating comparatively modest academic influence (Table 5).

Discussion

The findings of this study provide valuable insights into the characteristics of the editorial boards and academic productivity of nine ophthalmology journals in Türkiye. The data obtained yield a comprehensive analysis of the journals' publication metrics, citation performances, and international impacts. These results constitute an important basis for understanding the journals' current status and for

Table 2. National and international distributions of editorial board members in Turkish ophthalmology journals

Turkish academic ophthalmological journals	Practicing in Türkiye	Practicing outside Türkiye	Total
	n (%)	*n* (%)	*n* (%)
Archives of ophthalmological research	29 (93.55)	2 (6.45)	31 (100)
Beyoğlu eye journal	74 (89.16)	9 (10.84)	83 (100)
Turkish journal of ophthalmology	22 (78.57)	6 (21.43)	28 (100)
Türkiye Klinikleri journal of ophthalmology	119 (96.75)	4 (3.25)	123 (100)
Journal of Retina and Vitreous	37 (68.52)	17 (31.48)	54 (100)
MN ophthalmology	45 (100)	0 (0)	45 (100)
European eye research	47 (82.46)	10 (17.54)	57 (100)
Current retina journal	40 (88.89)	5 (11.11)	45 (100)
Turkish journal of clinical and experimental ophthalmology	33 (91.67)	3 (8.33)	36 (100)

n: Number, %: Distribution percentage. Data were collected from official journal websites between December 1 and 31, 2024. "Practicing in Turkey" refers to editorial board members whose primary institutional affiliation is within Türkiye at the time of data collection. "Practicing outside Türkiye" refers to editorial board members whose primary institutional affiliation is outside Türkiye. Percentages are calculated within each journal. Editorial board member locations were determined based on publicly available institutional information; in cases of ambiguity. Data were cross-checked with institutional or professional profiles. Descriptive statistics were calculated for all metrics (mean±standard deviation)

Table 3. Publication metrics and citation analysis of the editorial and advisory boards and editorial structure of Turkish ophthalmology journals: A bibliometric analysis using the iCite database

Turkish academic ophthalmological journals	Total pubs	Pubs per year	Total citations	Cites per year	(RCR)
	Mean±S.D.	Mean±S.D.	Mean±S.D.	Mean±S.D.	Mean±S.D.
Archives of ophthalmological research	28.23±26.94	2.16±1.58	250.13±417.25	1.13±0.5	0.75±0.37
Beyoğlu eye journal	46.99±45.78	2.91±1.96	599.33±1506.67	1.53±1.42	0.92±0.61
Turkish journal of ophthalmology	88.71±86.07	4.18±3.49	2108.93±3102.04	2.06±1.62	1.24±0.88
Türkiye Klinikleri journal of ophthalmology	34.81±57.06	2.16±2.53	415.06±1464.51	1.24±1.27	0.79±0.67
Journal of Retina and Vitreous	539.26±1848.42	55.8±332.95	10883.15±47387.05	2.53±2.66	1.42±1.17
MN ophthalmology	34.18±31.22	1.91±1.33	364.33±359.24	1.61±2.57	0.97±1.16
European eye research	57.37±52.16	3.11±2.21	936.37±1941.43	1.52±1.23	0.89±0.58
Current retina journal	37.95±22.56	1.97±1.07	484.98±706.87	1.78±2.81	0.97±1.2
Turkish journal of clinical and experimental ophthalmology	38.83±32.16	2.17±1.5	447.72±490.63	1.46±1.23	0.93±0.65
Editorial structure					
Editor-in-chief/co-editor	54.42±46.25	2.74±1.76	904.58±1555.69	1.85±1.83	1.07±0.89
Associate editor	63.48±46.23	3.35±1.98	712.62±608.19	2.15±3.12	1.21±1.38
Editorial/advisory board	186.33±1125.24	95.42±934.57	1885.45±16505.03	88.3±928.21	87.69±928.27

S.D.: Standard deviation, RCR: Relative citation ratio. Data were collected from iCite Database databases between December 1 and 31, 2024. Total pub: The total number of published articles indexed in the databases. Pubs per year: Average number of publications per year since the first indexed publication. Total citations: The cumulative number of citations received for all publications. Cites per year: Average number of citations received per year. RCR: A field-normalized metric that shows the citation impact of one paper relative to the average paper in its field. Some variations in metrics may be due to differences in journal indexing periods and database coverage. Editorial structure metrics are grouped by editorial position. Descriptive statistics were calculated for all metrics (mean±standard deviation)

shaping their future strategic directions.

Our analysis reveals that professors dominate editorial positions across the hierarchy, particularly at the Editor-in-Chief level (100%), with their representation gradually decreasing in Associate Editor and Editorial/Advisory Board positions. This pattern indicates that while academic

Table 4. Publication metrics and citation analysis of editorial and advisory boards and editorial structure of Turkish ophthalmology journals: A dimensions database analysis

Turkish academic ophthalmological journals	Total pubs	Total citations	Citations (mean)	FCR	RCR	Publications with citations
	Mean±S.D.	Mean±S.D.	Mean±S.D.	Mean±S.D.	Mean±S.D.	
Archives of ophthalmological research	37.2±29.9	272.53±284.39	11.32±22.93	2.24±3.7	1.2±1.11	72.59±15.48
Beyoğlu eye journal	63.65±52.18	647.37±782.98	61.85±419.95	2.28±5.22	2.78±14.78	71.04±12.65
Turkish journal of ophthalmology	123.04±119.07	3234.43±4571.34	50.58±140.32	7.72±22.31	2.06±4.64	83.37±12.28
Turkiye Klinikleri journal of ophthalmology	60.67±98.3	774.37±2460.66	12.9±34	3.36±11.7	0.93±1	70.16±15.93
Journal of Retina and Vitreous	99.65±73.26	1451.84±1410.5	14.29±9.12	2.13±1.15	1.27±1.2	74.75±15.42
MN ophthalmology	55.4±51.8	731.33±905.54	12.61±9.44	1.67±0.98	0.97±1.24	72.54±22.33
European Eye Research	87.04±75.74	1691.79±3069.42	15.86±16.59	2.12±1.71	1.04±0.6	74.42±13.74
Current retina journal	59.76±29.59	681.58±415.29	16.32±21.3	2.32±3.25	1.07±1.34	75.1±11.68
Turkish journal of clinical and experimental ophthalmology	60.78±37.2	771.81±655.5	12.15±6.05	1.83±0.72	0.96±0.51	77.88±12.37
Editorial structure						
Editor-in-chief and co-editor	91.92±48.81	1391.17±1679.2	28.59±38.31	5.48±8.11	1.52±1.35	81.01±15.52
Associate editor	82.45±48.48	1051.86±806.36	13.21±7.9	2±0.76	1.26±1.45	77.07±11.93
Editorial/advisory board	240.54±1300.47	1187.65±2517.68	210.8±1383.37	197.87±1384.55	196.28±1384.75	266.73±1374.88

S.D.: Standard deviation. FCR: Field citation ratio, RCR: Relative citation ratio. Data were collected from the Dimensions database between December 1 and 31. 2024. All values are presented as mean±standard deviation. Total Pubs: The total number of articles published by editorial board members. Total citations: The cumulative number of citations received. Citations (mean): Average number of citations per publication. FCR: A field-normalized citation metric. RCR: A field-normalized metric indicating citation impact. Publications with citations: Percentage of publications that have received at least one citation. Editorial structure metrics are grouped by editorial position

seniority remains a key factor in editorial appointments, there is some diversification at lower editorial levels. Similarly, a previous study from Türkiye by Tutuncu demonstrated that full professors predominate on editorial boards, while young or early-career academics are under-represented.[12] Our findings showed that associate and assistant professors are particularly limited in senior editorial positions. This reflects a lack of scientific innovation and diversity in academic publishing.[13,14]

Gender disparities were most pronounced at higher editorial levels. Male professors held the majority of Editor-in-Chief and Co-Editor positions, with no associate or assistant professors of either gender occupying these top roles. At the Associate Editor level, male professors continued to outnumber females, although female associate professors had slightly higher representation than their male counterparts. In the Editorial/Advisory Board, male professors remained the majority, although the presence of women increased among associate and assistant professors. Numerous studies consistently highlight systemic gender inequality in scientific publishing.[15-17] In this context, those authors emphasize male dominance in certain fields and teams through concepts such as "men's clubs" and "male islands." Similarly, Bransch and Kvasnicka reported that male dominance in editorial boards of top economics journals creates a barrier to female economists in the academic publication process.[18] Their findings show that both the likelihood of female authors publishing articles and the number of citations received by articles rise in line with the proportion of female editors. In addition, they noted that the presence of female editors positively affects article quality (as measured by citation counts). On the other hand, Ellemers *et al.* [19] highlighted the concept of "Queen Bee Syndrome," noting that senior female academics who have succeeded in male-dominated academic fields may exhibit greater prejudice against other women.

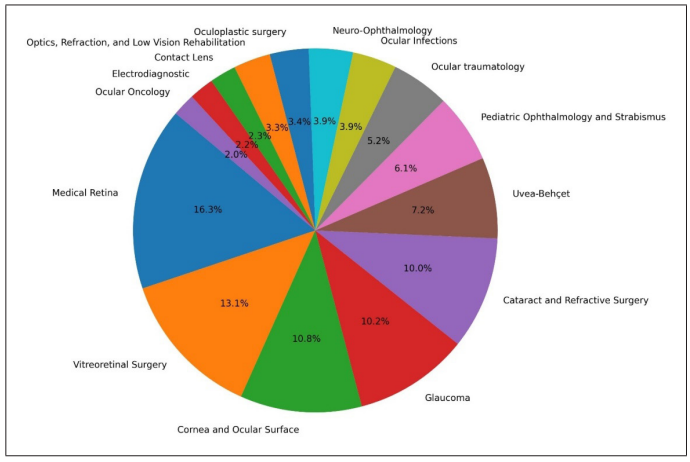

Fig. 3. Distribution of ophthalmology subspecialties represented on the editorial boards of Turkish journals. The pie chart illustrates the proportion of editorial board members across various ophthalmology subspecialties. Including medical retina, vitreoretinal surgery, cornea and ocular surface, glaucoma, cataract and refractive surgery, Uvea–Behçet, pediatric ophthalmology and strabismus, ocular traumatology, ocular infections, neuro-ophthalmology, oculoplastic surgery, optics, refraction and low vision rehabilitation, contact lens, electrophysiology/diagnostics, and ocular oncology. Each segment represents the percentage of total editorial board positions held by specialists in the respective subspecialty.

This imbalance points to the existence of structural gender-based barriers in accessing academic leadership positions. Amrein *et al*.[20] proposed a range of multidimensional strategies to address this issue, including transparent quota systems in editorial processes, mentorship programs for female academics, and ensuring equal access to research resources. Adopting gender-balanced approaches in editorial representation is of critical importance if ophthalmology journals in Turkey are to compete at the level of international standards and enhance their scientific productivity. The development of institutional policies, the establishment of diversity-focused goals by journal management, and the design of training programs to address implicit biases that perpetuate inequality may therefore be recommended.

Editorial boards predominantly consisting of members from Türkiye (87.25%) indicate that these journals primarily rely on local academic networks, with limited international participation. This is particularly apparent in journals such as Türkiye Klinikleri Journal of Ophthalmology (95.12%) and MN ophthalmology (100%), reflecting a national focus and a preference for local researchers. In contrast, journals such as the Turkish journal of ophthalmology (29.63%) and the Journal of Retina and Vitreous (35.29%) attracted higher levels of contributions from abroad. Similarly, Brinn and Jones examined 60 academic accounting journals (22 from the UK, 13 from the USA, and nine from Australia) and 437 editorial board members, finding that most editorial boards were mainly composed of academics from the journal's country of publication, indicating a strong "home country bias."[21] This geographical concentration in editorial leadership is further supported by Csomos comprehensive analysis of 11,915 journals from WOS's SSCI and SCIE databases and 15,795 editors-in-chief, which revealed that editors-in-chief are largely concentrated in the USA (33.90%), demonstrating that country's marked dominance in this field. Those authors also found a strong correlation between the geographical distribution of editors and the origin of publishing houses.[22] This indicates a notable lack of global diversity and interdisciplinary collaboration, which may limit these journals' citation impacts and academic interaction potential. In the future, enhancing publication quality and visibility, as well as promoting international collaborations, may be recommended to increase global participation. These steps could enhance the global influence of the journals, enabling them to reach a broader readership.

The geographical and institutional distributions of the editorial boards of ophthalmology journals in Türkiye revealed notable inequalities in academic productivity. Editorial positions are dominated by major metropolitan areas such as Ankara (31.61%), Istanbul (21.47%), and Izmir (13.12%1) due to advantages in terms of funding, technological infrastructure, and access to qualified human resources. In contrast, the lack of representation from regions such as Eastern and Southeastern Anatolia points to a grave inequity in access to scientific processes. In addition, while the marked representation of independent practitioners (8.10%) and private hospital physicians (6.48%) ensures a focus on clinical practice but raises the risk of sidelining basic sciences and long-term research. The balance between the historical legacy of traditional state universities (such as Ege, Ankara, and Gazi) and the dynamism of newer institutions such as the University of Health Sciences reflects the transformation in medical education in training. However, the lack of collaboration between these institutions limits the development of interdisciplinary studies. Hodgson's study highlighted a significant "institutional oligopoly" in the editorial structure of economics journals. Their findings show that editorial positions are heavily concentrated in a few prestigious universities, especially elite institutions in the USA (such as Harvard, MIT, Chicago, Yale, Princeton, and Stanford) and leading universities in the UK (including Oxford, Cambridge,

Table 5. Turkish ophthalmology association members by subspecialties based on Icite and dimensions databases

Turkish ophthalmology subspecialty categories	Icite			Dimensions		
	Pubs per year mean±S.D.	Cites per year mean±S.D.	RCR mean±S.D.	Citations mean±S.D.	FCR mean±S.D.	RCR mean±S.D.
Cataract and refractive surgery	2.18±1.37	1.06±0.41	0.72±0.31	12.51±6.87	1.83±0.93	0.84±0.30
Contact lens	3.52±3.57	1.98±1.58	1.23±0.79	40.18±181.71	6.79±12.61	1.79±2.34
Cornea and ocular surface	2.98±2.21	1.33±1.00	0.87±0.53	21.58±44.08	3.40±6.85	1.25±1.33
Electrodiagnostic	1.51±0.95	1.12±0.53	0.69±0.24	8.36±3.42	1.30±0.45	0.74±0.32
Glaucoma	2.81±1.84	1.32±0.86	0.83±0.49	15.96±25.72	2.49±3.83	0.94±0.73
Medical retina	2.70±2.35	1.63±1.90	0.95±0.86	12.33±7.80	1.71±0.67	0.96±0.87
Neuro-ophthalmology	1.94±1.27	0.98±0.35	0.69±0.25	7.86±3.66	1.59±1.24	0.94±1.02
Ocular infections	4.08±3.19	1.80±1.99	1.11±0.77	24.28±63.77	3.63±9.16	1.33±1.81
Ocular oncology	3.39±2.36	1.29±0.97	0.77±0.48	12.64±9.87	1.68±1.33	0.91±0.62
Ocular traumatology	2.39±1.27	1.54±1.81	0.88±0.75	16.63±29.89	2.70±4.74	1.01±0.95
Oculoplastic surgery	2.23±1.25	1.52±1.95	1.02±0.95	11.54±9.21	1.65±0.74	1.13±0.65
Optics. Refraction. and low vision rehabilitation	2.02±1.16	1.24±0.53	0.84±0.31	11.15±7.34	1.70±0.59	0.91±0.28
Pediatric ophthalmology and strabismus	1.56±0.89	1.04±0.60	0.73±0.44	8.85±5.04	1.48±0.66	0.87±0.39
Uvea-Behçet	2.88±1.74	2.01±2.45	1.13±1.05	14.04±10.64	1.93±0.67	1.21±1.20
Vitreoretinal surgery	2.43±1.3	1.99±2.45	1.10±1.05	13.42±8.33	1.83±0.87	0.99±0.96

S.D.: Standard deviation, FCR: Field citation ratio, RCR: Relative citation ratio. Data were collected from the iCite and Dimensions databases between December 01 and 31. 2024. All values are presented as mean±standard deviation. Pubs per year: Average number of publications per year (Icite). Cites per year: Average number of citations per year (Icite). RCR: A field-normalized metric indicating citation impact (Icite). Citations: Total number of citations (Dimensions). FCR: A field-normalized citation metric (Dimensions). Subspecialty categories were determined based on expertise classifications provided by the Turkish ophthalmological association. Descriptive statistics (mean±SD) were used for all variables

and the London School of Economics). This concentration limits opportunities for researchers from other institutions to access editorial roles and publish their work.[23] Lowe's study examined the editorial boards of accounting journals and found that board members were generally selected from more prestigious universities, suggesting the possibility of an "elite" bias in these selections.[24] Melhem's study on the editorial boards of international biomedical journals similarly points to the low representation of certain regions and suggests that the homogeneity of editorial boards may influence scientific publication decisions.[25] In the light of these findings, we believe that strategic steps aimed at enhancing the diversity of editorial boards in Türkiye could play a critical role in addressing regional disparities and supporting interdisciplinary and basic scientific research.

The evaluation of publication metrics for the editorial and advisory boards of ophthalmology journals published in Türkiye against global standards is crucial for understanding their place in the international academic arena. Tutuncu's study from Türkiye, which analyzed 219 Turkish national social science journals indexed in Tr Dizin, showed that journals with highly qualified editors have lower acceptance rates, reflecting higher standards.[26] The data from the current study revealed these journals' international performance, competitiveness, and development potential. This assessment not only helps clarify the current status of these journals but also serves as a roadmap for early-career academics. Young researchers can shape their academic careers and learn strategies for enhancing international impact by examining these journals' achievements and areas for development.

ICITE and dimensions analyses revealed significant performance differences among the editorial and advisory boards of Turkish ophthalmology journals. The Turkish Journal of Ophthalmology demonstrated the strongest

metrics with the highest publication, citation, and RCR values, while journals such as the Journal of Retina and Vitreous and European eye research exhibited strong but somewhat lower performance. Erdag and Citirik reported that the editorial board of the Turkish journal of ophthalmology demonstrated higher performance than other Turkish ophthalmology journals in terms of WOS publication count, h-index, and total publications in Scopus. However, no significant difference was found between journals in terms of average citation counts in WOS.[27] These analyses provide a framework for future efforts aimed at optimizing editorial practices and research dissemination strategies in the field.

The "Contact Lens" category demonstrates a higher citation impact compared to other subspecialties based on its metrics. "Electrodiagnostic" and "Neuro-Ophthalmology" have the lowest RCR values, reflecting limited academic activity in these fields. This situation can be explained by the fact that ophthalmologists specializing in electrodiagnostics are less common compared to ophthalmologists specializing in areas such as the retina.

Erdağ and Erda reported that retina specialists exhibited higher academic productivity compared to other subspecialties.[27] Tanya *et al*. [28] determined that among Canadian ophthalmologists, the subspecialty rankings based on H-index demonstrated that ocular oncology achieved the highest academic impact with an H-index. The use of different databases for academic productivity data and the varying training programs and working hours within the Ophthalmology sub-registration areas may have contributed to these inconsistencies.

These data can guide young ophthalmologists in their career planning while also serving as important reference points for institutions and health policymakers in resource allocation and strategy development.[28]

Similarly to Gershoni *et al.*'s [29] report, the most prevalent subspecialties among the analyzed position holders in the present study were retina, cornea, and glaucoma. In light of these data, and considering factors such as high income potential and popularity, ophthalmology leaders appear to have concentrated their focus on retina, cornea, and glaucoma subspecialties.

Several recommendations may be proposed to address challenges and enhance the global impact of these journals. These include improving transparency in editorial selection processes, promoting gender-balanced representation, fostering international collaboration, and addressing regional disparities through strategic diversity initiatives.

Limitations

The publication and citation counts presented in this study should be considered solely as quantitative indicators of editors' academic profiles. However, as emphasized in the literature, higher numbers of publications and citations do not always directly translate to academic quality or performance. These metrics can be influenced by various factors and are potentially subject to manipulation (such as excessive self-citation, citation circles, and salami slicing of publications). Such indicators alone are not, therefore, sufficient to evaluate the scientific contributions of editors, and the results should be interpreted with these limitations in mind.

There are a number of limitations to this study. For example, the presence of multiple entries for some editorial board members in the dimensions or ICITE databases, rather than verified unique names, may have affected the data accuracy. In addition, the existence of authors with identical names increases the likelihood of errors and flawed matches during the author selection process. Furthermore, the fact that not all ophthalmologists are active members of the TODNET.org database and that some physicians with advanced subspecialties had to be categorized under the general ophthalmologist category constitute other limitations of the study.

Conclusion

The editorial boards of ophthalmology journals in Türkiye exhibit geographical imbalances in terms of being concentrated in major cities, the predominance of full professors in editorial positions, limited representation of early-career academics, and a gender disparity favoring male academics. In addition, the predominance of Turkish citizens on editorial boards indicates a lack of international participation. The Turkish journal of ophthalmology exhibited the strongest publication and citation metrics, reflecting its primacy among Turkish ophthalmology journals.

Ethics Committee Approval: This study is a study focused on public internet databases. It did not require ethics committee approval.

Peer-review: Externally peer-reviewed.

Authorship Contributions: Concept: C.M.; Design: M.B.; Supervision: M.B., C.M.; Materials: M.B., C.M.; Analysis and/or Interpretation: A.H.R.; Literature Search: A.H.R.; Writing: A.H.R.

Conflict of Interest: None declared.

Use of AI for Writing Assistance: Not declared.

Financial Disclosure: The authors declared that this study received no financial support.

References

1. Balasubramanian S, Saberi K, Adusumalli S, Wagholikar KB, Ganguly N. Women representation among cardiology journal editorial boards. Circulation 2020;141:786-7. [CrossRef]
2. Reyes J, Seddon I, Watane A, Gedde S, Sridhar J. Association between preresidency peer-reviewed publications and future academic productivity or career choice among ophthalmology residency applicants. JAMA Ophthalmol 2023;141:178-83. [CrossRef]
3. Rivera PA, Atayde A, Wang L, Kombo N. Female authorship and ophthalmology journal editorial board membership trends over the last decade, 2012-2021. Am J Ophthalmol 2023;255:107-14. [CrossRef]
4. Dewidar O, Elmestekawy N, Welch V. Improving equity, diversity, and inclusion in academia. Res Integr Peer Rev 2022;7:4. [CrossRef]
5. Hoekman J, Frenken K, Tijssen RJ. Research collaboration at a distance: Changing spatial patterns of scientific collaboration within Europe. Res Policy 2020;39:662-73. [CrossRef]
6. Tomkins A, Zhang M, Heavlin WD. Reviewer bias in single- versus double-blind peer review. Proc Natl Acad Sci U S A 2017;114:12708-13. [CrossRef]
7. Herzog C, Hook D, Konkiel S. Dimensions: Bringing down barriers between scientometricians and data. Quant Sci Stud 2020;1:387-95. [CrossRef]
8. Hutchins BI, Baker KL, Davis MT, et al. The NIH Open Citation Collection: A public access, broad coverage resource. PLoS Biol 2019;17:e3000385. [CrossRef]
9. Hicks D, Wouters P, Waltman L, de Rijcke S, Rafols I. Bibliometrics: The Leiden Manifesto for research metrics. Nature 2015;520:429-31. [CrossRef]
10. National Institutes of Health (NIH). iCite. Available from: https://icite.od.nih.gov/. Accessed: December 1-31, 2024.
11. Digital Science. Dimensions. Available from: https://www.dimensions.ai/. Accessed: December 31, 2024.
12. Tutuncu L. Gatekeepers or gatecrasher? The inside connection in editorial board publications of Turkish national journals. Scientometrics 2024;129:957-84. [CrossRef]
13. Horta H. Academic inbreeding: Academic oligarchy, effects, and barriers to change. Minerva 2022;60:593-613. [CrossRef]
14. Macfarlane B, Jefferson AE. The closed academy? Guild power and academic social class. High Educ Q 2022;76:36-47. [CrossRef]
15. Larivière V, Ni C, Gingras Y, Cronin B, Sugimoto CR. Bibliometrics: global gender disparities in science. Nature 2013;504:211-3. [CrossRef]
16. Shah S, Shumway NB, Sarvis EW, Sena JA, Voice A, Mumtaz A, Sheikh AB. Gender Parity in Geriatrics Editorial Boards. Geriatrics (Basel) 2022;7:90. [CrossRef]
17. Auschra C, Bartosch J, Lohmeyer N. Differences in female representation in leading management and organization journals: establishing a benchmark. Res Policy 2022;51:104410. [CrossRef]
18. Bransch F, Kvasnicka M. Male gatekeepers: gender bias in the publishing process? J Econ Behav Organ 2022;202:714-32. [CrossRef]
19. Ellemers N, van den Heuvel H, de Gilder D, Maass A, Bonvini A. The underrepresentation of women in science: differential commitment or the queen bee syndrome? Br J Soc Psychol 2004;43:315-38. [CrossRef]
20. Amrein K, Langmann A, Fahrleitner-Pammer A, Pieber TR, Zollner-Schwetz I. Women underrepresented on editorial boards of 60 major medical journals. Gend Med 2011;8:378-87. [CrossRef]
21. Brinn T, Jones MJ. The composition of editorial boards in accounting: a UK perspective. Account Audit Account J 2008;21:5-35. [CrossRef]
22. Csomos G. Mapping the geography of editors-in-chief. J Data Inf Sci 2024;9:124-37. [CrossRef]
23. Hodgson GM, Rothman H. The editors and authors of economics journals: a case of institutional oligopoly? Econ J 1999;109:165-86. [CrossRef]
24. Lowe DJ, Van Fleet DD. Scholarly achievement and accounting editorial board membership. J Account Educ 2009;27:197-209. [CrossRef]
25. Melhem G, Rees CA, Sunguya BF, Ali M, Kurpad A, Duggan CP. Association of International Editorial Staff With Published Articles From Low- and Middle-Income Countries. JAMA Netw Open 2022;5:e2213269. [CrossRef]
26. Tutuncu L. Editorial board publication strategy and acceptance rates in Turkish national journals. J Data Inf Sci 2023;8:49-83. [CrossRef]
27. Erdag M, Citirik M. Assessing the H-Indexes of Editorial Board Members in Ophthalmology Journals Published in Türkiye. Beyoglu Eye J 2024;9:101-5. [CrossRef]
28. Tanya SM, He B, Tang J, et al. Research productivity and impact of Canadian academic ophthalmologists: trends in H-index, gender, subspecialty, and faculty appointment. Can J Ophthalmol 2022;57:188-94. [CrossRef]
29. Gershoni A, Tiosano A, Gabbay O, et al. Academic background, professional experience, and research achievements of United States academic ophthalmology leadership. Ir J Med Sci 2021;190:1-7. [CrossRef]

DOI: 10.14744/eer.2025.80488
Eur Eye Res 2026;6(1):97–99

EUROPEAN EYE RESEARCH

CASE REPORT

A rare complication of intravitreal dexamethasone implantation: Intralenticular Ozurdex implantation

Deniz Bagci, Cumali Degirmenci

Department Of Ophthalmology, Ege University, Izmir, Turkiye

Abstract

Intravitreal dexamethasone (DEX) implant is a device that continuously releases DEX after injection into the vitreous. It is used for indications such as diabetic macular edema (DME), non-infectious posterior uveitis, and retinal vein occlusion. The most common complications include intraocular pressure elevation and cataract. We present the case of a 59-year-old female referred for cataract surgery 18 months after receiving a DEX implant for DME. Slit-lamp biomicroscopy revealed a Grade III nuclear cataract and an intralenticular DEX implant. The patient subsequently underwent phacoemulsification with intraocular lens (IOL) implantation. Hydrodissection was deliberately omitted, and excessive manipulations were avoided. The posterior capsule remained intact, and a three-piece IOL was implanted within the capsular bag without intraoperative complications. Conclusion: Intralenticular Ozurdex implantation is a rare but clinically relevant complication. Careful injection technique, patient cooperation, and meticulous surgical management are essential to prevent and successfully manage this event.

Keywords: Diabetes; implantation; intralenticular; Ozurdex.

The dexamethasone (DEX) intravitreal implant (Ozurdex®, Allergan Inc., Irvine, CA, USA) is a biodegradable device that slowly releases 0.7 mg DEX into the vitreous cavity over several months.[1-3] It is commonly used for diabetic macular edema (DME), macular edema secondary to non-infectious posterior uveitis, and retinal vein occlusion.[3]

Although generally safe and effective, several complications have been reported, including cataract progression, transient intraocular pressure (IOP) elevation, conjunctival hemorrhage, implant migration into the anterior chamber, and, rarely, inadvertent implantation into the crystalline lens.[4,5] Intralenticular placement represents a unique scenario that may alter both the therapeutic efficacy of the implant and the progression of lens opacification.

Herein, we report a rare case of intralenticular DEX implant detected during cataract progression, and we discuss its surgical management and postoperative course.

Case Report

A 59-year-old female was referred to our clinic for cataract surgery, having received an intravitreal DEX implant in the right eye at another center 18 months earlier due to DME.

At presentation, best-corrected visual acuity (BCVA) was 1.80 logMAR in the right eye and P+P– in the left eye. IOP

* This case was presented as a poster at the 57th National Congress of the Turkish Ophthalmological Association. The 57th Turkish Ophthalmological Association (TOA) National Congress will be held in Antalya, Turkey on 8-12 November 2023.

Cite this article as: Erkan Pota Ç, Atlıhan YS. Analysis of tear meniscus and anterior segment alterations in keratoconus patients after scleral contact lens. Eur Eye Res 2026;6(1):97–99.

Correspondence: Cumali Degirmenci, M.D. Department of Ophthalmology, Ege University, Izmir, Turkiye
E-mail: cudegirmenci@yahoo.com

Submitted Date: 29.05.2025 **Revised Date:** 03.09.2025 **Accepted Date:** 11.09.2025 **Available Online Date:** 29.04.2026

measured 15 mmHg in the right eye and 36 mmHg in the left eye. Biomicroscopic examination revealed a Grade III nuclear cataract and an intralenticular DEX implant in the right eye (Fig. 1), and a Grade II nuclear cataract with rubeosis iridis in the left eye. Fundus examination demonstrated bilateral peripheral panretinal photocoagulation (PRP) scars. Fundus fluorescein angiography showed diffuse leakage without significant neovascularization (Fig. 2). Optical coherence tomography (OCT) revealed retinal thickening and an epiretinal membrane in the right eye (Fig. 3).

The patient first received an intravitreal bevacizumab injection in the right eye, followed by phacoemulsification and intraocular lens (IOL) implantation. Hydrodissection was deliberately omitted, and manipulations during phacoemulsification were minimized. The posterior capsule was confirmed to be intact, and a three-piece IOL was implanted into the capsular bag. No intraoperative complications occurred.

At 1 month postoperatively, BCVA improved to 0.7 logMAR. IOP was 21 mmHg under dual topical antiglaucomatous therapy. The IOL was well-centered, the cornea remained clear, and no anterior chamber reaction was observed. Fundus examination confirmed previous PRP. Macular OCT demonstrated persistent DME with a central retinal

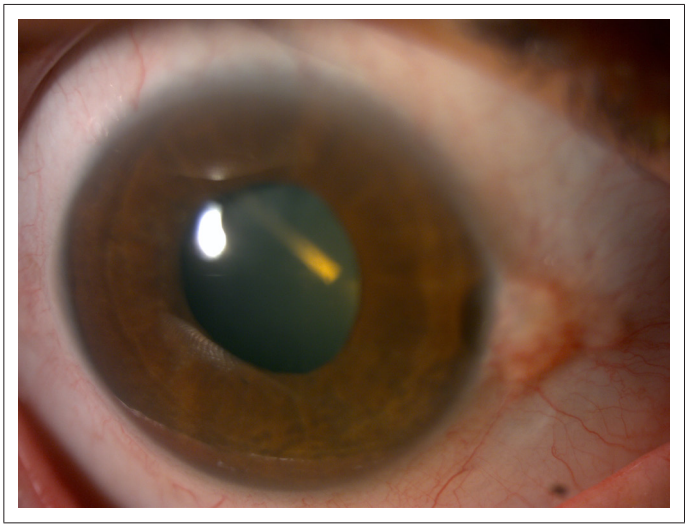

Fig. 1. Anterior segment photograph of the right eye showing intralenticular Ozurdex implantation, ×16 magnification.

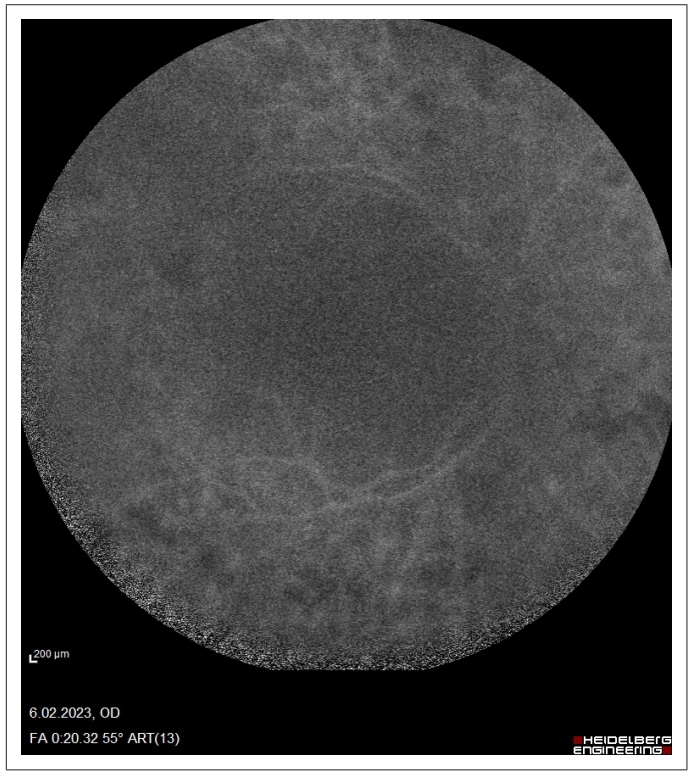

Fig. 2. Fundus fluorescein angiography of the right eye showing diffuse leakage without clear neovascularization.

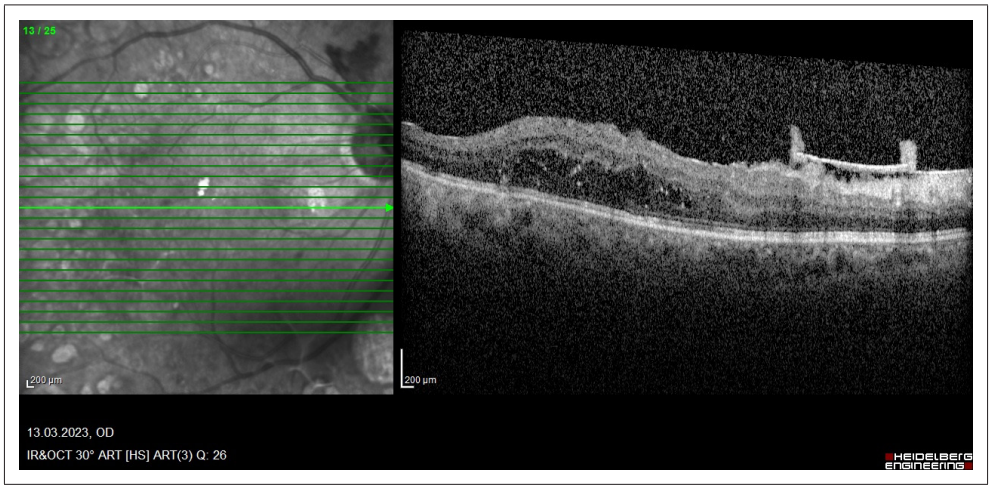

Fig. 3. Macular optical coherence tomography image of the right eye showing retinal thickening and an epiretinal membrane.

thickness of 470 µm, and three consecutive intravitreal bevacizumab injections were planned. Cyclocryotherapy was scheduled for the left eye due to neovascular glaucoma; however, the patient did not continue follow-up.

Discussion

Accidental intralenticular placement of a DEX implant is an uncommon but clinically important complication. Several factors may contribute, including inadequate injector control, poor visualization, or sudden patient movement during the injection.[6]

While intravitreal DEX is designed to release corticosteroid directly into the vitreous cavity, lenticular entrapment may alter its pharmacokinetics. Some reports suggest that such implants can remain stable and still exert therapeutic activity for several months, leading to partial or even prolonged suppression of macular edema.[7-9] However, this comes at the cost of accelerated cataract progression, often necessitating surgical removal.[7,10]

Cataract surgery in the presence of an intralenticular implant poses unique challenges. Hydrodissection is generally avoided to prevent posterior capsule rupture and implant migration.[7,10] In our case, careful phacoemulsification and capsular bag implantation of a three-piece IOL were performed successfully without complications.[6]

This case reinforces the importance of surgical expertise and careful intraoperative planning. Preventive measures are equally critical: adequate patient counseling, proper anesthesia, and stabilization of the globe during injection may reduce the likelihood of this complication.[5] From a management perspective, conservative observation may be acceptable if the implant does not compromise vision; however, cataract extraction is indicated when there is visual axis involvement or significant lens opacification.[8,9]

Conclusion

Intralenticular Ozurdex implantation is a rare but significant complication of intravitreal therapy. Although such implants may retain some therapeutic effect, cataract progression and visual axis compromise typically require surgical intervention. Careful intraoperative management, particularly omission of hydrodissection and minimization of lens stress, can ensure safe cataract extraction with preservation of capsular integrity. This case underscores the importance of preventive strategies, surgeon training, and patient cooperation to minimize the risk of such complications.

Ethics Committee Approval: This is a single case report, and therefore ethics committee approval was not required in accordance with institutional policies.

Informed Consent: Written informed consents were obtained from patient and his family.

Peer-review: Externally peer-reviewed.

Authorship Contributions:

Concept: D.B., C.D.; Design: C.D.; Supervision: C.D.; Resource: D.B., C.D.; Materials: D.B., C.D.; Data Collection and/or Processing: D.B.; Analysis and/or Interpretation: D.B., C.D.; Literature Search: D.B., C.D.; Writing: D.B., C.D.; Critical Reviews: C.D.

Conflict of Interest: None declared.

Use of AI for Writing Assistance: Not declared.

Financial Disclosure: The authors declared that this study received no financial support.

References

1. Pearce W, Hsu J, Yeh S. Advances in drug delivery to the posterior segment. Curr Opin Ophthalmol 2015;26:233-9. [CrossRef]
2. Wang J, Jiang A, Joshi M, Christoforidis J. Drug delivery implants in the treatment of vitreous inflammation. Mediators Inflamm 2013;2013:780634. [CrossRef]
3. Mohan S, Ratra D. Intravitreal Implants. Treasure Island (FL): StatPearls Publishing; 2023.
4. Garweg JG, Zandi S. Retinal vein occlusion and the use of a dexamethasone intravitreal implant (Ozurdex®) in its treatment. Graefes Arch Clin Exp Ophthalmol 2016;254:1257-65. [CrossRef]
5. Rahimy E, Khurana RN. Anterior segment migration of dexamethasone implant: risk factors, complications, and management. Curr Opin Ophthalmol 2017;28:246-51. [CrossRef]
6. Ertan E, Duman R, Doğan M. Dexamethasone intravitreal implant in the crystalline lens: a case report. Arq Bras Oftalmol 2020;83:242-5. [CrossRef]
7. Munteanu M, Rosca C. Repositioning and follow-up of intralenticular dexamethasone implant. J Cataract Refract Surg. 2013 Aug;39(8):1271-4. [CrossRef]
8. Poornachandra B, Kumar VBM, Jayadev C, Dorelli SH, Yadav NK, Shetty R. Immortal Ozurdex: A 10-month follow-up of an intralenticular implant. Indian J Ophthalmol 2017;65:2557. [CrossRef]
9. Carnevali A, Taloni A, Gatti V, et al. Effect of intralenticular dexamethasone implant: A case report. Eur J Ophthalmol 2024;34:NP80-3. [CrossRef]
10. Regan KA, Blake CR, Lukowski ZL, Iyer SSR. Intralenticular Ozurdex® - One Year Later. Case Rep Ophthalmol 2017;8:590-4. [CrossRef]

DOI: 10.14744/eer.2025.02997
Eur Eye Res 2026;6(1):100–102

EUROPEAN EYE RESEARCH

CASE REPORT[

Bilateral Acute Iris Transillumination Mimicking Anisocoria

Batuhan Aksoy,[1] Merve Iris,[2] Melih Tutuncu,[2] Didar Ucar[1]

[1]Department of Ophthalmology, Istanbul University-Cerrahpasa Faculty of Medicine, Istanbul, Turkiye
[2]Department of Neurology, Istanbul University-Cerrahpasa Faculty of Medicine, Istanbul, Turkiye

Abstract

Anisocoria, defined as a ≥0.4 mm difference in pupil diameter, may result from physiological or pathological causes. While often benign, it can occasionally indicate serious neurological or ophthalmological conditions. Bilateral acute iris transillumination (BAIT) is a rare, recently defined entity characterized by iris pigment dispersion and sphincter paralysis. A 54-year-old female presented to the emergency department on noticing unequal pupil sizes. Neurological examination and cranio-cervical magnetic resonance imaging were unremarkable. She was referred to ophthalmology for further evaluation. Slit-lamp examination revealed bilateral iris transillumination defects and pupillary mydriasis, more prominent in the left eye. No signs of uveitis, glaucoma, or optic nerve pathology were observed. On detailed anamnesis, she reported systemic moxifloxacin use 1 month earlier for an upper respiratory tract infection. Clinical findings and drug history supported a diagnosis of BAIT. BAIT should be considered in the differential diagnosis of anisocoria, especially when neurological imaging is normal. Early recognition may prevent unnecessary investigations and optimize patient care.

Keywords: Anisocoria; moxifloxacin; pupil disorders; uveitis.

Anisocoria is commonly defined as a difference of 0.4 mm or more in pupil diameter between the two eyes.[1] It can result from a wide spectrum of etiologies, ranging from benign physiological variations to potentially life-threatening conditions, and may be of either neurological or ophthalmological origin.

Among ophthalmological entities, bilateral acute iris transillumination (BAIT) and bilateral acute depigmentation of the iris (BADI) are recently described clinical syndromes. Both conditions are characterized by acute-onset, bilateral, and marked pigment dispersion from the iris. However, a distinguishing feature of BAIT is the presence of sphincter paralysis, which is absent in BADI.[2]

Herein, we present a case of BAIT associated with anisocoria that developed following oral moxifloxacin use for an upper respiratory tract infection. Written informed consent was obtained from the patient for publication of this case.

Case Report

A 54-year-old female presented to the emergency department after noticing unequal pupil sizes while looking in the mirror. She also complained of photophobia. Clinical examination confirmed anisocoria, and she was referred to the neurology department for further evaluation.

Neurological assessment revealed no ptosis, ophthalmoplegia, or cranial nerve deficits. Motor and

Cite this article as: Aksoy B, Iris M, Tutuncu M, Ucar D. Bilateral acute iris transillumination mimicking anisocoria. Eur Eye Res 2026;6(1):100–102.

Correspondence: Batuhan Aksoy , M.D. Department of Ophthalmology, Istanbul University-Cerrahpasa Faculty of Medicine, Istanbul, Turkiye
E-mail: draksoybatu@gmail.com
Submitted Date: 08.09.2025 **Revised Date:** 09.09.2025 **Accepted Date:** 30.09.2025 **Available Online Date:** 29.04.2026

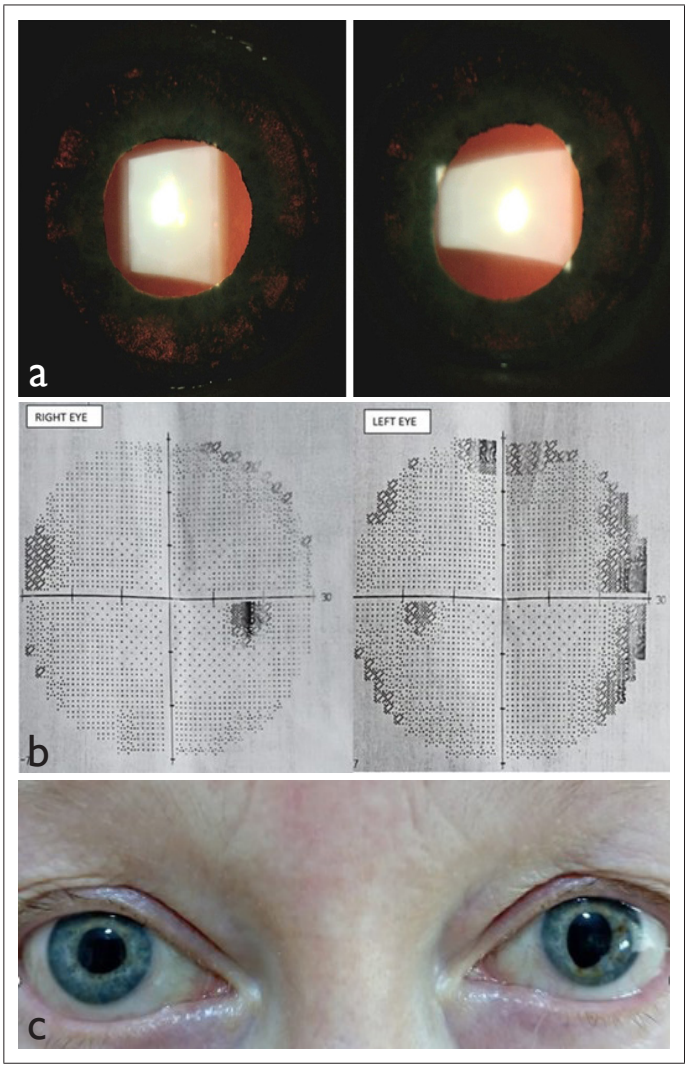

Fig. 1. **(a1 and a2)** Biomicroscopic photograph of iris transillumination deficiency (right eye is shown in the right side, left eye is shown in the left side). **(b)** Grey scale of Humphrey 30-2 SITA standard visual field test results with no abnormality other than rim defects, (left to right, consecutive right eye and left eye). **(c)** Photograph of anisocoria due to pupillary sphincter defect.

sensory examinations were within normal limits. Deep tendon reflexes were preserved, and there were no signs of cerebellar or extrapyramidal involvement.

Contrast-enhanced brain and cervical MRI showed no abnormalities. The patient denied any history of ocular trauma, chronic systemic disease, or prior intraocular surgery. Given the absence of neurological pathology, she was referred to the ophthalmology clinic for further evaluation.

Ophthalmic examination demonstrated best-corrected visual acuity of 0.0 logMAR along with mild impairment in color vision. Pupillary evaluation showed bilateral mydriasis with anisocoria; the right pupil measured 6 mm and the left 4 mm, both with poor reactivity to light. Slit-lamp examination revealed marked bilateral iris transillumination defects suggestive of pigment epithelial loss (Fig. a1, a2). Fundoscopic evaluation was unremarkable except for thin retinal architecture attributed to prior refractive surgery. Optical coherence tomography and Humphrey visual field testing revealed no structural or functional abnormalities (Fig. 1b).

Further anamnesis revealed that the patient had been prescribed oral moxifloxacin 400 mg once daily for 1 week to treat an upper respiratory tract infection approximately 1 month before presentation. Following completion of the antibiotic course, she developed bilateral ocular redness and was seen at an outside ophthalmology clinic, where she was treated with topical 0.1% nepafenac and a combination of moxifloxacin/dexamethasone eye drops. After resolution of the redness, she noticed persistent anisocoria and photophobia, prompting her emergency department visit (Fig. 1c).

In the absence of any neurological or intraocular pathology that could explain the anisocoria, the constellation of clinical findings – particularly the bilateral iris transillumination, mydriasis, poor pupillary reaction, and recent moxifloxacin use – supported a diagnosis of BAIT.

DISCUSSION

BAIT is a rare but increasingly recognized syndrome characterized by acute, bilateral loss of iris pigment epithelium, iris transillumination defects, and pupillary sphincter paralysis resulting in fixed or poorly reactive dilated pupils.[2,3] It has been strongly associated with systemic fluoroquinolone exposure, particularly moxifloxacin, and typically follows upper respiratory tract infections.

Although the precise pathophysiology remains unclear, immune-mediated toxicity to the iris pigment epithelium has been postulated. Pigment liberated into the anterior chamber can accumulate in the trabecular meshwork, increasing the risk for secondary ocular hypertension or glaucoma.[3] Therefore, close monitoring of intraocular pressure (IOP) is essential in these patients.

Anisocoria itself has a broad differential diagnosis, ranging from physiological variants to serious neurological conditions. Physiological anisocoria is generally <1 mm, remains constant under different lighting conditions, and is not associated with other neurological signs.[4,5]

In the context of BAIT, anisocoria results from iris sphincter paralysis due to pigment epithelial damage, leading to mydriatic and poorly reactive pupils. This

condition can closely mimic other causes of anisocoria with neurological implications, such as Horner syndrome, Adie's tonic pupil, or oculomotor nerve palsy.[3]

Horner syndrome presents with ptosis, miosis, and anhidrosis resulting from disruption of the sympathetic pathway. Anisocoria in Horner syndrome is typically more pronounced in dim lighting due to the affected pupil's inability to dilate.[4]

Adie's tonic pupil results from postganglionic parasympathetic denervation and is characterized by a dilated pupil that reacts poorly to light but constricts during accommodation. It is often unilateral and may be associated with diminished deep tendon reflexes (Adie's syndrome).[4]

Oculomotor nerve palsy usually manifests with ptosis, ophthalmoplegia, and a dilated, non-reactive pupil due to parasympathetic fiber involvement. It is most often caused by compressive lesions or ischemia.[4]

BAIT can be differentiated from these entities by the presence of bilateral iris transillumination, a history of recent fluoroquinolone exposure, absence of neurological signs, and symmetrical or asymmetrical mydriasis with poorly reactive pupils.

Recognition of BAIT is important to avoid misdiagnosis and prevent unnecessary diagnostic procedures, including neuroimaging and invasive testing. Treatment primarily involves the use of topical corticosteroids to reduce inflammation and pigment dispersion. Monitoring for elevated IOP is essential, as secondary glaucoma may develop and may be resistant to medical therapy, occasionally requiring surgical intervention.[6]

CONCLUSION

This case highlights the importance of thorough history taking – including recent drug exposure – and a detailed ophthalmologic examination in the differential diagnosis of anisocoria. In patients with recent systemic antibiotic use, especially fluoroquinolones, and characteristic iris changes, BAIT should be strongly considered.

Ethics Committee Approval: This is a single case report, and therefore ethics committee approval was not required in accordance with institutional policies.

Informed Consent: Written informed consent was obtained from the patient for the preparation of this work.

Peer-review: Externally peer-reviewed.

Authorship Contributions: Concept: B.A. ; Design: B.A., D.U. ; Supervision: M.T., D.U. ; Resource: B.A. ; Materials: - ; Data Collection and/or Processing: B.A. ; Analysis and/or Interpretation: B.A., M.İ., M.T., D.U. ; Literature Search: B.A., M.İ. ; Writing: B.A., M.İ., M.T., D.U. ; Critical Reviews: M.T., D.U.

Conflict of Interest: None declared.

Use of AI for Writing Assistance: Not declared.

Financial Disclosure: The authors declared that this study received no financial support.

REFERENCES

1. Lam BL, Thompson HS, Corbett JJ. The prevalence of simple anisocoria. Am J Ophthalmol 1987;104:69–73. [CrossRef]
2. Tugal-Tutkun I, Onal S, Garip A, Taskapili M, Kazokoglu H, Kadayifcilar S, et al. Bilateral acute iris transillumination. Arch Ophthalmol 2011;129:1312–9. [CrossRef]
3. Tuğal-Tutkun İ, Altan Ç. Bilateral Acute Depigmentation of Iris (BADI) and Bilateral Acute Iris Transillumination (BAIT)-an update. Turk J Ophthalmol 2022;52:342–7. [CrossRef]
4. Bakbak B, Gedik S. Anisocoria. Turk J Ophthalmol 2012;42:68–72. [CrossRef]
5. George AS, Abraham AP, Nair S, Joseph M. The prevalence of physiological anisocoria and its clinical significance - a neurosurgical perspective. Neurol India 2019;67:1500–3. [CrossRef]
6. Phulke S, Kaushik S, Kaur S, Pandav SS. Steroid-induced glaucoma: an avoidable irreversible blindness. J Curr Glaucoma Pract 2017;11:67–72. [CrossRef]

DOI: 10.14744/eer.2025.58561
Eur Eye Res 2026;6(1):103–116

EUROPEAN EYE RESEARCH

REVIEW ARTICLE

An overview of normal eye histology

Mozhgan Rezaei Kanavi,[1] Arian Rezaei[2]

[1]Ocular Tissue Engineering Research Center, Research Institute for Ophthalmology and Vision Science, Shahid Beheshti University of Medical Sciences, Tehran, Iran
[2]Sari Branch, Islamic Azad University, Faculty of Medicine, Sari, Iran

Abstract

This review, inspired by prior reviews and based on fundamental and clinical literature on normal human eye histology, describes both basic and specialized ocular histology while presenting distinctive histological images. By encompassing this review, both clinical ophthalmic practitioners and investigators in the field of basic and experimental eye research can better understand human ocular histology and determine the pathogenesis of various eye disorders.

Keywords: Clinical ophthalmic practitioners; Experimental eye research; Eye disorders; Eye histology.

Histology of the eye is the study of the ocular tissues and involves all aspects of tissue biology, with focusing on how cellular structures and arrangements optimize eye function. Understanding ocular histology is of great assistance in appreciating the pathophysiology of ocular disorders and their past and recent therapeutic approaches.[1] This review serves as an update to prior valuable reviews and scientific literature on the histology of the eye, presenting both basic/general and specialized ocular histology. For this purpose, in August 2025, all information regarding eye and adnexal histology needed for this review was extracted from relevant English articles in the PubMed, Web of Science, Cochrane Library, Embase, and Scopus databases, as well as from ophthalmology textbooks containing information about the histology of ocular components and ocular adnexa. We also included unique and high-quality photomicrographs from our eye pathology archive to enrich the review with a mini-atlas of normal eye histology.

Basic/General Ocular Histology

Ocular tissues are composed of two interactive components: Cells and extracellular matrix (ECM). The cell (Fig. 1) is the smallest unit of ocular tissues, consisting of a plasma membrane, cytoplasm, a membrane-bound nucleus, and several membrane-bound organelles. The ECM primarily consists of collagen fibrils, which support the cells, along with fluid that transports nutrients to the cells and removes wastes and secretory materials.[1,2]

Types of Ocular Tissues

There are four main types of ocular tissues: epithelial, connective, muscular, and nervous tissues.[2,3]

* The manuscript was orally presented at the Department of Ophthalmology, Faculty of Medicine, Ege University, Izmir, Türkiye in April 2025.

Cite this article as: Kanavi MR, Rezaei A. An updated review of ocular histology. Eur Eye Res 2026;6(1):103–116.

Correspondence: Mozhgan Rezaei Kanavi, M.D. Ocular Tissue Engineering Research Center, Research Institute for Ophthalmology and Vision Science, Shahid Beheshti University of Medical Sciences, Tehran, Iran
E-mail: rezaeikanavi@gmail.com

Submitted Date: 04.12.2025 **Revised Date:** 18.03.2025 **Accepted Date:** 29.03.2025 **Available Online Date:** 29.04.2026

Ocular epithelial tissues

The epithelial tissues in the eye, in addition to providing external protection, function as gatekeepers that control the passage of materials. Based on their shape and arrangement, the ocular epithelial tissues are categorized into squamous (stratified in the corneal and conjunctival epithelium), cuboidal (simple in lacrimal acini and stratified in sweat glands), and columnar (pseudostratified to stratified in the lacrimal sac epithelium) (Fig. 2).[2-5]

Ocular connective tissues

The connective tissues in the eye form the crucial connections and hold ocular tissues together. They can be classified into areolar (loose, such as conjunctival stroma), dense (such as corneal stroma), and specialized (such as fat, blood, lymph, and related inflammatory cells).[2,4,6] The connective tissues of the eye contain two types of cells: (1) fixed or resident cells, including fibroblasts, adipocytes (fat cells), macrophages, and mast cells, and (2) transient or wandering cells, including leukocytes that migrate from the bloodstream into the connective tissue in response to inflammation or tissue damage.[4,6]

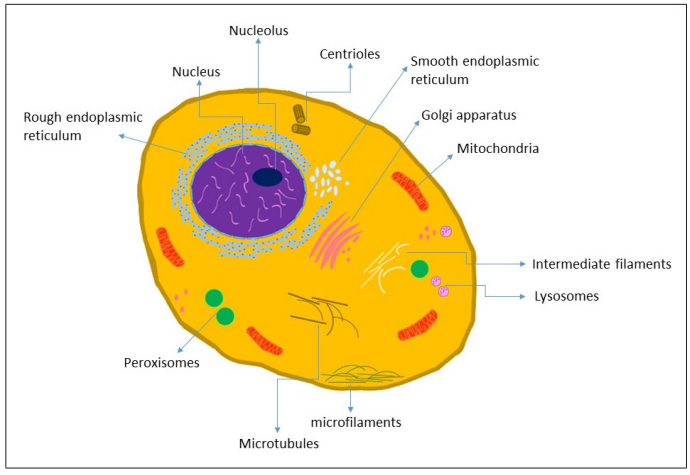

Fig. 1. A schematic image illustrating the structure of a typical cell, consisting of a nucleus (including the nucleolus) and cytoplasm that encompasses the cytoskeleton (microtubules, intermediate filaments, and microfilaments) along with intracytoplasmic organelles such as mitochondria, lysosomes, rough and smooth reticulum, peroxisomes, centrioles, and the Golgi apparatus.

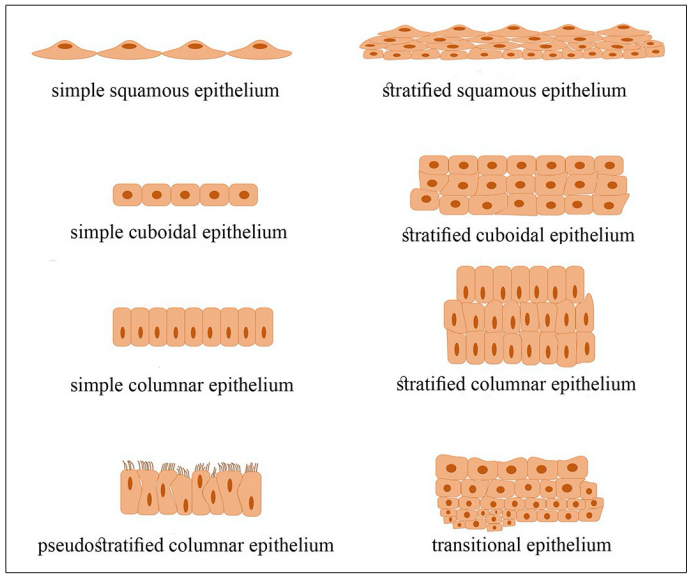

Fig. 2. A schematic image showing the types of epithelial tissues in the eye.

Inflammatory cells typically involved in the early phase of inflammation include: (1) polymorphonuclear leukocytes, which have a multi-segmented nucleus; (2) eosinophils, characterized by a bi-lobed nucleus and eosinophilic granular cytoplasm; and (3) basophils (tissue mast cells) that contain intracytoplasmic basophilic granules (Fig. 3).[7,8] The cells involved in the late phase include: (1) lymphocytes, which have a small, hyperchromatic nucleus and scant cytoplasm; (2) plasma cells, distinguished by an eccentric nucleus, a clock-face arrangement of nuclear chromatin, and a lucent curvilinear area adjacent to the nucleus composed of the Golgi apparatus; and (3) tissue monocytes (macrophages), referred to as histiocytes, which have eccentrically located indented nuclei and abundant eosinophilic cytoplasm (Fig. 4).[7,8]

Ocular muscular tissues

The muscular tissues of the eye consist of soft tissues that facilitate both voluntary and involuntary ocular movements. The eye contains both skeletal and smooth muscle types (Fig. 5). Examples of skeletal muscles include the orbicularis oculi, as well as the rectus and oblique extraocular muscles. Ocular smooth muscles consist of the superior tarsal muscle (of Müller), the sphincter and dilator muscles of the iris, and the ciliary body muscles.[4,8]

Ocular neural tissues

The neural tissues of the eye transmit electrical impulses between the eye and the brain, and are categorized into two main types: sensory and motor neurons. Each neuron (Fig. 6) comprises a cell body (soma), dendrites, an axon hillock, an axon, a myelin sheet, and an axon terminal. A collection of neurons forms a nerve, which is surrounded by a layer of connective tissue known as endoneurium. In addition, there is a layer of connective tissue around the fascicles of axons, called perineurium, and an outer layer of connective tissue that covers the nerve's surface. Neuroglial cells serve as supporting cells in the eye and include retinal astrocytes that surround retinal capillaries and maintain blood-retinal barrier, retinal microglial cells that act as resident tissue macrophages and play crucial

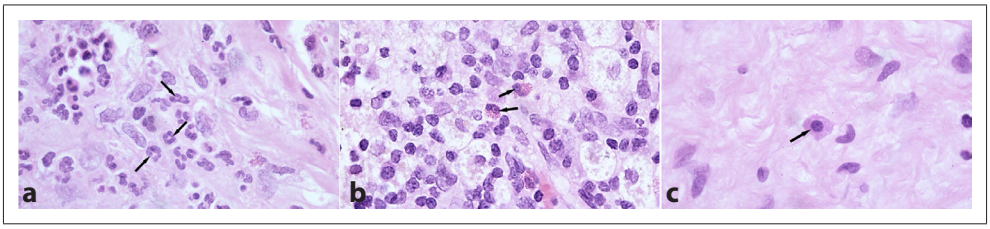

Fig. 3. Cells involved in the early phase of inflammation. **(a)** highlights polymorphonuclear leukocytes with multi-segmented nuclei (arrows). **(b)** illustrates eosinophils (arrows) with bi-lobed nuclei and eosinophilic granular cytoplasm. **(c)** shows a basophil (tissue mast cell) with a centrally located nucleus and intracytoplasmic basophilic granules (arrow).

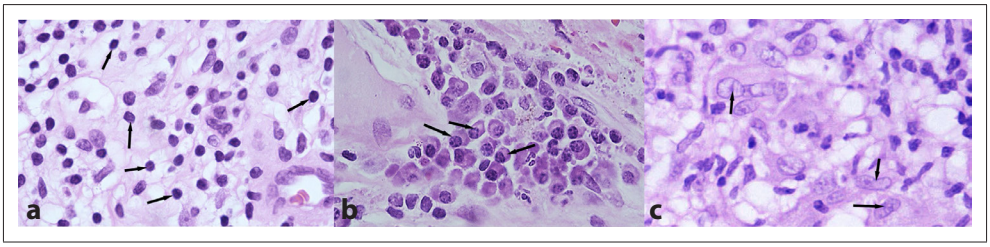

Fig. 4. Cells involved in the late phase of inflammation. **(a)** depicts lymphocytes (arrows) with small hyperchromatic nuclei and scant cytoplasm. **(b)** illustrates plasma cells (arrows), characterized by eccentric nuclei with a clock-face arrangement of nuclear chromatin. **(c)** shows a cluster of tissue monocytes (epithelioid cells) with indented nuclei and abundant eosinophilic cytoplasm (arrows).

roles in retinal homeostasis, oligodendrocytes in the intraorbital part of the optic nerve that form the myelin sheath, and Müller glial cells, which are a unique combination of radial glia, astrocytes, and oligodendrocytes that span the width of the mature retina.[4,9]

Specialized Ocular Histology

The eyeball (globe) (Fig. 7) is situated within the bony orbital cavity, alongside structures such as the lacrimal glands, muscles, tendons, fat, fasciae, vessels, and nerves. The outermost tissue layer of the globe is formed by the cornea and sclera. The middle layer is the vascular uveal layer, while the innermost layer is the retina. Other internal structures of the eye include the anterior and posterior chambers, aqueous humor, lens, vitreous body, and optic nerve head.[1,4,10]

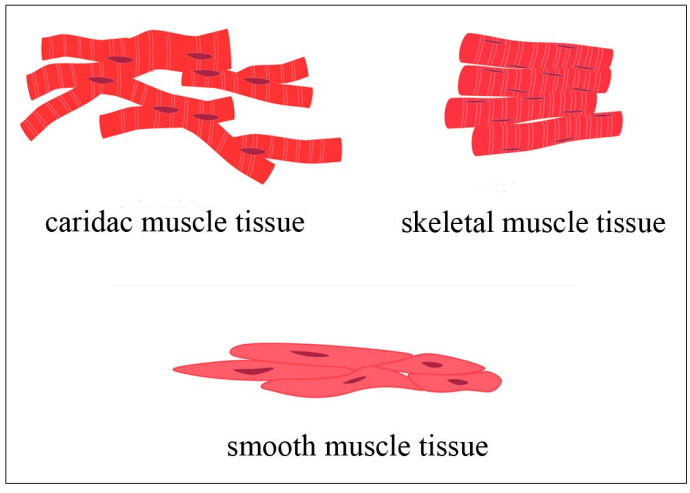

Fig. 5. A schematic image of the different types of muscle cells, including skeletal muscle cells, smooth muscle cells, and cardiac muscle cells. Note that only skeletal and smooth types are observed in ocular muscle tissue.

Detailed histology of the globe and the accessory external structures of the eye will be explained below.

The Eyeball (Globe)

The cornea

The normal cornea (Fig. 8) is an avascular tissue that constitutes the anterior-most 1/6 of the globe and is composed of six layers: epithelium, Bowman layer, stroma, pre-Descemet layer, Descemet membrane, and endothelium. The corneal epithelium, the outermost layer, consists of a 5–8 cell-layered non-keratinized stratified squamous epithelium with a thin and indistinct basement membrane, best visualized using periodic acid-Schiff (PAS) staining. Immediately beneath this membrane lies the acellular Bowman layer, made up of compactly packed, haphazardly organized collagen fibrils. Comprising 90% of the corneal thickness, the corneal stroma contains collagen-producing keratocytes (fibroblast-like cells) and regularly arranged bundles of Type I collagen (collagenous lamella), as well as fibril-associated collagens with interrupted triple-

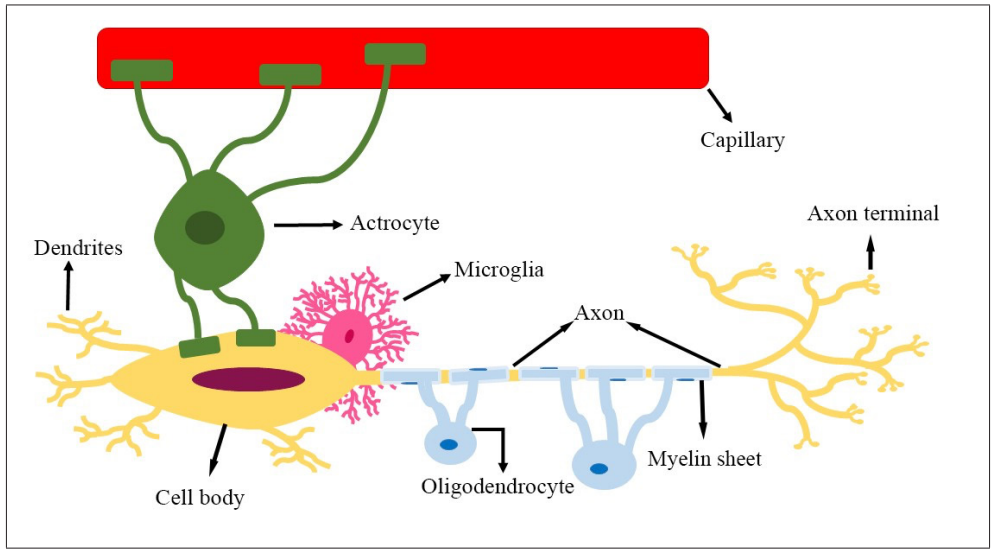

Fig. 6. A schematic image of a neuron illustrating the cell body, axon, dendrites, myelin sheaths, and axon terminal. Note the neuroglial cells, including astrocytes surrounding capillaries to maintain the blood-retinal barrier, microglial cells representing resident tissue macrophages, and myelin-forming oligodendrocytes.

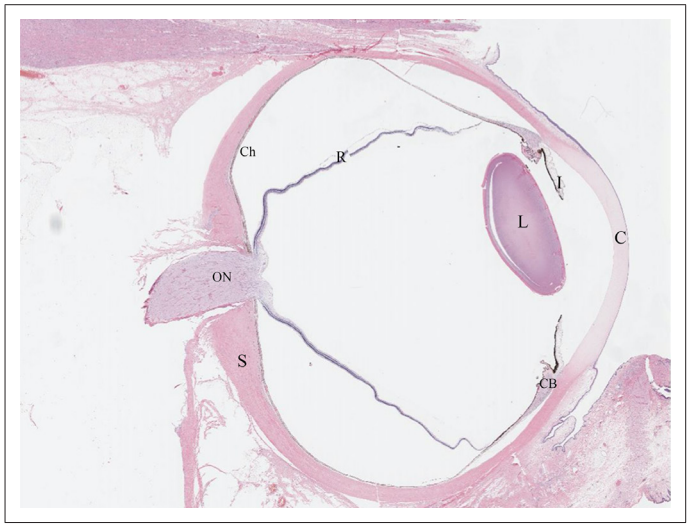

Fig. 7. A whole eye histological section. The image depicts a hematoxylin and eosin-stained section of the globe, illustrating the cornea (C), sclera (S), iris (I), ciliary body (CB), lens (L), choroid (Ch), retina (R), and optic nerve (ON).

helices collagens such as Type V collagen and hydrated ground substance, all of which are critical for the cornea's transparency and optical properties. The acellular pre-Descemet layer, also known as the Dua layer, is the most posterior part of the stroma and has a strong adhesion to the Descemet membrane. As a PAS-positive basement membrane, the Descemet membrane is produced by the corneal endothelium and is ultrastructurally composed of an anterior non-banded layer formed during embryogenesis and a posterior banded layer that develops throughout life. Forming the innermost layer of the cornea, the corneal endothelium consists of a monolayer of low cuboidal cells that appear hexagonal in shape and are primarily responsible for corneal deturgescence and transparency by actively pumping ions and water from the corneal ground substance into the aqueous humor. In contrast to the corneal epithelium, these endothelial cells have very limited proliferative potential.[1,4,7,11-14]

The sclera

The sclera is a whitish, relatively avascular dense fibrous connective tissue primarily composed of Type 1 collagen fibers oriented in various directions. It covers about 5/6 of the outer layer of the eye and functions as structural support for the globe's shape. The sclera connects to the cornea anteriorly at the limbal region, where corneal stem cells are situated. Posteriorly, its outer two-thirds merge with the dural sheath of the optic nerve, while the inner third forms a cribriform network called the lamina cribrosa, through which the axonal fibers of the retinal nerve fiber layer (NFL) pass to become the retrobulbar optic nerve. Histologically, the sclera consists of three indistinct layers: the episclera, stroma, and lamina fusca (Fig. 10). The episclera is a thin, loose, fibrovascular connective tissue that covers the outer surface of the scleral stroma. Comprising the majority of the scleral tissue, the scleral stroma is a lightly vascularized dense connective tissue made up of interlacing Type I collagen fibers alternating with networks of elastic fibers. The thickness and orientation of the scleral collagen lamellae are more variable than those in the corneal stroma. The ciliary arteries, vortex veins, and ciliary nerves pass

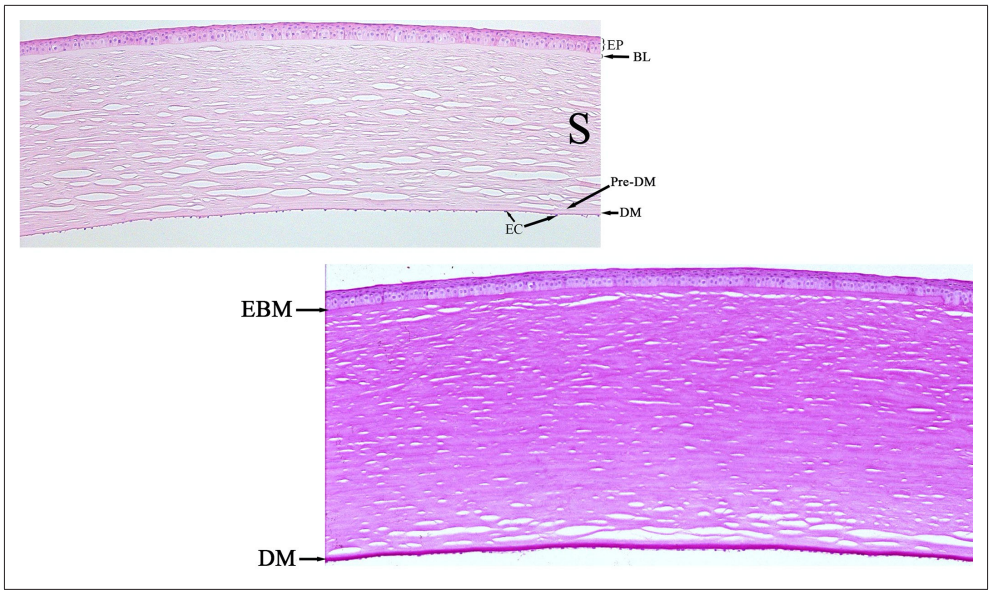

Fig. 8. Histology of a normal cornea. **(a)** depicts a full-thickness hematoxylin and eosin-stained corneal section, composed of epithelium (EP), Bowman layer (BL), stroma (S), pre-Descemet layer (Pre-DM), Descemet membrane (DM), and endothelial cells (EC).. Note the Periodic-acid Schiff (PAS)-reactive corneal epithelial basement membrane (EBM) and DM, as well as the corneal endothelial basement membrane on PAS stain in the **(b)**.

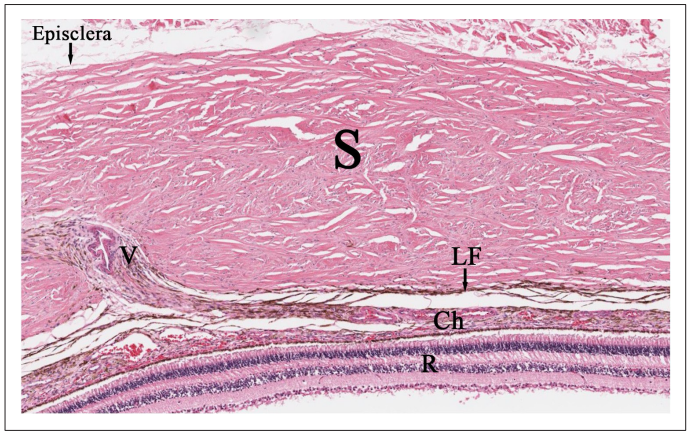

Fig. 9. Histology of a normal sclera. The image illustrates three indistinct layers of the sclera, consisting of the episclera as a thin outer fibrovascular connective tissue, a middle collagenous stroma (S), and the thin fibrovascular lamina fusca (LF) as the inner layer of the sclera overlying the uveal tissue. The section includes a transmural emissary canal, including vortex vein (V), as well as the choroid (Ch) and retina (R) (hematoxylin and eosin stain).

through the scleral stroma via transmural emissary canals to reach the underlying uveal or retinal tissue. The scleral spur is part of the posterior scleral stroma, situated between the posterior part of trabecular meshwork and the anterior insertion of the longitudinal ciliary body muscles (Fig. 10). The lamina fusca forms a loose attachment between the uveal tract and the sclera; it is a thin fibrovascular layer that contains fibroblasts and melanocytes. The strongest points of scleral-uveal bonding are located around the optic nerve and major emissary canals, as well as the anterior base of the ciliary body.[1,4,7,11,12,15]

The limbus

The limbus is a 1.0–1.5 mm transitional area between the peripheral cornea and the anterior part of the sclera. It begins anteriorly at a plane connecting the termination of the Bowman layer to the end of the Descemet membrane and extends posteriorly to a plane perpendicular to the ocular surface and passing through the anterior tip of the scleral spur. Histologically, the limbus is covered by a non-keratinized stratified squamous epithelium with palisades, which overlies the corneo-scleral stroma. The innermost section of the limbus comprises the main components of the aqueous outflow apparatus, including the trabecular meshwork and Schlemm's canal [Figure 10]. The limbal palisades host the limbal stem cells' niche, which, despite having low mitotic activity, possesses unlimited self-regeneration capacity.[12,13,16,17]

Aqueous outflow apparatus

The trabecular meshwork, Schlemm's canal, and collector channels constitute the aqueous outflow apparatus. Histologically, the trabecular meshwork is made up of fenestrated connective tissue trabecular beams covered by a monolayer of partially pigmented thin trabecular cells. The Schlemm's canal closely resembles a lymphatic vessel and is lined by a non-fenestrated monolayer of endothelial

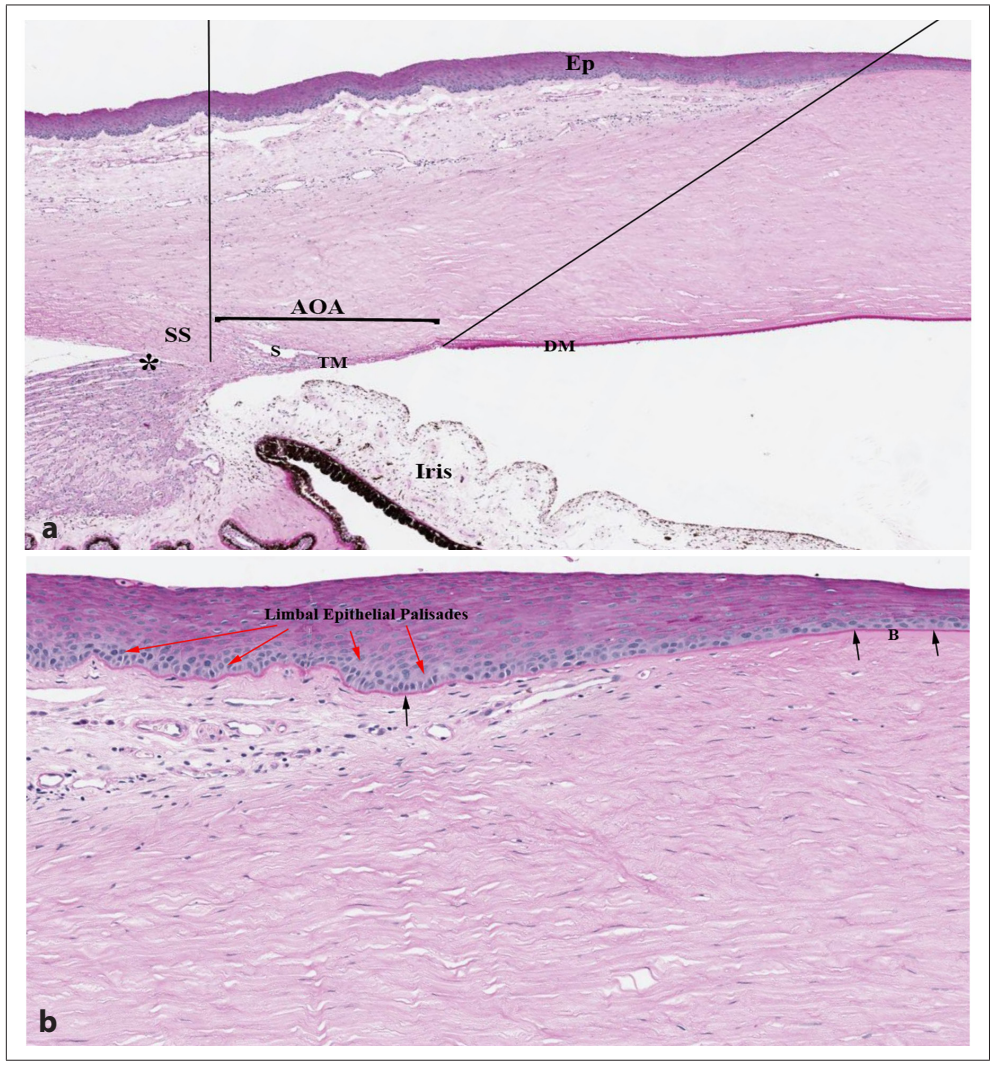

Fig. 10. Histology of the normal limbus. **(a)** depicts the limbal area, which starts anteriorly from an oblique plane connecting the termination of Bowman layer (BL) to the end of Descemet's membrane (DM). The limbus posteriorly limits to a plane perpendicular to the ocular surface, passing through the anterior tip of the scleral spur (SS). The innermost section of the limbus consists of the main parts of the aaqueous outflow apparatus (AOA), including the trabecular meshwork (TM) and Schlemm canal (S). Asterisk (*) illustrates the anterior insertion of the ciliary body just posterior to the scleral spur. A non-keratinized stratified squamous epithelium with palisades (Image a, and red arrows in image b) overlying the corneoscleral stroma constitutes the outermost part of the sclera. Black arrows **(b)** illustrate the Periodic-acid Schiff (PAS)-reactive epithelial basement membrane (PAS stain).

cells resting on a thin connective tissue wall (Fig. 11). Over 25 collector channels, originate from the Schlemm's canal, draining aqueous humor into the aqueous veins located in the episcleral area.[12,18,19]

The uveal tract

The uvea is a distinct, highly vascularized, and variably pigmented layer located inward from the sclera and cornea. It consists of the iris, ciliary body, and choroid (Fig.12).[1,4,7,11,12]

The iris

The iris is a variably pigmented, ring-shaped tissue situated behind the cornea, forming a circular pupil that controls the amount of light entering the eye. It comprises four layers: the anterior border layer, the iris stroma, the muscular layer, and the bi-layered iris pigment epithelium (Fig. 13). The anterior border layer consists of a condensation of the iris stroma, predominantly made up of melanocytes, and is characterized by numerous crypts and folds. The iris stroma contains connective tissue with abundant melanocytes,

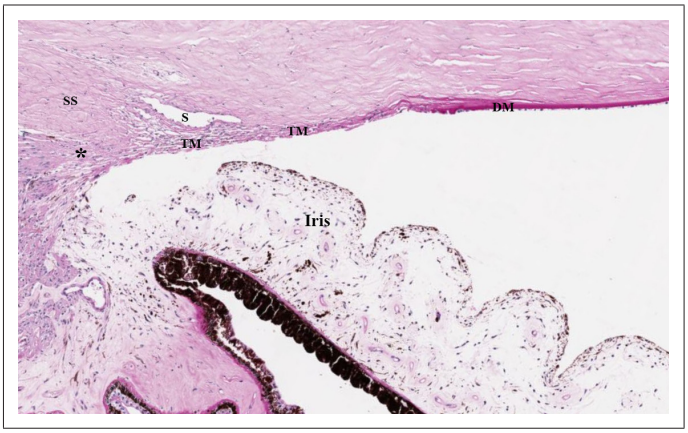

Fig. 11. Histology of the trabecular meshwork and Schlemm's canal. Note the fenestrated trabecular meshwork (TM) at the inner aspect of the limbal area, extending from the termination of Descemet membrane (DM) to the scleral spur (SS). The image depicts Schlemm canal (S), lined by a monolayer of endothelial cells. Asterisk (*) illustrates the anterior insertion of the ciliary body just posterior to the scleral spur (SS) (Periodic-acid Schiff stain).

Fig. 12. A semi-schematic image of the uveal tract representing the iris, ciliary body, and choroid, highlighted in yellow, blue, and green, respectively.

fibroblasts, scattered nerves, blood vessels with thick collagen cuffs, and two types of pigment-laden clump cells. Type I clump cells, or Koganei cells, are histiocytic cells that contain phagocytosed pigment, while Type II cells are variants of neuroepithelial cells. The muscular layer of the iris comprises smooth muscle cells, including the flat and radially arranged dilator muscle, which lies just anterior to the iris pigment epithelium and extends from the middle area of the iris to the iris root. The sphincter muscle, thicker than the dilator muscle, is positioned at the pupillary border in a radial arrangement. The iris pigment epithelium consists of a double layer of anterior and posterior cuboidal epithelium arranged apex-to-apex, which contains intracytoplasmic heavily packed melanin granules that block light rays, ensuring that light passes through the pupil into the eye. The number and size of melanin granules in the anterior border layer melanocytes determine iris color, while the granules in the iris pigment epithelium do not contribute to this variation.[1,4,7,11,12]

The ciliary body

The ciliary body is a thickened, ring-shaped uveal tissue located deep to the limbus. It spans the inner wall of the eye from the iris root to the choroid at the ora serrata and suspends the lens in place via thin suspensory fibers made of fibrillin (zonular fibers). The primary functions of the ciliary body are to control lens shape and produce aqueous humor. It consists of two parts: the anterior pars plicata, which contains ciliary processes, and the posterior pars plana (Fig. 14). The zonular fibers extend from the valleys of the ciliary processes along the pars plana toward the lens. The inner face of the ciliary body is lined by a double layer of epithelia: an inner non-pigmented layer and an outer pigmented layer. The inner layer comprises highly eosinophilic columnar epithelial cells rich in mitochondrial content and ion channels, which are responsible for aqueous humor production. The outer layer is a melanin-rich simple columnar epithelium that is continuous with the retinal pigment epithelium (RPE). The ciliary muscle forms the bulk of the ciliary body and is composed of three bundles of smooth muscle: longitudinal (the outermost), radial (the middle), and circular (the innermost) muscle fiber layers (Fig. 14). These muscular bundles function as a unit during accommodation. Histologically, differentiating between the muscle layers is challenging, and the muscle fibers appear wedge-shaped in cross-section. A fibrovascular connective tissue lies between the pigmented ciliary epithelium and the ciliary muscle fibers.[1,4,7,11,12]

The choroid

The choroid is the middle layer of the posterior part of the eyeball, consisting of pigmented loose connective tissue and a dense network of blood vessels that extend from the ora serrata to the optic nerve. It is composed of three main layers: The lamina fusca, stroma, and choriocapillaris (Fig. 15). The lamina fusca is made up of pigmented melanocytes that have delicate attachments to the sclera. Deep to the lamina fusca is the stromal layer, which consists of loosely vascularized connective tissue containing arterioles, venules, melanocytes, fibrocytes, nerves, and inflammatory cells. The innermost layer of the choroid, closest to the RPE, is the choriocapillaris, which contains small blood

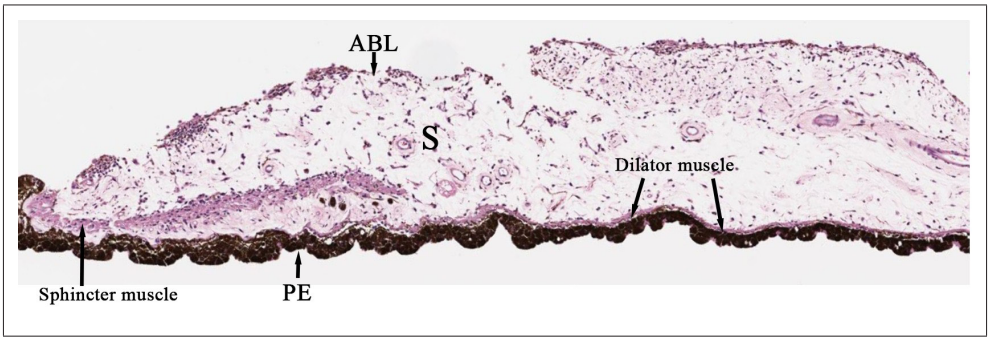

Fig. 13. Histology of a normal iris. The picture depicts the four layers of the Iris composed of the anterior border layer (ABL), iris stroma (S), the muscular layers (sphincter and dilator muscles), and the bi-layered iris pigment epithelium (PE) located at the posterior part of the iris (hematoxylin and eosin stain).

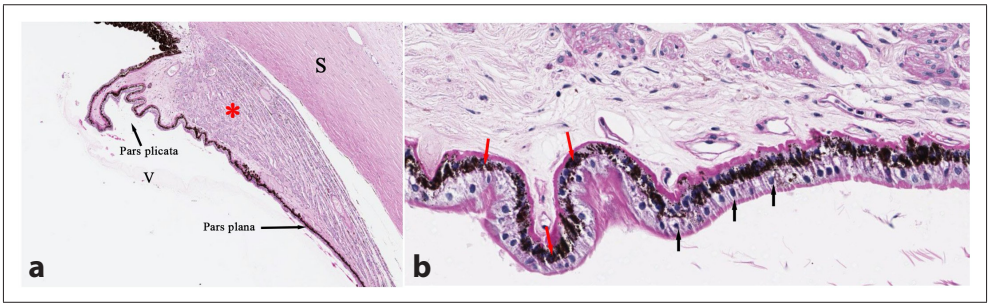

Fig. 14. Histology of the normal ciliary body. Histological section of the ciliary body (Image a) illustrating the plicated ciliary processes anteriorly (pars plicata) and the flattened part of ciliary body posteriorly (pars plana). The ciliary muscles, comprising the main bulk of the ciliary body (asterisk), composed of smooth muscle bundles, and the anterior vitreous (V) are also demonstrated in the image **(a)** Note the double-layered ciliary body epithelium in image **(b)** composed of an inner non-pigmented epithelium (black arrows) and an outer pigmented epithelium (red arrows) (hematoxylin and eosin stain).

vessels (capillaries) adjacent to the Bruch membrane and is responsible for nourishing the outer retina.[1,4,7,11,12,20]

The lens

The lens is a biconvex, transparent disc-shaped structure located behind the pupil. It separates the aqueous and vitreous chambers and comprises four parts: the capsule, epithelium, cortex, and nucleus (Fig. 16). The capsule surrounds the entire lens and is a thick membrane primarily composed of Type IV collagen and glycoprotein, serving as the basement membrane of the lens epithelial cells. This PAS-positive membrane is thickest at the anterior and near-equatorial regions (12–21 μm) and thinnest posteriorly (2–9 μm) (Fig. 16). Immediately beneath the anterior lens capsule is a monolayer of cuboidal epithelial cells that are mitotically active and elongate toward the equatorial parts. From these areas, the elongated cells migrate centrally, produce crystalline proteins, lose their nuclei and organelles, and ultimately differentiate into lens fibers. Notably, the epithelial cells are absent posterior to the lens equator.

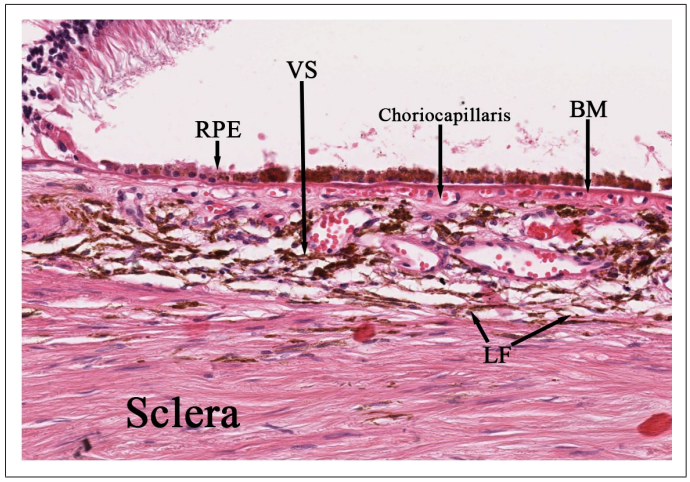

Fig. 15. Histology of a normal choroid. The image illustrates the three main histological layers of the choroid, consisting of the outer lamina fusca (LF), vascularized stroma (VS), and the innermost choriocapillaris, whose capillaries adjoin the Bruch membrane (BM). Note the retinal pigment epithelial cells (RPE) overlying the BM (hematoxylin and eosin stain).

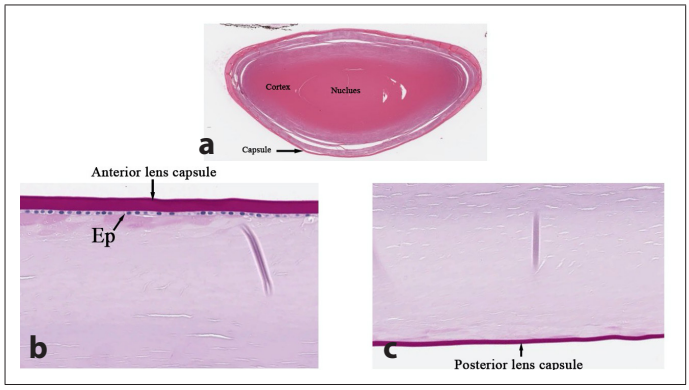

Fig. 16. Histology of a crystalline lens. Four parts of the lens, including the lens capsule, epithelium, cortex, and nucleus, are illustrated in image **(a)** on hematoxylin and eosin stain. Images **(b, c)** depict the periodic acid-Schiff (PAS)-reactive lens capsule on PAS stain, which is thickest anteriorly and thinnest posteriorly.

The lens fibers make up the bulk of the lens, and mature fibers are densely packed with lens crystalline proteins, which increase the refractive index of the lens. Newly formed fibers, resulting from the postnatal maturation of the lens epithelial cells, comprise the lens cortex and are continuously added to existing fibers, compressing them in a lamellar pattern. The fetal lens nucleus, along with the oldest lens fibers, forms the nucleus, where the lens fibers are densely packed.[1,4,7,11,21,22]

The vitreous

The vitreous body constitutes 80% of the eyeball's volume and is a water-rich (99%), transparent, avascular, gelatinous connective tissue composed of collagen fibrils (Fig. 14), few hyalocytes, and hyaluronic acid (hyaluronan) molecules.

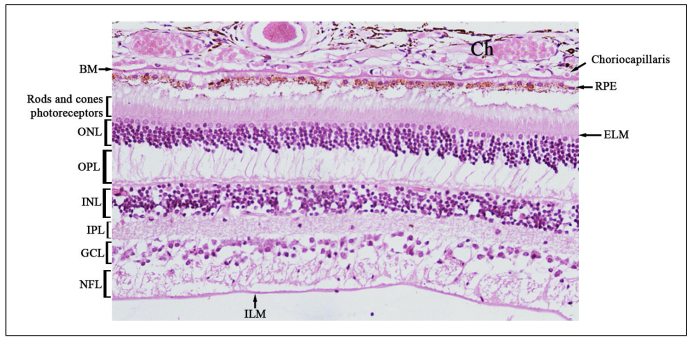

Fig. 17. Histology of a normal retina. The image illustrates a monolayer of retinal pigmented epithelium and nine distinct layers of the neurosensory retina, including rods and cones (inner and outer segments of photoreceptors), external limiting membrane (ELM), outer nuclear layer (ONL), outer plexiform layer (OPL), inner nuclear layer (INL), inner plexiform layer (IPL), ganglion cell layer (GCL), nerve fiber layer (NFL), and internal limiting membrane (ILM). The choriocapillaris of the choroid (Ch) and Bruch membrane (BM) are also demonstrated in the image (hematoxylin and eosin stain).

Hyaluronic acid acts as a filler in the interfibrillar spaces, separating the collagen fibrils and doubling the viscosity of the vitreous viscosity compared to water. The vitreous body has two main topographic regions: the core (central) and cortical (peripheral) vitreous. The cortical vitreous is firmly attached to the posterior lens capsule anteriorly, to the anterior and posterior areas of the ora serrata (vitreous base), and to the macula and optic nerve head.[7,11,12,20]

The retina

The retina fundamentally consists of two distinct layers: the RPE, which is the outer layer, and the inner neurosensory retina (Fig. 17). It constitutes the inner lining of the posterior two-thirds of the eyeball. Continuous with the pigmented ciliary epithelium and the underlying Bruch membrane, the RPE is a monolayer of hexagonal cells that contain abundant melanosomes and lipofuscin. These cells appear cuboidal to columnar in histological cross-sections and possess apical microvilli that closely fit with the outer segments of photoreceptors. The "blood-retinal barrier" is formed by the lateral membranes of the RPE cells, which encompass intercellular tight junctions (zonulae occludentes) near their apices. Bruch membrane, a PAS-reactive lamina located between the RPE cells and the choroid, consists of five layers. The innermost layer is formed by the basement membrane of RPE cells, followed by the inner collagenous zone, a middle porous band of elastic fibers, the outer collagenous zone, and the basement membrane of the choriocapillaris endothelial cells. The outer collagenous layer is continuous with the connective tissue interspersed between the capillaries. This series of connective tissue layers in Bruch membrane renders it highly permeable to small molecules.[7,12,20]

The neurosensory retina, continuous with the non-pigmented ciliary epithelium, is a multilayered structure composed of photoreceptors, neurons, and glial cells. Histologically, the neurosensory retina comprises nine distinct layers (Fig. 17): rods and cones (photoreceptors and their inner and outer segments), external limiting membrane (ELM), outer nuclear layer (ONL), outer plexiform layer (OPL), inner nuclear layer (INL), inner plexiform layer (IPL), ganglion cell layer (GCL), NFL, and internal limiting membrane (ILM). The ELM forms where the supportive Müller cells connect to the photoreceptors through zonulae adherents, and it is not a true membrane. The ONL consists of the cell bodies (nuclei) of photoreceptors, while the OPL is formed by synapses between the axons of photoreceptors and the dendrites of intermediate neurons (bipolar and horizontal cells). The cell bodies

(nuclei) of these intermediate neurons (bipolar, horizontal, and amacrine cells), along with Müller cells, make up the INL. The IPL encompasses synapses between the axons of bipolar cells and the dendrites of ganglion and amacrine cells. The GCL contains the cell bodies (nuclei) of ganglion cells, whose axons form the non-myelinated NFL. The ILM at the retina-vitreous interface is created by the basement membrane of Müller cells. Histological features vary depending on the retinal region. For instance, the macular area consists of a multilayered GCL, and within its central 1.5 mm (the fovea), the OPL fibers run obliquely, creating the Henle fiber layer. The foveola, a small crater at the center of the fovea, consists solely of cone photoreceptors. Overall, the density of the retinal GCL and the thickness of the inner layers decrease toward the peripheral retina, such that the nine histological layers of the neurosensory retina may be absent at the far-peripheral regions near the ora serrata, where cystic changes can occur.[1,4,7,11,12,20,23]

The optic nerve

The non-myelinated axons of retinal ganglion cells (RGCs) converge and turn 90° as they emerge from the optic disc, located at the posterior pole of the eye ball, referred to as the optic nerve head. This head includes the intraocular portion of the optic nerve and is situated anterior to the lamina cribrosa (Fig. 18). The lamina cribrosa is a fenestrated region in the posterior sclera through which the optic nerve axons pass. The retrolaminar portion of the optic nerve is myelinated due to the presence of oligodendrocytes and is thicker than the optic nerve head. This part of the optic nerve tissue consists of the axons of RGCs and supportive glial cells, including oligodendrocytes, astrocytes, and microglial cells. The optic nerve is surrounded by a meningeal sheath composed of dura mater, arachnoid mater, and pia mater (Fig. 18). The external sheath of dura, continuous with the sclera surrounding the lamina cribrosa, is made up of dense connective tissue. The middle sheath, the arachnoid, creates a subarachnoid space filled with cerebrospinal fluid. The internal thin fibrovascular sheath, pia mater, extends into the optic nerve tissue and divides the nerve fibers into bundles.[1,4,7,11]

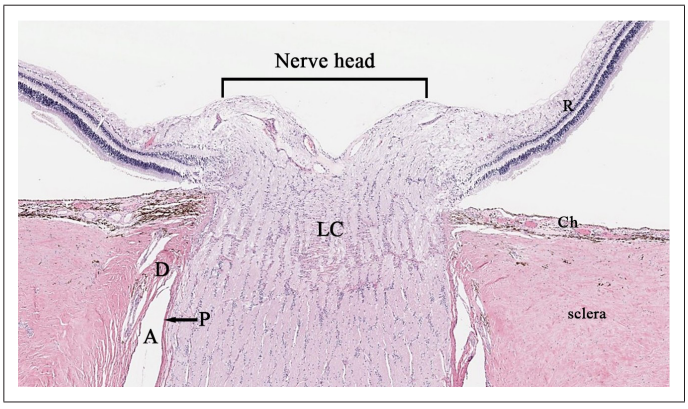

Fig. 18. A histological section of the optic nerve. Note the intraocular part of the optic nerve, referred to as the optic nerve head, anterior to the lamina cribrosa (LC), composed of non-myelinated retinal ganglion cell (RGC) axons. A meningeal sheath, consisting of dura (D), arachnoid (A), and pia (P) mater, surrounds the retrolaminar portion of the optic nerve. This part of the optic nerve comprises myelinated axons as well as supportive glial cells. The sclera, choroid (Ch), and retina (R) are also demonstrated in the image (hematoxylin and eosin stain).

Extraocular Tissues

The eyelids

The eyelid is comprised of four main histological layers: skin, orbicularis oculi muscle, tarsal plate, and palpebral conjunctiva at the tarsal level (Fig. 19). The thinnest skin on the body forms the anterior aspect of the eyelid, presenting as keratinized stratified squamous epithelium (epidermis) over an extremely loose connective tissue called the dermis. The epidermis contains melanocytes, antigen-presenting Langerhans cells, and Merkel cells. The dermis, in addition to delicate collagen fibrils, vessels, lymphatics, and nerve fibers, includes several key components: (1) eyelashes and associated holocrine sebaceous glands of Zeis, concentrated at the lid margin, with secretions consisting of whole secreting cells; (2) modified apocrine sweat glands (of Moll) that open onto the eyelash follicles with secretions containing the apical parts of the secreting cells (decapitation secretion); (3) eccrine sweat glands distributed throughout the eyelid skin, with secretions that do not contain any part of

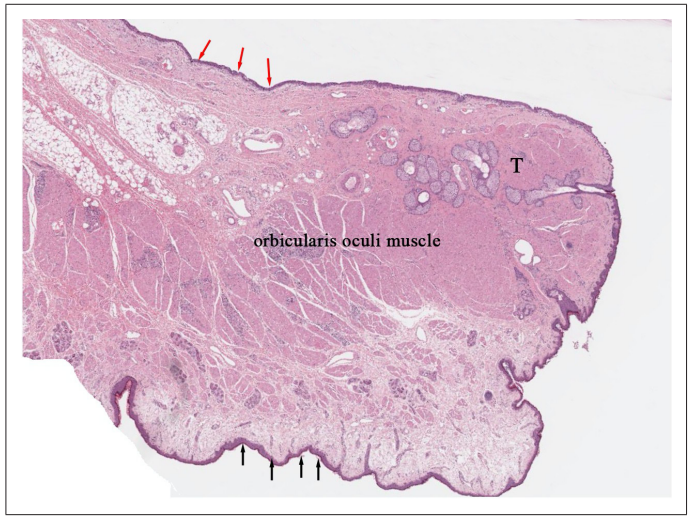

Fig. 19. A histological section of a normal eyelid. The image depicts a hematoxylin and eosin-stained section of the eyelid at the tarsal level, consisting of skin (black arrows), orbicularis oculi muscle, tarsal plate (T), and palpebral conjunctiva (red arrows).

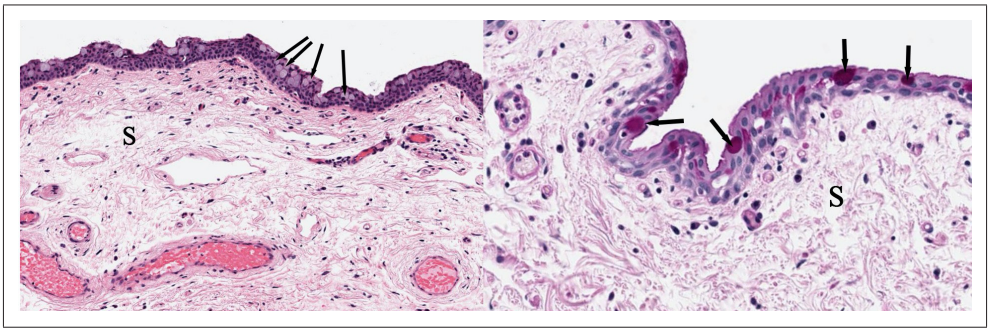

Fig. 20. Histology of a normal conjunctiva. Note the non-keratinized stratified squamous epithelium of the conjunctiva in (a) (hematoxylin and eosin stain), containing mucus-secreting goblet cells (arrows) that are Periodic acid-Schiff (PAS)-reactive in (b) (arrows) (PAS stain). (a) depicts vascularized loose connective tissue of the conjunctival stroma with scattered chronic inflammatory cells.

the secreting cells; and (4) pilosebaceous units (vellus hairs). In addition to the orbicularis oculi (a striated skeletal muscle), the aponeurotic portion of the levator palpebrae superioris (also a skeletal muscle) and the Müller muscle (a smooth muscle) are present in the eyelid. The tarsal plate, which reinforces the eyelid, is a thick band of dense collagenous connective tissue that houses the meibomian glands (sebaceous glands). The accessory lacrimal glands of Krause and Wolfring are also located in the eyelid; the former is found at the conjunctival fornices, and the latter is situated near the upper margin of the superior tarsal plate and along with the lower margin of the inferior tarsal plate.[1,4,7,11,12,24]

The conjunctiva

The conjunctiva is a transparent mucous membrane that connects the outer surface of the eye with the inner surface of the eyelid. It can be divided into palpebral, forniceal, and bulbar parts. Histologically, the conjunctiva consists of a non-keratinized stratified squamous epithelium with approximately five cell layers, which contains PAS-reactive mucus-secreting goblet cells (Fig. 20), immune system Langerhans cells, and scattered indistinct melanocytes. The conjunctival stem cells, characterized by slow cycling and high self-renewal capacity, are present in the basal layer of the conjunctival epithelium and distributed throughout the bulbar and forniceal parts. A delicate basement membrane separates the conjunctival epithelium from the underlying stroma (substantia propria), which is a richly vascularized loose connective tissue containing lymphatic channels, nerves, occasional accessory lacrimal glands (Krause and Wolfring), and resident lymphocytes, plasma cells, histiocytes, and mast cells. In addition, occasional lymphoid follicles, a subtype of mucosa-associated lymphoid tissue, may also be present.[7,12,13]

In contrast to the bulbar conjunctiva, the palpebral conjunctiva displays epithelial ridges. At the fornix, the conjunctiva features infoldings of conjunctival epithelium rich in goblet cells, known as the pseudoglands of Henle (Fig. 21). The caruncle and the plica semilunaris are specialized regions of the conjunctiva. The caruncle, as a transitional zone between the conjunctiva and the skin, is the most medial part of the bulbar conjunctiva and consists of non-keratinized squamous epithelium containing sebaceous glands, hair follicles, and sweat glands. The plica semilunaris, located just temporal to the caruncle, is a fold of bulbar conjunctiva composed of goblet cell-rich non-keratinized squamous epithelium overlying a stroma that includes smooth muscle fibers. Lying between the conjunctiva and the sclera is the collagenous sheath of Tenon's capsule, which separates the globe and the anterior portions of extraocular muscles from the orbital fat. It is attached to the sclera anteriorly by fine bands of connective tissue behind the sclero-corneal junction and merges with the optic nerve sheath posteriorly.[1,4,7,11,24]

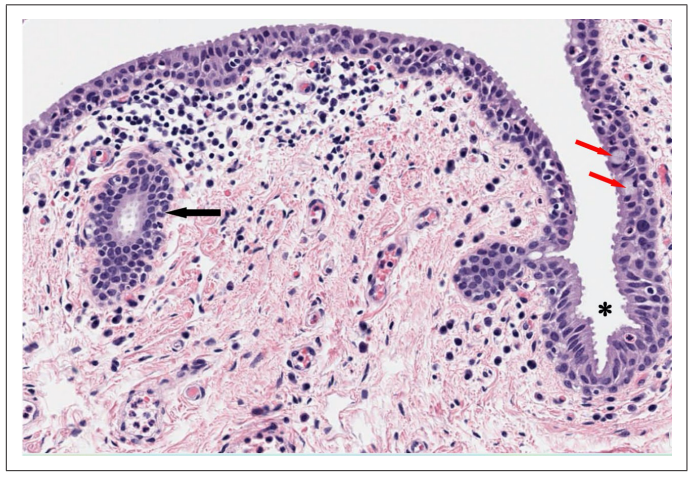

Fig. 21. A histological section of the forniceal conjunctiva. Note the presence of pseudoglands of Henle (black arrow) resulting from conjunctival epithelial infoldings (asterisk) containing goblet cells (red arrows) (hematoxylin and eosin stain).

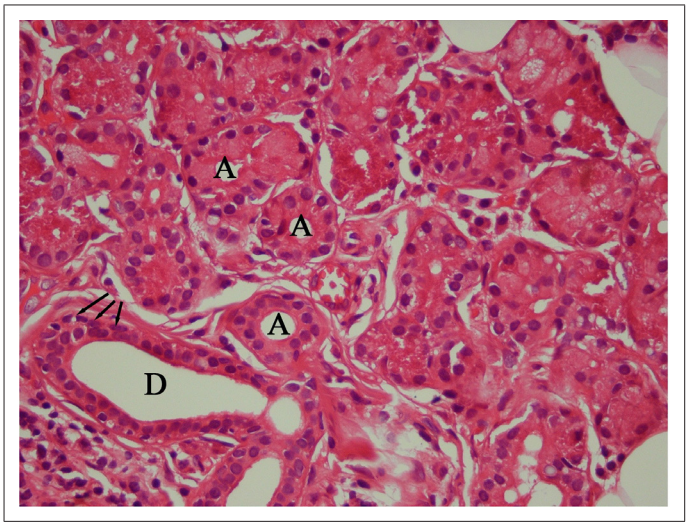

Fig. 22. Histology of normal lacrimal glands. The image depicts the tubuloacinar components of the lacrimal gland, composed of acini (A) and a draining duct (D). Note the round structures of acini consisting of cuboidal epithelial cells with peripherally located round nuclei and abundant basophilic intracytoplasmic granules. Flattened myoepithelial cells (arrows) are present in the outer layer of the ductal epithelium (hematoxylin and eosin stain).

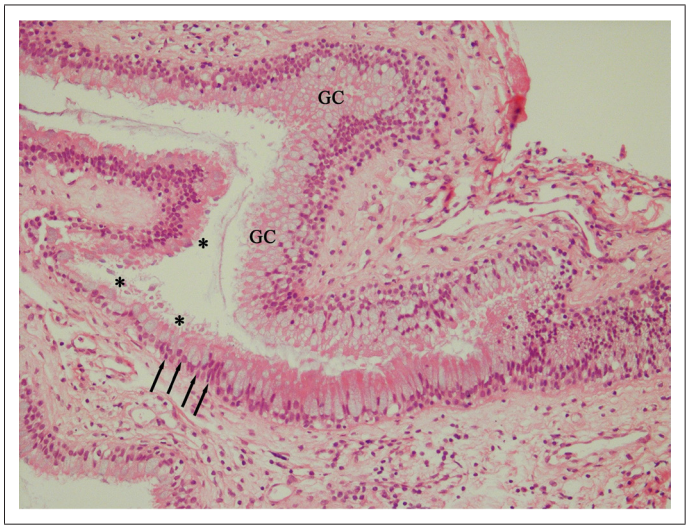

Fig. 23. A histological section of a normal lacrimal sac. Note the presence of a pseudostratified columnar epithelium of the lacrimal sac (arrows), which displays microvilli (asterisks) at the superficial epithelial layer and contains numerous mucus-secreting goblet cells (GC) (hematoxylin and eosin stain).

The lacrimal glands and excretory system

The lacrimal apparatus consists of secretory and excretory parts. The main and accessory lacrimal glands make up the secretory part, while the lacrimal puncti, lacrimal canaliculi, lacrimal sac, and nasolacrimal duct comprise the excretory section.[12]

The main lacrimal glands

The main lacrimal glands are exocrine glands located at the supratemporal aspect of the orbit and are histologically divided into lobules by loose connective tissues. The lobules are composed of tubulo-acinar components (Fig. 22), in which the acini are rounded structures containing cuboidal epithelial cells with peripherally located round nuclei and abundant basophilic intracytoplasmic secretory granules. Secretions from the acini drain into ductal components situated within the fibrovascular stroma and are lined by an inner low cuboidal epithelium. Flattened myoepithelial cells surround the ductal epithelium in the larger ducts, and small clusters of chronic inflammatory cells, such as lymphocytes and plasma cells, may be present in the stroma. The lacrimal gland secretes the aqueous component of the tear film, including immunoglobulin A.[1,4,7,11,12,25,26]

The accessory lacrimal glands

The accessory lacrimal glands of Krause and Wolfring make up about 10% of the total lacrimal secretory system and are located at the proximal tarsal margin and/or in the fornix. Their histological features are similar to those of the main lacrimal glands.[12]

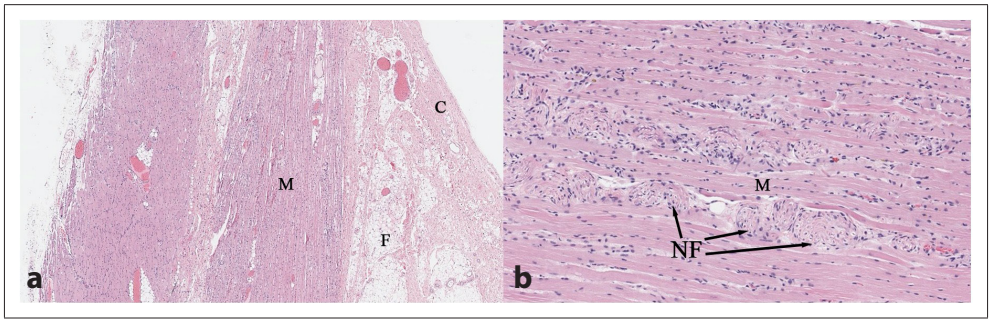

Fig. 24. Histology of normal orbital tissues. **(a)** illustrates orbital tissue composed of orbital fat (F), fibrovascular connective tissue (C), and extraocular muscles (M). **(b)** depicts the presence of neural fascicles (NF) running between the extraocular muscle fibers (M) (hematoxylin and eosin stain).

The lacrimal excretory system

The puncti, canaliculi, lacrimal sac, and nasolacrimal duct make up the lacrimal excretory system. The lacrimal puncti are openings at the medial canthus that drain tears into the lacrimal canaliculi, which then lead to the lacrimal sac. From the lacrimal sac, the tears exit through the nasolacrimal duct into the nose. The puncti and lacrimal canaliculi are lined by non-keratinized stratified squamous epithelium surrounded by connective tissue. The lacrimal sac and nasolacrimal duct are lined with pseudostratified columnar epithelium resting on a broad basement membrane (Fig. 23). The superficial epithelial layer contains microvilli that may assist in the reabsorption of lacrimal fluid within the lacrimal sac. The epithelium also includes numerous mucus-secreting goblet cells arranged as solitary or mucous glands. Large lipid droplets and secretory vacuoles are present in the apical portions of the epithelial cells. Lymphocytes and macrophages may be found in the underlying stromal connective tissue, partly penetrating the epithelium. Particularly in the lower section of the nasolacrimal duct, the epithelium contains ciliated epithelial cells that may facilitate draining flow.[4,7,11,12,26,27]

The orbital tissue

In addition to the lacrimal glands, the histology of normal orbital tissue includes fat, connective tissues containing nerves and vessels, as well as extraocular muscles and tendons (Fig. 24).[11,12]

Conclusion

This review, using basic and clinical textbooks as well as valuable review papers on ocular histology, along with illustrating original histological figures, presents an updated and high-quality version of our knowledge on eye histology, and is crucial for comprehending what occurs in ocular injuries. By describing the basic and specialized ocular histology in this review, both clinical ophthalmic students and researchers in the field of basic and experimental eye research can better understand human eye histology and discover the pathogenesis of ophthalmic disorders.

Peer-review: Externally peer-reviewed.

Authorship Contributions: Concept: M.R.K.; Design: M.R.K., A.R.; Supervision: M.R.K.; Resource: M.R.K.; Materials: M.R.K., A.R.; Data Collection and/or Processing: M.R.K., A.R.; Literature Search: M.R.K., A.R.; Writing: M.R.K., A.R.; Critical Reviews: M.R.K.

Conflict of Interest: None declared.

Use of AI for Writing Assistance: Not declared.

Financial Disclosure: The authors declared that this study received no financial support.

References

1. Pradeep T, Mehra D, Le PH. Histology, Eye. (Updated 2023 May 1). In: StatPearls. Treasure Island (FL): StatPearls Publishing; 2025 Jan. Available at: https://www.ncbi.nlm.nih.gov/books/NBK544343/
2. Mescher AL. Junqueira's Basic Histology, Text & Atlas. 17th ed. McGrow Hill: LANGE; 2024.
3. Cleveland Clinic. Body Tissue. 2025 April 6. Available at: https://my.clevelandclinic.org/health/body/body-tissue
4. Awh C, Wilson MW. Basic Histology of the Eye and Accessory Structures. EyeWiki. American Academy of Ophthalmology. 2025 April 20. Available at: _https://eyewiki.org/Basic_Histology_of_the_Eye_and_Accessory_Structures#Accessory_Structures
5. Cleveland Clinic. Epithelium. 2025 April 6. Available at: https://my.clevelandclinic.org/health/articles/22062-epithelium
6. Cleveland Clinic. Connective Tissue. 2025 April 6. Available at: https://my.clevelandclinic.org/health/body/connective-tissue
7. Rapuano CJ, Stout JT, McCannel CA. Ophthalmic Pathology and Intraocular Tumors. San Francisco: American Academy of Ophthalmology; 2025-2026.
8. Cleveland Clinic. Muscles. 2025 April 6. Available at: https://my.clevelandclinic.org/health/body/21887-muscle
9. Cleveland Clinic. Nerves. 2025 April 6. Available at: https://my.clevelandclinic.org/health/body/22584-nerves
10. Nilsson DE. Eye evolution and its functional basis. Vis Neurosci 2013;30:5–20. [CrossRef]
11. Yanoff M, Sassani JW. Basic Principles of Pathology, Ocular Pathology. 9th ed. Philadelphia: Elsevier; 2025. [CrossRef]
12. Rapuano CJ, Stout JT, McCannel CA. Fundamentals and Principles of Ophthalmology. San Francisco: American Academy of Ophthalmology; 2025-2026.
13. Rapuano CJ, Stout JT, McCannel CA. External Disease and Cornea. San Francisco: American Academy of Ophthalmology; 2025-2026.
14. Sridhar MS. Anatomy of cornea and ocular surface. Indian J Ophthalmol 2018;66:190–4. [CrossRef]
15. Coudrillier B, Pijanka J, Jefferys J, et al. Collagen structure and mechanical properties of the human sclera: analysis for the effects of age. J Biomech Eng 2015;137:041006. [CrossRef]
16. Singh V, Shukla S, Ramachandran C, et al. Science and Art of Cell-Based Ocular Surface Regeneration. Int Rev Cell Mol Biol 2015;319:45–106. [CrossRef]
17. Yoon JJ, Ismail S, Sherwin T. Limbal stem cells: Central concepts of corneal epithelial homeostasis. World J Stem Cells 2014;6:391–403. [CrossRef]
18. Tripathi RC, Tripathi BJ. Functional anatomy of the anterior chamber. Jakobiec FA, editors. Ocular Anatomy, Embryology and Teratology. Philadelphia: Harper & Row; 1982.

19. Rapuano CJ, Stout JT, McCannel CA. Glaucoma. San Francisco: American Academy of Ophthalmology; 2025-2026.
20. Rapuano CJ, Stout JT, McCannel CA. Retina and Vitreous. San Francisco: American Academy of Ophthalmology; 2025-2026.
21. Rapuano CJ, Stout JT, McCannel CA. Lens and Cataract. San Francisco: American Academy of Ophthalmology; 2025-2026.
22. Hejtmancik JF, Shiels A. Overview of the lens. Prog Mol Biol Transl Sci 2015;134:119–27. [CrossRef]
23. Joyce C, Le PH, Sadiq NM. Histology, Retina. (Updated 2023 Aug 8). In: StatPearls. Treasure Island (FL): StatPearls Publishing; 2025 Jan. Available at: https://www.ncbi.nlm.nih.gov/books/NBK546692/
24. Cochran ML, Lopez MJ, Czyz CN. Anatomy, Head and Neck: Eyelid. (Updated 2023 Aug 14). In: StatPearls. Treasure Island (FL): StatPearls Publishing; 2025 Jan. Available at: https://www.ncbi.nlm.nih.gov/books/NBK482304/
25. National University of Singapore. Orbit-Lacrimal Gland-Normal Histology. NUS Pathweb. 2025 April 6. Available at: https://medicine.nus.edu.sg/pathweb/normal-histology/orbit-lacrimal-gland/
26. Remington LA. Ocular Adnexa and Lacrimal System. Remington LA, editors. Clinical Anatomy and Physiology of the Visual System. St. Louis: Butterworth-Heinemann; 2012.p.159–81. [CrossRef]
27. Paulsen F, Thale A, Kohla G, Schauer R, Rochels R, Parwaresch R, Tillmann B. Functional anatomy of human lacrimal duct epithelium. Anat Embryol (Berl) 1998;198:1–12. [CrossRef]

DOI: 10.14744/eer.2025.57441
Eur Eye Res 2026;6(1):117

EUROPEAN EYE RESEARCH

LETTER TO THE EDITOR

Does 'Turkish ophthalmology' need clarification? What truly constitutes our field?

Aslan Aykut

Department of Ophthalmology, Marmara University Faculty of Medicine, Istanbul, Turkiye

Dear Editor,

I read the article "The 100 most-cited articles in Turkish ophthalmology: A bibliometric analysis of research trends and scientific impact" with great interest.[1] By limiting their search to the seven ophthalmology journals published in Turkey, the authors provide a clear picture of our national journals, their citation performance, and their most active subspecialties. This journal-centered approach usefully shows how domestic periodicals collect citations, build professional networks, and uphold editorial standards. Nevertheless, the phrase "Turkish ophthalmology" in the title can be understood in several different ways. It may refer to the physical location of a journal, the institutional address of the authors, the language of the paper, or the eye-health problems that matter most to Turkish patients. Focusing on only one of these meanings may leave aside the large body of high-quality work that Turkish researchers publish in international journals. In our own bibliometric review of uveal-melanoma papers, we traced Turkish-affiliated authors across the global literature. We observed strong cross-border collaboration along with citation patterns that differ from those reported for Turkish journals.[2] Viewed together, the two studies suggest that place of publication, author affiliation, article language, and public-health relevance each answer a different policy question, and merging them under one label can blur the real contribution of Turkish ophthalmology.

For this reason, I kindly propose that future bibliometric studies state their working definition of "Turkish ophthalmology" directly in the title or subtitle, for example, "ophthalmology journals published in Turkey" or "ophthalmic papers from Turkish institutions." When possible, combining more than one of these angles in the same analysis would give a fuller and more balanced view of our scientific output.

I thank Reyhan *et al.*[1] for their careful work and hope that this short note will encourage clearer terms in future studies.

Peer-review: Externally peer-reviewed.

Conflict of Interest: None declared.

Use of AI for Writing Assistance: Not declared.

Financial Disclosure: The authors declared that this study received no financial support.

References

1. Reyhan AH, Berhuni M, Yilmaz IE. The 100 most-cited articles in turkish ophthalmology: A bibliometric analysis of research trends and scientific impact. Eur Eye Res 2025;5:39–46.[CrossRef]
2. Aykut A, Sarigul Sezenoz A. Turkish uveal melanoma research: A bibliometric analysis (1987–2024). Eur Eye Res 2024;4:141–9. [CrossRef]

Cite this article as: Aykut A. Does 'Turkish ophthalmology' need clarification? What truly constitutes our field?. Eur Eye Res 2026;6(1):117.

Correspondence: Aslan Aykut, M.D. Department of Ophthalmology, Marmara University Faculty of Medicine, Istanbul, Turkiye
E-mail: aslanaykut81@gmail.com

Submitted Date: 07.07.2025 **Revised Date:** 20.07.2025 **Accepted Date:** 28.08.2025 **Available Online Date:** 29.04.2026